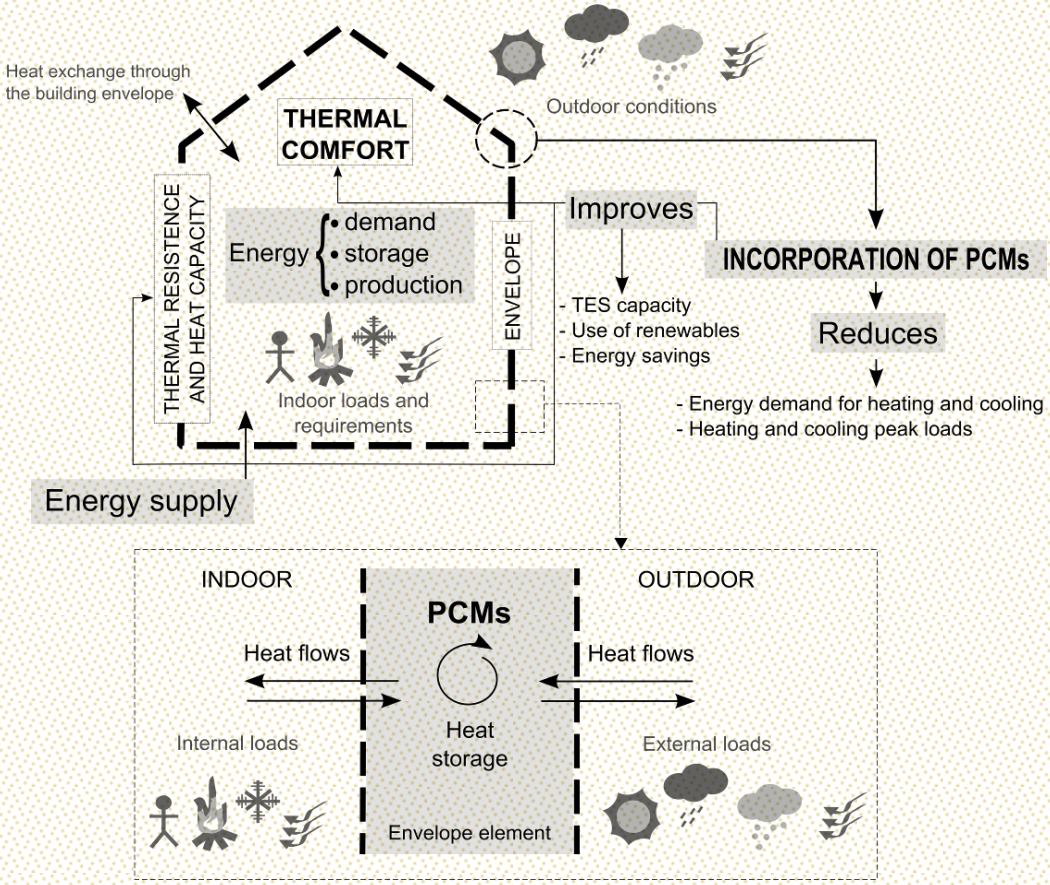

Nelson Miguel Lopes Soares

THERMAL ENERGY STORAGE WITH PHASE CHANGE MATERIALS (PCMs) FOR THE IMPROVEMENT OF THE ENERGY PERFORMANCE OF BUILDINGS

PhD thesis in Sustainable Energy Systems
supervised by Professor José Joaquim da Costa, Professor Adélio R. Gaspar and Professor Paulo Santos
and submitted to the Department of Mechanical Engineering, Faculty of Sciences and Technology of the University of Coimbra

September, 2015

· U C ·

UNIVERSIDADE DE COIMBRA

UNIVERSIDADE DE COIMBRA

THERMAL ENERGY STORAGE WITH PHASE CHANGE MATERIALS (PCMs) FOR THE IMPROVEMENT OF THE ENERGY PERFORMANCE OF BUILDINGS

by

Nelson Soares

M.Sc. in Energy for Sustainability in the specialization area of Indoor Climate and Comfort by the University of Coimbra (2011)

M.Sc. in Civil Engineering in the specialization area of Constructions by the University of Coimbra (2008)

Thesis submitted to the Department of Mechanical Engineering
in partial fulfillment of the requirements for the degree of

Doctor of Philosophy in Sustainable Energy Systems

by the

FACULTY OF SCIENCES AND TECHNOLOGY
UNIVERSITY OF COIMBRA

Thesis Supervisors

José Joaquim da Costa, Assistant Professor
Department of Mechanical Engineering of the University of Coimbra

Adélio Rodrigues Gaspar, Assistant Professor
Department of Mechanical Engineering of the University of Coimbra

Paulo Fernando Antunes dos Santos, Assistant Professor
Department of Civil Engineering of the University of Coimbra

Coimbra, 2015

This thesis is framed in the context of the Sustainable Energy Systems focus area of the MIT-Portugal Program. It is also framed within the Initiative Energy for Sustainability of the University of Coimbra and within the Research Project "*Energy and Mobility for Sustainable Regions*" (EMSURE) CENTRO-07-0224-FEDER-002004. As a visiting student at MIT, the candidate also worked in the MIT-Kuwait Signature Project "*Sustainability of Kuwait's Built Environment*". The research carried out was funded by the Portuguese Foundation for Science and Technology (FCT) through the PhD scholarship SFRH/BD/51640/2011 in the framework of the MIT-Portugal Program. The work was also supported by the Portuguese Association for the Development of Industrial Aerodynamics (ADAI); the Portuguese Associated Laboratory for Energy, Transports and Aeronautics (LAETA), and the Portuguese Institute for Sustainability and Innovation in Structural Engineering (ISISE).

Abstract

The improvement of the energy efficiency of buildings during their operational phase is an active area of research. The markets are looking for new technologies, namely new thermal energy storage (TES) systems, which can be used to reduce buildings' dependency on fossil fuels, to make use of renewable energy sources and to contribute to match energy supply and demand efficiently. The main goals of this thesis are: (*i*) to evaluate the heat transfer with solid–liquid phase-change through small TES units filled with phase-change materials (PCMs), providing experimental data to be used in the design of new TES systems for buildings and in the validation of numerical models, and (*ii*) to provide some guidelines for the incorporation of PCM-drywalls in buildings aiming to reduce the energy demand for heating and cooling by making use of the latent heat from the phase-change processes of PCMs.

The first part of this thesis refers to the experimental study of the heat transfer through a vertical stack of metallic rectangular cavities filled with different PCMs (a microencapsulated and a free-form PCM). The research carried out aims: (*i*) to analyze the melting and solidification processes of the PCM within the enclosures, (*ii*) to evaluate the influence of the aspect ratio of the cavities on the heat transfer and (*iii*) to discuss which type of PCM is better for specific cases. As a result, a big amount of experimental data for benchmarking and validation of numerical models is made available to the scientific community. Moreover, the results allow discussing which arrangement of the TES unit is better for specific applications considering the thermal regulation effect during charging, the influence of subcooling during discharging, and the influence of natural convection during both processes. It is shown that the effect of natural convection in the free-form PCM must be considered in any simulation to better describe the charging process. During discharging, subcooling must also be considered. On the contrary, the effect of natural convection and subcooling can be neglected when considering the microencapsulated PCM.

The second part of this thesis concentrates on the dynamic simulation of energy in buildings considering the latent heat from PCMs' phase-change processes. The energy system under investigation is extended to an air-conditioned residential single-zone room. The main goals are: (*i*) to develop a holistic methodology to optimize the incorporation of PCM-drywalls in different typologies of construction and (*ii*) to provide guidelines for the incorporation of PCM-drywalls in different climates. Two studies are carried out: (*i*) a multi-dimensional optimization study combining *EnergyPlus* and *GenOpt* tools to optimize the incorporation of PCM-drywalls in lightweight steel-framed (LSF) residential buildings in Europe, and (*ii*) an *EnergyPlus*-based parametric study to optimize the incorporation of PCM-drywalls in heavyweight residential buildings in Kuwait. It is shown that an optimum PCM-drywall solution can be found for each European climate and that the incorporation of PCM-drywalls can contribute for heating and cooling energy savings in LSF construction. The results show that PCM-drywalls are particularly interesting for LSF construction in Mediterranean climates leading to higher energy savings. PCM-drywalls can also be used to reduce the annual energy demand for cooling in Kuwait by almost 5%.

Keywords: Phase change materials; PCMs; Thermal energy storage; Heat transfer; Building applications; Thermal performance optimization; Buildings energy simulation.

Resumo

O aumento da eficiência energética dos edifícios durante o seu período de utilização é uma área de investigação global, com um mercado exigente à procura de novas soluções que permitam aumentar a independência energética dos edifícios, impulsionando o uso de energias renováveis e reduzindo o consumo de combustíveis fósseis. Neste contexto, o desenvolvimento de novos sistemas para armazenamento e aproveitamento de energias renováveis, nomeadamente da energia solar térmica, poderá contribuir para a construção de edifícios mais sustentáveis e com menores consumos de energia associados à climatização. Os principais objetivos desta tese são: (i) avaliar a transferência de calor com mudança de fase sólido–líquido através de uma pequena unidade para armazenamento de energia térmica preenchida com materiais de mudança de fase (PCMs), fornecendo resultados experimentais que possam ser usados no desenvolvimento de novos sistemas para armazenamento de calor latente para os edifícios e na validação de modelos numéricos; (ii) fornecer algumas diretrizes para a utilização de placas de gesso cartonado com PCMs (*PCM-drywalls*) visando reduzir o consumo de energia associado à climatização ao tirar proveito do calor latente envolvido nos processos de mudança de fase dos PCMs.

Na primeira parte da tese estuda-se por via experimental a transferência de calor através da unidade para armazenamento de energia térmica. Esta unidade é constituída por um arranjo vertical de cápsulas de secção retangular preenchidas com diferentes tipos de PCMs (microencapsulado e/ou livre). As principais linhas de investigação são: (i) caracterizar os processos de mudança de fase dos PCMs durante as fases de carga e descarga, (ii) avaliar o impacto do fator de forma das cavidades na transferência de calor e (iii) discutir qual é o melhor tipo de PCM para diferentes aplicações em edifícios. Um vasto conjunto de resultados experimentais para *benchmarking* e validação de modelos numéricos é disponibilizado à comunidade científica. Os resultados permitem ainda discutir qual é a melhor configuração da unidade de armazenamento, considerando o seu efeito termorregulador durante a fase de carga, a influência do fenómeno de *subcooling* durante a fase de descarga e a influência da convecção natural durante ambas as fases. Verifica-se que os efeitos da convecção natural têm que ser considerados na modelação da transferência de calor durante a fase de carga do PCM livre. Durante a descarga, o efeito do *subcooling* deve também ser considerado. Pelo contrário, os efeitos da convecção natural e do *subcooling* podem ser desprezados na modelação da transferência de calor durante ambas as fases, quando se considera a unidade preenchida com o PCM microencapsulado.

Na segunda parte da tese, o estudo é alargado à escala do compartimento. Para considerar a contribuição do calor latente envolvido na mudança de fase dos PCMs nas necessidades de energia para climatização, é efetuada a simulação dinâmica do comportamento térmico do compartimento. Os principais objetivos são: (i) desenvolver uma metodologia integrada para otimizar a incorporação de *PCM-drywalls* em diferentes tipos de construção e (ii) fornecer algumas diretrizes para a incorporação das mesmas placas de gesso com PCMs em edifícios residenciais, considerando diferentes climas. Dois cenários são avaliados: (i) no primeiro, a ferramenta de simulação dinâmica *EnergyPlus* é combinada com a ferramenta de otimização *GenOpt* para otimizar a incorporação de *PCM-drywalls* em edifícios de construção leve em aço enformado a frio considerando diferentes climas Europeus; (ii) no segundo cenário, é feito um estudo paramétrico usando o *EnergyPlus* para avaliar a incorporação de *PCM-drywalls* na construção tradicional de inercia térmica forte no Kuwait. Verifica-se que existe uma solução ótima para cada um dos climas investigados e que a incorporação de *PCM-*

drywalls contribui para a redução das necessidades de energia para climatização em ambos os tipos de construção. Os resultados demonstram ainda que estas placas são particularmente promissoras para a construção de inércia térmica fraca nos climas Mediterrânicos.

Palavras-chave: *Phase change materials*; PCMs; Armazenamento de energia térmica; Transferência de calor; Aplicações em edifícios; Otimização do desempenho térmico; Simulação térmica de edifícios.

Acknowledgements

This thesis presents the results of my research carried out in the framework of the Sustainable Energy Systems Doctoral Program of the University of Coimbra, within the MIT-Portugal Sustainable Energy Systems Program, an initiative of the Portuguese Foundation for Science and Technology (FCT). My work was funded by FCT under the PhD scholarship SFRH/BD/51640/2011, from September 2011 to August 2015. Wining this MIT-Portugal Program scholarship gave me an exceptional opportunity to participate in an outstanding, vibrant and multidisciplinary school program. Moreover, it supported my visit to the Massachusetts Institute of Technology (MIT) for developing research in the MIT Sustainable Design Lab. For these reasons, I would like to express my gratitude to FCT and the MIT-Portugal program for the great opportunity to participate on such international, interactive and collaborative platform.

I would like to thank my main advisor Professor José Costa for accepting me as a Ph.D. student at the Department of Mechanical Engineering of the University of Coimbra. He is a constant source of inspiration and motivation, always willing to critically review my results, to teach me and to share with me his knowledge, expertise and experience. I thank him for his constant generosity and friendship. He provides encouragement, guidance and scientific support to make research possible, always trusting and allowing the freedom to pursue one's own ideas.

I also thank to my advisors Professor Adélio Gaspar and Professor Paulo Santos for their time, friendship, encouragement and scientific support. They have been tireless in supporting my work, always willing for keen and exciting discussions about my research.

I want to express my very special gratitude to Professor Christoph Reinhart for having accepted to be a member of my Ph.D. thesis committee and for hosting me in his research group at MIT during my seven months visit. I would like to thank the great inspiration and motivation he gave me, and all the thoughts, ideas and experience he shared with me. I would like to express my appreciation for his time and guidance towards the formulation and realization of a research problem in the framework of the MIT-Kuwait Signature Project called "*Sustainability of Kuwait's Built Environment*". Joining his team at the MIT Sustainable Design Lab was very enriching for me, both personally and professionally. I feel privileged to have been given the opportunity to work in such an active, professional and enthusiastic environment in which everybody works on exciting research projects.

I am thankful for the privilege to be a research member of both the Portuguese Association for the Development of Industrial Aerodynamics (ADAI) and the Associated Laboratory for Energy, Transports and Aeronautics (LAETA). I acknowledge all the support provided by ADAI to participate in international schools and conferences, and for the implementation of my research plan. I am also grateful for the opportunity to be a research member of the Portuguese Institute for Sustainability and Innovation in Structural Engineering (ISISE). I acknowledge the support given by ISISE for me to participate in international events.

My research was also developed in the framework of the Initiative Energy for Sustainability (EfS) of the University of Coimbra. This Initiative provided me an outstanding multidisciplinary environment that was very important for the development of my research. I acknowledge the several grants provided by the EfS Initiative for supporting my visit to the MIT and my presence in several international conferences. I am also grateful for the support provided for attaining international events through the Research Project "*Energy and Mobility for Sustainable Regions*" (EMSURE) CENTRO-07-0224-FEDER-002004.

I would like to thank the UK Energy Research Centre (UKERC) for the opportunity and support to participate in the UKERC International Summer School 2013.

I also acknowledge Paulo Pais for his assistance in the construction of the experimental setup developed for part of my research.

Finally, I want to thank my parents, sisters and friends for all their love and encouragement.

Nelson Soares, September 2015

CONTENTS

CHAPTER 1

Introduction

This chapter presents the background information and the main motivation for the research carried out in this thesis. The main challenges of incorporating PCMs in buildings and some benefits from considering TES systems for the improvement of the energy performance of buildings during their operational phase are also addressed. This chapter aims to emphasize how the developed research can contribute for the advancement of knowledge in the covered research fields. Chapter I is divided into four sections. Section I.1 introduces the general setting and the main motivation for the research developed. An extensive survey was made to provide a comprehensive review of previous studies related to the evaluation of how and where PCMs are used in passive latent heat TES systems, and how these construction elements can be used to improve the energy performance of buildings. Some research gaps were also identified during the survey. This study was already published in the paper "*Review of passive PCM latent heat thermal energy storage systems towards buildings' energy efficiency*" by Soares *et al*. [1]. The most important research topics identified in the literature review are presented in Section I.2. More attention will be devoted to this extensive literature review in Chapters II and V. Section I.3 presents the research questions and the main goals of the research carried out. Finally, Section I.4 provides an overview of the structure of the thesis.

I.1 Background and motivation

Nowadays, the improvement of the energy performance of buildings during their operational phase is a prime objective for energy policy at regional, national and international levels, as remarked by Pérez-Lombard *et al.* [2]. In developed countries, *Buildings* is one of the leading sectors with respect to energy consumption. Taking the EU as an example, the buildings sector accounts for around 40% of the total final energy consumption and produces nearly 40% of the total CO_2 emissions [3,4]. Most of it is due to the increase in the living standards and in occupants' comfort demands, mainly for heating and cooling. In a non-sustainable approach, buildings are increasingly dependent on active systems to ensure indoor thermal comfort. This produces an increase in the energy consumption as well as an increase in the associated greenhouse gas emissions. Consequentially, there is a surge in the operational phase cost of buildings. The reduction of the energy consumption for air-conditioning and the improvement of the energy conservation are crucial to promote energy efficiency and sustainability of buildings. Furthermore, the enforcement of the use of renewable energy sources is decisive concerning the reduction of buildings' energy dependency.

The economic panorama and the EU's main legislation concerning the reduction of the energy consumption of buildings have been challenging the buildings industry and academic community to innovate and to develop new products and technologies for improving the energy performance of buildings and to make use of renewable energy sources. The development of new systems to take advantage of solar thermal energy for reducing cooling and heating energy demands can be very helpful for the challenging energy performance requirements for new buildings and retrofitting. The exportation of these new technologies, mainly to the emerging economy countries in great need of housing, could also be a great opportunity for the R&D companies. Moreover, the research carried out in the development of new solar based technologies will definitely contribute for the advancement of knowledge in the research field.

It should be remarked that the concern about the reduction of the energy demand during the operational phase of buildings is no longer a problem of the western world and the energy-importing countries. Some oil-exporting countries have also recognized the importance of reducing the energy consumption of buildings to balance the energy domestic market and exportation [5]. Therefore, the improvement of the energy performance of buildings is a global area of research with a market looking for new materials, systems and technologies that could be used to reduce buildings' dependency on fossil fuels, to make use of renewable energy sources, to contribute to a more environmental-friendly and efficient energy use, to contribute to match energy supply and demand efficiently (by increasing the energy storage capacity), and to improve indoor thermal comfort in a more sustainable and cost-effective way.

Nowadays, PCMs can be used in TES applications to take advantage of solar thermal energy in a passive way. Here, "passive" means that the solid–liquid phase-change processes occur without resorting to mechanical equipments. In comparison to the traditional materials used in construction, PCMs provide a large heat capacity over a limited temperature range (due to the high energy quantities involved in the solid–liquid phase-change processes) and they could act like an almost isothermal reservoir of heat. As the temperature increases and reaches the melting temperature, PCMs change phase from solid to liquid. Since this reaction is endothermic, they absorb heat. When the temperature decreases and reaches the solidifying temperature, PCMs change phase from liquid to solid. This time they release the stored heat since the reaction is exothermic. An updated review on the main challenges and applications of TES was recently carried out by Kousksou *et al.* [6].

The principles of PCMs' use are very simple; however, evaluating the effective contribution of the latent heat for the enhancement of the energy performance of the whole building is challenging. The optimization of integrating PCMs within passive latent heat TES systems and the optimal integration of these elements within the building is also complex. This entails including the major design parameters, namely the phase-change temperature of the PCM, its thermal mass quantity and

its position within the TES system and/or, the position of the TES system within the building. Moreover, such parameters need to be specified for given indoor loads and also for specific climatic conditions. Therefore, the approach for the assessment of the potential of PCMs in buildings' design should be different for residential buildings or commercial buildings, or even high or low thermal inertia buildings. The approach should also be different if the inclusion of PCMs is to be optimized to reduce cooling energy demand during summer or heating energy demand during winter.

Another challenge is to evaluate how PCMs can be incorporated in constructions elements in order to avoid liquid leakage. Several ways of containment and different techniques for incorporating PCMs in construction materials have been studied over the last years. A review on the topic can be found in Soares *et al.* [1]. Two of the most well-known techniques are the microencapsulation and the macroencapsulation techniques. In the former, the PCM is encapsulated within a micropolymeric capsule. The final result is a powder-like material that can be mixed with other materials (such as gypsum, cement mortars, etc.). In the latter, the macrocapsule may be the only way of confinement in order to avoid liquid leakage. The macrocapsules are typically made of high-conductivity materials in order to enhance the heat transfer to the PCM-bulk, as PCMs have typically low thermal conductivity. These macrocapsules can then be incorporated in multilayer solutions of the envelope of buildings and in new TES systems.

The research carried out in this thesis is framed within the design and optimization of PCM based TES systems for buildings, which is a worldwide active area of research. The problems to be studied lie in the mainstream area of thermal heat storage in buildings considering the latent heat from the solid–liquid phase-change processes of PCMs. This involves the dynamic simulation of energy in buildings (DSEB) considering latent heat, and the development of reliable experimental setups to evaluate the heat transfer with solid–liquid phase-change through small elements. It is believed that this work will give new and relevant contributions to the present knowledge in these research fields.

I.2 Review of research trends

The number of articles concerning the integration of PCMs in buildings has been increasing during the last decade. In fact, the incorporation of PCMs in TES applications has been a R&D topic of great interest for scientists at universities, in research centers and in industry, and a lot of work has been developed and published worldwide, as reviewed by several authors. Most review papers deal with the general problem of TES using PCMs, focusing on both the PCMs characterization/classification and applications. However, during the last years more specific issues were reviewed and it is

foreseeable that the review articles concerning the problem of integrating PCMs in buildings will gradually be more specialized on certain subjects, as a consequence of the large amount of work that is being developed worldwide [1].

The research topics range from the most general to very specific ones, covering issues such as: (*i*) the kind of PCMs and the main criteria for their selection [1,7–20]; (*ii*) the thermophysical properties of different PCMs [8,10–15,18,20–22] and the main techniques for their measurement [1,11,23–26]; (*iii*) the long-term stability of PCMs [12,14,25,27]; (*iv*) the hysteresis, the phase segregation and the subcooling problems [14]; (*v*) the different techniques for encapsulation and containment [17,19,20,25,28–33], including microencapsulation [34–38]; (*vi*) the description of PCM emulsions [39] and PCM slurries [36,39,40]; (*vii*) the description of several impregnation methods [1]; (*viii*) the main properties of shape-stabilized TES materials [41]; (*ix*) the combination of thermal insulation and thermal energy storage properties [42]; (*x*) the description of some heat transfer enhancement techniques [1,14,22,28,43–45]; (*xi*) the mathematical and numerical modeling of phase-change problems [28,46–51]; (*xii*) the description of several passive applications for buildings and their thermal performance analysis [1,9,13,16,19,21,25,26,31,38,43,52–60]; (*xiii*) the DSEB with PCMs [1,47]; (*xiv*) the free cooling of buildings with TES systems with PCMs [29,55,61–63]; (*xv*) the design of ventilation and air-conditioning systems with PCMs [43,62,64,65] and other active systems for buildings [21,25,53,55,66]; (*xvi*) the integration of PCMs in domestic hot water systems [67,68]; (*xvii*) the latent heat storage in solar collectors [69,70] and other solar systems [9,22,70–72]; (*xviii*) the thermal management of photovoltaics [73–79]; (*xix*) the thermal control of electronic devices [9,44]; (*xx*) the exergy assessment [80] of PCM-based systems; (*xxi*) the use of PCMs for cold storage applications [81] and (*xxii*) other TES applications [82,83].

Many of these review papers pointed out that the study of solid–liquid phase-change of PCMs is of great interest from the theoretical point of view and for the development of new TES systems for buildings. Moreover, Soares *et al.* [1] identified several research gaps providing some recommendations for future work, such as: (*i*) the design of new passive TES systems to take advantage of solar thermal energy; (*ii*) the assessment of the stability and convergence of numerical results, and the importance of validating the numerical predictions using appropriated experimental data (together with a suitable uncertainty analysis); (*iii*) the importance of the effects of hysteresis, subcooling and natural convection phenomena in the numerical simulation of the heat transfer with solid–liquid phase-change, and (*iv*) the development of methodologies to couple DSEB techniques with multi-dimensional, multi-criteria and/or multi-objective optimization analysis to help decision-making in the optimization of both the configuration of TES systems and their location within the building.

Soares *et al.* [1] also pointed out that passive TES systems with PCMs can contribute to (*i*) increase indoor thermal comfort; (*ii*) improve the thermal resistance and the heat capacity of the envelope of the building; (*iii*) decrease the energy demand for heating and cooling; (*iv*) decrease the air-conditioning power needed and the heating and cooling peak-loads; (*v*) take advantage of renewable energy sources such as solar thermal energy; (*vi*) save money during the operational phase and (*vii*) contribute for the reduction of CO_2 emissions associated to heating and cooling. Fig. I.1a shows a sketch of the building as a thermodynamic system. The main advantages of incorporating TES systems with PCMs in buildings are also presented in Fig. I.1a.

In this thesis, two energy systems whose physical domains differ in scale are studied: the element of the envelope of the building (Fig. I.1b) and the building itself (Fig I.1a). At the envelope element scale, the thermal performance of the energy system is mainly influenced by the external and internal boundary conditions and by the thermophysical properties of the PCM. At the level of the building, a DSEB methodology is required to evaluate the influence of PCMs in the energy performance of the entire room considered as a model.

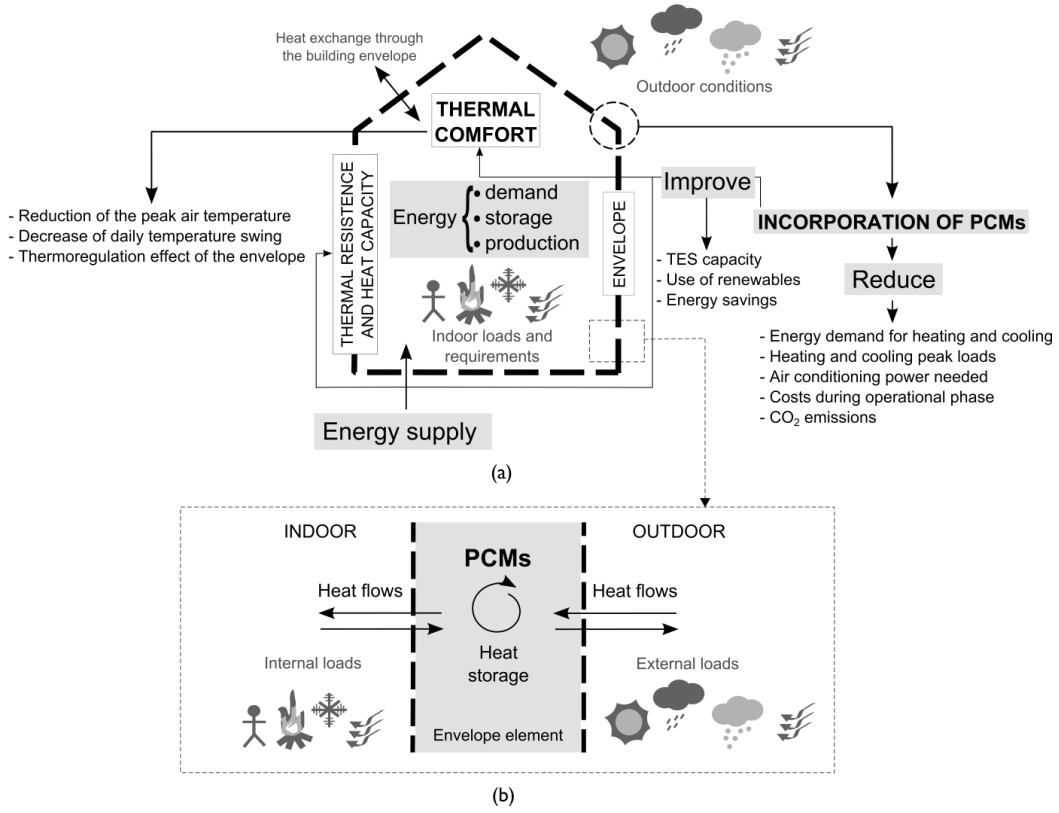

Fig. I.1 (a) Sketch of the building as a thermodynamic system and main advantages of incorporating TES systems with PCMs in buildings. (b) Sketch of the physical domain of the envelope element as an energy system.

I.3 Research questions and main goals

A typical thermodynamic system is characterized by its physical boundary and the exchanges of the physical entities that "flow" through it, such as matter, energy, work, heat or entropy. The problems investigated in this thesis are particularly devoted to the evaluation of the heat flows through the boundary of the energy systems under investigation and to the enhancement of the heat storage capacity of the systems by taking advantage of the latent heat involved in the phase-change processes of PCMs. The research is divided into two main parts, each one referring to a specific scale of the energy system under investigation.

The first part is devoted to the experimental analysis of the heat transfer with solid–liquid phase-change. In this case, the scale of the energy system will be restricted to the scale of the TES unit under investigation. The containment of the TES unit is the boundary of the system. The imposed boundary conditions during the charging and discharging experiments will be controlled in order to evaluate their influence on the thermal performance of the system. Therefore, the main goals of Part A are to evaluate the heat transfer with solid–liquid phase-change through small TES units to be used in the design of new TES systems for buildings, and to provide experimental data for benchmarking purposes and validation of numerical models. The first research question to be addressed is *what is the best configuration of the TES unit for different buildings' applications?* The results of Part A are very useful for the academic community that is investigating the heat transfer with solid–liquid phase-change through vertical rectangular cavities. Moreover, the results can be used by researchers and R&D teams for the design of new TES systems.

In the second part of this thesis, the scale of the energy system will be enlarged to the scale of the building itself. In this case, the boundary of the system is the envelope of the building. As the thermal performance of the building is strongly influenced by the characteristics of the envelope and by the internal and external heat loads, a DSEB approach is required. Therefore, the behavior of users and the climatic conditions will have a great influence on the energy demand for air-conditioning. The main goal of Part B is to reduce the energy demand for heating and cooling during the operational phase of the building by taking advantage of the latent heat involved in the phase-change processes of PCMs. A particular TES system is investigated – the so-called PCM-drywalls. In this TES system, the microencapsulated PCMs are incorporated in the porous structure of a gypsum drywall. These boards can then be used as an envelope finishing inner layer. Part B aims to provide some guidelines for the optimum incorporation of PCM-drywalls in residential buildings by considering different typologies of buildings (lightweight and heavyweight construction) and different climatic conditions. Considering this, the second research question to be addressed in this thesis is *how and where should PCM-drywalls be best incorporated in the envelope of the building to improve its*

energy performance? The results of Part B are very useful for architects and engineers who want to include PCM-drywalls in the design of more sustainable and energy efficient buildings and in the design of retrofitting strategies for the enhancement of the energy performance of existing buildings.

I.4 Thesis outline

Fig. I.2 sketches the content of this thesis. Part A comprises Chapters II to IV. In Chapter II some fundamentals of the heat transfer with solid–liquid phase-change are presented. In Chapter III, an experimental setup is presented to evaluate the heat transfer with solid–liquid phase-change through a small TES unit. In Chapter IV, a parametric analysis is carried out to evaluate the influence of the configuration of the TES unit, the impact of the imposed boundary conditions during the experiments, and the influence of the type of PCM on the thermal performance of the TES unit. Part B comprises Chapters V to VII. In Chapter V, a literature review on different passive TES systems for buildings is provided. In Chapter VI, a methodology for the optimization of the incorporation of PCM-drywalls in low-rise LSF residential buildings in different European climates is presented. In Chapter VII, a parametric study is carried out to evaluate how PCM-drywalls can be used to reduce cooling energy demand and peak-loads in low-rise residential heavyweight buildings in Kuwait. The final remarks and conclusion are given in Chapter VIII.

To sum up, in Part A it is experimentally shown that natural convection and subcooling can be neglected when studying the heat transfer with the microencapsulated PCM. This supports the use of the EnergyPlus PCM-model in the DSEB addressed in Part B.

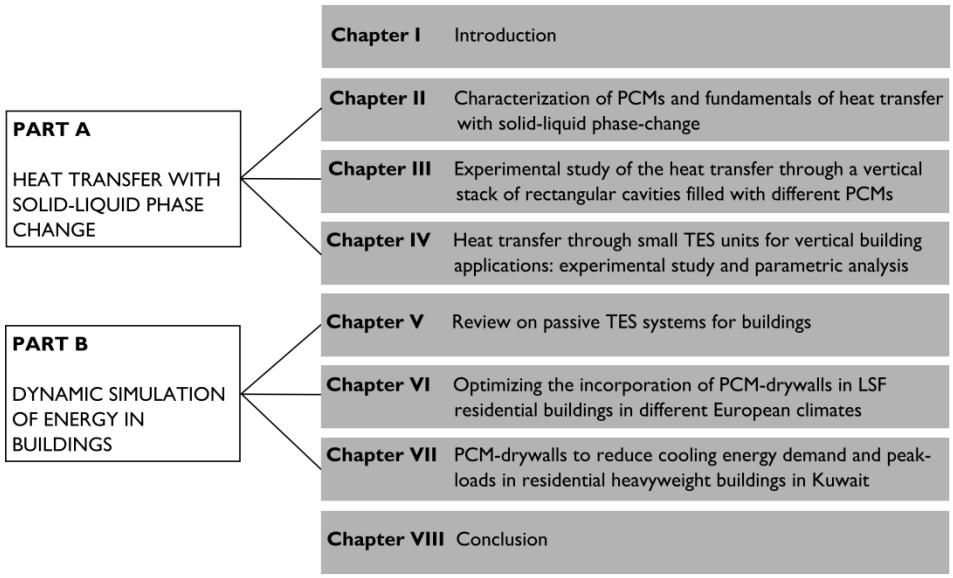

Fig. I.2 Thesis outline.

PART A

HEAT TRANSFER WITH SOLID–LIQUID PHASE-CHANGE

Chapter II

Characterization of PCMs and fundamentals of heat transfer with solid–liquid phase-change

This chapter introduces the different types of PCMs and the main criteria for their selection, and some techniques to incorporate PCMs into construction elements. The basic thermodynamics of TES in buildings and the most important fundamentals of the heat transfer with solid–liquid phase-change are also discussed in this chapter. The main thermophysical properties of PCMs are discussed as they are the basis for the development and design of new TES systems. The numerical modeling of the heat transfer with solid–liquid phase-change and some heat transfer enhanced techniques are also discussed. This chapter summarizes part of the literature review which has been published in the paper "*Review of passive PCM latent heat thermal energy storage systems towards buildings' energy efficiency*" by Soares *et al.* [1]. Chapter II is divided into four sections. Section II.1 introduces different types of PCMs and provides a description of the basic requirements for a material to be used as a PCM. The different types of PCMs are then compared with respect to their most important properties, advantages and disadvantages. Section II.2 presents the main methods for incorporating PCMs in construction elements avoiding liquid leakage. Section II.3 introduces some methods to measure the main thermophysical properties of PCMs. Section II.4 discusses the modeling of solid–liquid phase-change.

II.1 Phase change materials (PCMs)

II.1.1 Definition of PCM

In Chapter I, the principle of phase-change and the way PCMs work were introduced. From a hot-topic and mediatic point of view, solid–liquid PCMs have recently been "rediscovered" and applied to a wide range of technologies, including those related to buildings. However, the incorporation of PCMs in construction elements is not new in the literature and has been the subject of study for many decades. In the past, the term PCM was frequently replaced by the name of the material itself, and the use of the term PCM alone was not widespread. Nowadays, this terminology is used to cover a wide range of materials for many applications, appearing almost as a kind of labeling, and in this way immediately linking the research or the commercial product to TES applications. In their work, Hyun *et al.* [84] state that "*the nebulous term phase-change material (PCM) simply refers to any substance that has a large heat of fusion and a sharp melting point*". This cleaver definition demystifies the PCM terminology. It also enables to highlight the importance of matching the phase-change temperature range of the PCM with each specific application, in order to take advantage of the latent heat involved in the solid–liquid phase-change processes.

II.1.2 Types of PCMs and main criteria for their selection

Ideally, materials to be used in phase-change TES systems should have a melting/solidification temperature in the practical range of application and they must have a high latent heat of fusion and a high thermal conductivity. Moreover, to be used in the design of TES systems, PCMs should have desirable thermophysical, kinetic, chemical and economic properties as suggested by many authors [11,14,21,22,25,28,52,62]. PCMs should also have desirable environmental properties to decrease the environmental impact of the TES systems during their lifecycle. The main criteria for the selection of PCMs are summarized in Table II.1.

Table II.1 Main criteria that govern the selection of PCMs.

Thermal and physical properties	– Suitable phase-change temperature in the desired operating temperature range; – high thermal conductivity; – high latent heat of phase transition per unit mass; – high specific heat and high density; – congruent melting and long term thermal stability; – favourable phase equilibrium and no segregation; – small volume variation on phase-change; – small vapour pressure at operating temperature.
Kinetic properties	– High nucleation rate and little or no supercooling of the liquid phase; – high rate of crystallization.
Chemical properties	– Completely reversible melting/solidification cycles; – long term chemical stability and no degradation after a large number of melting/solidification cycles; – no corrosiveness and capability with construction materials; – nontoxic, non-flammable and non-explosive.
Economic properties	– Abundant and available; – cost-effective.
Environmental properties	– Low embodied energy; – separation facility from the other materials and recycling potential; – low environmental impact and non-polluting.

PCMs are mainly classified as organic, inorganic and eutectic. Organic PCMs are further described as paraffins and non-paraffins. The non-paraffins include a wide selection of organic materials such as fatty acids, esters, alcohols and glycols [52]. Of most interest in this group are the fatty acids which are subdivided into six groups: caprylic, capric, lauric, myristic, palmitic and stearic [52]. An update on the developments in organic solid–liquid PCMs and their application in TES systems was recently reviewed by Sharma *et al.* [16]. Inorganic PCMs are further described as hydrated salts and metallics (metals have too high melting temperatures for passive building applications). A eutectic is a composition of two or more components, each of which melts and solidifies congruently forming a mixture of the component crystals during crystallization [21].

Eutectic PCMs are subdivided into organic-organic, organic-inorganic and inorganic-inorganic. Several authors have presented a comparison of the advantages and disadvantages of the different types of PCMs [10–12,14,21,22,24,25,31,53,66,85]. The main advantages and disadvantages of each type are compared and summarized in Table II.2. In this thesis, commercial paraffin waxes (organic PCMs) will be used.

Table II.2 Comparison between different types of PCMs: advantages and disadvantages [10–12,14,21,22,24,25,31,53,66,85].

Classification	Advantages	Disadvantages
Organic: Paraffins and non-paraffins	– Availability in a large temperature range; – high latent heat of fusion (fatty acids have high heat of fusion values comparable to that of paraffins [11]); – solidification with little or no subcooling; – congruent phase-change; – self-nucleation properties; – no segregation and good nucleation rate; – predictable and thermally and chemically stable, *i.e.* good stability of material properties during repeated thermal cycles; – low vapour pressure in the melted form; – not dangerous, non-reactive and non-corrosive (fatty acids could be milddly corrosive [11]); – compatibility with conventional construction materials; – recyclable.	– Low thermal conductivity; – lower volumetric latent heat storage capacity, *i.e.* lower phase-change enthalpy; – lower density; – flammable (possible to use fire-retardant additives [86]); – non-compatibility with plastic containers; – more expensive (commercial paraffins are cheaper and more available than pure paraffins and fatty acids are 2–2.5 times more expensive than technical grade paraffins [11]); – relatively large volume change (however some fatty acids could undergo small volume changes [52]).
Inorganic: Hydrated salts	– Higher volumetric latent heat storage capacity, *i.e.* higher melting enthalpy; – higher latent heat of fusion ; – low cost and readily available; – sharper phase-change; – higher thermal conductivity; – non-flammable; – lower volume change; – compatible with plastics; – it is better to use salt hydrates than paraffins to reduce the manufacturing/disposal environmental impact [87].	– Poor nucleating properties and subcooling problems; – incongruent melting and dehydration in the process of thermal cycling; – phase segregation during transition and thermal stability problems; – their application could require the use of some nucleating and thickening agents; – decomposition and phase separation; – non-compatible with some construction materials; – corrosive to most metals and slightly toxic.
Eutectic	– Sharp melting temperature (could be used to deliver the desired melting temperature required); – volumetric thermal storage density slightly above organic compounds; – no segregation and congruent phase-change [11].	– Limited data are available on their thermophysical properties; – some fatty eutectics have quite strong odour and therefore they are not recommended for use in PCM-wallboards [22].

II.1.3 Main thermophysical properties of PCMs

Fig. II.1 shows the main potential fields of application of PCMs in TES applications: temperature control and storage/release of heat with high storage density and small temperature change. Fig. II.1 shows that the latent heat can be stored without a significant change of the temperature of the

material (read on the temperature axis); that is why PCMs can be used for temperature control of TES applications. On the other hand, the figure also shows that PCMs are able to store large amounts of heat (due to latent heat) at a small temperature change as the phase-change processes occurs within a limited phase-change temperature range (read on the stored heat axis). These two features will be studied in more detail in Chapters III and IV, when evaluating the thermal behavior of small TES units filled with PCMs for TES applications. It should be pointed out that the behavior of common PCMs is slightly different from that of ideal PCMs. In common PCMs, as shown in Fig. II.1, the ideal melting-peak temperature of the isothermal phase-change process of pure PCMs, T_{mp}, is replaced by a phase-change melting temperature range, ΔT_{m}.

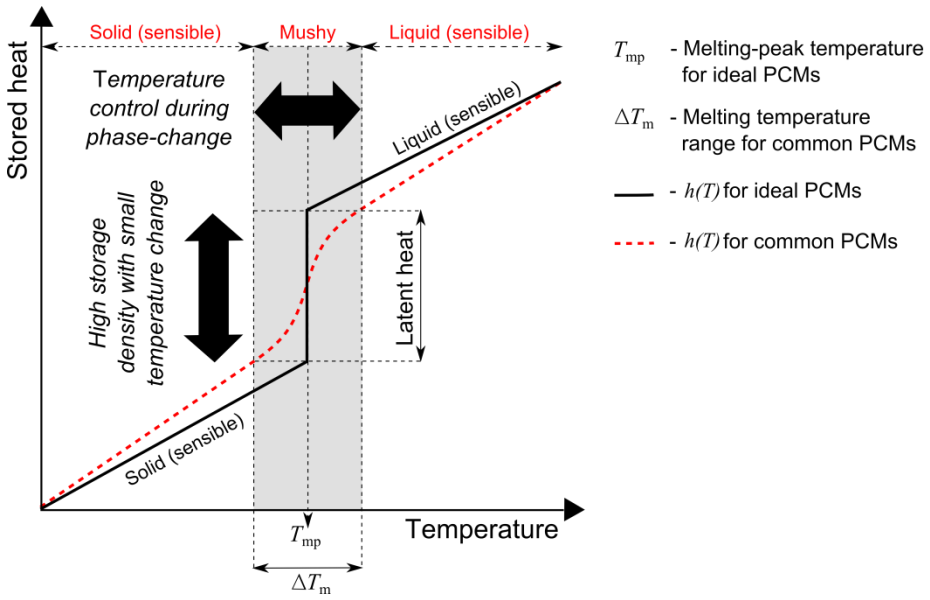

Fig. II.1 Potential fields of application of PCMs: (*i*) temperature control and (*ii*) storage and supply of heat with high storage density and small temperature change.

The storage capacity of an ideal PCM can be characterized via four main parameters, namely the heat capacity of the solid and liquid phases, the latent heat of fusion and the melting-peak temperature. However, for common PCMs, more than specifying these variables, the enthalpy-temperature curve $h(T)$ should be provided, as it describes the material with much more precision. Therefore, the enthalpy-temperature relationship $h(T)$ is one of the most important properties of PCMs as it includes many information about the phase-change processes.

In ideal situations, the enthalpy-temperature curve $h(T)$ should be equal during the reversible charging (melting) and discharging (solidification) cycles. However, the $h(T)$ curve could be influenced by other phenomena such as subcooling, hysteresis and cycling stability. Fig. II.2 shows the temperature variation during melting and solidification of an ideal PCM with subcooling. When

subcooling (also called supercooling) is verified, a temperature significantly below the solidifying temperature of the PCM has to be reached to start crystallization and to release the latent heat stored in the material. As remarked by Mehling and Cabeza [88], if the heat released upon solidification is larger than the sensible heat lost due to subcooling, the temperature rises again to the solidifying temperature of the PCM, T_{sp}, which ideally should be equal to T_{mp}. However, if this does not happen, or if the rate of heat lost to the ambient is larger than the rate of heat released during crystallization, the temperature will not rise to the solidifying temperature again, and a real hysteresis will be caused by subcooling. Therefore, subcooling can cause negative effects when performing dynamic experiments, and it can be a serious problem in technical applications of PCMs. Subcooling can depend on the size of the PCM sample and also on the type and shape of the container used in a macro-scale approach.

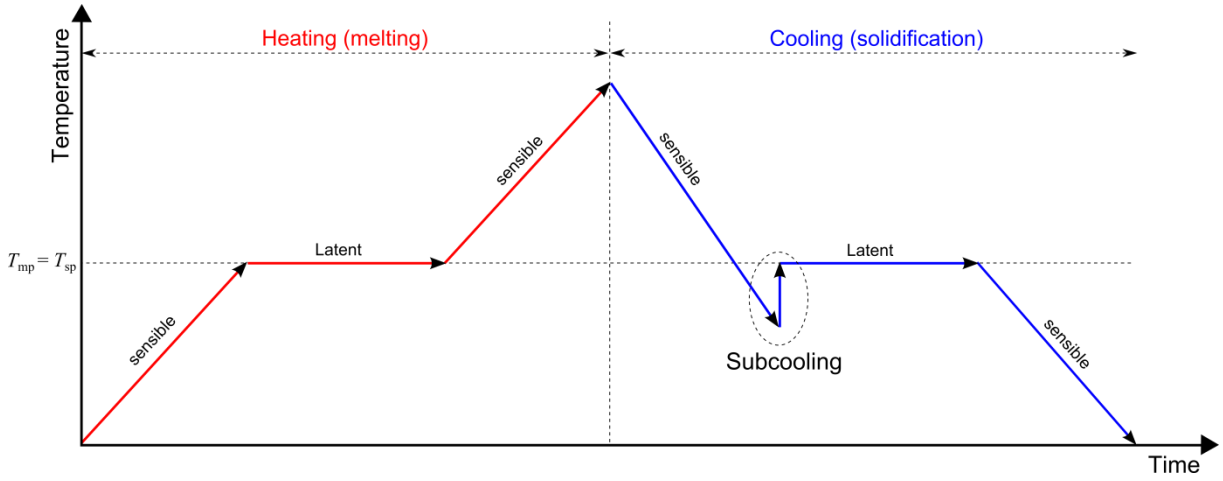

Fig. II.2 Sketch of the evolution of temperature during charging (melting) and discharging (solidification) processes of an ideal PCM with subcooling.

Regarding hysteresis, it started to be understood as a property of the PCM-based sample. However, it can be caused by the measurement conditions (mainly in calorimetry experiments as PCMs have a high heat storage density in a small temperature range). In this case, it is called apparent hysteresis [88]. Fig. II.3 shows different causes that can lead to hysteresis. Due to hysteresis, there are typically different data from charging and discharging experiments. Therefore, the results must be provided for both heating and cooling experiments.

Another aspect to take into account when dealing with the heat transfer with solid–liquid phase-change, is the effect of natural convection in the molten PCM as it is one of the major factors that affect phase transition processes [89]. In Chapters III and IV, the effects of subcooling, hysteresis

and natural convection will be evaluated in more detail, considering small TES units filled with PCMs for building applications.

Regarding the cycling stability of PCMs, PCM-composites and PCM-based elements, one of the main problems is the phase separation. PCMs must show a reproducible phase-change in order to maintain the heat storage capacity required for a designed application. It should be remarked that a PCM that shows phase separation will show a reduction of the melting enthalpy after repeated cycling [88]. For PCM-based elements, cycling stability can also refer to the capacity to avoid liquid leakage after repeated melting and solidification cycles. A recent review on the thermal stability of PCMs used in TES systems was carried out by Rathod and Banerjee [27].

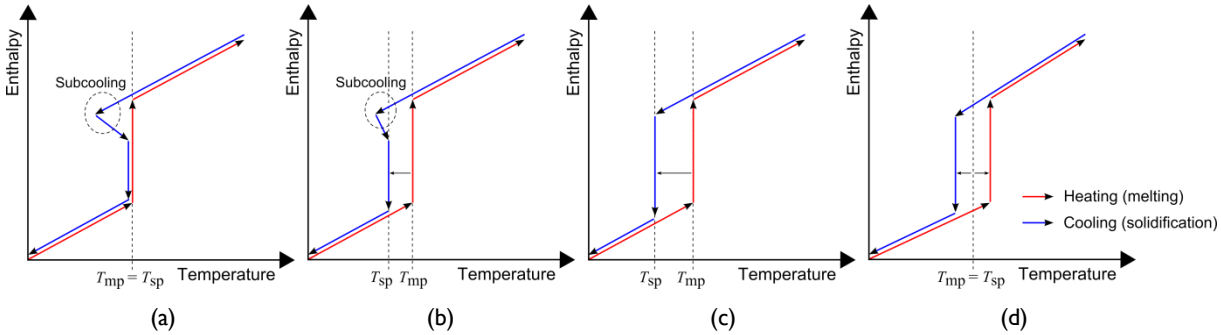

Fig. II.3 Real hysteresis as a material property caused by subcooling when: (a) the temperature rises again to the solidifying temperature of the PCM; (b) the temperature does not rise again to the solidifying temperature of the PCM. (c) Real hysteresis caused by slow heat release or a real difference between the phase-change temperatures. (d) Apparent hysteresis caused by non-isothermal conditions in the measurements.

Finally, PCMs and PCM-based composites should have a good thermal conductivity to improve the storage and release of latent heat in a given volume of the material in a short period. As PCMs have typically low thermal conductivity, some strategies can be used to improve this feature. This feature will be discussed below.

II.2 Construction materials with PCMs

II.2.1 Incorporation of PCMs in construction elements to avoid liquid leakage

Once the PCMs have been selected, based primarily on the temperature range of application and on their thermophysical properties, it is important to evaluate how they could be incorporated within passive TES systems (construction materials or building elements) to prevent liquid leakage during the liquid phase. Hawes *et al.* [90] considered the direct incorporation, the immersion and the

encapsulation to be the three most promising methods of incorporating PCMs in conventional construction materials. Additionally, PCMs can also be used in the form of shape-stabilized PCMs (SSPCMs).

Both direct incorporation and immersion methods integrate PCMs directly in conventional construction materials. The first method is the simplest and cheapest one. The liquid or powdered PCM is directly mixed with the construction material (such as gypsum, concrete or plaster) during production [25,31] and no extra equipment is required. However, some problems of leakage and eventual incompatibility with some materials may occur. In the immersion method, the porous material, such as gypsum boards, bricks or concrete blocks, is immersed into the melted PCM absorbing it by capillary action. The same problems of long-term leakage and eventual interaction with some building structures may be pointed out [91].

PCMs can be encapsulated before incorporation into construction elements. As stated by Regin *et al.* [30], the PCM containment should (i) meet the requirements of strength, flexibility, corrosion resistance and thermal stability; (ii) act as a barrier to protect the PCM from harmful interaction with the environment; (iii) provide sufficient surface for heat transfer, and (iv) provide structural stability and easy handling. As mentioned before, two types of encapsulation can be defined: the microencapsulation and the macroencapsulation.

Tyagi *et al.* [34] defined the former technique as the process by which individual particles or droplets of solid or liquid material (the core) are surrounded or coated with a continuous film of polymeric material (the shell) to produce capsules in the micrometer to millimeter size range, known as microcapsules. As suggested by these authors [34], microencapsulation prevents leakage during the liquid phase, which contributes to greatly expand the possibilities of integrating PCMs in construction materials such as gypsum [92], cement mortars [93–96], lime [97], concrete [95,98], artificial marble, sealants, paints, textiles and other coatings. Several physical and chemical methods have been developed for the production of microcapsules: pan coating, air-suspension coating, centrifugal extrusion, vibrational nozzle, spray drying, interfacial polymerization, *in situ* polymerization and matrix polymerization [34,99]. Some authors concluded that the microencapsulation technique could also contribute to improve heat transfer by increasing the heat exchange surface [21] and to control the volume variations during phase-change [12]. Khudhair and Farid [54] noted that the microencapsulation technique may affect the mechanical strength of some construction materials and other authors pointed out some supercooling problems [100]. A recent update on the microencapsulation methods of PCMs as a TES medium was reviewed by Jamekhorshid *et al.* [37].

The macroencapsulation is the technique in which PCMs are packaged in a container, such as tubes, spheres, panels, or other receptacles, and then incorporated into TES systems. The

macrocapsules must be designed to fit well the intended application. The thermal and geometric parameters of the container required for a given amount of PCM have a direct influence on the heat transfer characteristics and affect the melting time and the performance of the PCM-based TES element [28]. Hence, the container should be optimized to increase the heat transfer rate during the phase-change processes and to avoid loss of material, corrosion and PCMs' changes in volume problems. With macroencapsulation, the function of the construction structure can be less affected and the encapsulation can help to overcome some flammability problems of PCMs. However, it may have the disadvantages of poor thermal conductivity and tendency for solidification at the edges [25].

In recent years, a new kind of compound PCM, the so-called shape-stabilized PCMs (SSPCMs) or form-stable composite PCMs, has been attracting the interest of many researchers [101–110] due to their high apparent specific heat, suitable thermal conductivity, the ability to keep the shape of the PCM-board stabilized during phase-change processes, and a good performance of long-term multiple thermal cycles [25]. In this technique, the PCM (like paraffin) is dispersed in another phase of supporting material (like high-density polyethylene) to form a stable composite material [25]. Since the mass percentage of paraffin can be as much as 80%, the total energy is comparable to that of the PCM itself [101]. Some applications of SSPCMs in building walls, ceilings and floors have been studied by many authors [111–119] showing that the interest in this new kind of materials is rising. Other studies have been devoted to the preparation and characterization of different SSPCMs such as the works carried out by Cao *et al.* [120], Memon *et al.* [121], Chung *et al.* [122] and Wang *et al.* [123]. The development of new nano-PCM based form-stable composites is also an active area of research. Sayyar *et al.* [124] recently proposed a gypsum wallboard incorporated with nano-PCMs. In this wallboards, the fatty acids were supported by graphite interconnected nanosheets to form a shape-stable nano-PCM composite. These authors carried out a numerical study to evaluate the contribution of this TES system in the energy performance of a designed test cell. The authors found that the incorporation of nano-PCM into wallboards can reduce the energy demand for maintaining the indoor temperature within the comfort zone by 79%. A recent update on the preparation, thermal properties and applications of SSPCMs can be found in the review paper by Fang *et al.* [41].

All the techniques described above deal with the solid–liquid phase-change of PCMs. However, Whitman *et al.* [125] proposed a solid–solid PCM, for potential integration in buildings. Solid–solid PCMs may have some advantages for building applications mainly those related with liquid leakage and volume expansion problems of solid–liquid PCMs.

II.2.2 Heat transfer enhancement techniques

PCMs have typically low thermal conductivity leading to inadequate heat transfer and slow charging and discharging rates. Hence, heat transfer enhancement techniques are required for most PCM-based passive TES applications. Several techniques have been proposed for different applications with PCMs such as: (*i*) the dispersion of high conductivity particles in the PCM (e.g. Cu, Al, graphite, etc.) [107,108,126,127]; (*ii*) the impregnation of high conductivity porous material with the PCM (e.g. graphite matrix [128–134] or metal foams [128,135–141]); (*iii*) inserting fibrous materials like carbon fibers [142–149]; (*iv*) microencapsulation to enhance the heat transfer surface [99,150,151], and (*v*) placing of structures of high conductivity materials in the PCM bulk (e.g. metal fins to enhance the heat transfer rate) [152–160]. The use of TES units with metallic fins to improve the heat transfer to the PCM-bulk by conduction will be studied in more detail in Chapters III and IV.

In many passive TES systems, the PCM is not in direct contact with the main heat source (for example the solar radiation) nor with the indoors environment. During winter, a reduction of the heat transfer rate and a delay in the heat transfer process should be avoided to take advantage of solar thermal energy for heating. The color and the thermal conductivity of the finishing material of the TES system could enhance the heat transfer rate [161], absorbing a greater fraction of solar radiation and transferring more heat to the PCM by conduction. During summer, adequate solar protection and night ventilation techniques are the most basic strategies to make passive TES systems work properly (reducing the energy demand for cooling). In most cases, as pointed out by Rodriguez-Ubinas *et al.* [66], with the integration of some low consumption devices, it is also possible to accelerate the heat exchange across the surface of the PCM (by convection) and help to complete their charging-discharging cycles. As it was concluded by Koo *et al.* [162], the convective heat transfer coefficient influences the thermal heat storage capacity of a PCM-wallboard, the time shift and the optimal average melting-peak temperature. Najjar and Hasan [163] concluded that PCMs can be used in a greenhouse for reducing the maximum air temperature difference by 3–5 °C during 24 h. This narrowing of the temperature fluctuation can be further improved by enhancing the convection heat transfer between the TES system and the air inside the greenhouse. David *et al.* [164] developed a numerical model to evaluate several convective heat transfer correlations from the literature for natural, mixed and forced convection flows. The results showed that the convective heat transfer highly influences the storage/release processes in the case of PCM-walls.

II.3 Methods to measure the main thermophysical properties of PCMs

II.3.1 Thermal characterization and enthalpy-temperature curve

The thermal performance of a passive TES system is directly related to the thermophysical properties of the chosen PCM. If a new system is to be developed or optimized, the thermophysical properties of the PCM must be known *a priori*. However, the product datasheet of the majority of commercial PCMs does not specify the thermophysical properties of both solid and liquid phases, which are crucial for modeling. Moreover, data provided by the PCM manufacturers could be erroneous, uncertain and overoptimistic [21]. This inconsistency is stated and measured by several authors [165,166].

When an effort is carried out to match experimental and numerical results many uncertainties related to the measurements and several numerical errors have to be considered. This is not easy to accomplish in standard thermal analysis, but it is even harder to do when a material changes its phase in time with the variation of temperature. Therefore, the characterization of PCMs and PCM-composites is essential to provide reliable data for modeling. This is a challenging task considering conventional equipments and methods, which are commonly designed to test solid or liquid materials. Moreover, the majority of techniques is designed to test small, pure and homogeneous materials which typically do not exhibit subcooling, hysteresis, significant variation of the thermal conductivity with temperature and temperature change during their solid–liquid phase-change processes. Since most of the commercial PCMs to be used in construction elements are not pure (as pure substances are very expensive), the uncertainty of the measurements for characterizing PCMs is an active area of research. Cabeza *et al.* [23] reviewed the conventional and unconventional technologies available for the thermophysical characterization of PCMs, describing different equipments and techniques to evaluate the main properties of PCMs, namely the specific heat, the latent heat of fusion, the melting/solidification temperature and the enthalpy–temperature curve, and the thermal conductivity and diffusivity of the materials. Nowadays, the techniques most commonly used to determine the thermal properties of PCMs are the conventional Differential Scanning Calorimetry (DSC) and the T-history method.

The latent heat of fusion, the specific heat capacity and the melting/solidification temperature of PCMs can be obtained by using conventional DSC techniques [25]. Generally speaking, DSC experiments allow to measure the quantity of heat that can be absorbed or released by a body subjected to a change of temperature (heat transfer by conduction), in which the difference in the amount of heat required to increase the temperature of two different samples in identical conditions (the test sample and a reference one which properties are known) is measured as a function of temperature. The thermal reaction of the sample to be characterized is then compared with the

thermal reaction of the reference sample [24]. The most commonly used DSC methods are the dynamic and the step methods. In the first one, the heating and cooling are continuous while in the latter the heating and cooling are not continuous, and small heating/cooling ramps are followed by periods in which the temperature is kept constant to allow the sample reaching thermal equilibrium, as explained by Cabeza *et al.* [23]. Barreneche *et al.* [167] investigated the most appropriate DSC operation method for the characterization of the two most common PCMs – paraffins and hydrated salts. Castellón *et al.* [168] also evaluated the accuracy of both DSC methods (dynamic and step methods) in the determination of the enthalpy-temperature relationship of the commercial paraffin PCM – RT 27. More detailed information about these two methods can be found in refs. [23,88,169].

The traditional DSC measurements require three experiments – for baseline, calibration and sample analysis – in order to determine the specific heat capacity as a function of temperature $c_p(T)$. Therefore, this method is complex, expensive and very time-consuming, mainly when testing PCMs since the heating/cooling rates have to be very small. From the curve $c_p(T)$, the storage capacity $h(T)$ can be calculated by integration over T. As discussed by Dumas *et al.* [170], the enthalpy-temperature relationship $h(T)$ is one of the most important properties of PCMs as, in the buildings field, this curve is many times required to generate transient thermal simulations in some software programs (as the *EnergyPlus* to be used in Chapters VI and VII) and to describe the thermal behavior of different parts of a modeled structure. However, the literature shows that measurements using conventional DSC techniques are usually not suitable to determine $h(T)$ of PCMs as the results are very influenced by the heating/cooling rates and the mass of the sample. The T-history method is preferable to determine this curve with sufficient precision as described in ref. [23]. In short, the main limitations of conventional DSC measurements are: (i) some heat transfer phenomena are omitted, such as the convection in the sample, the non-uniformity of the temperature in the sample and the time needed to heat or cool the sample (inertia) [24]; (ii) only small quantities of the material are analyzed, although the equivalent heat capacity calculated using the DSC curves is clearly influenced by the sample mass and heating rate [88,171]; (iii) the analysis instrumentation is complex, time-consuming and expensive and the phase-change cannot be visually observed [10]. Kuznik and Virgone [172] stated that the DSC results can be used to show the difference between the melting and the solidification temperatures which characterizes the hysteresis of the PCM. However, it should be pointed out that, for several authors, this hysteresis may be caused by the measurement conditions as explained in Section II.1.3. Lazaro *et al.* [173] carried out a set of Round Robin Tests to compare the results of different DSC measurements performed by different institutions and considering the same reference material. These authors showed that $h(T)$ curves determined by using a dynamic DSC method can be influenced by several aspects and they proposed a methodology to avoid their influence.

DSC analysis was used in several studies to evaluate the thermal characteristics of PCMs [165,166,174–178] as well as PCM-composites with other materials [175,179–181]. Sittisart and Farid [86] also used DSC results to show that the addition of fire retardants into a form-stable PCM (for reducing its flammability) had little effect on the latent heat value and did not change its thermal properties significantly. Sari-Bey *et al.* [182] have used DSC measurements for the thermophysical characterization of polymer matrix composites containing microencapsulated PCM – Polycaprolactone/Micronal® DS 5001 X composites. The measurements were carried out for different concentrations at different temperatures. Sharma *et al.* [183] prepared new eutectic materials as novel form-stable PCMs for TES applications in buildings. These new materials were characterized by using DSC measurements and the DSC results showed that only a few eutectics were found satisfactory for building applications regarding their composition, desired temperature range and latent heat of fusion. Eddhahak-Ouni *et al.* [184] evaluated the specific heat capacity of Portland cement concretes embedded with the microencapsulated PCM – Micronal® DS 5001 X by using DSC measurements while Sari [185] used DSC measurements to evaluate the latent heat storage properties of kaolin-based composite PCMs for building applications fabricated using vacuum impregnation method.

In Chapter III, the Modulated DSC (MDSC) method will be used to provide an easier, faster and cheaper way to measure the specific heat capacity of PCMs. The MDSC from TA Instruments (Q100 model) installed in the Chemical Engineering Department of the University of Coimbra was used to determine the specific heat (of both solid and liquid phases), the latent heat and the melting/solidifying temperature of different PCMs (free-form and microencapsulated PCMs). It should be pointed out that the MDSC method has seldom been used for the characterization of PCMs. Borreguero *et al.* [186] used the MDSC method for obtaining an apparent heat capacity dependent on temperature to be used in the developed one-dimensional mathematical model based on the Fourier heat conduction equation. Regarding the definition of $h(T)$ curves of PCMs by using the MDSC method, further research has to be carried out, since some problems are verified during phase-change. A methodology to determine the $h(T)$ curve of PCMs with sufficient accuracy using the MDSC method has never been proposed before. Therefore, interlaboratory comparison using different techniques will be required to guarantee the precision and accuracy of this method.

More techniques for measuring the $h(T)$ curve of PCMs are presented by Cabeza *et al.* [23] namely the twin-bath method proposed by Paksoy [187] and the energy balance setup designed at the University of Zaragoza and described in ref. [129]. This method is particularly interesting for PCM-composite samples, which are bigger than those typically employed in the T-history method.

The T-history method proposed by Zhang and Jiang [188] is a simple method for determining the melting-peak temperature, heat of fusion, specific heat and thermal conductivity of PCMs. This

method is based on an air enclosure where temperature is maintained constant, and two samples which are introduced at a different temperature: the PCM sample and the reference sample (usually pure water). During the heating and cooling experiments, the temperature evolutions of both the air enclosure and the two samples are measured. Temperature-time curves of the PCM samples are drawn and their thermophysical properties are obtained by comparing the curves with the temperature-time curve of the other material taken as a reference [31]. Compared with other methods, such as conventional calorimetry methods (DSC and DTA), the T-history method has the following features: (i) it has been designed to test large samples [24], (ii) the experimental setup is simpler, (iii) it is able to measure different thermophysical properties of several samples of PCMs simultaneously, and (iv) it allows one to observe the phase-change process of each PCM sample [188]. Zhang and Jiang [188] measured the thermophysical properties of several PCMs using the T-history method and they found a desirable agreement between their results and data available in the literature. Hasan *et al.* [189] also used the T-history and DSC methods for characterizing PCMs for thermal control of photovoltaics. The T-history method has been improved by several authors [190–192]. For example, Marín *et al.* [190] made some improvements based on a method of finite increments to obtain the $h(T)$ curve of PCMs using the T-history method. Moreover, these authors used the $h(T)$ curves of PCMs for studying other properties such as subcooling and hysteresis. Lázaro *et al.* [193] also provided more information about the T-history method to measure $h(T)$ curves of PCMs. A deeper understanding of the T-history method is provided in the review article by Solé *et al.* [194]. Several studies, such as the ones carried out by Gunther *et al.* [169] and Rathgeber *et al.* [195], were also devoted to the assessment of the more suitable methods and the required accuracy of the measurements when determining the enthalpy of PCMs as a function of temperature via DSC and T-history methods.

The DTA technique is an alternative method to DSC measurements in which the heat applied to the sample and the reference remains the same [25]. DSC measures the energy required to keep both the sample and the reference sample at the same temperature, while DTA measures the difference in temperature between the sample and the reference sample when they are both subjected to the same heat.

The methods described above are typically used for the thermal characterization of small-scale samples. Therefore, problems arise when the thermal characterization of large-scale PCM-composite samples are required, as construction materials with PCMs often behave differently compared to the PCM itself. Several experimental setups for measuring the main thermophysical properties of large-scale test-samples are found in the literature. Barreneche *et al.* [196] developed two devices to determine the effective thermal conductivity of construction materials with PCMs and the temperature-time response curves. The large-scale test-samples (0.3 m × 0.3 m × 0.3 m) have a

gypsum or Portland cement matrix which incorporates 5 wt% and 15 wt% of a microencapsulated PCM – Micronal® DS 5001. Another setup for testing the steady and the transient thermal performance of large-scale test-samples with PCMs was proposed by de Gracia *et al.* [197]. The experimental setup was used to calculate the thermal transmittance and the heat storage capacity of the test-sample and to evaluate the dynamic thermal response of the test-sample under daily temperature oscillation. Recently, an inter-laboratory study was carried out by Barreneche *et al.* [198] to compare the performance and feasibility of some experimental setups such as the ones presented in refs. [186,196,197]. The three experimental setups were used to measure the effective thermal conductivity, the total amount of heat accumulated, and the specific heat of large-scale test-samples. Three kinds of gypsum blocks with PCMs were used as test-samples: blocks incorporating the microencapsulated PCM – Micronal® DS 5001, blocks with a suspension of water/PCM, and gypsum blocks with the impregnated PCM – RT 21. The results obtained with the different experimental setups were compared and the inter-laboratory study showed that the results are relatively consistent with each other. Karkri *et al.* [110] used a transient guarded hot-plate setup to evaluate the overall thermophysical properties (e.g. heat capacity and latent heat) of 48 mm × 48 mm × 4.8 mm SSPCMs test-samples with different compositions while the periodic temperature method was used to determine the thermal conductivity and thermal diffusivity of the materials. Mandilaras *et al.* [199] proposed a hybrid methodology for the evaluation of the effective heat capacity of a SSPCM attached to an insulation panel. The thermal response of the test-sample was measured by using a dynamic operated heat flow meter apparatus, providing different boundary conditions in two test cases: the first one was used to define and optimize the artificial effective heat capacity curves; the second one was used to validate the results. Another experimental methodology to evaluate the storage properties of large-scale PCM-wallboards samples was proposed by Eddhahak-Ouni *et al.* [200].

To evaluate the thermal reliability of construction materials with PCMs, accelerated thermal cycle tests and melting-solidification performance tests can be performed. Considering previous research, the number of cycles must be large enough, since the lifetime of components are decades long for building applications. Dutil *et al.* [51] suggest that 5000 thermal cycles are suitable for building applications. Harikrishnan *et al.* [201] also pointed out that it is very important to find the optimum number of thermal cyclic operation of PCM-composites in order to predict the life time of the effective use of the materials in TES applications for buildings. In their study, these authors estimated an average life cycle of about 13–14 years for PCM-composites by considering 5000 thermal cyclic operation conditions. Sari [185] carried out 1000 melting-freezing cycles to evaluate the thermal reliability and chemical stability of three different kinds of kaolin-based composite PCMs. The thermal characteristic reliability of fatty acid binary mixtures as PCMs was evaluated by Fauzi *et*

al. [202] by using a thermal cycling test setup for 1000, 2000, 3000 and 3600 heating-cooling cycles. Another kind of study was carried out by Behzadi and Farid [203] to evaluate the potential changes with time in the thermal characteristics of organic PCMs when heated above their melting-peak temperature in order to evaluate the long term thermal stability of organic PCMs. Regarding the characterization of the morphology and structure of construction materials with PCMs, scanning electronic microscopy (SEM) and Fourier infrared spectroscopy (FTIR) methods are usually used. The SEM technology was used by several authors, like in the studies presented in refs. [110,182,184,185,204,205] while FTIR was used in refs. [185,202,206]. Further information about the methods used for the morphological and structural characterization of PCMs and PCM-based composites and to evaluate the physicochemical stability and mechanical properties of these materials can be found in the extensive review articles by Cabeza *et al.* [207] and Memon [19].

II.3.2 Thermal conductivity and thermal diffusivity

Many of the methods described in the previous section can be used to measure the thermal conductivity of construction materials with PCMs. There are also several commercial equipments for measuring the thermal conductivity of materials such as the Laser Flash (LFA), the UNITHERM 6000 Guarded Hot Plate setup and the C-THERM TCI™ Thermal Conductivity Analyzer. Further details about these experimental setups can be found in ref. [23].

Some authors [172,174,178] have used the guarded hot plate apparatus [208] to measure the thermal conductivity of PCMs. Jaworski and Abeid [209] also measured the thermal conductivity of gypsum-based composites incorporating microencapsulated PCMs using a miniature plate apparatus where the heat flows through the square cross-section sample, along with the measurement of the temperature difference between the two surfaces. Boudenne *et al.* [210] and Boudenne *et al.* [211] proposed a periodic method to determine simultaneously both thermal conductivity and diffusivity of various materials at room temperature and as a function of temperature. As described by Cabeza *et al.* [23], this method is based on the use of a small temperature modulation in a parallelepiped-shape test-sample, and allows obtaining all the thermophysical parameters in only one measurement with their corresponding statistical confidence bounds.

In the course of the work leading to this thesis, the Transient Plane Source (TPS) method was used to measure the thermal conductivity of different PCMs. The Hot Disk® thermal constants analyzer TPS 2500 S installed in the Chemical Engineering Department of the University of Coimbra was used to test solid, liquid and powder samples. Regarding free-form PCMs, the experiments were carried out in both solid and liquid phases and different sample holders were used in the

experiments. For the assessment of the thermal conductivity of microencapsulated PCMs only a powder sample holder was required. In the literature, there is a gap regarding the evaluation of the thermal conductivity of microencapsulated PCMs. Typically, the provided information refers to the thermal conductivity of the PCM itself or to the properties of the polymeric capsule used to enclose the PCM. The preliminary tests carried out showed that the thermal conductivity of these PCMs depends on compaction. Moreover, the measured values showed to be lower than those typically specified in the literature. Hence, the variation of the thermal conductivity of microencapsulated PCMs with the level of compaction must be evaluated. Another challenge to accomplish in the future is to determine the variation of the thermal conductivity of PCMs within a temperature range covering phase-change. In this case, the sample holders will be associated to a thermostatic bath and the experiments are to be repeated for several temperatures. Therefore, the knowledge of the variation of the thermal conductivity of PCMs obtained by an alternative way based on the TPS method may be seen as a future area of research. Other researchers have used the Hot Disk® thermal constants analyzer TPS 2500 S to measure the thermal conductivity of PCM-composites such as Eddhahak-Ouni *et al.* [184] and Zhang *et al.* [205].

Borreguero *et al.* [186] developed a home-made experimental setup to obtain the thermal conductivity of large-scale test-samples made of gypsum with different contents of a microencapsulated PCM. In a recent paper, Toppi and Mazzarella [92] proposed some experimental correlations to calculate the main properties of a gypsum based composite material with a microencapsulated PCM as a function of its composition, aimed at avoiding the need of measuring the thermal properties of the material each time its composition changes. These correlations may be very useful when choosing the composition of the material to obtain predefined required properties.

II.4 Modeling solid–liquid phase-change

As remarked by Verma *et al.* [49], the mathematical modeling of a PCM-based TES system can be used for the optimum selection of materials and to assist in the optimal design of the system. When the PCM undergoes phase-change, both solid and liquid phases are present. Therefore, the difficulty in solving numerically a solid–liquid phase-change problem is the presence of a moving boundary on which heat and mass balance conditions have to be met. Furthermore, it is also difficult due to the presence of other materials which do not change phase, and due to PCMs' inherent non-linear nature at the moving interface, for which the displacement rate is controlled by the latent heat lost or absorbed at the boundary [50], so that the position of the boundary is not known *a priori* and becomes part of the solution. Additionally, the two phases have different thermophysical properties [11]. In the literature, this solid–liquid interface boundary is known as the Stefan problem. Solutions

to phase-change problems include analytical and numerical solutions, using one-, two- or three-dimensional models to solve the energy equation, which could be formulated in various ways with the phase-change being accounted for in different representations [28]. Very few analytical solutions are available in closed form. They are mainly for the one-dimensional case of an infinite or semi-infinite region with simple initial boundary conditions, and constant thermal properties [50].

There are several techniques for solving the Stefan problem. In their work, Dutil *et al.* [50] made a detailed and comprehensive review on the mathematical modeling and simulation of TES with PCMs. These authors provided essential mathematical bases for numerical modeling using either first or second law approaches and fixed [212], moving or adaptative meshes. In the authors view, the second law models are intended to complement and not to replace the first law models. The first law models have some shortcomings because they do not consider the effect of time duration through which the heat is stored or retrieved, the temperature at which the heat is supplied, and the temperature of the surroundings. Second law models address those issues which lead to optimal designs and operations [50]. In general, a time variant mesh approach offers good accuracy but it is limited to simple problems and geometries, while the fixed mesh approach (in which the latent heat of fusion is usually absorbed into the material's specific heat or enthalpy) is much simpler in practical applications and multidimensional problems [11]. Dutil *et al.* [50] also collected the most recent works published on the field of numerical modeling of PCMs used in thermal storage applications, organized according to the geometry of the problem (cartesian/rectangular, spherical and cylindrical) and specific configurations or applications (packed beds, finned surfaces, porous and fibrous materials and slurries).

Phase-change problems are usually solved with finite-difference, finite-element, finite-volume or control-volume finite-element-based methods. Generally, two approaches are used: (i) the latent heat of fusion is artificially absorbed into the specific heat of the material (effective heat capacity formulation), or (ii) the latent heat of fusion is directly described by the enthalpy changes (enthalpy formulation). The latter formulation treats the enthalpy as the dependent variable in the energy conservation equation which is integrated by expressing the heat flow in terms of enthalpy [153,154]. It is noted that when the PCM is a pure substance, the phase-change occurs at a single temperature, while in the case of mixtures, alloys and impure materials the phase-change takes place over a temperature range, and there appears a mushy region between solid and liquid zones. For pure PCMs the only unknown variable is the melting-peak temperature, the enthalpy is a temperature dependent variable and the enthalpy method constructs the latent heat flow through the volume integration with the use of the enthalpy of the system [153,154,213–219]. For the non-pure PCMs the solution of the energy equation in terms of enthalpy typically requires the knowledge of the enthalpy-temperature functional dependency and the function relating the thermal conductivity and

the temperature [10]. The effective heat capacity formulation introduces the concept of an equivalent heat capacity, and considers the phase-change latent heat as a great quantity of heat in sensible form in the whole phase transition temperature interval [212,220]. As stated by Chen *et al.* [220] with this method, the phase-change heat transfer problem can be transformed into a "single-phase" non-linear conduction problem in the whole calculation region and the location of phase-change interface can be determined when the temperature distribution is gained.

Dutil *et al.* [50] pointed out the importance of stability and convergence of the numerical method used, and stressed the importance of validating the numerical results using appropriate experimental data (together with a suitable uncertainty analysis). Other active area of research is related to the evaluation of the effect of hysteresis and subcooling phenomena in the numerical results, as pointed out before.

CHAPTER III

Experimental study of the heat transfer through a vertical stack of rectangular cavities filled with different PCMs

This chapter presents the experimental setup developed in the Mechanical Engineering Department of the University of Coimbra to evaluate the heat transfer through a vertical stack of rectangular cavities filled with different PCMs: the free-form PCM – Rubitherm® RT 28 HC and the microencapsulated PCM – Micronal® DS 5001 X. The heat transfer through the small TES unit is experimentally analyzed in terms of both melting and solidification processes. This chapter provides data that are useful for benchmarking and validation of numerical models. In terms of practical applications, the main goals are to: (*i*) discuss which PCM type is better for specific building applications, and (*ii*) evaluate the influence of natural convection and subcooling phenomena during charging and discharging. Chapter III summarizes the results which have been published in the paper "*Experimental study of the heat transfer through a vertical stack of rectangular cavities filled with phase change materials*" by Soares *et al.* [221]. This chapter is divided into five sections. Section III.1 introduces the problem and provides the background literature review. Section III.2 describes the experimental setup developed, the instrumentation and the experimental procedure. The description of the TES unit and the thermophysical characterization of the PCMs under investigation is also provided in Section III.2. Section III.3 presents and discusses the results achieved for both charging and discharging phases. Section III.4 provides the final remarks. In Section III.5, the main conclusions are provided. Chapter III introduces the experimental setup and procedures that will be used in the parametric study described in Chapter IV for evaluating the influence of the configuration of the TES unit and the influence of the imposed boundary conditions on the heat transfer processes.

III.1 Introduction

It is known by now that commercial paraffin waxes to be used as PCMs in passive TES applications for buildings have typically low thermal conductivity (~ 0.2 W m^{-1} K^{-1}), which can be problematic regarding the energy performance of these elements. The incorporation of fins of high-conductivity material within rectangular macrocapsules containing PCMs has been one of the techniques used to improve the heat transfer through the PCM bulk. These TES units can then be integrated in PCM-enhanced vertical envelope solutions such as PCM-bricks [222,223], PCM-concrete walls [224], PCM-shutters [153,154,225], PCM-window blinds [226–229], ventilated facades [230] and PCM-panels [231]. They can also be used to take advantage of the off-peak electrical energy for indoor heating [213], to serve as vertical heat sinks [232] and to passively improve the energy performance of photovoltaics (PV/PCM systems) and solar panels (SP/PCM systems) [70,159,233–237] by controlling the operating temperature. For these reasons, solid–liquid phase-change in rectangular cavities is of great interest either from the theoretical point of view and/or for the development of new TES systems.

Several experimental and numerical studies have been devoted to evaluate the effect of natural convection in vertical rectangular cavities filled with free-form PCMs [158,159,232–236,238–247]. The term "free" means that the macrocapsule is the only way of containment in order to avoid liquid leakages. Therefore, the molten paraffin can move freely inside the cavity due to buoyancy forces. On the other hand, microencapsulated PCMs can also be chosen to fill up the internally finned cavities. In this case, the migration of the PCM within the enclosure due to the buoyancy forces may be considered negligible. Typically, considering vertical applications, horizontal fins are added to the vertical heated/cooled walls of the cavity to provide additional heat transfer surface in the TES system. These units are different from those commonly used in electronic devices mainly in what concerns the orientation of both the enclosure and fins. In recent years, different PCM-based heat sinks with vertical fins emerging from top and bottom heated surfaces have been extensively studied [160,248–253]. However, since the heat transfer mechanisms during the phase-change processes depend on the configuration and orientation of both system and fins, the main findings regarding the influence of natural convection in the molten PCM within these heat sinks can only be carefully applied to vertical/horizontal building applications.

Some of the most important findings about the natural convection inside rectangular fins-enhanced enclosures filled with commercial paraffin waxes for vertical building applications are pointed out in the recent literature related with the thermal control of PV/PCM and SP/PCM systems [233–236]. It has been claimed that the performance of these panels can be improved by placing a PCM-fins-enhanced latent-heat TES unit on the panels back to passively lower the high operating temperature of the systems. Some of these studies were recently reviewed by Ma *et al.* [74], Du *et al.* [75], Browne *et al.* [78] and Makki *et al.* [79]. Hasan *et al.* [77] also reviewed the main advantages and disadvantages of different thermal control techniques for building integrated PV including the one with PCMs.

One of the first numerical models of a PV/PCM system that has been validated with realistic experimental conditions, for identically sized geometries, was proposed by Huang *et al.* [233]. These authors used the experimental data to validate the two-dimensional finite volume heat transfer model conjugated hydrodynamically to solve the Navier-Stokes and energy equations. Several experiments were carried out with a single flat aluminum plate system and two PV/PCM systems filled up with the free-form PCM – RT 25, with and without metal fins. The experimentally validated numerical model was then used for design purposes. A parametric study was carried out considering several configurations of the system: different ambient temperatures and insolation rates, different geometrical parameters of the PV/PCM system and several configurations of the fins. Temperature and velocity fields and vortex formation within the system were predicted for each configuration. The authors pointed out that the fins enable a more uniform temperature distribution within the

PV/PCM system and that natural convection in the molten PCM increases the heat transfer within the PCM, further improving the capacity of the thermal control effect on the panel. However, they have remarked that the relationship between the number and geometry of fins and the convective flow requires further study. The results have shown that for the two fins PV/PCM system filled up with a 20 mm PCM depth (with a melting temperature of 32 °C), the temperature on the front surface of the TES unit was maintained under 36.4 °C for 80 minutes considering an insolation rate of 1000 W m^{-2} and an ambient temperature of 20 °C. The results have also shown that for the same system filled up with a 40 mm PCM depth (with a melting temperature of 26.6 °C), the temperature on the front surface of the system was maintained under 33 °C for 150 minutes considering an insolation rate of 750 W m^{-2} and the same ambient temperature of 20 °C.

The same two fins PV/PCM geometry was considered in the numerical study carried out by Biwole *et al.* [234]. For validation purposes, these authors compared the numerical results (isotherms and velocity fields) to those obtained from experiments. The results have shown that adding a PCM-fins-enhanced capsule on the back of the solar panel can maintain the operating temperature below 40 °C for 80 minutes under a constant solar radiation of 1000 W m^{-2}. The same temperature was reached by the panel without PCM after only 5 minutes. The authors have also pointed out that adding high-conductivity fins accelerates the phase-transition, as well as the attenuation of the operating temperature.

Huang *et al.* [235] evaluated the impact of different internal fins-arrangements (number, dimension and shape) on the heat transfer processes with phase-change. For a macrocapsule filled with the free-form PCM − RT 25 and a certain fins arrangement, these authors found that during melting, the temperature rise of the PV/PCM system can be reduced by more than 30 °C when compared with the data of a single flat aluminum plate.

Huang et al. [159] developed a three-dimensional numerical model to simulate the temperature rise of a PV/PCM system and the results were compared with those obtained from using a previously developed and experimentally validated two-dimensional finite-volume heat transfer model. They found that the two-dimensional model can reflect correctly the three-dimensional model predictions for simple line-axis systems.

Huang *et al.* [236] carried out an experimental study for evaluating the effect of natural convection on the molten PCM and PCM crystalline segregation by considering different systems enhanced with internal fins. The results have shown that although the metal fins can improve the heat transfer inside the system, the thermal regulation period declines when increasing the number of fins. Therefore, these authors have suggested that when the PCM has completely melted, the operating temperature rises faster due to fins which may mitigate the idea that adding fins make PV/PCM

systems more efficient. In order to achieve a quick thermal dissipation response with a longer thermal regulation period, a modified PV/PCM system combining two commercial paraffin waxes with different melting temperatures was investigated by Huang [237].

Kamkari *et al.* [254] carried out an experimental investigation to evaluate the influence of the inclination angle of a rectangular enclosure on the convection-driven melting process of a PCM – lauric acid with high Prandtl number. The results showed that the inclination of the cavity has a significant impact on the formation of natural convection currents and, consequently, on the heat transfer rate and melting time of the PCM. Kamkari and Shokouhmand [255] experimentally evaluated the melting process of a PCM within a transparent rectangular enclosure with and without horizontal partial fins. The experimental results were used to calculate melted fractions, heat transfer rates and Nusselt numbers during the melting process of the PCM. The authors also defined two parameters to evaluate the thermal performance of the TES unit in the presence of horizontal partial fins: the melting enhancement ratio and the overall fin effectiveness. Both parameters increase with increasing the number of fins. An experimental effort to visualize temperature field and melting front evolution during solid–liquid phase change process of a PCM (lauric acid) within a vertical rectangular enclosure was also carried out by Shokouhmand and Kamkari [243]. These authors also evaluated the influence of natural convection during the melting process of the PCM.

As stated by Dutil *et al.* [51], mathematical and numerical modeling is very important for the optimum design of PCM-systems and for materials' selection. However, modeling of phase-change within rectangular enclosures is very challenging due to the non-linear behavior of the melting front and to the presence of a moving boundary, where heat and mass balance conditions have to be met. Furthermore, additional phenomena must be considered in the simulation problem such as: (i) hysteresis; (ii) subcooling; (iii) crystalline segregation; (iv) volume expansion; (v) natural convection in the molten PCM and in the air-layer that accommodates the PCM volume expansion in the cavity; (vi) motion of the solid in the melt, and (vii) variation of density and other thermophysical properties along with the temperature evolution. Regarding the term "hysteresis", Dumas *et al.* [170] have recently suggested that it may be inappropriate for PCMs. In fact, they suggest that hysteresis may be related to a misunderstanding of the DSC measurements as explained in Chapter II. As remarked by Assis *et al.* [256], due to the difficulties of an accurate modeling, it has become a frequent practice to neglect some of the phenomena mentioned above and to approximate the remaining ones when a numerical solution is attempted. Therefore, the development of well instrumented and controlled experimental setups is crucial to provide benchmarking results for validation purposes. However, in the literature, there is still a lack of detailed experimental results which can be easily reproduced for validating numerical models that account for subcooling and natural convection in the molten PCM domain inside vertical fins-enhanced rectangular cavities. This chapter aims at providing experimental

data for benchmarking and validation of numerical models that can be used for the design of new latent-heat TES systems (including vertical stacks of rectangular cavities filled with different types of PCMs) for buildings or other applications. It also aims at providing information about the influence of natural convection and subcooling phenomena during solid–liquid phase-change processes.

III.2 Experimental setup and procedure

III.2.1 Experimental apparatus and instrumentation

Fig. III.1 provides a 3D sketch and a photographic view of the experimental setup developed. It is composed by three main modules: the heating (A), the cooling (C) and the test-sample (B) modules. The last one has a fixed position and accommodates the TES unit (the vertical stack of rectangular cavities filled with PCMs). Modules A and C are both movable along a horizontal axis, allowing to implement cycles of heating (charging the TES unit by melting the PCM bulk) and cooling (discharging/solidifying the PCM).

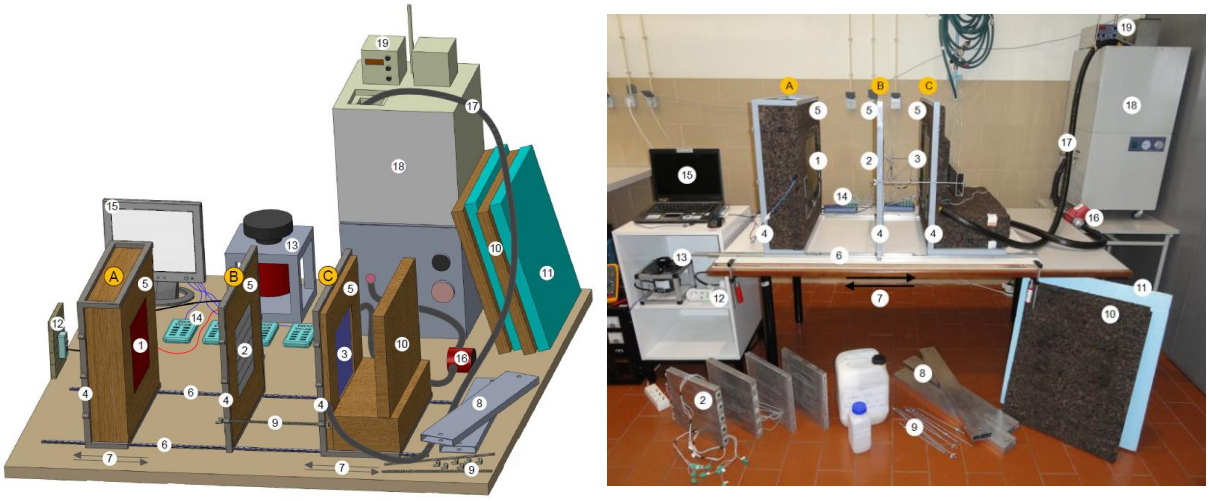

(a) (b)

A - Movable heating module
B - Fixed test module
C - Movable cooling module

① - Hot-plate
② - TES unit filled with PCM
③ - Cold-plate
④ - Rigid iron skeleton of the modules
⑤ - Thermal insulation boundary - cork
⑥ - Rails for linear motion
⑦ - Linear motion of the heating/cooling modules
⑧ - Accessories for compressing and joining the modules
⑨ - Threaded rods and nuts for the junction of the modules
⑩ - Movable thermal insulation layer - cork
⑪ - Movable thermal insulation layer - XPS
⑫ - Digital wattmeter
⑬ - Variac (*Lübcke Vario*)
⑭ - Pico® USB TC-08 thermocouple data logger
⑮ - PicoLog® data acquisition program
⑯ - Circulator pump *Grundfos* UPE 25-60
⑰ - Water circulation - insulated flow
⑱ - Water bath *Heto Lab Equipment* DBT KB21
⑲ - *HetoTherm* DBT 200 thermostat

Fig. III.1 (a) Three-dimensional sketch and (b) photographic view of the experimental setup.

The heating module holds the 0.3 m × 0.3 m heat source fed by an electrical resistance − the hot-plate with maximum power of 100 W. Both sides of the electrical resistance are covered with a mica layer and then sandwiched between two 8 mm thick aluminum flat plates, which ensure the uniformity of the temperature on the surface. The hot-plate is then coupled to a variable transformer, which is used to step up and/or step down the voltage (allowing the control of the power level). The charging experiments were carried out considering a 34 W power level (power density of about 378 W m^{-2}).

The cooling module holds the 0.31 m × 0.31 m heat exchanger fed by a thermo-regulated water flow − the cold-plate. The thermo-regulated water flow (of about 4 L min^{-1}) is ensured by a circulator pump coupled to a constant temperature water bath (*Heto Lab Equipment* DBT KB21). The cold-plate is based on a double-coil made of a 2 mm thick copper tube (Ø10 mm), framed by a 7 mm thick iron border (Fig. III.2). The coil is sandwiched between a high conductivity plate and a thermal insulation layer. The surface of the cold-plate in contact with the TES unit is made of a 5 mm thick aluminum flat plate to ensure the uniformity of the temperature on the surface. For further improvement of the temperature uniformity, the space surrounding the cooper coil is filled up with fine aluminum swarfs. The back layer of the cold-plate is made of a 4 mm thick cork sheet, on which a 10 mm thick Perspex plate is fixed.

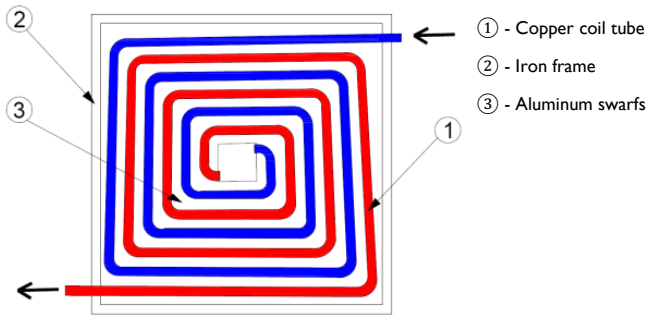

Fig. III.2 Sketch of the double-coil inside the cold-plate and direction of the water flow.

Nine K-type thermocouples, coupled three by three, are placed on the aluminum surfaces of both the hot and cold plates for monitoring the variation of temperature during the experiments (Fig. III.3a). THP and TCP represent, respectively, the average temperature measured on the surfaces of the hot and cold plates facing the TES unit. Twenty-one thermocouples are evenly distributed on the front and back surfaces of the test-sample, respectively, for measuring the surface temperature transient evolution (Fig. III.3b). The subscripts "H" and "C" refer to the surface of the TES unit facing the hot-plate and the cold-plate, respectively. The positioning of these thermocouples aims at

monitoring the thermal stratification during the experiments, as well as the effect of the root of the fins. Fig. III.3b shows how the thermocouples are distributed on the surfaces of the test-sample.

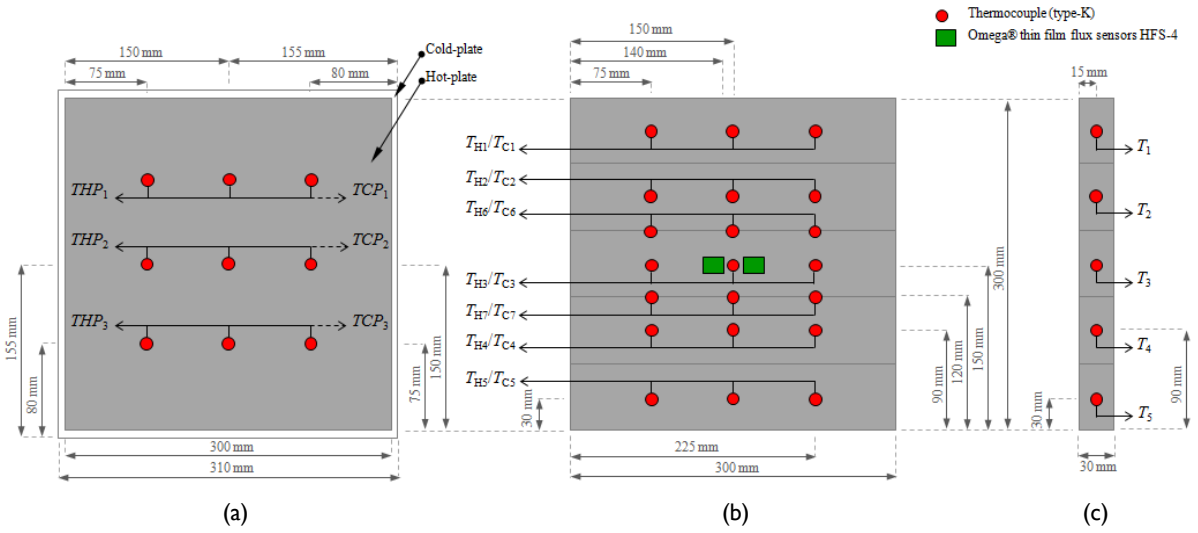

Fig. III.3 Sketch of the distribution of the thermocouples and the heat flow meters (a) on the surfaces of the cold and hot plates; (b) on the front and back surfaces of the TES unit; (c) within the TES unit (inserted up to a depth of 150 mm).

Two heat flux meters (Omega® thin film flux sensors HFS-4) are placed on each side of the test-sample as sketched in Fig. III.3b. The heat flux measured may not be representative of the overall heat flux crossing the vertical walls of the sample due to the thermal stratification during the phase transition of the PCM and to the effect of the root of the fins. However, the local heat flux evolution can be helpful for validating numerical codes.

Five thermocouples are positioned on the mid-plane of the TES unit at half-height of each cavity (inserted laterally at a depth of 150 mm) as shown in Fig. III.3c. It is not possible to evaluate the probe positions uncertainty during the melting and solidification processes because the envelope of the TES unit is opaque. To avoid the movement of the thermocouple wires during phase-change processes, each of them was attached to a very rigid support of about 14 cm length. Moreover, when positioning the thermocouples in the cavities, an end-to-end guiding line procedure was carried out to align each thermocouple. Therefore, any displacement of the thermocouples' tip in the PCM bulk during phase-change processes is minimized.

The thermocouples were calibrated all together, connected to the respective Pico® TC-08 data logger, using the calibration bath *Heto Lab Equipment* DBT KB21 (accuracy of ±0.1 °C) equipped with the *HetoTherm* DBT 200 thermostat and a PT100 probe, for a temperature range of 10–50 °C. The DBT KB21 bath was filled with 7 L of distilled water. It is stable to ±0.005 °C at a temperature

range between −30 °C and 100 °C. For starting the calibration, the reference bath temperature was set to a specific value. When the bath temperature was stabilized, the probe thermocouples were immersed into the water at the same depth and temperature readings were recorded by the data acquisition system. The procedure was repeated in nine rounds considering steps of five degrees from 10 °C to 50 °C. At each round, and after stabilization, n = 31 readings were recorded for each thermocouple (or group of thermocouples as shown in Fig. III.3) considering time steps of 10 s. Based on the n number of measurements for each probe i, the average measured temperature was calculated. Once all the measurements have been taken, the linear least-squares curve-fitting method was used to fit a line to the recorded data for each thermocouple (or group of thermocouples). The R-square value is greater than 0.999 for all the calculated regression lines. The precision of the sensors is indicated in Table III.1, based on the standard deviation (σ) of the set of data values.

Table III.1 Precision range of the calibration measurements based on the standard deviation.

Measurement	Precision (°C)	Measurement	Precision (°C)	Measurement	Precision (°C)
T_{H1}	±1.17	T_{C4}	±1.08	T_1	±0.86
T_{H2}	±1.10	T_{C5}	±0.97	T_2	±0.85
T_{H3}	±1.03	T_{C6}	±1.01	T_3	±0.84
T_{H4}	±0.93	T_{C7}	±1.02	T_4	±0.86
T_{H5}	±0.88	THP_1	±0.99	T_5	±0.88
T_{H6}	±0.99	THP_2	±1.06		
T_{H7}	±1.08	THP_3	±0.98		
T_{C1}	±1.07	TCP_1	±1.02		
T_{C2}	±1.13	TCP_2	±0.94		
T_{C3}	±1.15	TCP_3	±0.99		

III.2.2 Experimental procedure

For better understanding the modular operation of the experimental setup, Fig. III.4a sketches the cross-section of the overall apparatus (before compressing the modules). Figs. III.4b and III.4c represent the configuration of the experimental setup during the charging and discharging experiments, respectively. Before starting the charging experiment, the test-sample filled up with the PCM is pre-cooled at 13 °C (as sketched in Fig. III.4c) and the hot-plate is pre-heated at 55 °C. This procedure is repeated before starting every charging experiment. The heating module is then moved towards the fixed test-sample module and, at the same time, the cooling module is pulled back and replaced by a thermal insulation board (to simulate a boundary with negligible heat fluxes). The heating module and the back-insulated test-module are then tightly compressed with the help of some accessories as shown in Fig. III.4b. The 34 W power level is kept constant during the charging experiment. When the temperature within the PCM bulk reaches 55 °C, the charging experiment is stopped, and a cooling experiment can start. The heating module is then pulled back and replaced by

a thermal insulation board. Simultaneously, the cooling module is moved towards the test-sample module. The modules are then compressed as shown in Fig. III.4c. Before the cooling experiment starts, the cold-plate is pre-cooled at 14 °C, which is the temperature selected for the discharging experiment (temperature of the thermo-regulated water flow). The discharging experiment is stopped when the temperature measured in the mid-plane of the TES unit reaches the value specified on the thermostat of the cold water bath (14 °C). Each experiment was repeated thrice to check the repeatability of the results. The results were compared and deviations were found to be negligible.

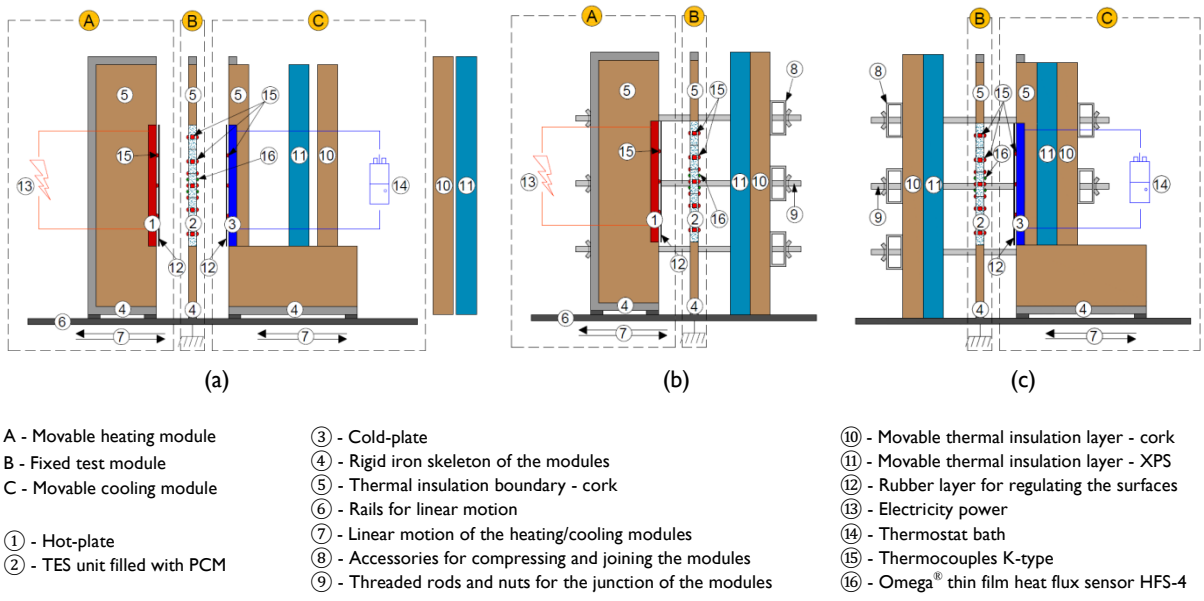

Fig. III.4 Sketch of the cross-section of the experimental setup before compressing the modules: (a) overall modular setup; (b) charging phase, and (c) discharging phase.

III.2.3 PCMs selection and test-sample

Fig. III.5 shows a sketch of the 0.3 m × 0.3 m × 0.03 m test-sample (PCM container made of aluminum) with 5 rectangular cavities. Each cavity of the sample has an aspect ratio $A = H'/L$ of about 2.154. The 2 mm thick aluminum side walls are supposed to provide an uniform rate of heat transfer to the enclosed PCM. The horizontal 4 mm fins are added to those vertical heated/cooled walls of the container to provide extended surface area for heat transfer to the PCM.

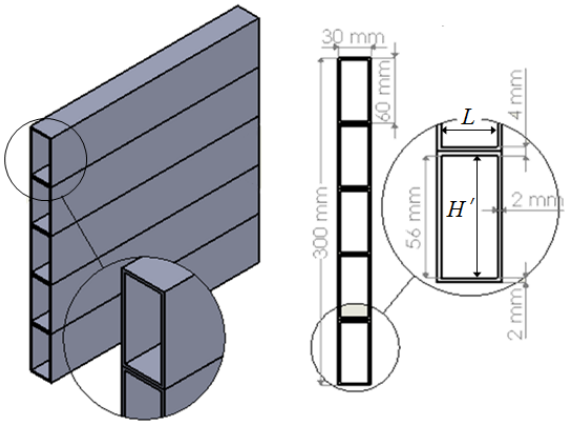

Fig. III.5 (a) Three-dimensional view and (b) cross-section sketch of the 5-cavities TES unit (A = 2.154).

The cavities of the TES unit are to be filled up with two different commercial paraffin-based PCMs: the Micronal® DS 5001 X (from BASF®) with a melting-peak temperature (T_{mp}) around 26 °C and the Rubitherm® RT 28 HC with T_{mp} around 28 °C. The first PCM is microencapsulated and the second one is a free-form paraffin wax, *i.e.*, the metallic macrocapsule is the only confinement to prevent liquid leakages. The reason for choosing these PCMs is that they are both organic PCMs, showing attractive features for building applications, as described in Chapter II [1,10,14]. The main thermophysical properties of the selected PCMs are listed in Table III.2. The product datasheet of Rubitherm® RT 28 HC [257] does not specify the latent heat of fusion, just a heat storage capacity of 245 ±18.4 kJ kg^{-1} in the range of 21 °C to 36 °C. A single value of 2 kJ kg^{-1} K^{-1} is provided for the specific heat of both phases. However, this property should have different values for the liquid and solid phases. Rouault *et al.* [258] estimated such values (shown in Table III.2) based on the properties of the n-octadecane, claiming that this is the main component of the RT 28 HC. On the other hand, the Micronal® DS 5001 X datasheet [259] specifies neither the specific heat capacity nor the heat conductivity. However, these values are crucial for the purpose of numerical modeling. The sensible heat capacity values for both the liquid and solid phases may be estimated based on the properties of the n-alcane, which is the main component of this PCM, according to Cui [260]. More detailed information about the properties of the Micronal® DS 5001 X can be found in the recent paper by Giro-Paloma *et al.* [261]. These authors argued that this material shows a phase-change temperature between 26.09 °C and 27.81 °C, a melting enthalpy between 114.98 kJ kg^{-1} and 142.55 kJ kg^{-1} and a solidification enthalpy between 117.85 kJ kg^{-1} and 137.85 kJ kg^{-1}. They also estimated a value of 995 ±3 kg m^{-3} for the density, as an average of the densities of two different materials: the polymeric shell (1000–1200 kg m^{-3}) and the paraffin wax core (760–880 kg m^{-3}) [261]. In their recent work, Sari-Bey *et al.* [182] also present some thermophysical properties of the Micronal® DS 5001 X, which are listed in Table III.2.

Table III.2 Thermophysical properties of the PCMs used in the experiments (values found in the literature).

	Rubitherm® RT 28 HC	Micronal® DS 5001 X
Melting temperature range (°C)	27–29 [257]	26.1–27.8 [261]
Melting-peak temperature (°C)	28 [257]	26 [259]
Solidifying temperature range (°C)	29–27 [257]	26.1–27.8 [261]
Solidifying peak temperature (°C)	27 [257]	26 [259]
Heat storage capacity (kJ kg^{-1})	245 ±18.4 [21–36 °C] [257]	145 [259] 115.0 –142.6 [261]
Latent heat (kJ kg^{-1})	≈ 245 [258]	≈ 110 [259]
Specific heat capacity (J kg^{-1} K^{-1})	2000 [257]	
– solid phase	1650 [258]	1610.5 [182]
– liquid phase	2200 [258]	1995.0 [182]
Heat conductivity (W m^{-1} K^{-1})	0.2 [257]	
– solid phase		0.24 [182]
– liquid phase		0.15 [182]
Density – solid phase (kg m^{-3})	880 [257]	≈ 250–350 [259] 995 ±3 [261] 920 [182]
Density – liquid phase (kg m^{-3})	770 [257]	≈ 250–350 [259] 995 ±3 [261] 920 [182]
Volume expansion (%)	12.5 [257]	n.a. [259]
Kinematic viscosity (mm^2 s^{-1})	3.1 [258]	n.a. [259]

For better characterizing the PCMs used in this study, calorimetric measurements related with the physical transformations of the samples under heating/cooling were performed on a modulated differential scanning calorimetry (MDSC) equipment from TA Instruments (Q100 model). The heat flow was calibrated at 0.5 °C min^{-1} using indium as standard, whereas the heat capacity measurement was calibrated at 2 °C min^{-1} using sapphire as standard. The samples were analyzed in aluminum pans with an ordinary aluminum lid. A dry nitrogen purge flow of 50 mL min^{-1} was applied in both calibration and measurements. The thermal behavior was studied using the equipment in the conventional dynamic DSC mode, with a ramp of a constant heating/cooling rate of about 0.5 °C min^{-1}, within the temperature range of –20 °C to 50 °C for the microencapsulated PCM, and 0 °C to 50 °C for the free-form PCM. Figs. III.6a and III.6b show, respectively, the DSC signal and temperature plots during the heating and cooling ramps for the free-form PCM – RT 28 HC and for the microencapsulated PCM – DS 5001 X. For the heat capacity measurements, a heating rate of 2 °C min^{-1}, a modulation period of 120 s and a temperature amplitude of ±0.53 K were employed. The measured thermophysical properties are listed in Table III.3. The measured values are in good agreement with the values found in literature (Table III.2).

The sample cavities were completely filled with the Micronal® DS 5001 X product (1035 g ±0.05 g of PCM). A vibrating mechanism was used to compact the PCM within the cavity. Regarding the Rubitherm® RT 28 HC, only 95% of the total volume of each cavity was filled with the PCM to

take into account the volume expansion during melting. Therefore, a permanent air-layer allows accommodating the PCM volume expansion in each cavity.

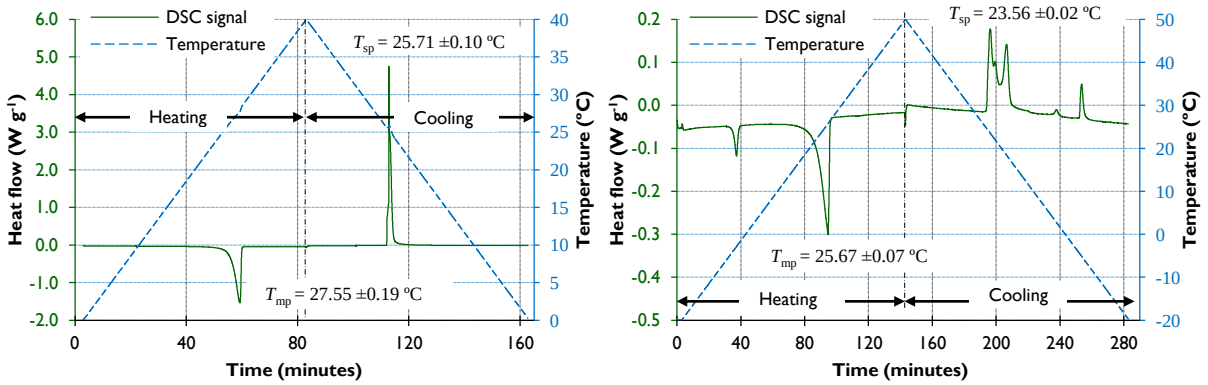

Fig. III.6 Heat flow and temperature evolution during a dynamic DSC measurement with constant heating/cooling rates of 0.5 °C min^{-1}: (a) free-form PCM – RT 28 HC; (b) microencapsulated PCM – DS 5001 X.

Table III.3 Measured thermophysical properties of the PCMs used in the experiments.

	Rubitherm® RT 28 HC	Micronal® DS 5001 X
Melting-peak temperature (°C)	27.55 ±0.19	25.67 ±0.07
Solidifying peak temperature (°C)	25.71 ±0.10	23.56 ±0.02
Heat storage capacity (kJ kg^{-1})		
– heating	≈ 258.1 ±5.1 [20°C–30°C]	≈ 111.3 ±1.4 [12°C–28°C]
– cooling	≈ 251.9 ±6.7 [20°C–27°C]	≈ 108.9 ±1.5 [10°C–25°C]
Specific heat capacity (J kg^{-1} K^{-1})		
– solid phase	1652 ±105 [0°C–20°C]	1972 ±276 [5°C–10°C]
– liquid phase	2021 ±120 [35°C–45°C]	1547 ±263 [35°C–45°C]

III.3 Results and discussion

Figs. III.7a and III.7b show the sketch of the physical domain for the charging and discharging phases of the PCM, respectively. T_{H} is the average temperature measured on the front surface of the TES unit and T_{C} is the average temperature measured on the back surface of the container. As stated before, the front side of the TES unit faces the heating module and the back side faces the cooling module. T is the measured temperature of the PCM in the mid-plane of the container. Subscripts 1 to 5 refer to the location of the thermocouples (from top to bottom). THP and TCP are defined above.

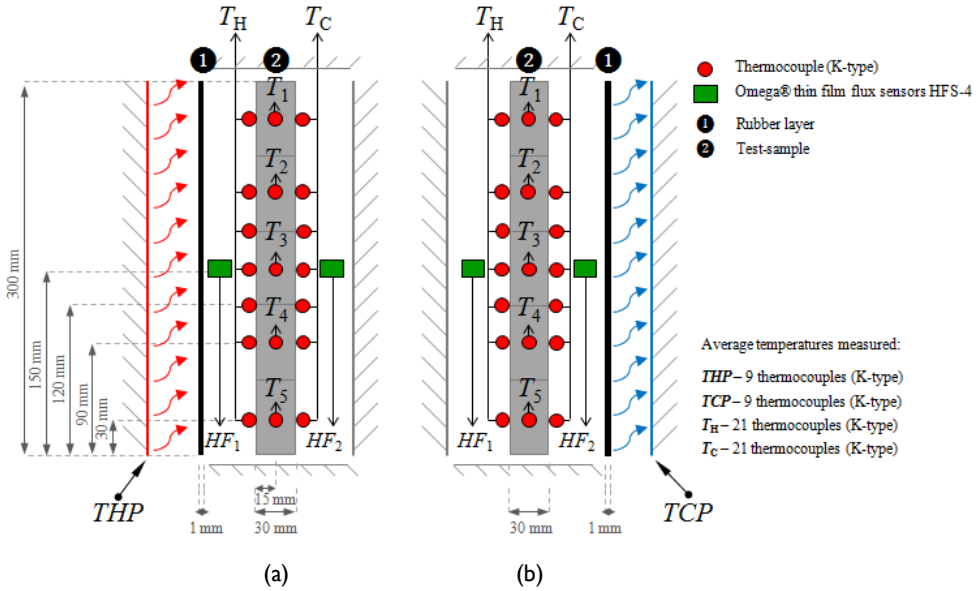

Fig. III.7 Sketch of the physical domain with the measured variables: (a) charging phase; (b) discharging phase.

During the heating phase, all the boundaries of the physical domain can be considered as surfaces with negligible heat flux, except the left one, which has a known temperature THP varying with time. During the cooling phase, the right frontier has also a known temperature TCP varying with time and the heat fluxes are considered negligible in all the other boundaries. HF_1 and HF_2 are the average heat fluxes measured on the centre of the front and back surfaces of the TES unit, respectively. In the front surface, the heat flux is considered positive when entering the TES unit. In the back surface, the heat flux is considered positive when leaving the test-sample.

III.3.1 Charging phase

III.3.1.1 Results for benchmarking and validation of numerical models with free-form PCMs

Fig. III.8 shows the evolution of the measured temperatures and heat fluxes during the charging experiment with the TES unit filled with the free-form PCM – RT 28 HC. T_{reg} is the value of the control-temperature reached on the hot surface of the TES unit, t_{reg} is the time of temperature control (thermal-regulation period), and t_m is the time required for complete melting of the PCM in the mid-plane of the cavities. Table III.4 shows the average measured values to be used for roughly drawing the curves shown in Figs. III.8a and III.8b. As stated before, each experiment was repeated thrice for the same conditions to check the repeatability of the results. All of the data presented in this section, for each variable and for each time step considered, are taken as the mean of the corresponding values measured in the three experiments. The variance with respect to the mean and the corresponding standard deviation (σ) were calculated for all variables. The maximum standard

deviation considered for each variable during charging is the maximum value computed as shown in Figs. III.8a and III.8b.

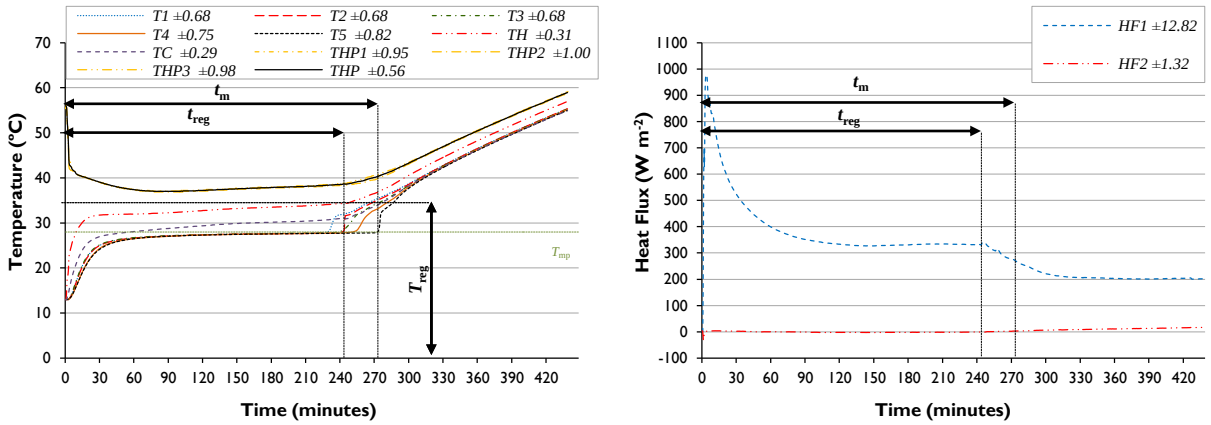

(a) (b)

Fig. III.8 Evolution of the average measured (a) temperatures and (b) heat fluxes for the 34 W power level charging phase of the 5-cavities TES unit filled with the free-form PCM – RT 28 HC.

Fig. III.8a shows three different phases during the heating process from 13 °C up to 55 °C: (*i*) solid (sensible heating); (*ii*) solid–liquid phase-change (latent heat), and (*iii*) liquid (sensible heating). Fig. III.8b shows that the measured heat flux remains constant during melting as latent heat is stored in the system. It was observed that conduction is initially the main mechanism of heat transfer with a linear temperature increase with time for the temperature on both surfaces of the TES unit and inside the PCM-bulk (Fig. III.8a). It is interesting to remark that the temperature of the cold surface T_C is always a few degrees higher than the monitored temperatures at the mid-plane of the cavities (T_1 to T_5), until the PCM melts in such points. This illustrates the effect of the heat transfer from the hot to the cold vertical wall of the TES unit, directly conducted along the horizontal fins. It is then expected that, within each cavity, the PCM starts melting not only on the hotter surface, but all around due to the contact with the aluminum confining surfaces.

In the mid-plane of the cavities, before completely melting, the temperature of the PCM is maintained below the melting-peak temperature with a gradual increase from the temperature attained at t = 30 minutes, which is approximately the time when the melting process starts near the hot surface. Therefore, during the melting process, the temperature in the PCM domain remains nearly constant. The heat transferred by convection through the melted PCM balances the latent heat used for the phase-change at the solid–liquid interface and the temperature on the surfaces of the TES unit remains approximately constant, below the control-temperature (T_{reg}) during the thermal-regulation period (t_{reg}). After 230 minutes, the melting front reaches the upper monitored

point in the mid-plane of the TES unit, and the local temperature T_1 increases sharply above T_{mp} due to natural convection flow (Fig. III.8a) and to the sensible heat transfer in the liquid phase. At the same time, the temperature in the solid phase locations maintains its very slow conduction-dominated increase with time.

Table III.4 Results for benchmarking and validation of numerical models with natural convection for the 5-cavities TES unit filled with the free-form PCM – RT 28 HC (34 W power level charging phase).

Time (s)	T_1 (°C)	T_2 (°C)	T_3 (°C)	T_4 (°C)	T_5 (°C)	THP (°C)	T_H (°C)	T_C (°C)	HF_1 (W m^{-2})	HF_2 (W m^{-2})
0	13.00	13.00	13.00	13.00	13.00	56.00	13.00	13.00	0.82	3.94
180	13.10	13.09	13.20	13.10	13.08	43.45	22.50	14.94	970.00	1.02
210	13.29	13.27	13.31	13.18	13.25	42.85	23.24	15.63	968.25	2.26
660	18.14	17.97	18.31	16.96	16.88	40.60	28.81	22.09	778.01	3.86
1140	22.48	22.32	22.62	21.19	21.06	39.95	31.04	25.44	622.76	3.38
1770	24.97	24.93	25.08	24.28	24.09	39.05	31.76	26.94	525.59	2.25
2340	25.85	25.82	25.93	25.49	25.38	38.35	31.89	27.44	472.54	1.23
3420	26.59	26.58	26.65	26.43	26.42	37.45	31.99	28.03	406.48	0.23
3600	26.66	26.65	26.72	26.52	26.51	37.35	31.99	28.11	398.56	0.24
4440	26.90	26.89	26.96	26.82	26.84	37.05	32.09	28.46	370.97	-0.07
5520	27.13	27.12	27.16	27.06	27.08	37.00	32.33	28.83	349.39	-1.24
6120	27.20	27.20	27.24	27.19	27.18	37.00	32.47	29.04	342.06	-2.17
7770	27.41	27.39	27.42	27.40	27.37	37.30	32.93	29.59	329.56	-2.22
9060	27.53	27.50	27.52	27.48	27.47	37.60	33.24	29.90	327.03	-2.62
11760	27.66	27.62	27.67	27.65	27.62	38.00	33.64	30.30	333.71	-1.70
13170	27.79	27.66	27.72	27.70	27.68	38.25	33.94	30.57	332.92	-1.26
13650	27.93	27.70	27.76	27.73	27.70	38.35	34.09	30.67	332.94	-1.17
14130	31.27	27.80	27.87	27.76	27.71	38.50	34.26	30.87	331.38	-0.70
14400	31.84	27.88	28.08	27.78	27.72	38.55	34.31	30.94	332.99	-0.91
14550	31.93	28.10	28.39	27.82	27.73	38.60	34.36	30.99	331.53	-0.64
14700	32.10	31.62	28.89	27.85	27.74	38.60	34.37	30.94	340.13	-1.41
14970	32.43	31.95	30.17	27.95	27.75	38.80	34.69	31.33	324.85	0.86
15210	32.99	32.56	31.54	28.22	27.76	39.05	35.10	31.87	311.99	0.85
15690	34.08	33.64	32.81	31.13	27.78	39.50	35.76	32.69	292.69	2.39
16050	34.82	34.43	33.71	32.53	27.81	39.95	36.37	33.43	279.35	2.30
16290	35.29	34.92	34.19	33.00	27.87	40.20	36.73	33.80	274.95	2.90
16530	35.74	35.36	34.67	33.61	32.04	40.60	37.20	34.41	263.51	3.36
17130	36.90	36.59	36.05	35.27	34.29	41.55	38.46	35.84	246.10	4.40
17790	38.25	38.05	37.74	37.35	37.04	42.90	40.09	37.73	225.09	6.27
18180	39.15	38.99	38.78	38.51	38.28	43.65	41.01	38.73	218.13	6.76
19890	43.00	42.91	42.81	42.67	42.53	47.10	44.79	42.67	205.85	8.77
26310	55.35	55.31	55.25	55.16	55.01	58.95	57.00	54.91	201.30	16.78

As the PCM starts melting close to the hot vertical surface of the cavities (T_H), one may analyze the melted vertical layer as a fluid layer enclosed in a vertical cavity with a gradually increasing width. It is generally accepted that, in rectangular differentially heated cavities, the onset of natural convection occurs for values of the Rayleigh number above 1800. As the properties of the PCM investigated (RT 28 HC) are rather similar to the thermophysical properties of the n-Octadecane (Table III.5), it is expected that the behavior of the free-form PCM – RT 28 HC will be

similar as well. The Rayleigh number characterizing natural convection inside a differentially heated vertical cavity can be defined as:

$$\mathrm{Ra} = \frac{g\beta\left(T_{\mathrm{H}} - T_{\mathrm{mp}}\right)L_c^{\,3}}{\nu^2} \cdot \frac{\mu c_{\mathrm{p}}}{k} \qquad \text{(III.1)}$$

where, for the purpose of this analysis, the vertical hot and cold surfaces are assumed to be at temperatures T_{H} and T_{mp}, respectively, and separated by L_{c} (the cavity width). The melting front may be considered plane and vertical, at least before the onset of natural convection. Considering the well-known properties of the n-Octadecane (Table III.5), and (T_{H}–T_{mp}) = 4°C, as seen in Fig. III.8a, one can make the exercise of determining the minimum width of the melted vertical layer required for the onset of natural convection. It was found that, for L_{c} equal to 3 mm, Ra = 1984. Therefore, natural convection is expected to occur in the cavity after a certain time, when the thickness of the melted layer will become large enough to guarantee $\mathrm{Ra} > 1800$, *i.e.*, roughly for $L_{\mathrm{c}} > 3$ mm.

Therefore, the overall thermal stratification in the test-sample is primarily caused by the natural convection flow, that probably starts some slow recirculating motion in the upper region of the melted PCM in each cavity; a second effect is the quicker heating of the gaseous layer on the top of each cavity (beneath each fin). By tending to increase the temperature of the fin itself, the latter promotes heating of the bottom wall of each upper-neighbor cell, an effect that does not apply to the lower-level cavity. The result of these mechanisms might be named as a cumulative or stack thermal stratification effect. As the melting front advances, the increasing volume of liquid PCM gives place to buoyancy forces that are more important in the vicinity of the hot vertical wall and, at some moment, become large enough to overcome the viscous forces, creating a global recirculating flow around a still solid core. Although slow, the liquid motion will enhance the heat transfer to the solid–liquid interface. The domain of melted PCM will thus be always warmer in the upper part of each cavity where the melting front will progress faster.

Table III.5 Thermophysical properties of the n-Octadecane.

PCM	ρ_{l} liquid density (kg m^{-3})	μ_{l} liquid viscosity (10^{-3} N s m^{-2})	k_{l} liquid thermal conductivity (W m^{-1} K^{-1})	$c_{\mathrm{p,l}}$ liquid specific heat (kJ kg^{-1} K^{-1})	β liquid thermal expansion coefficient (10^{-4} K^{-1})
n-Octadecane	774	3.9	0.152	2.18	8.5

Temperatures T_1 to T_5 measured at the centre of the five cavities show the above mentioned cumulative stratification effect. After $t_{\mathrm{m}} \approx 273$ minutes (Fig. III.8a), the PCM can be considered melted

in practically the whole mid-plane of the TES unit, where the heat transfer is now dominated by natural convection. The temperature rises with a smaller slope than at the beginning of the conduction-dominated process because the specific heat capacity is higher in the liquid than in the solid PCM. When the melting process ends, the temperatures on both surfaces of the TES unit quickly rise because heat is no longer absorbed by the phase-change process.

Fig. III.8b shows that the heat flux measured on the centre of the back surface of the TES unit (HF_2) remains practically constant during the entire charging process. On the other hand, the time evolution of the heat flux on the front surface (HF_1, in contact with the hot-plate) presents three inflection points. When the heating module is placed in contact with the test module, the heat flux increases sharply due to the high temperature difference between the two surfaces (≈42 °C). After 4 minutes, the heat flux shows an exponential decay until a value of about 330 W m^{-2} is reached at t ≈ 123 minutes, remaining nearly constant up to a new inflection point. This period corresponds to the melting of the PCM (when the latent heat is stored). When the phase-change is almost finishing and the heat transfer is dominated by convection, the heat flux starts decreasing while the temperature in the front surface of the TES unit starts increasing. The last inflection point at t ≈ 312 minutes marks the end of the sharp rise of the temperature of the PCM in the middle section of the cavities. From this moment on, both temperatures on the hot-plate and on the front surface of the TES unit increase linearly, keeping a roughly constant difference (≈2 °C) between each other while the heat flux on the front surface of the TES unit remains practically constant (≈200 W m^{-2}). The difference between T_{H} and THP is due to the presence of the rubber layer used to accommodate the thermocouples. By choosing an instant during that period and applying Fourier's law, a value for the heat conductivity of the rubber layer can be determined. The determined value of about 0.1 W m^{-1} K^{-1} is close to the tabled values for this type of materials.

Considering $E_{\mathrm{st,ex}}$ as the stored energy in the time range t_{i}–t_{f} (240–19020 s), calculated as indicated in Eq. (III.2) using numerical integration, its value is determined by considering the local measurements of HF_1 and HF_2. $E_{\mathrm{st,th}}$ in Eq. (III.3) is the theoretical stored energy for the same period, considering the total amount of PCM incorporated in the TES unit and the total heat capacity of the aluminum structure and the air-layer. In Eq. (III.3), m is mass of the material; L_{f} is the latent heat of fusion of the PCM; T_{i} and T_{f} are the average measured initial and final temperatures, respectively, T_{mp} is the melting-peak temperature of the PCM, and c_{p} is the specific heat. Subscript "s" and "l" refer to the solid and liquid phases of the PCM, respectively.

$$E_{\mathrm{st,ex}} = S\left[\int_{t_{\mathrm{i}}}^{t_{\mathrm{f}}} HF_1(t)dt - \int_{t_{\mathrm{i}}}^{t_{\mathrm{f}}} HF_2(t)dt\right] \qquad \text{(III.2)}$$

$$E_{\mathrm{st,th}} = m_{\mathrm{PCM}}\left[c_{\mathrm{p,s}}\left(T_{\mathrm{mp}} - T_{\mathrm{i}}\right) + L_f + c_{\mathrm{p,l}}\left(T_{\mathrm{f}} - T_{\mathrm{mp}}\right)\right]_{\mathrm{PCM}} + m_{\mathrm{Al}}\left[c_{\mathrm{p}}\left(T_{\mathrm{f}} - T_{\mathrm{i}}\right)\right]_{\mathrm{Al}} + m_{\mathrm{Air}}\left[c_{\mathrm{p}}\left(T_{\mathrm{f}} - T_{\mathrm{i}}\right)\right]_{\mathrm{Air}} \quad \text{(III.3)}$$

The estimated values of $E_{\mathrm{st,ex}}$ and $E_{\mathrm{st,th}}$ are approximately 608 kJ and 509 kJ, respectively, which means that the error of considering the local measurements of HF_1 and HF_2 instead of the overall heat fluxes crossing the vertical surfaces of the test-sample is about 16.25%. This may be explained by a significant non-uniformity of the heat flux along the vertical direction on both the front and back surfaces of the test-sample, mainly due to the thermal-bridge effect of the fins, but also to the observed stratification. An additional contribution for this deviation may be the heat stored by the insulation material surrounding the test-sample along the process, particularly during the final phase of sensible heating. Therefore, the measured heat fluxes are not representative of the overall heat fluxes crossing the vertical surfaces of the test-sample, but they can be used for monitoring purposes.

III.3.1.2 Results for benchmarking and validation of numerical models with microencapsulated PCMs

Figs. III.9a and III.9b show the evolution of, respectively, the measured temperatures and the heat fluxes on both front and back surfaces of the TES unit filled with the microencapsulated PCM – DS 5001 X, during the 34 W power level charging phase. Fig. III.9a depicts the three phases of the heat storage during the heating process from 13 °C up to 55 °C: (*i*) solid (sensible heating); (*ii*) solid–liquid phase-change (latent heat); and (*iii*) liquid (sensible heating). Table III.6 shows the values of the variables measured during the experiments.

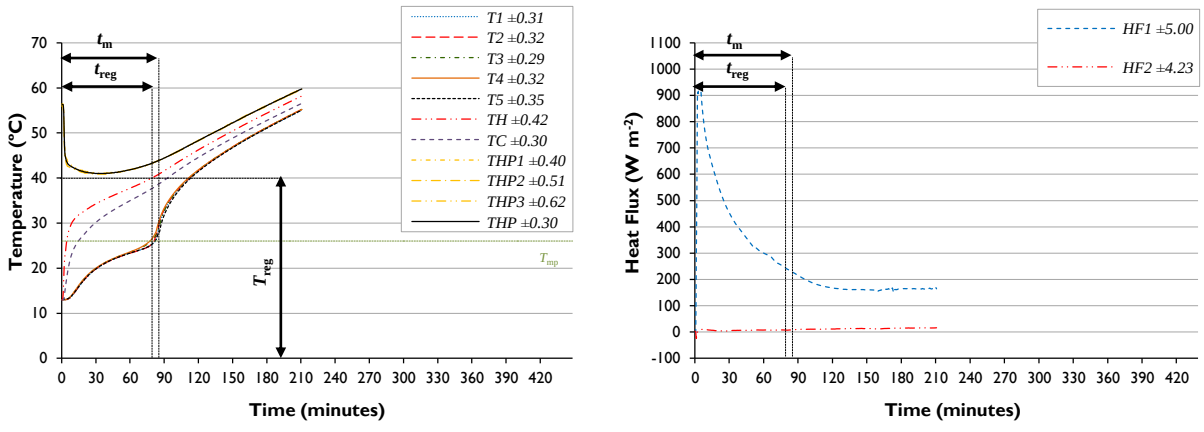

(a) (b)

Fig. III.9 Evolution of the average measured (a) temperatures and (b) heat fluxes for the 34 W power level charging phase of the 5-cavities TES unit filled with the microencapsulated PCM – DS 5001 X.

Table III.6 Results for benchmarking and validation of conduction-dominated numerical models for the 5-cavities TES unit filled with the microencapsulated PCM – DS 5001 X (34 W power level charging phase).

Time (s)	T_1 (°C)	T_2 (°C)	T_3 (°C)	T_4 (°C)	T_5 (°C)	THP (°C)	T_H (°C)	T_C (°C)	HF_1 (W m^{-2})	HF_2 (W m^{-2})
0	13.00	13.00	13.00	13.00	13.11	56.35	13.00	13.00	-1.17	3.39
120	13.01	13.01	13.01	13.01	13.14	48.85	20.93	13.79	913.07	-0.77
180	13.01	13.01	13.01	13.01	13.15	44.65	23.49	15.83	927.54	3.87
270	13.02	13.05	13.06	13.09	13.20	43.45	26.61	18.49	946.01	8.87
300	13.03	13.09	13.12	13.16	13.24	43.15	27.37	19.29	917.74	9.74
570	14.02	14.09	14.25	14.33	14.18	42.35	30.41	23.81	734.75	8.66
990	16.40	16.49	16.69	16.78	16.53	41.60	32.16	26.71	609.28	6.03
1500	18.77	18.85	19.00	19.06	18.88	41.15	33.57	29.06	498.57	4.02
1710	19.51	19.59	19.72	19.78	19.62	41.05	34.09	29.91	464.30	4.51
2280	21.07	21.12	21.24	21.27	21.16	41.00	35.34	31.74	396.22	6.34
3150	22.68	22.69	22.86	22.90	22.74	41.45	36.94	33.97	322.85	7.58
3690	23.43	23.45	23.70	23.77	23.51	41.90	37.93	35.21	296.80	7.84
4440	24.48	24.50	25.15	25.36	24.59	42.80	39.36	36.93	257.58	7.88
4590	24.74	24.84	25.60	25.85	24.92	43.00	39.67	37.33	250.43	8.16
4800	25.47	25.68	26.46	26.87	25.60	43.40	40.14	37.84	240.37	7.06
4980	26.69	27.64	27.64	28.48	26.64	43.70	40.57	38.33	233.28	7.85
5160	30.08	30.74	29.78	31.05	28.49	44.00	41.00	38.84	225.49	8.85
5310	31.94	32.37	31.97	32.68	30.97	44.25	41.40	39.27	219.26	9.47
5730	35.20	35.42	35.34	35.69	34.69	45.15	42.50	40.53	201.65	10.29
6240	37.96	38.05	38.11	38.31	37.67	46.20	43.89	42.04	184.62	10.94
6690	39.87	39.90	40.00	40.12	39.66	47.25	45.00	43.29	175.31	11.50
6990	40.96	40.98	41.09	41.17	40.80	47.85	45.77	44.09	170.48	11.29
7740	43.37	43.39	43.48	43.53	43.27	49.55	47.57	45.94	163.10	12.27
10050	49.33	49.49	49.49	49.52	49.38	54.50	52.81	51.17	163.02	13.76
12630	55.00	55.19	55.19	55.24	55.08	59.75	58.19	56.54	164.82	16.28

As the PCM is microencapsulated, conduction is the predominant mechanism of heat transfer, therefore no significant thermal stratification is observed due to natural convection. These results are in agreement with the results achieved by Zhang *et al.* [262]. These authors have claimed that for microencapsulated PCMs, the effect of the liquid-phase natural convection in the PCM core is weak and can be neglected due to suppression by micron-sized capsulation shells [262].

Two main inflection points can be observed on the time evolution of the measured temperatures and heat fluxes. After the initial sharp increase of both the heat flux and the temperature on the front surface, when the heating module is placed in contact with the test-sample, the heat flux experiences an exponential decay and the temperature of the PCM rises similarly in each cavity. The second inflection is observed when the melting-peak temperature is reached at the centre of the PCM-filled cavities, and it marks the end of the melting process. From this moment on, the temperature of the PCM rises sharply, while the temperature on the surfaces of the test-sample also increase at a higher rate. This indicates that the heat is no longer absorbed by the phase-change process. After 120 minutes, the heat flux on the front surface of the TES unit remains almost constant (Fig. III.9b), as well as the difference between T_H and T_C (Fig. III.9a).

$E_{st,ex}$ is determined as indicated in Eq. (III.2) for the time range from t_i = 270 s to t_f = 7170 s using numerical integration. $E_{st,th}$ is calculated as indicated in Eq. (III.4). C_{eff} is the overall heat storage capacity of the microencapsulated PCM. The estimated values of $E_{st,ex}$ and $E_{st,th}$ are about 210 kJ and 193 kJ, respectively, which means that the error of considering the local measurements of HF_1 and HF_2 is about 8.5%. This deviation is lower than the one determined in the previous section for the experiment with the free-form PCM, as the heat transfer is closer to a pure diffusion process with no thermal stratification.

$$E_{st,th} = \left[mC_{eff}\right]_{PCM} + \left[mc_p\left(T_f - T_i\right)\right]_{Al} \quad \text{(III.4)}$$

III.3.2 Discharging phase

III.3.2.1 Results for benchmarking and validation of numerical models with free-form PCMs

Fig III.10 shows the results of the discharging phase for the TES unit filled with the free-form PCM – RT 28 HC, with the cooling water temperature, T_{water}, set to 14 °C. Results show three phases during discharging from 55 °C down to 14 °C: (i) sensible cooling (liquid); (ii) liquid–solid phase-change (latent heat); and (iii) sensible cooling (solid).

Four parameters were defined to characterize the discharging process: (i) t_{cr} is the time required for starting the crystallization process; (ii) t_{sc} is the period during which subcooling occurs; (iii) ΔT_{sc} is the difference between the solidification temperature of the PCM (T_{sp}) and a lower temperature reached by the PCM at the end of the initial sensible cooling, due to subcooling phenomenon (T_{sp}^{*}), and (iv) t_{sol} is the time required for solidifying all the PCM in the mid-plane of the cavities. Table III.7 shows the values of the measured variables to be used for roughly drawing the curves shown in Figs. III.10a and III.10b.

The time evolution of the measured temperatures shows a mainly conduction-dominated solidification process. The evolution is especially steep at the beginning (up to $t = t_{cr}$), after which occurs the solidification itself while the latent heat is released at a nearly constant temperature. After $t = t_{sol}$, when the PCM in the mid-plane of the cavities is solidified, the temperature quickly drops to the temperature of the cold-plate. In analogy with the charging experiments, the importance of the effect of fins is well depicted from Fig. III.10a, since the temperature of the front surface T_H is well below the monitored temperatures T_1 to T_5 of the PCM (and the phase-change temperature) during the whole solidification period. Therefore, the solidification of the PCM will start on every solid walls of the cavity, predominantly over the cold surface at T_C, and progress towards the central zone. The liquid PCM will thus be trapped in a gradually shrinking cavity, inhibiting free convection flow. As

previously suggested by Longeon *et al.* [263], natural convection in the liquid domain of the PCM does not play an important role during the discharging process. These authors suggested that, at the beginning of the process, a slow convective flow appears in the liquid domain but it gradually disappears as the solidification front moves. The temperature of the liquid domain behind the solidification front remains almost constant (at the solidification temperature of the PCM), inhibiting natural convection [263]. Therefore, no significant thermal stratification due to natural convection is found during the first period of the discharging process (sensible heat transfer – liquid phase).

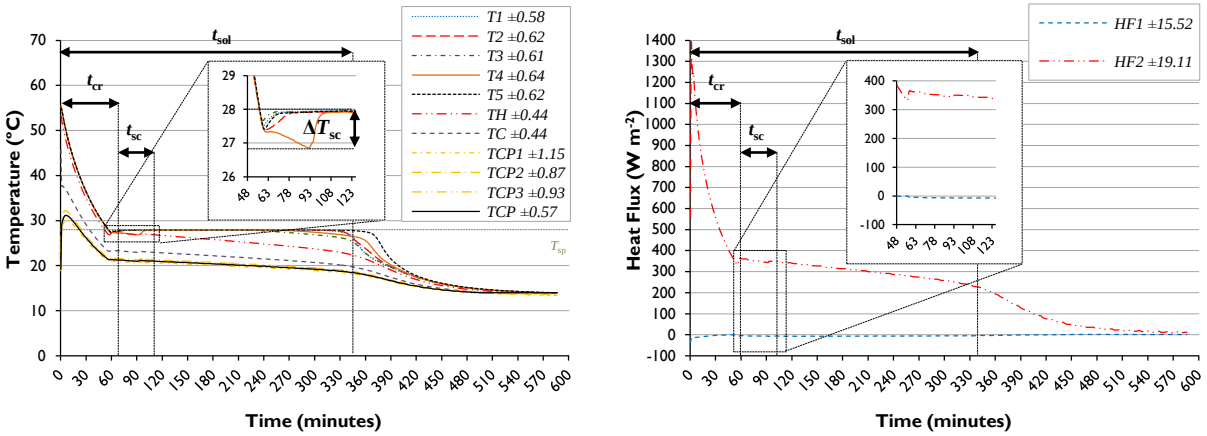

(a) (b)

Fig. III.10 Evolution of the average measured (a) temperatures and (b) heat fluxes for the discharging process of the 5-cavities TES unit filled with the free-form PCM – RT 28 HC and T_{water} = 14 °C.

It was also observed that before solidification starts, the PCM is locally cooled below the phase-change temperature due to the subcooling effect. As stated by Mehling and Cabeza [88], subcooling consists of the need to reduce the PCM temperature below the phase-change temperature in order to start crystallization. The effect of subcooling is clearly shown in Fig. III.10a. After the drop of temperature due to subcooling, the temperature in the PCM domain increases to its phase-change temperature, absorbing a small portion of latent heat. This can result in an apparent reduction of the latent heat released [264]. Moreover, subcooling delays the solidification process and it also may reduce the solidification temperature of the PCM [88,264] as explained in Chapter II.

Table III.7 Results for benchmarking and validation of numerical models with natural convection − discharging phase with T_{water} = 14 °C considering the 5-cavities TES unit filled with the free-form PCM – RT 28 HC.

Time (s)	T_1 (°C)	T_2 (°C)	T_3 (°C)	T_4 (°C)	T_5 (°C)	TCP (°C)	T_H (°C)	T_C (°C)	HF_1 (W m^{-2})	HF_2 (W m^{-2})
0	55.37	55.32	55.30	55.20	55.04	19.20	53.34	45.77	-36.22	556.95
60	54.72	54.65	54.73	54.68	54.60	29.00	52.34	37.63	-13.59	1392.90
240	51.87	51.69	51.76	51.78	51.73	30.90	49.44	37.31	-13.63	1227.95
480	48.52	48.35	48.39	48.46	48.42	31.05	46.34	36.23	-12.43	1007.54
1500	38.62	38.47	38.46	38.51	38.57	27.25	36.99	30.54	-5.13	620.81
3330	28.14	28.06	28.07	28.09	28.16	21.45	27.01	23.31	-0.84	332.22
3390	27.88	27.81	27.84	27.84	27.91	21.30	26.90	23.20	-1.75	347.32
3450	27.65	27.60	27.73	27.63	27.68	21.30	26.86	23.19	-6.68	365.97
3510	27.53	27.46	27.67	27.46	27.47	21.30	27.03	23.29	-6.57	363.43
3570	27.54	27.40	27.71	27.37	27.41	21.35	27.20	23.34	-5.54	362.32
3630	27.60	27.40	27.77	27.34	27.45	21.35	27.27	23.37	-5.05	361.79
3720	27.68	27.41	27.83	27.33	27.55	21.30	27.30	23.33	-4.77	361.01
3900	27.80	27.48	27.90	27.34	27.72	21.25	27.29	23.34	-5.64	361.39
4110	27.88	27.59	27.93	27.31	27.85	21.25	27.27	23.30	-6.37	355.90
4200	27.90	27.64	27.93	27.29	27.87	21.25	27.26	23.29	-6.70	354.43
4560	27.93	27.84	27.92	27.17	27.89	21.15	27.16	23.19	-6.69	352.20
4740	27.93	27.89	27.92	27.12	27.91	21.10	27.07	23.11	-6.62	351.58
5340	27.94	27.91	27.93	26.90	27.92	21.00	26.86	22.99	-6.76	345.34
5460	27.95	27.92	27.93	26.86	27.92	21.00	26.84	22.96	-7.04	343.50
5670	27.94	27.91	27.92	27.05	27.92	21.15	27.06	23.14	-7.51	350.21
5790	27.95	27.92	27.94	27.52	27.93	21.15	27.07	23.14	-7.27	349.59
5940	27.95	27.92	27.94	27.78	27.94	21.10	27.04	23.10	-6.90	349.11
6090	27.95	27.91	27.93	27.87	27.93	21.05	27.00	23.06	-6.61	349.05
6240	27.95	27.92	27.94	27.91	27.94	21.00	26.94	23.01	-7.35	348.57
12810	27.96	27.93	27.91	27.94	27.94	20.10	25.30	21.84	-7.14	299.07
14400	27.96	27.94	27.72	27.92	27.94	19.90	24.81	21.51	-6.89	286.90
15210	27.95	27.94	27.56	27.88	27.94	19.70	24.61	21.34	-6.80	281.59
17580	27.90	27.93	26.99	27.52	27.93	19.25	23.87	20.81	-6.03	262.93
18450	27.84	27.90	26.74	27.30	27.93	19.10	23.54	20.59	-5.89	252.85
19350	27.68	27.80	26.43	27.04	27.90	18.95	23.19	20.34	-5.53	242.36
19950	27.45	27.56	26.13	26.83	27.87	18.75	22.87	20.11	-5.58	232.94
20640	26.57	26.21	25.42	26.53	27.79	18.45	22.39	19.76	-4.05	220.64
21150	24.36	24.86	24.06	26.19	27.67	18.25	21.91	19.43	-4.19	209.57
21870	22.01	23.07	22.16	24.73	27.32	17.80	21.14	18.87	-3.47	185.31
23070	19.99	20.33	20.18	20.83	22.72	16.90	19.50	17.74	-1.86	141.62
24900	17.73	17.82	17.74	17.90	18.20	15.60	17.20	16.06	-1.02	85.60
26280	16.48	16.53	16.46	16.53	16.66	14.90	16.06	15.21	-0.11	60.35
27660	15.60	15.64	15.58	15.62	15.70	14.45	15.24	14.66	0.69	41.89
29310	14.92	14.94	14.89	14.90	14.99	14.05	14.61	14.19	1.01	27.42
30570	14.57	14.59	14.54	14.56	14.64	14.00	14.30	14.00	0.71	22.88
31560	14.38	14.39	14.34	14.35	14.43	14.00	14.11	14.00	0.57	17.79
33210	14.15	14.15	14.11	14.12	14.18	14.00	14.00	14.00	0.56	16.71
35160	14.00	14.00	14.00	14.00	14.00	14.00	14.00	14.00	0.45	12.65

III.3.2.2 Results for benchmarking and validation of numerical models with microencapsulated PCMs

Figs. III.11a and III.11b show the results of discharging considering the test-sample filled with the microencapsulated PCM – DS 5001 X and T_{water} = 14 °C, where t_{liq} is the time required for starting the solidification process. Table III.8 shows the values of the measured variables to be used for drawing the curves shown in Figs. III.11a and III.11b.

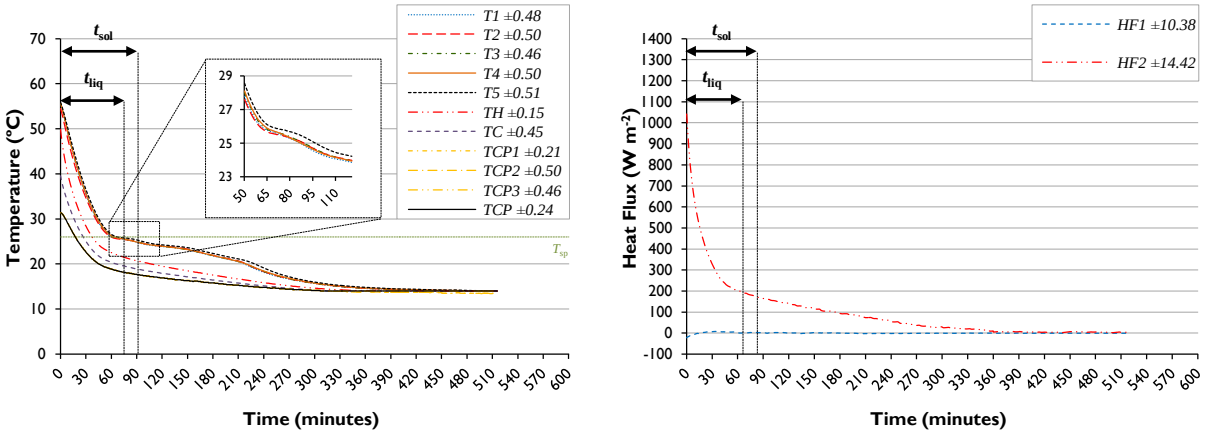

(a) (b)

Fig. III.11 Evolution of the average measured (a) temperatures and (b) heat fluxes for the discharging phase of the 5-cavities TES unit filled with the microencapsulated PCM – DS 5001 X and T_{water} = 14 °C.

Table III.8 Results for benchmarking and validation of conduction-dominated numerical models – discharging phase with T_{water} = 14 °C considering the 5-cavities TES unit filled with the microencapsulated PCM – DS 5001 X.

Time (s)	T_1 (°C)	T_2 (°C)	T_3 (°C)	T_4 (°C)	T_5 (°C)	TCP (°C)	T_H (°C)	T_C (°C)	HF_1 (W m^{-2})	HF_2 (W m^{-2})
0	55.57	54.52	55.71	55.69	55.81	31.30	49.84	39.57	-21.54	1041.54
120	54.30	53.14	54.45	54.43	54.74	31.10	46.76	37.81	-16.41	912.46
1230	40.74	39.65	40.93	40.99	41.92	25.00	32.44	28.16	3.49	428.75
2130	32.82	32.29	33.05	33.16	33.87	21.50	26.54	23.56	8.01	283.77
2700	29.19	28.90	29.42	29.53	30.10	20.00	24.26	21.79	6.26	235.81
3000	27.78	27.59	28.01	28.11	28.57	19.50	23.51	21.16	5.99	220.98
3420	26.42	26.32	26.60	26.70	27.05	19.00	22.79	20.60	4.62	206.09
3600	26.08	25.98	26.18	26.31	26.59	18.90	22.53	20.39	1.95	202.20
3780	25.86	25.77	25.92	26.03	26.26	18.70	22.30	20.17	0.67	198.36
3960	25.73	25.63	25.77	25.84	26.06	18.50	22.07	20.00	0.85	192.75
4530	25.44	25.44	25.53	25.51	25.81	18.10	21.49	19.53	2.75	180.59
4800	25.27	25.32	25.37	25.31	25.69	18.00	21.21	19.33	2.81	173.83
5280	24.93	25.05	25.03	24.96	25.42	17.70	20.80	18.97	2.68	167.00
5490	24.74	24.87	24.88	24.80	25.27	17.60	20.64	18.86	1.90	162.72
5550	24.68	24.81	24.83	24.76	25.22	17.60	20.60	18.81	1.13	161.73
6030	24.33	24.45	24.47	24.42	24.82	17.40	20.26	18.54	2.26	154.77
6120	24.27	24.39	24.40	24.36	24.75	17.30	20.21	18.50	2.76	154.45
6540	24.09	24.19	24.18	24.17	24.48	17.20	19.91	18.29	2.57	147.03
8550	23.44	23.56	23.41	23.43	23.82	16.40	18.73	17.36	0.11	120.73
9270	22.95	23.09	22.99	23.02	23.47	16.20	18.34	17.04	0.95	113.81
11610	21.22	21.36	21.28	21.30	21.76	15.50	17.16	16.13	0.24	86.83
12660	20.45	20.62	20.50	20.50	21.08	15.20	16.67	15.74	-1.99	73.34
13470	19.34	19.53	19.56	19.60	20.36	15.00	16.29	15.44	-1.84	66.89
15270	17.32	17.45	17.46	17.57	18.04	14.60	15.53	14.89	-1.09	45.18
15720	16.97	17.08	17.09	17.20	17.58	14.50	15.34	14.73	-1.14	42.56
17160	16.10	16.13	16.12	16.21	16.46	14.20	14.86	14.37	-0.57	29.16
18480	15.47	15.51	15.48	15.57	15.77	14.00	14.53	14.09	-0.28	26.47
20760	14.75	14.78	14.76	14.83	15.00	14.00	14.13	14.00	0.14	17.37
21000	14.70	14.73	14.71	14.78	14.94	14.00	14.13	14.00	-0.11	14.62
22680	14.44	14.47	14.46	14.52	14.65	14.00	14.01	14.00	-0.33	5.06
24420	14.27	14.30	14.30	14.35	14.45	14.00	14.00	14.00	-0.55	4.31
30930	14.00	14.00	14.00	14.00	14.00	14.00	14.00	14.00	-0.37	3.97

Initially, both the measured temperatures and the heat flux on the back surface of the test-sample decrease rather steeply. However, when the temperature in the PCM domain drops to the solidification temperature of the PCM, the decrease of the measured variables slows down as the latent heat is released. When the solidification of the PCMs starts no significant subcooling effect is verified. Therefore, the effect of subcooling during discharging is insignificant for the cavities filled with the microencapsulated PCM. When the solidification starts the temperatures in the PCM domain stabilize near the solidification temperature of the PCM, but after some time, a slow cooling brings the measured values to the temperature of the cooling water.

Fig. III.11a also shows that a second temperature stabilization around 24 °C appears during the discharging phase. As stated by Longeon *et al.* [263], this may be due to the solid–solid transition of the microencapsulated paraffin. The effect of the fins is depicted from the figure, since the temperature T_{H} of the front surface is always well below the temperature of the PCM bulk. The heat transfer process is dominated by conduction and no significant thermal stratification is found.

III.4 Overall addition remarks

Table III.9 summarizes the values of the main parameters presented in the sections above.

Table III.9 Values of the main parameters measured during the experiments.

PCM type	Charging			Discharging				
	t_{m} (s)	t_{reg} (s)	T_{reg} (°C)	t_{sol} (s)	t_{liq} (s)	t_{cr} (s)	t_{sc} (s)	ΔT_{sc} (°C)
RT 28 HC	16350	14850	34.5	20400	–	3510	2730	1.1
DS 5001 X	4890	4740	40.0	4740	4020	–	–	–

Regarding building applications, cavities filled with the free-form PCM – RT 28 HC are more attractive for enhancing the thermal-regulation period (t_{reg}) and for reducing the control-temperature value on the hot surface of the system (T_{reg}). On the other hand, cavities filled with the microencapsulated PCM – DS 5001 X are better for elements where it is crucial to reduce the time required for melting all the PCM within the system (t_{m}). For the same test-sample configuration and heating power level, the time required to completely melt the free-form PCM on the mid-plane of the TES unit is roughly thrice the time required for melting the microencapsulated PCM, in spite of the advection effect of natural convection in the liquid domain. Considering the total amount of energy stored and released, the free-form PCM can be used for storing more energy during a charging/discharging cycle because its heat storage capacity is higher.

III.5 Conclusion

This chapter aimed at experimentally studying the fins-enhanced heat transfer in a small PCM latent-heat TES unit, consisting of a vertical stack of rectangular cavities, during both melting and solidification processes. The main goals were to provide detailed data for benchmarking and validation of numerical models, and to discuss which PCM is better for filling the TES unit regarding different building applications. For this purpose, an experimental apparatus was built. It is essentially composed by three main modules: the heating, the cooling and the test-sample modules. The test-sample module is fixed and the heating and cooling modules are movable in order to allow the performance of heating and cooling cycles, and thus the melting and solidification of the PCM inside the TES units. During charging, a horizontal heat flux was imposed by a constant electric power in one of the vertical faces of the TES unit. During discharging, a cold-plate with a water circuit fed by a thermostatic water bath was used. The 5-cavities aluminum TES unit was filled with two kinds of PCMs: a free-form PCM (RT 28 HC) and a microencapsulated PCM (DS 5001 X).

It is concluded that during charging of the free-form PCM, (i) conduction is initially the dominant mode of heat transfer; (ii) the phase-change occurs at a characteristic temperature threshold; (iii) after some time, the natural convection flow ensues and becomes the dominant heat transfer mechanism; (iv) a thermal stratification was caused by the natural convection in the molten PCM and by the air-layer on the top of each cavity. Therefore, natural convection must be considered in every simulation. Moreover, it was concluded that conduction is the dominant mode of heat transfer during the entire charging of the microencapsulated PCM without any thermal stratification. Regarding building applications, cavities filled with free-form PCMs are more attractive to be used in systems in which the main purpose is to enhance the thermal-regulation period and to reduce the control-temperature value on the hot surface of the cavities in order to enhance the overall energy performance of the TES system. These two parameters are improved due to natural convection. On the other hand, cavities filled with microencapsulated PCMs are better for elements where it is crucial to reduce the time required for melting all the PCM. The mentioned parameters are both reduced when considering the microencapsulated PCM.

Regarding discharging, it is concluded that for both analyzed PCMs, the discharging phase is mainly governed by conduction. It is also concluded that the effect of natural convection and subcooling can be neglected when modeling microencapsulated PCMs. Regarding the free-form PCM, subcooling effect must be considered in the future simulations to well describe the heat transfer during discharging.

The vertical stack of rectangular cavities filled with PCMs (TES unit) is described and studied from its conceptual point of view. In the next chapter, a parametric study is carried out to evaluate

the influence of the aspect ratio of the cavities and the type of the PCM on both melting and solidification processes, as well as the influence of the boundary conditions imposed during the charging and discharging experiments. These experimental results are intended to be a good benchmarking reference for validating numerical models to be used in the optimization of practical applications, such as PCM-bricks, PCM-shutters, PV/PCM systems, SP/PCM systems, among other systems.

CHAPTER IV

Heat transfer through small TES units for vertical building applications: experimental study and parametric analysis

Based on the experimental setup and experimental procedure presented in Chapter III, several experiments were carried out to evaluate the thermal performance of the TES unit by varying (i) the aspect ratio of the cavities; (ii) the type of PCM, and (iii) the boundary conditions imposed during charging and discharging. This chapter provides further data, which are aimed to serve as a good benchmarking reference for the validation of numerical models to be used in the design and optimization of new TES systems for buildings. Chapter IV presents the results which are described in the paper "*Experimental evaluation of the heat transfer through small PCM-based thermal energy storage units for building applications*" by Soares *et al.* [265]. This chapter is divided into four sections. Section IV.1 introduces the problem and provides an overview of some TES systems incorporating vertical stacks of rectangular cavities filled with PCMs for buildings. Section IV.2 describes the experimental procedure for the parametric study. The description of the experiments carried out is also presented in this section. Section IV.3 presents and discusses the results obtained for both charging and discharging experiments. Finally, Section IV.4 provides the main conclusions of the parametric study.

IV.1 Introduction

In the previous chapter, an experimental setup to evaluate the heat transfer through a small TES unit was introduced. Two types of PCMs were used in the experiments: a free-form PCM and a microencapsulated PCM. To improve the heat transfer through the PCM bulk, the small TES unit was made of aluminum and provided with some horizontal fins connecting the heated/cooled vertical walls, thus forming a vertical stack of rectangular cavities. The TES unit was studied from its conceptual point of view and only one test sample with five rectangular cavities (aspect ratio A = 2.145) was investigated. Moreover, the same boundary conditions were imposed for all the charging and discharging experiments. This chapter is focused on the parametric study of the heat transfer through similar test-samples filled with the same PCMs: the free-form PCM – Rubitherm® RT 28 HC and the microencapsulated PCM – Micronal® DS 5001 X. The main goal of this chapter is to investigate the influence of the aspect ratio of the cavities and the impact of different experimental conditions on the thermal performance of the TES unit. Therefore, further experimental data for benchmarking and validation of numerical models are provided in this chapter. These results are aimed to be used in the design and optimization of vertical TES applications for buildings, such as PCM-bricks, PCM-shutters, PCM-window blinds, PCM-panels, PV/PCM systems and SP/PCM systems.

As stated in Chapter III, important results concerning the analysis of the heat transfer through a vertical stack of rectangular cavities filled with commercial free-form paraffin waxes are pointed out in several studies related with the thermal management of PV/PCM and SP/PCM systems [70,159,233–236]. It has been claimed that the thermal performance of these systems can be improved by placing a TES unit with PCMs on the panels' back to mitigate high operating temperatures. The main challenge here is to achieve lower operating temperatures with a longer thermal regulation period. The development of well instrumented and controlled experiments as the one presented in Chapter III is important to evaluate the influence of different fins-arrangements and to analyze the impact of natural convection and subcooling phenomena on the heat transfer with phase-change. Further experimental and numerical studies have been devoted to evaluate the effect of natural convection in vertical rectangular enclosures filled with free-form PCMs, such as the works presented in refs. [158,232,238–244,254,255].

As stated by Soares *et al.* [1], some of the most promising passive latent heat TES systems for buildings (for some climates and certain typologies of buildings) are those related with harnessing solar thermal energy for heating during winter and those optimized to reduce overheating during summer. It is also claimed that the development of hybrid and adaptable systems to solve the winter and summer challenges at the same time is an upcoming area of research. It is suggested that the design of portable, rotary and movable Trombe wall systems, or even shutters or window blinds systems with PCMs associated with the glazed facade, can be a good way to reduce the energy demand for both heating and cooling. These systems can integrate a vertical stack of rectangular cavities filled with PCMs in their configuration, which is the case of the exterior PCM-shutter proposed by Soares *et al.* [153] (Fig. IV.1). This TES system was designed to take advantage of solar thermal energy for winter night time indoor heating in Coimbra, Portugal (Mediterranean climate). The shutter is to be opened during the day to maximize the direct solar gains through the glass window, while charging the system by melting the PCM bulk [153]. During the night, the system is to be closed to minimize the heat losses through the window and to allow its discharging (releasing the stored energy indoors). Afterwards, the right-side and the left-side shutters can be switched to solve both the summer and the winter challenges. A two-dimensional phase-change heat diffusion model based on the enthalpy formulation was used to evaluate the performance of the PCM-shutter. The results were promising, however the influence of the natural convection, hysteresis and subcooling phenomena were not considered in the numerical model.

Alawadhi [225] proposed a different PCM-shutter system for reducing the solar heat gains through the glazed facade during the working hours in hot climates (such as the one in Kuwait). The system is made of aluminum rolling slats filled with the PCM – P116 instead of the traditional insulation foam. A numerical study was carried out using a finite element method to evaluate the

thermal effectiveness of the TES system. The results have shown that the PCM-shutter can reduce the heat gains through the windows by almost 24% (considering a thickness of about 0.03m for the system) in comparison with the traditional foam-system. Further exterior window shading elements with PCMs were studied by Mehling [266] and Buddhi *et al.* [267].

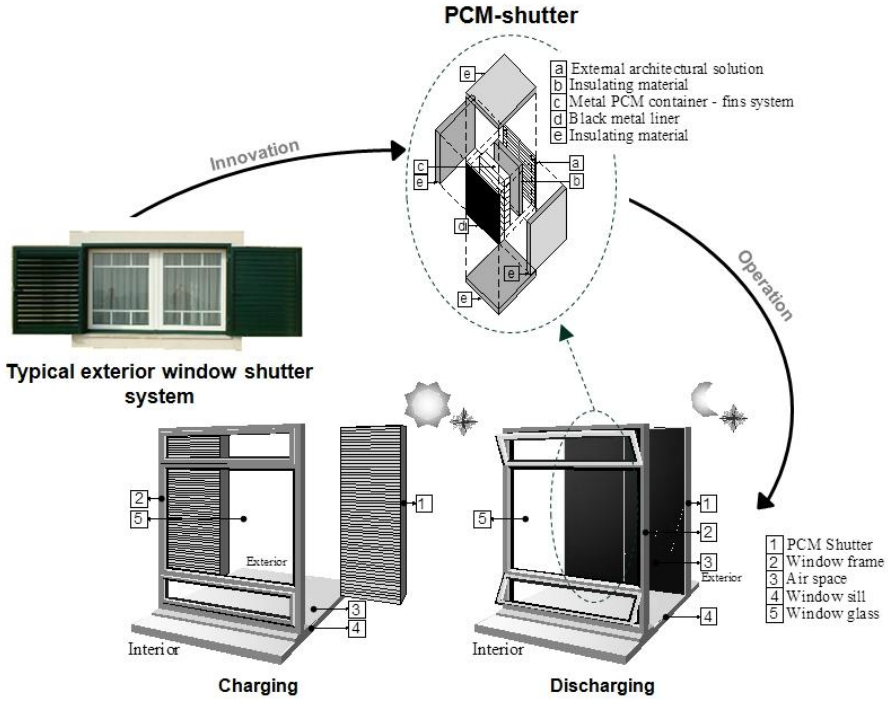

Fig. IV.1 Sketch of the configuration and operation of the PCM-shutter system proposed by Soares *et al.* [153].

Another TES system to make use of solar thermal energy – interior PCM-window blinds – was proposed from its conceptual point of view by Soares *et al.* [226] and Soares [227] (Fig. IV.2). The system is intended to operate cyclically and it is composed by a set of rotary vertical or horizontal segments, which can rotate around their vertical or horizontal shafts. Moreover, all the segments might be assembled together and collected within the wall. Each segment section consists of an aluminum cavity to be filled up with PCMs. The aluminum enclosures are covered on one side with an insulation layer, which is essential to control the direction of the heat flux, especially during the discharging phase of the system, as shown in Fig. IV.2. In Mediterranean climates, during clear winter days with low temperature, solar energy is an abundant resource. Accordingly, the metallic cavities filled with PCMs must face the Southern glazed facade during the day to collect the solar heat gains through the window and to allow the charging of the system (melting of the PCM bulk). During the night, the blinds must be rotated around their shafts so that the insulation layer will face the window to minimize the heat losses and to allow the discharging of the system indoors. During summer, or even during winter days whenever occupants want to benefit from direct solar gains or

daylighting, the window blinds can be adjusted or assembled together and collected within the wall. With this configuration, the PCM-window blinds system shows many advantages in comparison to a traditional Trombe wall: (*i*) the system is movable; (*ii*) the huge mass of the Trombe wall and the big amount of material can be replaced by a thin layer of metallic cavities filled with PCMs; (*iii*) some performance problems associated with the direction of the heat flux and the heat losses during winter nights are overcome by making use of the insulation layer combined with the rotary nature of the system; (*iv*) the daylighting can be controlled if desired, and (*v*) the system does not need any external protection during summer to avoid overheating, or during winter nights to avoid heat losses.

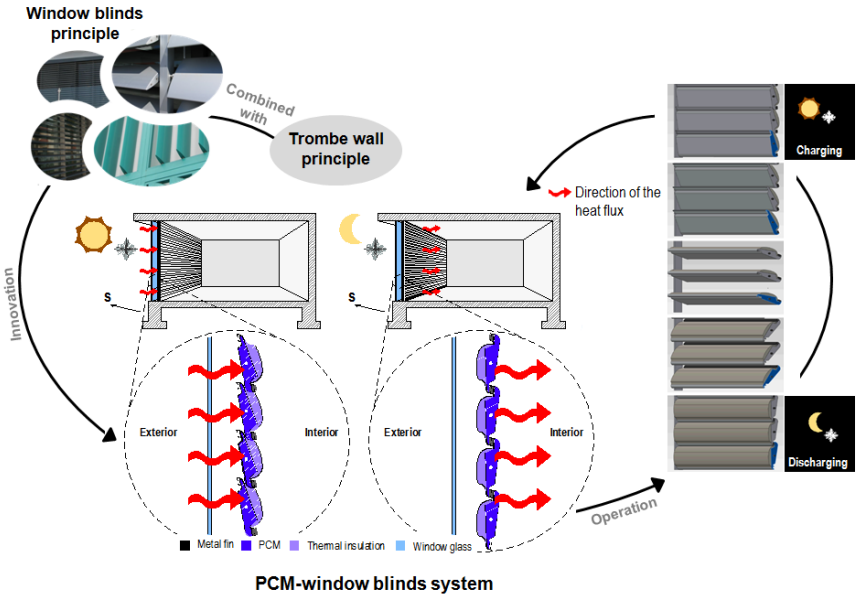

Fig. IV.2 Sketch of the configuration and operation of the interior PCM-window blinds system proposed in refs. [226] and [227].

The first prototype of a PCM-window blinds system was recently presented by Silva *et al.* [228]. An outdoor full-scale lightweight test cell composed by two compartments placed side-by-side was built in Aveiro, Portugal (Mediterranean climate). The interior window blinds system was associated to the southward window facade. In the PCM-enhanced compartment, the cavities of the blinds were filled up with the free-form PCM – Rubitherm® RT 28 HC. In the reference compartment, the cavities were considered empty. The indoor temperature was monitored from 28th January to 6th February, 2014. The results have shown that, for the proposed case study, the PCM-window blinds system can be used to reduce winter overheating problems in lightweight construction with big windows facing south. The maximum indoor air temperature measured in the reference room was about 53.8 °C in comparison with the 37.2 °C measured in the PCM-enhanced room. In another paper, the same research team presented the results of a similar experimental

study carried out during summer to evaluate the performance of the PCM-window blinds prototype during this season [229]. The results showed that the compartment with the PCM-window blinds system has a thermal regulating capacity of the indoor temperature of about 18–22%. The maximum and minimum temperature peaks decreased by 6% and 11%, respectively, in comparison with the reference compartment. Although the promising results, more research should be conducted in order to optimize: (*i*) the thickness and shape of the cavities; (*ii*) the thickness of the insulation layer; (*iii*) the inclusion of metallic fins to enhance the heat transfer surface; (*iv*) the melting-peak temperature of the PCM, and (*v*) the quantity and type of PCM for filling up the macrocapsules. Moreover, further work is needed to evaluate the performance of this system considering the influence of internal loads and air-conditioning set points, other climates, seasons, and typologies of construction. The use of solar thermal energy for reducing heating energy demand during winter as proposed by Soares *et al.* [227] has also to be further evaluated from both numerical and experimental points of view. In this context, experimental results like the ones presented in this chapter are important for the validation of numerical models to be used in the optimization of this kind of system.

Another TES system incorporating PCM-filled rectangular cavities in its structure is the PCM-brick proposed by Silva *et al.* [222] and further studied by Vicente *et al.* [223]. This TES system is associated with the opaque envelope of the building. It is composed by a typical Portuguese hollow clay brick enhanced by an aluminum macrocapsule filled with the free-form PCM – Rubitherm® RT 18 (Fig. IV.3). The experimental results were promising regarding the attenuation and time delay of the indoor air temperature fluctuation when considering this kind of PCM-enhanced masonry wall. However, more research should be carried out to optimize the configuration of the metallic rectangular enclosure itself to ensure that the PCM volume is optimized.

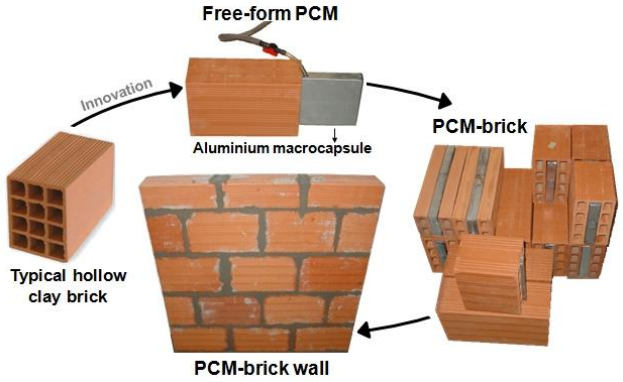

Fig. IV.3 Sketch of the configuration of the PCM-brick system adapted from refs. [222] and [223].

All of the TES systems described above are not optimized yet regarding the configuration of the TES unit itself. This would greatly benefit from accurate numerical models that must take into

account several features such as: (*i*) the aspect ratio of the cavities; (*ii*) the influence of adding fins with different sizes and shapes to enhance the heat transfer surface; (*iii*) the non-linear behavior of the melting front and the presence of a moving boundary where heat and mass balance conditions have to be met, in the case of free-form PCMs; (*iv*) the hysteresis of the PCM; (*v*) the subcooling problem; (*vi*) the crystalline segregation; (*vii*) the volume expansion of the PCM during melting; (*viii*) the natural convection in the molten free-form PCM and in the air-layer to be used to accommodate the PCM volume expansion in the cavity; (*ix*) the motion of the solid in the melt in the case of free-form PCMs, and (*x*) the variation of density and other thermophysical properties of the PCM along with the temperature evolution. As pointed out in Chapter III, due to the difficulties of considering all of these features when modeling the heat transfer with solid–liquid phase-change in rectangular cavities, further experimental studies as the one presented in this chapter are required to evaluate which phenomena must be considered and, on the other hand, which ones can be neglected or simplified when a numerical solution is attempted.

IV.2 Experimental procedure

Fig. IV.4 shows the three configurations of the TES unit considered in the parametric study.

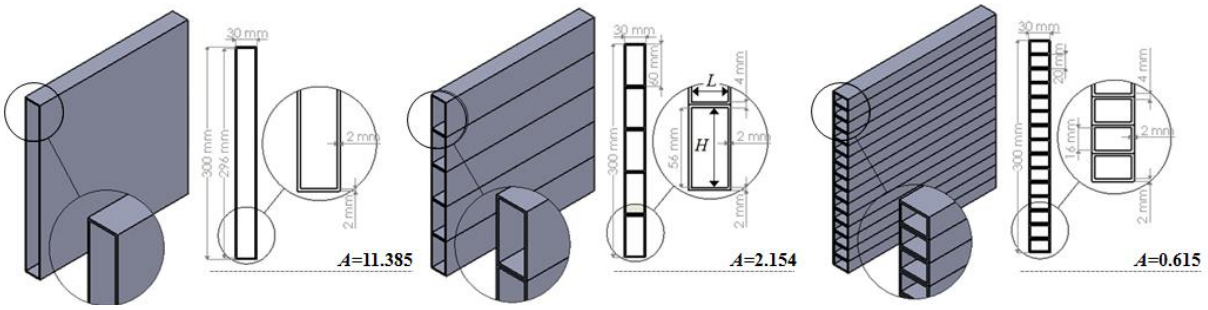

Fig. IV.4 Sketch of the three aluminum test-samples used as PCM containers: (a) 1 single rectangular cavity (A = 11.385); (b) 5-cavities (A = 2.154); (c) 15-cavities (A = 0.615).

The same experimental setup, instrumentation and procedures described in Chapter III are used in the parametric analysis. As explained in Section III.2.2, before starting a charging experiment, the TES unit is pre-cooled at 13 °C and the hot-plate is pre-heated at 55 °C. The heating module is then moved towards the fixed test-sample module and, at the same time, the cooling module is pulled back and replaced by a thermal insulation board. The power level is kept constant during each experiment. When the temperature within the PCM bulk reaches 55 °C, the charging experiment is

stopped, and a cooling experiment starts. Before the cooling experiment starts, the cold-plate is pre-cooled at the temperature selected for the experiment (temperature of the thermo-regulated water flow, T_{water}). The heating module is then pulled back and replaced by a thermal insulation board. Simultaneously, the cooling module is moved towards the fixed test-sample module. The discharging experiment is stopped when the temperature measured in the mid-plane of the TES unit reaches the value specified on the thermostat of the cold water bath. In the parametric study, the effects of the following parameters are evaluated:

- the type of PCM – two PCMs are tested: the free-form PCM – Rubitherm® RT 28 HC and the microencapsulated PCM – Micronal® DS 5001 X;
- the aspect ratio of the cavities (and number of fins) – three different test-samples are used (Fig. IV.4);
- the power input level – for the charging experiments, the power input level is set at 34 W and 68 W (power density values of about 378 W m^{-2} and 756 W m^{-2}, respectively);
- the temperature of the thermo-regulated water flow – four temperatures are considered for the discharging experiments: 14, 17, 20 and 23 °C.

A total of 12 charging and 21 discharging experiments were carried out as shown in Fig. IV.5. Each experiment was repeated thrice to check the repeatability of the results as explained in Chapter III.

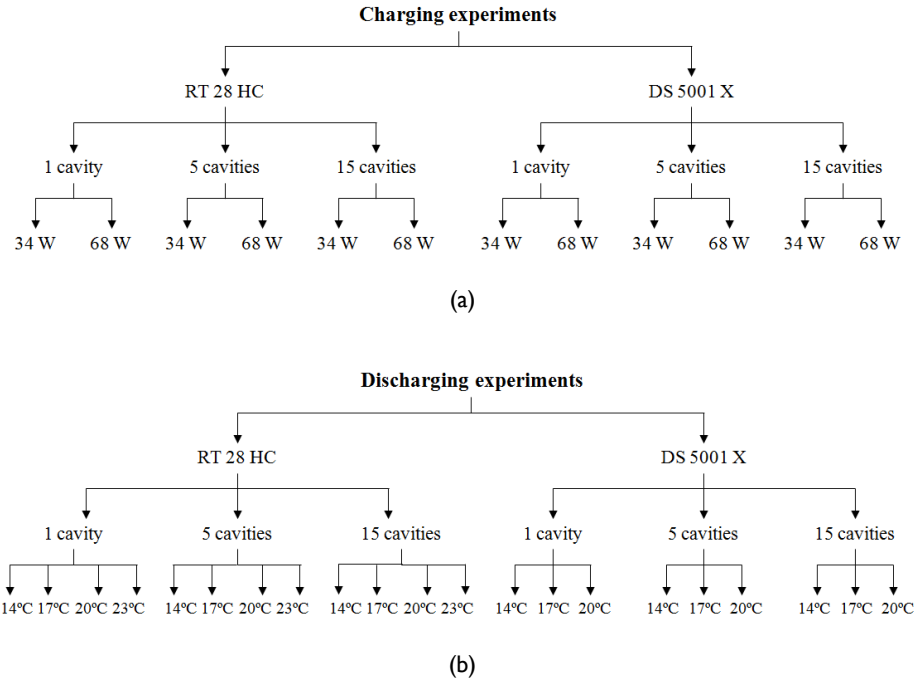

Fig. IV.5 Sketch of the parametric configurations for the (a) charging and (b) discharging experiments.

IV.3 Results and discussion

IV.3.1 Charging phase

Fig. IV.6 depicts the time evolutions of the measured temperatures from the upper (T_1) to the bottom points (T_5) in the mid-plane of the TES unit filled with the free-form PCM, for different cavity aspect ratios and power levels. The transient evolutions of the measured average temperatures on both the front (T_H) and back (T_C) surfaces of the TES unit are also shown for each charging experiment, as well as the evolution of THP. This figure shows three different phases during the charging process from 13 up to 55 °C, with storage of (i) sensible heat (solid); (ii) latent heat (solid–liquid phase-change); and (iii) sensible heat (liquid). Like in Section III.3.1.1, three parameters are defined to characterize the charging phase: (i) T_{reg} is the value of the control-temperature reached on the hot surface of the TES unit; (ii) t_{reg} is the thermal-regulation period, and (iii) t_m is the time required for complete melting the PCM in the mid-plane of the cavities.

The results show that adding fins increases the heat transfer rate to the PCM bulk, reducing the values of T_{reg} and t_{reg}. Moreover, it also reduces the effect of natural convection and the thermal stratification, leading to a more uniform temperature distribution in the TES unit. Natural convection plays an important role after the first stages of melting, which are dominated by conduction. As the phase-change process continues, buoyancy forces induce the motion of the fluid due to the temperature gradient. Therefore, natural convection enhances the melting process in the cavities from top to bottom, causing a significant thermal stratification. The buoyancy effects become progressively more significant at the later stages of the melting process.

The best relationship between the aspect ratio of the cavities and the convection flow, when using free-form PCMs (such as the RT 28 HC), depends on the purpose for which the TES unit is to be used. If the main goal is to reduce the value of the control-temperature on the hot surface of the unit (T_{reg}) and the time required for complete melting the PCM (t_m), more fins should be added to increase the heat transfer rate to the PCM bulk. On the other hand, if the main purpose is to increase the thermal-regulation period on the hot surface of the cavity (t_{reg}), the natural convection flow should be enhanced and the number of fins should be reduced. It should be remarked that the higher the number of fins, the heavier the system, which can be problematic for some vertical building applications. Moreover, the higher the numbers of fins, the lower the volume of PCM, and less energy will be stored and released during charging and discharging, respectively.

The heat transfer process is also very influenced by the imposed power level. As expected, for the same test-sample configuration, the greater the power level, the shorter the time required to

completely melt the PCM and likewise the thermal-regulation period. Similar results regarding the influence of the power level were attained from the experiments with the microencapsulated PCM.

Fig. IV.7 shows the same monitored temperatures obtained in a similar series of charging experiments considering the TES units filled up with the microencapsulated PCM – DS 5001 X.

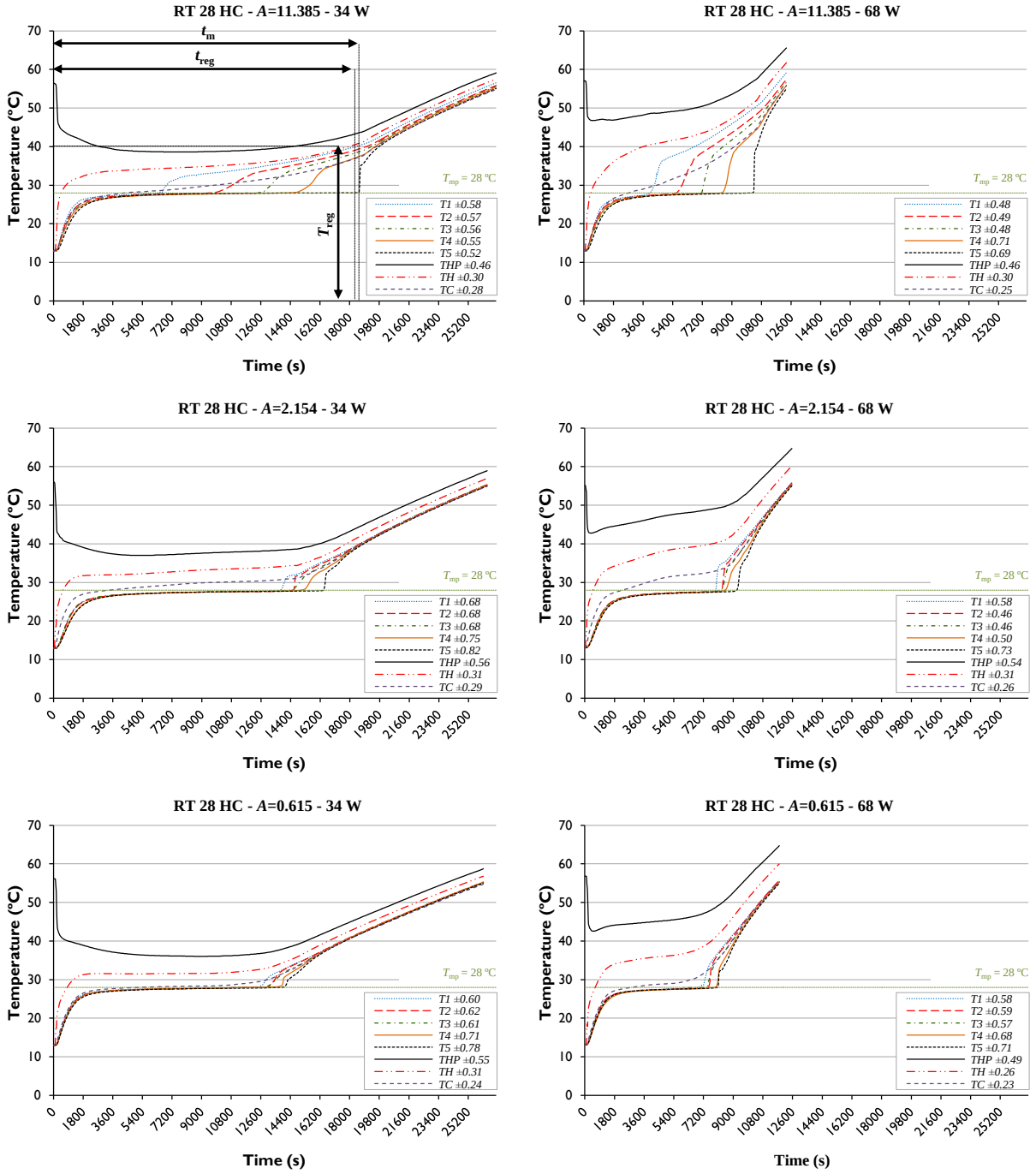

Fig. IV.6 Evolution of the measured average temperatures during charging for different cavity aspect ratios and power levels, considering the TES units filled with the free-form PCM – RT 28 HC.

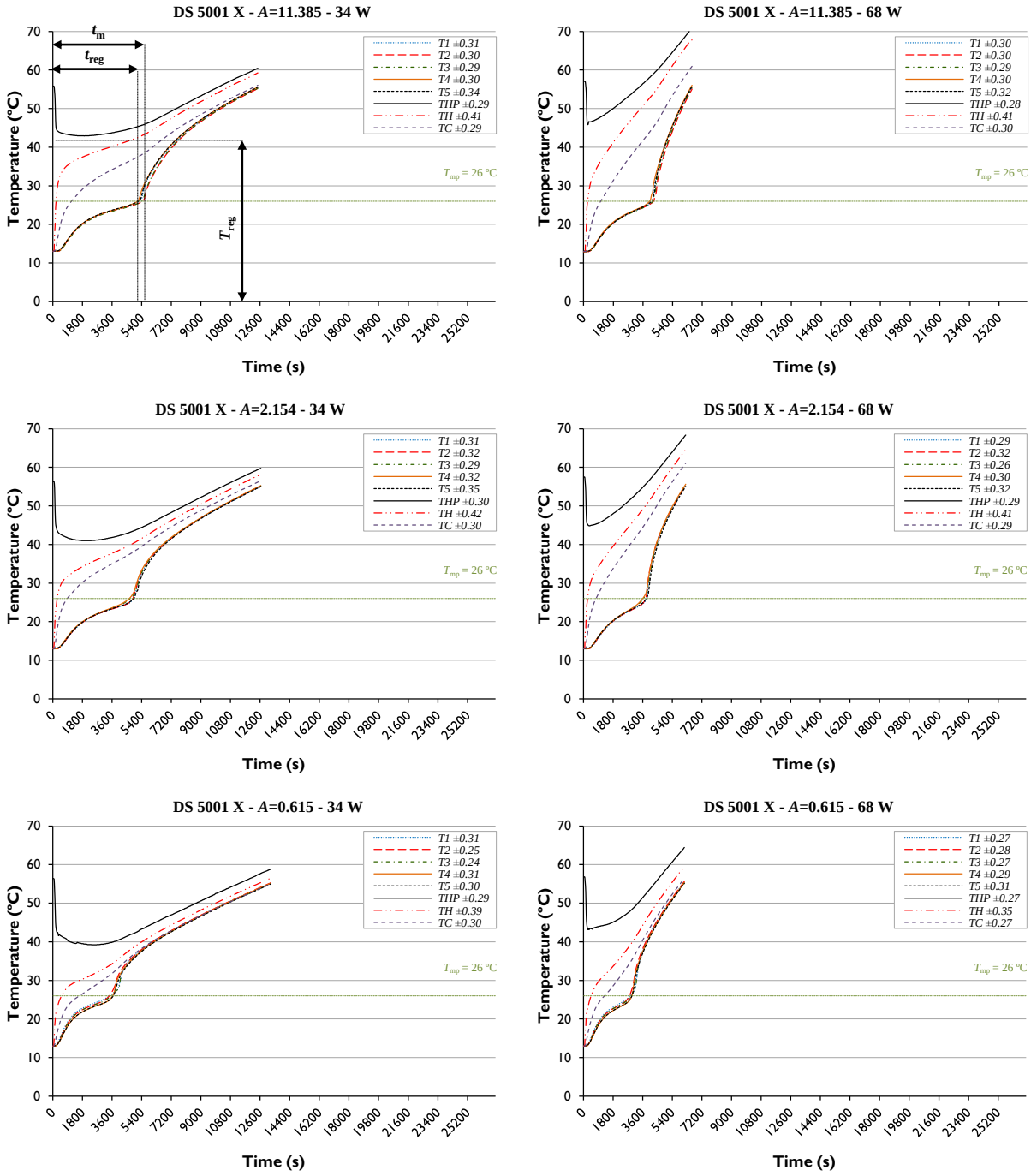

Fig. IV.7 Evolution of the measured average temperatures during charging for different cavity aspect ratios and power levels, considering the TES units filled with the microencapsulated PCM – DS 5001 X.

In this case, conduction is the only heat transfer mechanism across the micro-porous medium during the entire process. Therefore, no significant thermal stratification effect is observed. The influence of decreasing the aspect ratio of the cavities follows the same trend as with the free-form PCM, *i.e.*, a reduction of the time required for the charging process, as a result of the increased rate of heat transfer to the PCM (whose overall volume in the system is smaller). By comparing Figs

IV.6 and IV.7, it is observed that, for the same test-sample configuration and heating power level, the time required to completely melt the free-form PCM in the mid-plane of the TES unit is roughly thrice the time required for melting the microencapsulated PCM, in spite of the advection effects of natural convection in the free-liquid phase. This is mainly due to the significantly lower latent heat of the microencapsulated PCM, and also to its lower sensible heat capacity, for equivalent volumes contained in the TES unit.

Fig. IV.8 shows the influence of the aspect ratio of the cavities on the three parameters defined above for characterizing the charging process (for each PCM and power level considered in the experiments). Cavities filled with free-form PCMs (such as the RT 28 HC) are more attractive to be used in systems in which the main purpose is to enhance the thermal-regulation period (t_{reg}), and to reduce the control-temperature value on the hot surface of the TES unit (T_{reg}). Photovoltaic panels are a good example of systems where such effects can improve the overall energy performance of the system. On the other hand, cavities filled with microencapsulated PCMs (such as the DS 5001 X) are more interesting for elements where it is crucial to reduce the time required for melting all the PCM (t_m). A good example of this kind of systems can be construction solutions (like PCM-bricks, PCM-shutters, etc.) designed to store solar thermal energy during the day to be released afterwards during the night.

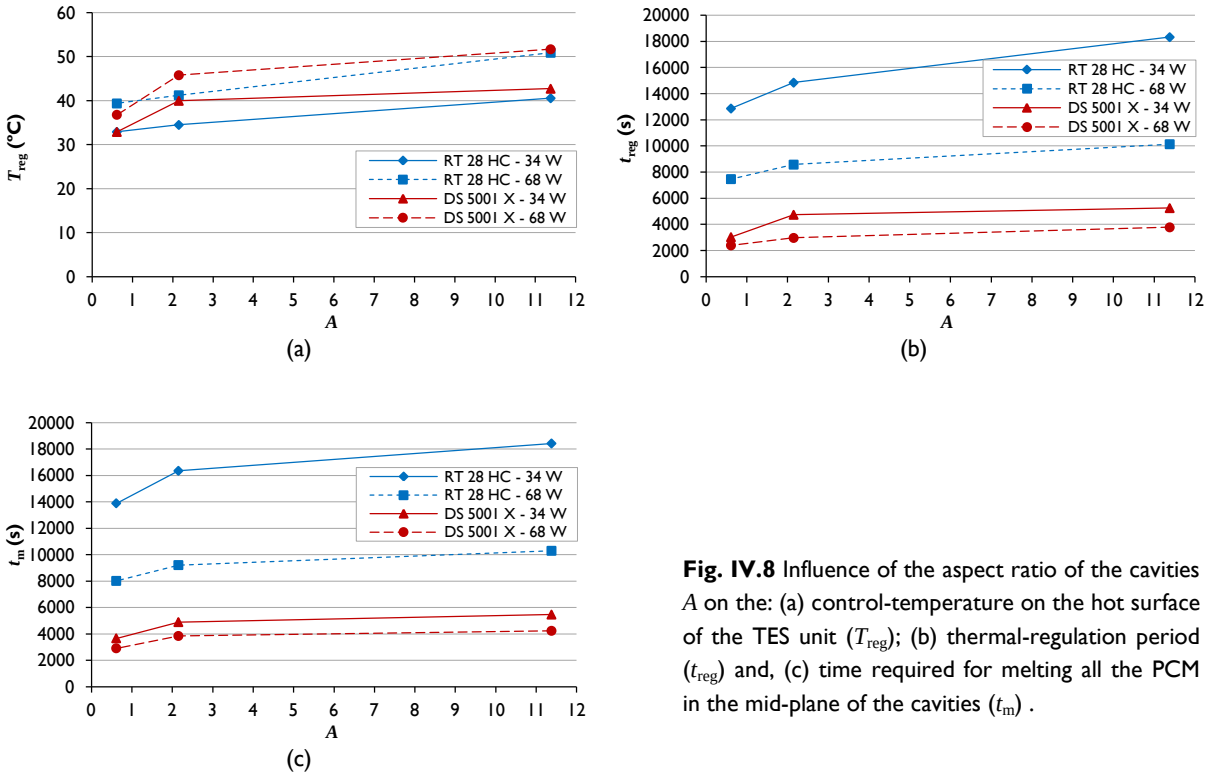

Fig. IV.8 Influence of the aspect ratio of the cavities A on the: (a) control-temperature on the hot surface of the TES unit (T_{reg}); (b) thermal-regulation period (t_{reg}) and, (c) time required for melting all the PCM in the mid-plane of the cavities (t_m) .

IV.3.2 Discharging phase

Figs. IV.9, IV.10 and IV.11 show the transient evolution of the measured average temperatures for the discharging phase of the 1, 5 and 15-cavities TES units, respectively, filled with the free-form PCM, considering different temperatures for the cooling water (T_{water}).

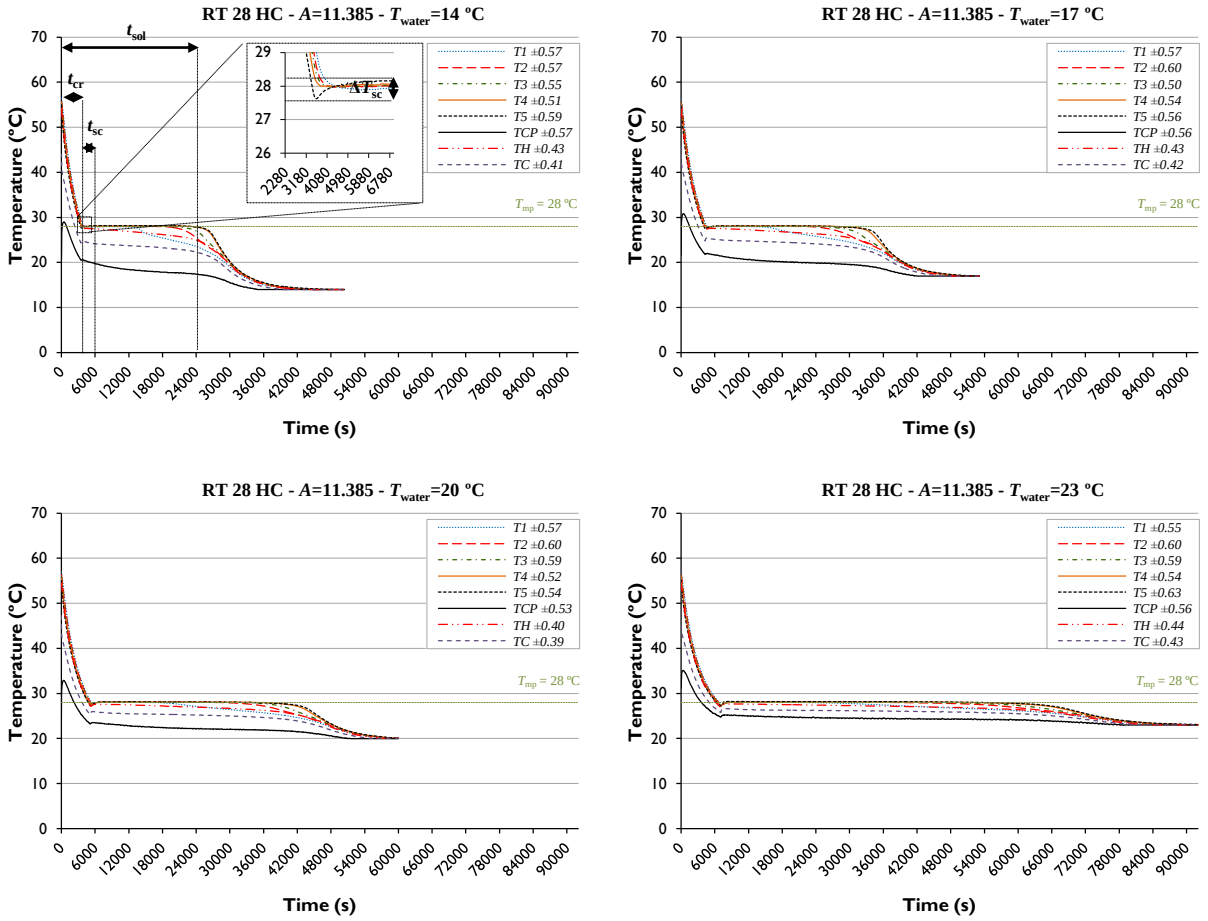

Fig. IV.9 Evolution of the measured average temperatures during discharging: single-cavity TES unit (A =11.385) filled up with the free-form PCM – RT 28 HC and different values of T_{water}.

As described in Chapter III, four parameters are defined for characterizing the discharging process of the free-form PCM: (*i*) t_{cr} is the time required for starting the crystallization process; (*ii*) t_{sc} is the period during which subcooling occurs, (*iii*) ΔT_{sc} is the difference between the solidification temperature of the PCM (T_{sp}) and a lower temperature reached by the PCM at the end of the initial sensible cooling, due to the subcooling (T_{sp}^{*}), and (*iv*) t_{sol} is the time required for solidifying all the PCM in the mid-plane of the cavities. The results show the three phases during the discharging process from 55 °C down to T_{water}: (*i*) sensible heat (liquid); (*ii*) latent heat (liquid–solid phase-change); and (*iii*) sensible heat (solid).

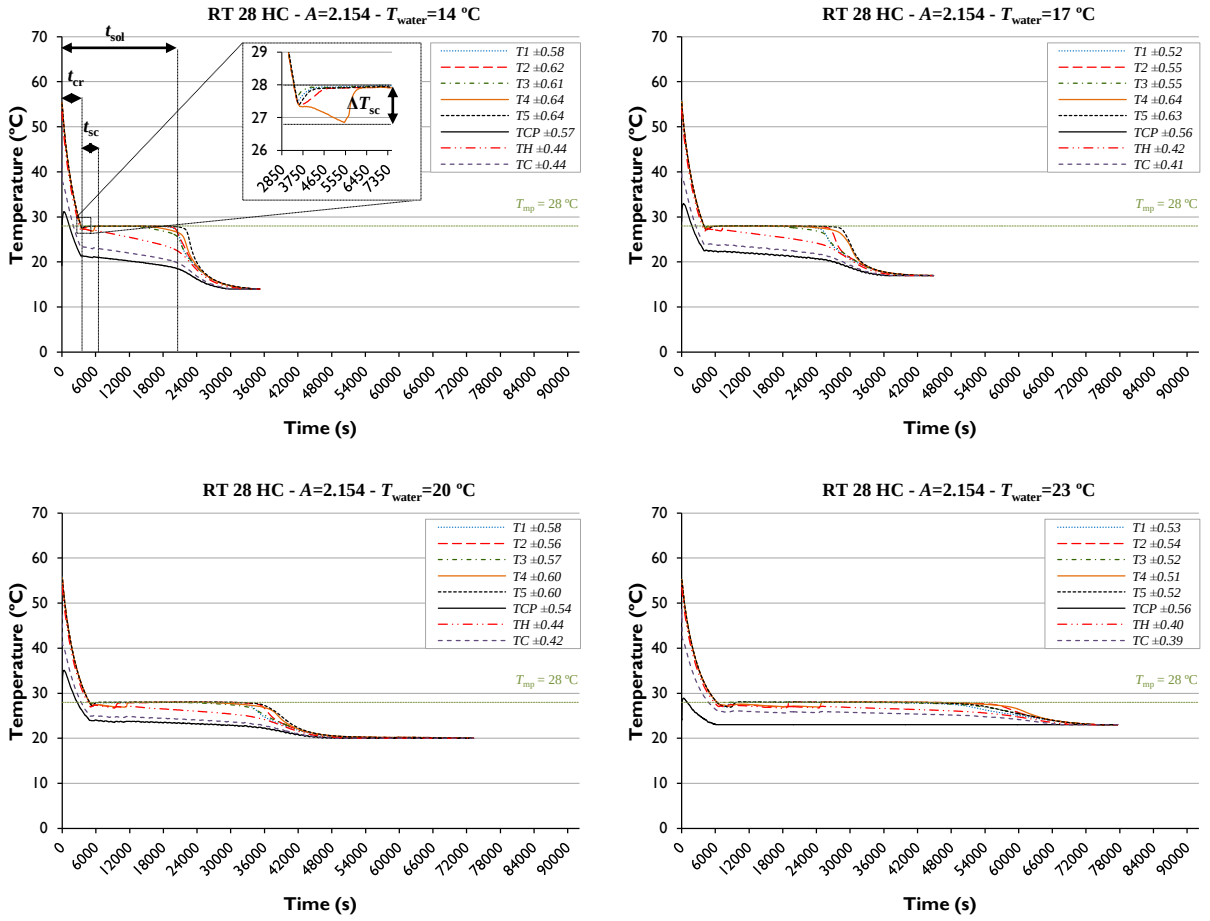

Fig. IV.10 Evolution of the measured average temperatures during discharging: 5-cavities TES unit (A = 2.154) filled up with the free-form PCM – RT 28 HC and different values of T_{water}.

The results show that the discharging process is globally dominated by conduction. In comparison with the charging process, natural convection does not play a significant role during the first cooling period of the solidification process (sensible heat transfer – liquid phase). However, a remarkable thermal stratification is observed as the solidification ends, but it is inverted: T_1 is always the first one to drop down from the phase-change temperature and, in most cases, the end of solidification in the mid-plane occurs from top to bottom. This feature is more pronounced in the single-cavity container where T_1 drops down much earlier than T_2 and the remaining temperatures on the mid-plane of the TES unit. Like in the charging experiments, the main promoter of the top-to-bottom progression of the phase-change front may be the air-layer on top of the cavity, which will cool down quicker in the first stage and will always be colder than the PCM (at some intermediate value between T_H and T_C). This can be better understood, if one thinks that: (*i*) this air-layer is being cooled by three surfaces (the fin, the top wall, and both the front and back walls), with a much higher surface area-to-volume ratio; (*ii*) its thermal diffusivity (≈ 25 mm² s⁻¹) is much greater than that of the liquid PCM (≈ 0.12 mm² s⁻¹), and (*iii*) the free convection motion keeps the liquid PCM almost

uniformly at the phase-change temperature during the solidification period. Further research must be carried out to better characterize the thermal stratification after the end of solidification. However, the results show that natural convection in both liquid PCM and air-layer domains must be considered in modeling to well describe the heat transfer during discharging of free-form PCMs.

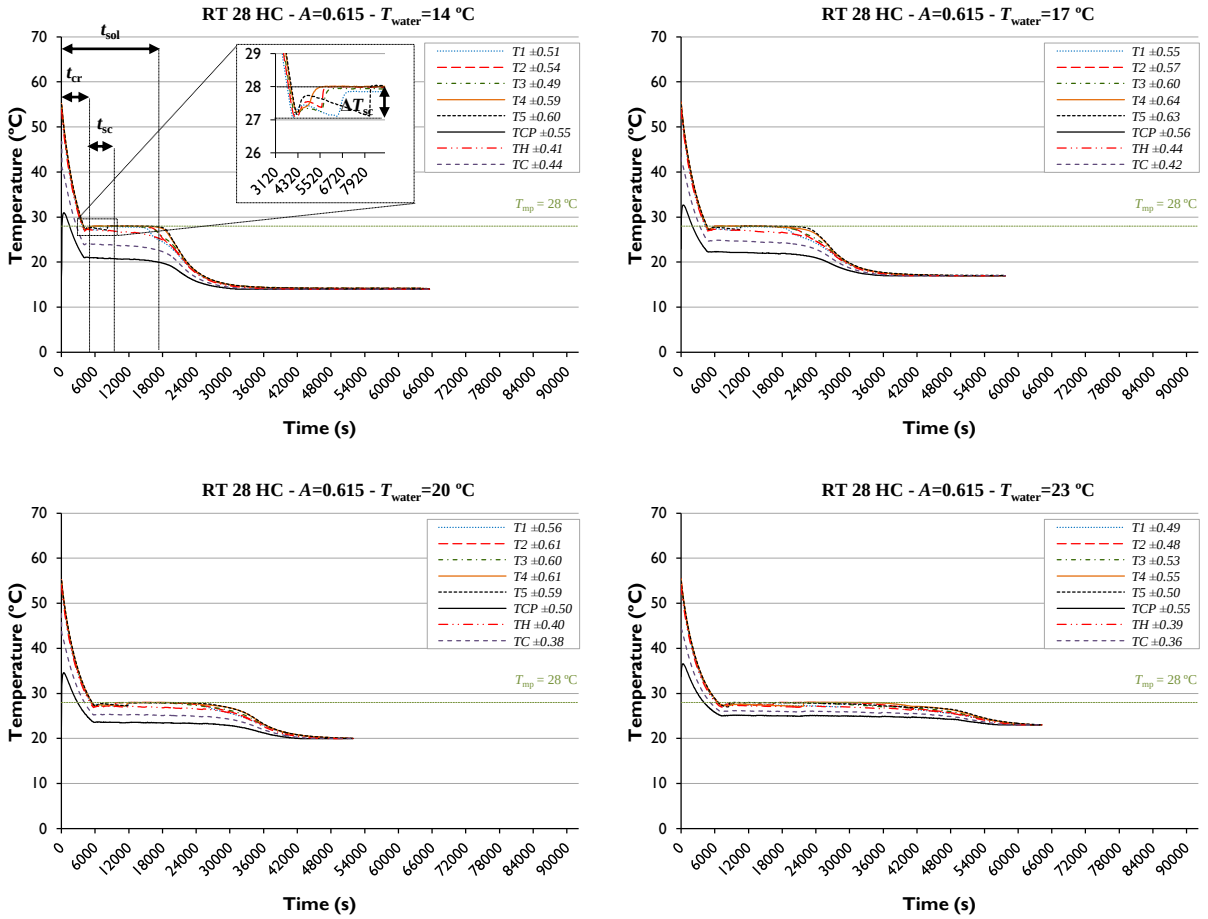

Fig. IV.11 Evolution of the measured average temperatures during discharging: 15-cavities TES unit (A = 0.615) filled up with the free-form PCM – RT 28 HC and different values of T_{water}.

Fig. IV.12 shows the relation between the aspect ratio of the cavities and the time required for starting the crystallization process (t_{cr}) for the experiments with the free-form PCM. The higher the value of the cooled water (T_{water}), the lower the heat transfer rate during the first period of the discharging process and the higher the value of t_{cr}. Moreover, when comparing the results achieved for the single-cavity and the 5-cavities TES units, it was verified that adding fins reduces the time required for starting the crystallization process. This is mainly due to the improvement of the heat transfer rate by conduction. On the other hand, when passing from 5 to 15 cavities, adding fins increases the time required for starting crystallization. This change is caused by the enhancement of

the subcooling effect, *i.e.*, there is a point when adding more fins cannot compensate the reduction of the value of the temperature below the phase-change temperature to start crystallization and more time is required to attain that temperature. Therefore, increasing the heat transfer rate by adding more fins can increase the subcooling effect by reducing the temperature required to start crystallization.

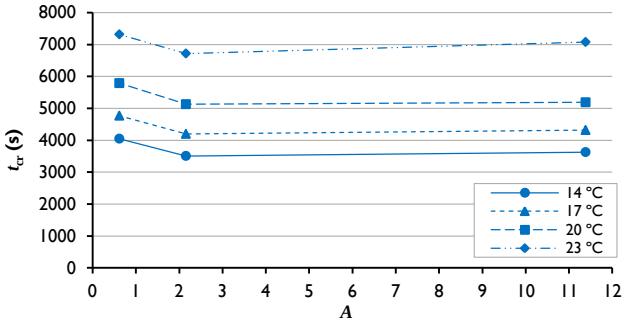

Fig. IV.12 Influence of the aspect ratio of the cavities A on the time required for starting the crystallization process (t_{cr}). Discharging experiments with the free-form PCM – RT 28 HC.

Fig. IV.13 shows the relation between the aspect ratio of the cavities and the value of ΔT_{sc}. It can be seen that ΔT_{sc} is higher for the 5-cavities test sample. Adding fins reduces the influence of the cooled water boundary condition on the ΔT_{sc} value. Fig. IV.14 shows the influence of the aspect ratio of the cavities on the subcooling period (t_{sc}) for the experiments with the free-form PCM. It is concluded that, for the same number of fins, the higher the solidification rate, the lower the duration of subcooling. This tendency is more significant for the 5 and 15-cavities test samples. Therefore, the value of t_{sc} can be reduced by decreasing the temperature of the cooled water. On the other hand, for the same value of T_{water}, the higher the heat transfer rate during the discharging phase, the longer the subcooling period. Therefore, increasing the number of fins enhances subcooling effect in the free-form PCM by enhancing the value of t_{sc}.

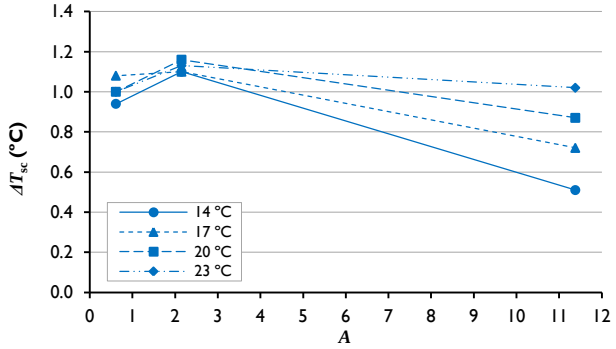

Fig. IV.13 Influence of the aspect ratio of the cavities A on the difference between the solidifying temperature of the PCM and the dropped temperature due to subcooling (ΔT_{sc}). Discharging with the free-form PCM – RT 28 HC.

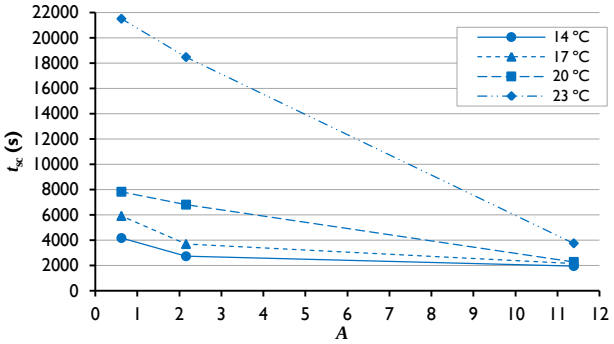

Fig. IV.14 Influence of the aspect ratio of the cavities A on the subcooling period (t_{sc}). Discharging experiments with the free-form PCM – RT 28 HC.

Figs. IV.15, IV.16 and IV.17 show, respectively, the evolution of the measured temperatures for the discharging phase of the single, 5 and 15-cavities TES units filled with the microencapsulated PCM – DS 5001 X, considering different values of T_{water}. It is observed that a second temperature stabilization around 24 °C appears. This transition is more significant for the experiments with lower cooling rates during the discharging process, *i.e.*, experiments with higher value of the cooling water temperature or with lower numbers of fins.

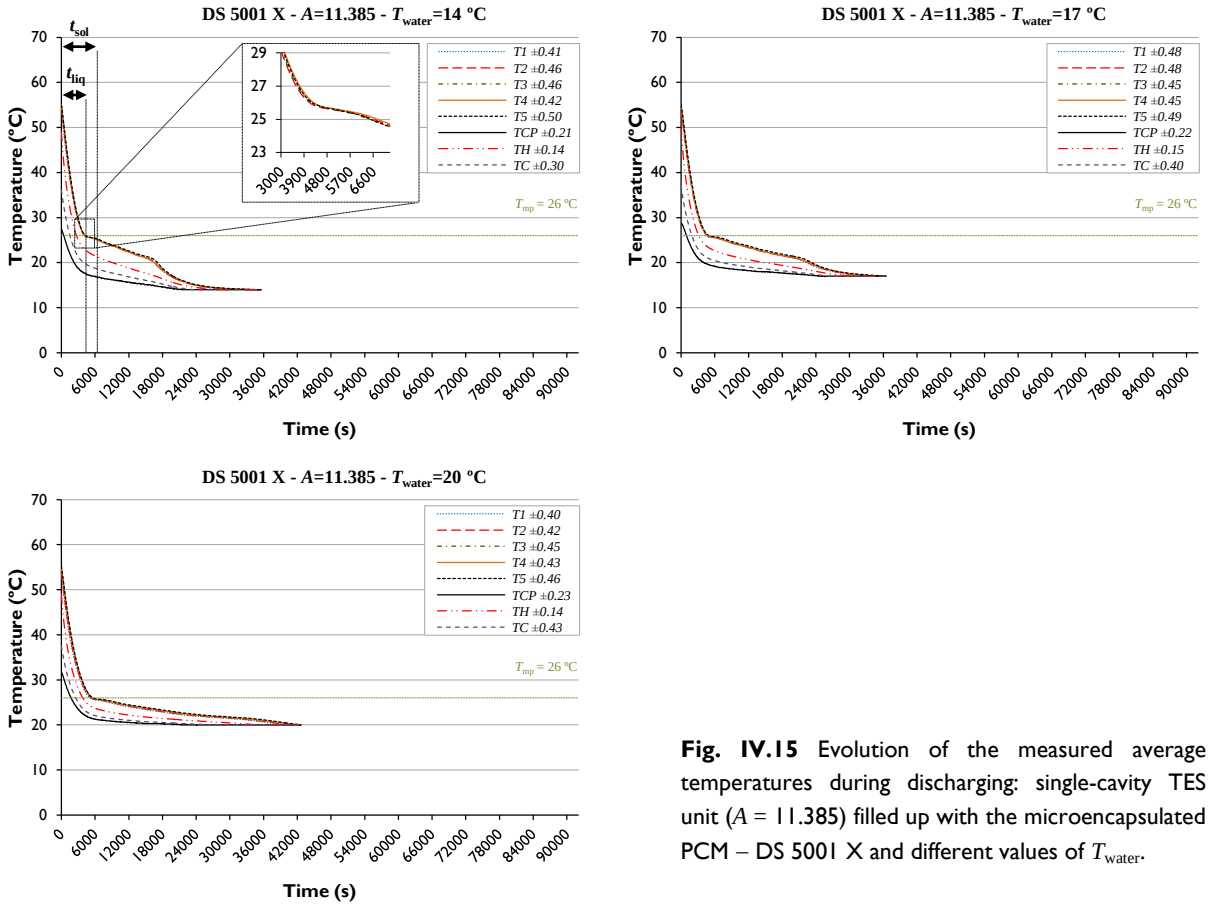

Fig. IV.15 Evolution of the measured average temperatures during discharging: single-cavity TES unit (A = 11.385) filled up with the microencapsulated PCM – DS 5001 X and different values of T_{water}.

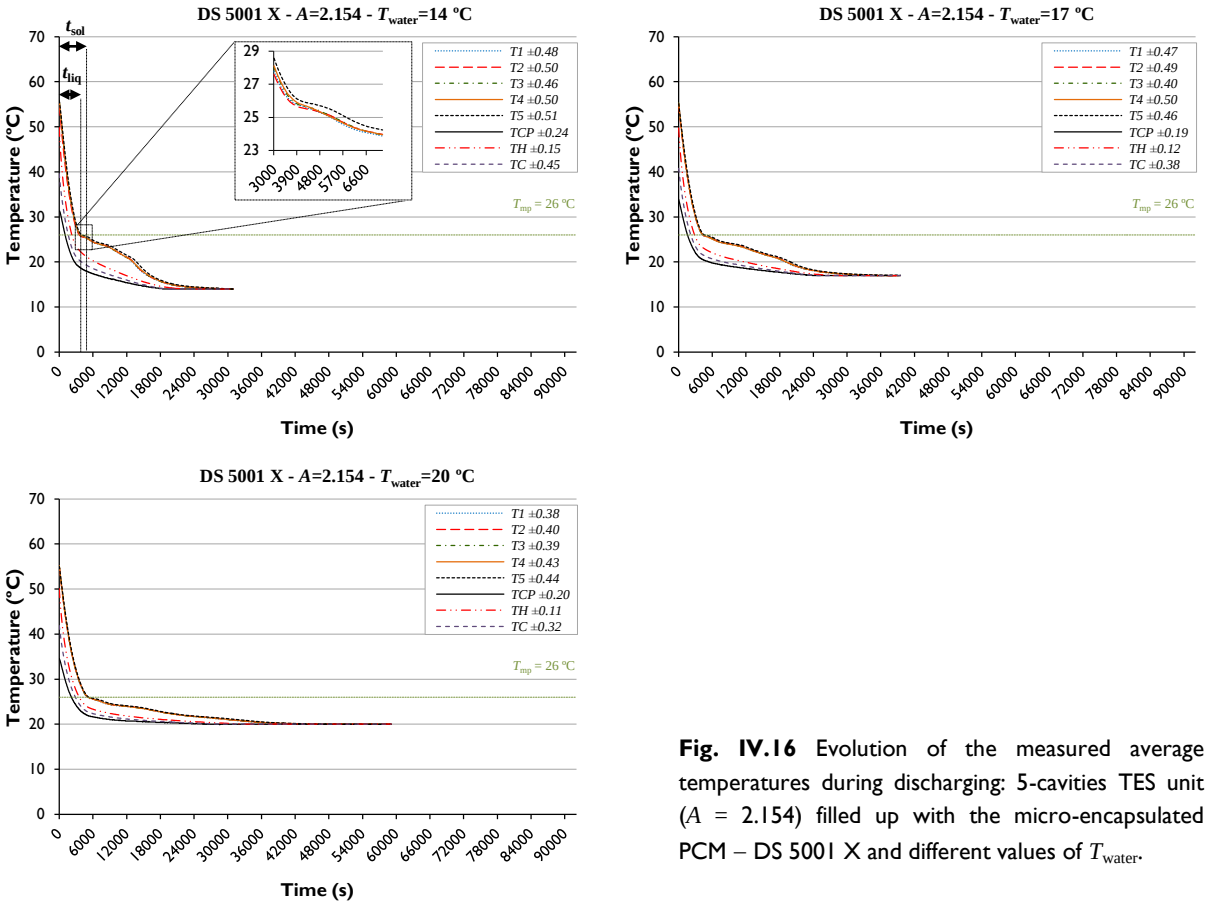

Fig. IV.16 Evolution of the measured average temperatures during discharging: 5-cavities TES unit (A = 2.154) filled up with the micro-encapsulated PCM – DS 5001 X and different values of T_{water}.

Fig. IV.18 shows the influence of the aspect ratio of the cavities on the time required for starting the solidification process (t_{liq}), considering the experiments with the microencapsulated PCM. It can be seen that the value of t_{liq} can be reduced either by increasing the number of fins or lowering the temperature of the cooling water, because both parameters increase the rate of heat removal from the PCM.

Fig. IV.19 shows the influence of the aspect ratio of the cavities on the phase-change temperature achieved after subcooling (T_{sp}^{*}) for all the experiments. For the free-form PCM, the higher the number of fins, the lower the value of the phase-change temperature after subcooling. Hence, increasing the heat transfer rate by adding more fins increases the subcooling effect by reducing the value of the phase-change temperature after subcooling. In this case, the difference between the melting and the solidifying temperature is increased, and the hysteresis effect turns out to be more significant. For the microencapsulated PCM, the higher the number of fins, the higher the value of the phase-change temperature because no subcooling occurs.

Fig. IV.20 shows the relationship between the aspect ratio of the cavities and the time required for solidifying all the PCM in the mid-plane of the cavities (t_{sol}) for all the experiments.

Results show that increasing the number of fins undoubtedly enhances the solidification rate and reduces the time required for solidifying the PCM in the mid-plane of the TES unit. Moreover, the lower the value of the cooled water boundary condition, the higher the heat transfer rate and the lower the time required for solidifying the PCM. The discharging phase can be problematic when considering building applications, mainly when the stored energy has to be released during a relatively short period of time. Therefore, adding fins is unquestionably a good technique for improving the release of the stored energy by improving the solidification rate during the discharging process.

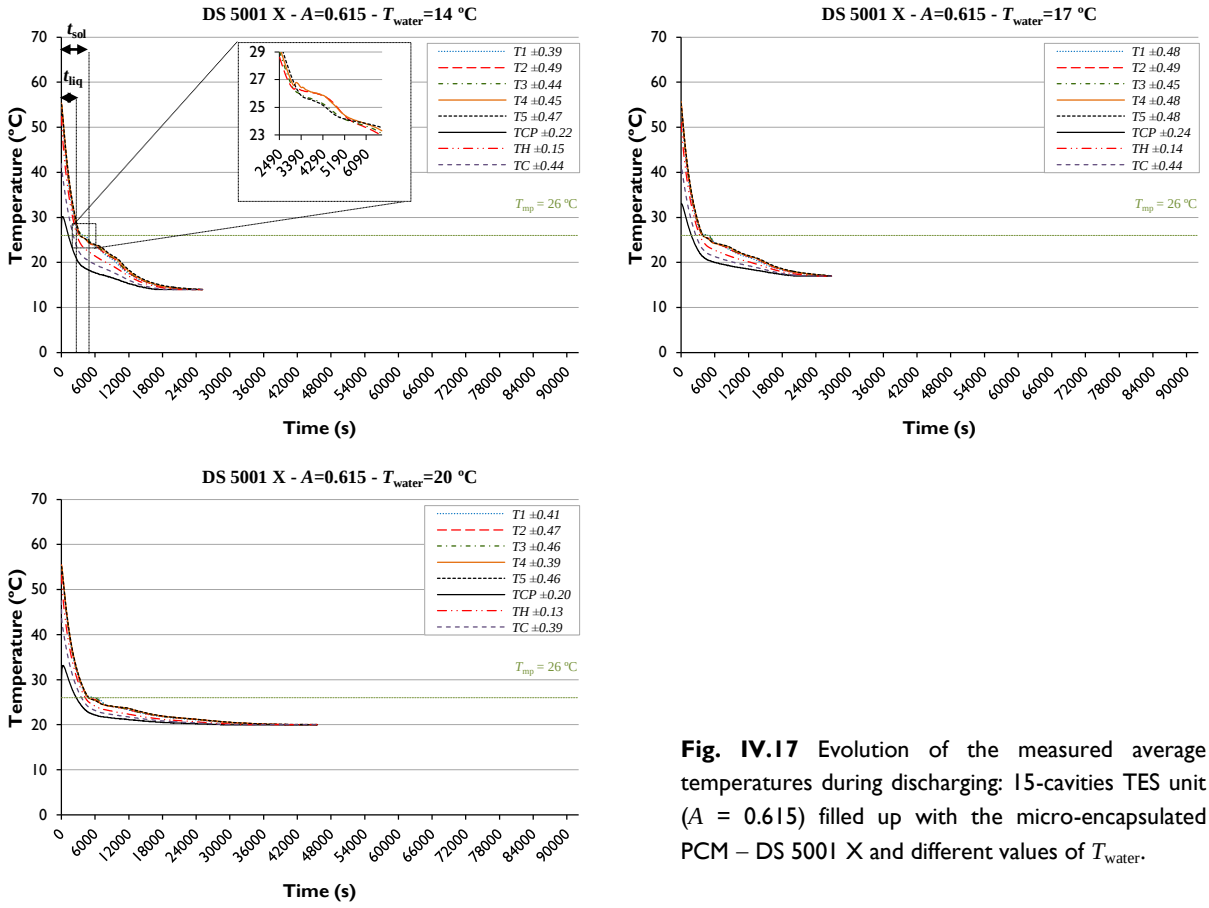

Fig. IV.17 Evolution of the measured average temperatures during discharging: 15-cavities TES unit (A = 0.615) filled up with the micro-encapsulated PCM – DS 5001 X and different values of T_{water}.

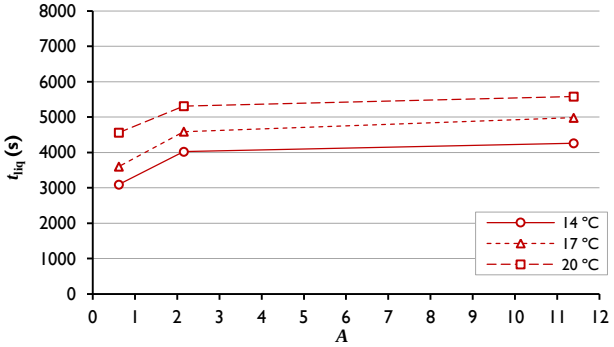

Fig. IV.18 Influence of the aspect ratio of the cavities A on the time required for starting the solidification process (t_{liq}). Discharging experiments with the microencapsulated PCM – DS 5001 X.

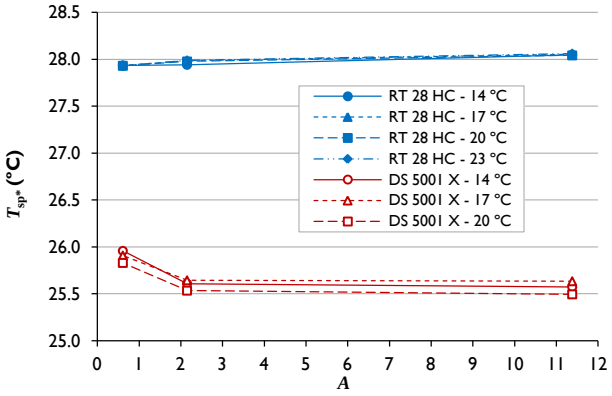

Fig. IV.19 Influence of the aspect ratio of the cavities A on the phase-change temperature achieved after subcooling (T_{sp}^*) for all the discharging experiments.

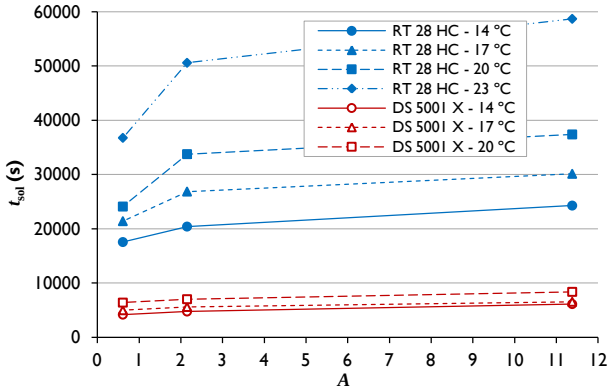

Fig. IV.20 Influence of the aspect ratio of the cavities A on the time required for solidifying all the PCM in the mid-plane of the cavity (t_{sol}) for all the discharging experiments.

IV.4 Conclusion

This chapter aimed at experimentally evaluating the heat transfer through small TES units with horizontal metallic fins emerging from vertical heated/cooled surfaces. These TES units can be used for the thermal management of vertical TES buildings' systems. They are made up of a vertical stack of metallic rectangular cavities to be filled up with different PCMs. A parametric study was carried out to evaluate the thermal performance of different TES units by considering three test-samples with different cavity aspect ratios, two types of PCMs (the free-form PCM – Rubitherm® RT 28 HC and the microencapsulated PCM – Micronal® DS 5001 X), two input power levels during charging, and four temperatures of the cooling water flow during discharging. A total of 12 charging and 21 discharging experiments were carried out.

This chapter provided a large set of benchmarking results for numerical validation purposes. The results also allow discussing which arrangement is better for specific building applications considering the thermal regulation effect of the TES unit during charging, the influence of subcooling during discharging, and the influence of natural convection during both processes. During charging,

the influence of the aspect ratio of the cavities on three parameters was investigated: (i) the control-temperature on the hot surface of the unit; (ii) the thermal-regulation period, and (iii) the time required for melting all the PCM in the mid-plane of the TES unit. During discharging, five parameters were evaluated: (i) the time required for solidifying all the PCM in the mid-plane of the TES unit; (ii) the time required for starting the crystallization process; (iii) the subcooling period; (iv) the phase-change temperature achieved after subcooling, and (v) the difference between the solidifying temperature of the PCM and the lower temperature due to subcooling.

It was verified that during the charging of the free-form PCM, conduction is initially the dominant mode of heat transfer. After some time, the natural convection flow ensues and becomes the dominant mechanism causing a thermal stratification from top to bottom. Therefore, natural convection in both PCM-liquid and air-layer domains must be considered in modeling to well describe the heat transfer during charging. Decreasing the aspect ratio of the cavities reduces the effect of natural convection. Adding fins also: (i) improves heat transfer by conduction, reducing the time required for melting; (ii) reduces the value of the control-temperature on the hot surface of the TES unit, and (iii) reduces the thermal-regulation period. Regarding the microencapsulated PCM, conduction is the dominant mode of heat transfer during charging, without any significant thermal stratification. Adding fins increases the heat transfer rate, but it also reduces the period during which temperature control is ensured. Regarding building applications, cavities filled with free-form PCMs are more attractive to be used in systems in which the main purpose is to enhance the thermal-regulation period and to reduce the control-temperature value on the hot surface of the TES unit. Cavities filled up with microencapsulated PCMs are better for elements where it is crucial to reduce the time required for melting all the PCM in the TES unit.

In both the free-form and the microencapsulated PCM, the discharging phase is mainly governed by conduction. Therefore, adding fins is unquestionably a good technique for improving the release of the stored energy by improving the solidification rate during the discharging process and by reducing the time required for solidifying all the PCM in the TES unit. Moreover, the lower the value of the cooled boundary condition, the higher the solidification rate. Natural convection in both PCM-liquid and air-layer domains must be considered in numerical modeling to well describe the heat transfer during discharging of free-form PCMs. The effect of natural convection and subcooling can be neglected when modeling microencapsulated PCMs. For the free-form PCM, adding fins enhances the subcooling effect by increasing the period during which subcooling occurs and by reducing both the temperature required to start crystallization and the phase-change temperature after subcooling. Therefore, subcooling delays the solidification process and reduces the solidifying temperature of the PCM, which can increase the hysteresis problem. Subcooling effect must be considered in the future simulations to well describe the discharging phase of free-form PCMs.

In short, it was concluded that the effects of natural convection in the free-form PCM are important and must be considered in any simulation to well describe the charging process. During discharging, subcooling must also be considered. The effect of natural convection and subcooling can be neglected when modeling cavities filled with the microencapsulated PCM. As stated before, the experimental results presented in this chapter are intended to be a good benchmarking reference for validating numerical models to be used in the design and optimization of practical building applications with rectangular cavities filled up with PCMs, such as PCM-bricks, PCM-shutters, PCM-window blinds, PV/PCM systems, SP/PCM systems, among other systems.

PART B

DYNAMIC SIMULATION OF ENERGY IN BUILDINGS

CHAPTER V

Review on passive TES systems for buildings

In this chapter, an overview of the main passive TES systems with PCMs for buildings is made. Some research gaps and future outlook are also pointed out during the next sections. This chapter summarizes part of the literature review which have been published in the paper "*Review of passive PCM latent heat thermal energy storage systems towards buildings' energy efficiency*" by Soares *et al.* [1]. Chapter V is divided into six main sections. Section V.1 presents some features related to building physics. In Section V.2 several passive TES systems for buildings are introduced and discussed. In Section V.3, the dynamic simulation of energy in buildings with latent heat from solid–liquid phase-change processes of PCMs is discussed and several software tools are presented, namely the *EnergyPlus* which will be used in Chapters VI and VII. Section V.4 discusses the lifecycle assessment of passive TES systems with PCMs and Section V.5 the economic impact analysis of this kind of systems. Finally, the contribution of passive TES systems towards net zero energy buildings (NZEBs) is discussed in Section V.6.

V.1 Building Physics

V.1.1 Building as a thermodynamic system

In a sustainable approach, buildings should be designed to ensure indoor thermal comfort of occupants during the whole year, with a minimum auxiliary energy demand for heating and cooling. The envelope of the building plays an important role in the delay and decay of the outdoor temperature fluctuation [268]. If the storage and insulation properties of the envelope were optimized to maintain the indoor air temperature in a comfortable range without heating and/or cooling energy consumption, a passive ideal energy conservation building with a passive ideal energy conservation envelope would be achieved [85]. However, the building is a quite complex thermodynamic system, submitted to many internal and external solicitations, and a theoretical passive ideal energy conservation building is difficult to attain.

The external solicitations are principally due to the local outdoor climatic conditions mainly the air temperature, the wind speed and the solar radiation. Internal solicitations come from internal heat loads related to the occupancy of the building. For specified climatic conditions, air exchange rate, size of the room, thickness of the building envelope and occupation rate and activity, the indoor

air temperature is closely related to the thermophysical properties of the materials of the envelope of the building, mainly their thermal resistance and heat capacity. Therefore, improving the thermal performance and heat capacity of the envelope of the building is crucial to reduce the energy consumption for heating and cooling. TES in the envelope of the building, or even in the partition elements, is a key target to attain more energy efficient buildings and PCMs could play an important role in this field. As explained in the first part of this thesis, due to the latent heat involved in their phase-change processes, PCMs provide a large heat capacity over a limited temperature range, and more thermal energy could be stored in the envelope of the building, in comparison with traditional sensible materials. Moreover, this feature can be very helpful for the effective use of renewable energy sources, mainly solar thermal energy. As the thermal improvements due to the inclusion of PCMs depend on the climate, design and orientation of the construction elements, but also on the amount, position and type of PCM, these studies require a detailed dynamic simulation of the thermal behavior of the building in the conditions of use established *a priori*.

V.1.2 Lightweight and heavyweight construction

Lightweight buildings such as steel or wood-framed construction, show certain advantages over heavyweight buildings, such as masonry or concrete construction. The motivation for using lightweight construction arises from overriding requirements for speed of construction and architectural flexibility for retrofitting purposes. Furthermore, modular lightweight construction is very suited to the economy of mass production with superior quality achieved by factory-based quality control. In comparison with heavyweight buildings, lightweight construction may be environmentally less sensitive since the weight of construction is much lower and the disruption on site is reduced. This reduces the energy necessary for the production and transportation of materials and reduces the quantity of waste materials [269]. Efficient factory production techniques are also much less wasteful and most of the building components could be easily separated and selected for recycling in the end of the building's life. However, lightweight buildings typically lead to buildings with low thermal mass [269].

Regarding thermal comfort, this low thermal mass and the consequent risk of comfort problems (such as overheating), may be the main disadvantage of lightweight construction. It also has lower thermal inertia, and it is more vulnerable to large temperature fluctuations due to external and internal loads. Considering both residential and office lightweight buildings, the integration of passive latent heat TES systems with PCMs could increase the thermal storage capacity of the building and help to avoid overheating problems during the summer due to internal loads or solar heat gains. The thermoregulation potential of PCMs could be optimized to decrease the amplitude of the indoor temperature fluctuation and to reduce the cooling peak loads. During winter, the integration of

passive TES systems with PCMs could be used to take advantage of solar thermal energy for heating. Moreover, PCM-based TES systems can be very effective in shifting the heating and cooling loads to off-peak electricity periods [270]. PCMs store 5–14 times more heat per unit volume than sensible storage materials such as water, masonry or rock [11]. Regarding heavyweight construction, the integration of PCMs in the building could lighten the construction's weight maintaining the heat capacity of the elements.

In short, the behavior of buildings with high or low thermal inertia is different, and the integration of PCMs in these buildings should reflect those behavior. An example of a methodology developed to assess PCM effectiveness in passively cooling building envelopes by taking into account the thermal inertia of the building was carried out by Castell and Farid [271].

V.1.3 Daily cycle optimization

The thermal performance of each PCM-based passive TES system depends on the indoor thermal loads, on the climatic conditions, mainly on the solar radiation and ambient temperature, on the characteristics and use of the building, on the design parameters such as shading elements, on the configuration and orientation of the TES system, on the location of the system within the building, but also on the amount, location and type of PCM chosen. For example, considering a PCM-based construction solution, which intends to take advantage of solar thermal energy for heating during winter, the volume of melted PCM depends on the extension of the sunshine period and amount of solar radiation, and on the thermophysical properties of the PCM, mainly the phase-change temperature, the latent heat of fusion and the thermal conductivity. The objective of the optimization process is to increase the storage/release capacity using as little PCM as possible [174]. The stored energy in a complete daily cycle is proportional to the PCM volume while the PCM is melting, after that, only sensible heat is absorbed. On the other hand, the released energy is proportional to the solidified volume of PCM during the discharging period. Remark that, due to the low thermal conductivity of PCMs, which mostly fall into the range of 0.2 to 0.7 W m^{-1} K^{-1}, these systems have an inherent disadvantage of slow heat transfer during the charging and discharging processes. If the PCM mass is overestimated, the time needed for the heat to penetrate the PCM could become larger than the sunshine period, and the melting process cannot be completed. Likewise, if the PCM mass is overestimated, the time needed for the heat to be released indoors could become larger than the discharging period, and the solidification process cannot be completed. Therefore, insufficient thermal storage is achieved when PCM neither totally solidifies nor melts [270]. If PCMs are not properly selected for the appropriate temperature range or, if the TES system does not work during the time and for the purpose predicted, the potential of PCMs will not be achieved.

Considering the use of PCMs to avoid overheating during summer, the previous remarks must also be considered. The volume of PCM should be selected in a manner that all the PCM mass should be completely melted and solidified during a phase-change daily cycle [272]. Some authors have concluded that the daily cycle optimization could be extended to yearly cycle optimization [273,274]. In this approach the thermal energy could be stored/released to make an impact in the transitions seasons (spring and autumn).

V.2 Overview of the main PCM-based passive TES systems for buildings

V.2.1 PCM-wallboards

Wallboards are very suitable for the incorporation of microencapsulated PCMs. They are cheap and widely used in building applications, especially in lightweight construction. Many studies, numerical/simulation [174,273–280], experimental [175,177,281–283] or both numerical and experimental [91,162,172,178,180,186,220,284–286], have been carried out to assess the performance of PCM enhanced wallboards. The efficiency of these elements depends on several factors such as: (*i*) how the PCM is incorporated in the wallboard; (*ii*) the orientation of the wall; (*iii*) the climatic conditions, (*iv*) the amount of direct solar gains; (*v*) the internal heat gains; (*vi*) the color of the surface; (*vii*) the ventilation and infiltration rates; (*viii*) the thermophysical properties of the chosen PCM mainly the temperature range over which phase-change occurs, and (ix) the latent heat capacity per unit area of the wall.

Kuznik *et al.* [174] carried out an optimization study using interior/exterior temperature evolutions within a period of 24 h to optimize the thickness of a PCM-wallboard to enhance the thermal behavior of a lightweight internal partition wall. The PCM-wallboard was composed of 60 wt.% of microencapsulated paraffin, which has a melting temperature of about 22 °C. The optimal thickness was found to be equal to1 cm. This 1 cm thick PCM-wallboard allows a doubling of the thermal inertia of the building. Kuznik *et al.* [178] carried out an experimental research in a full-scale test cell under controlled thermal and radiative conditions, to evaluate the performance of walls, with and without PCMs, during a summer day. These authors used the same PCM-composite described in the previous study to show that the PCM-wallboard reduces both the air temperature fluctuations in the room and the overheating effect. The authors also concluded that the available storage energy is twice as high for a 5 mm thick PCM-wallboard, which corresponds to an equivalent concrete layer of about 8 cm. Kuznik and Virgone [172] have carried out a comparative study, using cubical test cells, with and without a PCM-composite, to provide experimental data to be used for validation of numerical modeling. The effect of hysteresis was clearly exhibited in the experimental results, and the authors concluded that it must be taken into account correctly in numerical modeling

to predict the real thermal behavior of the construction element. In order to evaluate the potential of a PCM-wallboard constituted of 60 wt.% of microencapsulated paraffin within a copolymer, a renovated office building in Lyon was monitored during one year by Kuznik *et al.* [177]. A room was equipped with PCM-wallboards in the lateral walls and in the ceiling, and another room, identical to the first one, was not equipped but also monitored. The results showed that PCM-wallboards can enhance the thermal comfort of occupants.

Shilei *et al.* [281] evaluated the impact of a PCM-wallboard with 26 wt.% of fatty acids on the indoor thermal environment under the winter climatic conditions of the northeast of China. The experimental results showed that the PCM-wallboard can improve indoor thermal environmental for that conditions. Chen *et al.* [220] also evaluated the potential of including PCM layers for energy savings during the winter season in Beijing. Ahmad *et al.* [180] studied three types of PCM-wallboards for lightweight envelopes: a polycarbonate panel filled with paraffin granulates (melting temperature of 26 °C), a polycarbonate panel filled with polyethylene glycol PEG 600 (melting temperature of 25 °C), and a PVC panel filled with PEG 600 and coupled to a vacuum isolated panel. The numerical and experimental results showed that the last type is the most convenient for the authors' purpose. Athienitis *et al.* [285] concluded that gypsum wallboards (with 25 wt.% of butyl stearate) attached on the vertical walls of an experimental outdoor test room in Montreal, reduced the total heating load of approximately 15%. A gypsum board containing 45 wt.% of PCMs reinforced with additives was also studied by Oliver [287]. The thermal storage capacity of different construction materials with similar use and position in buildings than PCM-wallboards were evaluated and compared. It was concluded that an 1.5 cm thick board of gypsum with PCMs stores five times more the thermal energy of a laminated gypsum board, and the same energy as a 12 cm thick brick wall within the comfort temperature range (20–30 °C).

Diaconu and Cruceru [277] evaluated the potential of a three-layer sandwich-type insulating panel (with outer layers consisting of PCM-wallboards and a middle layer consisting of a thermal insulation material) for air conditioning and heating energy savings in continental temperate climate. As it was pointed out by these authors, the PCM-wallboard layers have different functions: the external layer has a higher value of the PCM melting-peak temperature and it is active during the hot season, the internal layer with a melting-peak temperature of the PCM close to the setpoint temperature of the heating system is active during the cold season. The authors carried out a year-round simulation of a room with the described system, and they concluded that it can contribute to annual energy savings (12.8% for heating and 1% for cooling) and to reduce the peak value of the cooling/heating loads by 35.4%. Diaconu [288] developed a simplified model for the heat exchange between the indoor environment and the ambient considering a PCM-enhanced wall with a PCM-wallboard in the inner layer. The main goal of the author was to evaluate the influence of occupancy pattern and ventilation on the energy savings potential of the wall system.

Bernardi *et al.* [289] evaluated the effect of gypsum panels incorporating microencapsulated PCMs on the thermal stability of cultural heritage objects. These gypsum panels with PCMs were tested in the S. Croce Museum in Florence, Italy, where the microclimatic monitoring has shown dangerous thermal conditions for the preservation of the works of art. Both laboratory and field studies carried out by the authors confirmed the effectiveness of PCMs as thermal storage solutions. Rodriguez-Ubinas *et al.* [290] evaluated the influence of PCM-drywalls in retrofitting of buildings. The results showed that the thermal performance of PCM-drywalls is strongly influenced by the window to wall ratio and by the shading factor. The authors highlighted the importance of combining the choice of the PCM-drywall with these two parameters in order to increase indoor thermal comfort, reduce the peaks and temperature fluctuations and to solve overheating problems. Chwieduk [291] numerically investigated the possibility of using thin and light PCM panels into external walls, aiming at substituting the large and heavy external walls used in high latitude countries. On the basis of the simulation studies of the dynamics of external walls with different configurations, the author proposed some guidelines for designing the building envelope with the PCM panels incorporated into its structure. Barzin *et al.* [292] experimentally investigated the use of DuPont Energain® PCM-wallboards on the interior walls in combination with an underfloor heating system incorporating PCMs. Several experiments were carried out in two identical test huts at the Tamaki Campus, University of Auckland. The authors used a price-based control method to evaluate the efficiency of the use of energy. The experimental results over a period of five days showed a total energy saving and electrical cost saving equal to 18.8% and 28.7%, respectively. The highest energy saving achieved during this period was 35% with a corresponding cost saving of about 44.4%. Biswas *et al.* [293] combined experimental and numerical analysis to evaluate the energy saving potential of a prototype nano-PCM enhanced wallboard. This nano-PCM is shape-stable for convenient incorporation into lightweight building components.

V.2.2 Other PCM enhanced walls

Evers *et al.* [294] evaluated the thermal performance of enhanced cellulose insulation with paraffin and hydrated salts for use in frame walls. The thermally-enhanced frame walls were heated and allowed to cool down in a dynamic wall simulator that replicated the sun exposure in a wall of a building on a typical summer day. The results showed that the paraffin-based insulation reduced the average peak heat flux by up to 9.2% and reduced the average total daily heat flow up to 1.2%. Joulin *et al.* [165] compared the numerical and experimental results of a PCM conditioned in a parallelepipedic polyefin envelope to be used in passive solar walls. Carbonari *et al.* [295] analyzed sandwich panels containing PCMs for prefabricated walls. The numerical and experimental results showed good accuracy, and demonstrated that PCMs can be useful for correcting the summer

behavior of lightweight enclosures, thanks to the possibility of absorbing incoming thermal flux blocking the temperature in an intermediate wall layer at values which coincide with the PCM phase-change temperature. A comparison between the experimental results also demonstrated that adding an air-layer between the PCM and the external metal finishing layer is capable of improving the performance of the system. A new structural insulated panel (SIP) outfitted with PCMs was proposed by Medina *et al.* [176]. The so-called PCMSIP system was experimentally evaluated during the summer and it was concluded that this system can reduce the heat fluxes through the wall during peak-times. The PCMSIP system also leads to a more constant indoor air temperature and to a more regular temperature on the surface of the wall. The results indicated that a PCMSIP with 10 wt.% and 20 wt.% of PCM caused the peak heat flux to decrease by an average of 37% and 62%, respectively. The average reduction in the daily heat transfer across the system was about 33% and 38% for PCM concentrations of 10 wt.% and 20 wt.%, respectively.

Halford and Boehm [296] evaluated the potential of a PCM layer, which is placed between two layers of insulation material in a configuration known as resistive-capacitive-resistive, for summer peak load shifting. The PCM layer itself was a PCM perlite mixture which is hermetically sealed inside of a poly/foil packaging. The numerical results showed that, depending upon the temperature regime selected for the inner wall, a maximum of 11–25% reduction in the peak-load can be achieved, when compared to the "mass but no phase-change" case, and a 19–57% decrease over the "insulation only" case. The thermal performance of an idealized envelope wall containing PCM layers was numerically modeled, analyzed, and optimized by Mathieu-Potvin and Gosselin [297]. These authors concluded that the phase-change temperature and position of the PCM layer have a large influence on the shielding performance of the wall. Moreover, they pointed out that genetic algorithms are a useful tool to rapidly optimize the configuration of the system. Huang *et al.* [298] carried out a detailed theoretical investigation and evaluated the TES capacity and the temperature control achieved by using a passive PCM-augmented cavity wall system with two types of PCMs (solid–solid GR41 and GR27). The system is composed by two main masonry layers separated by the PCM layer and the cavity. The performance of a south-east oriented system was predicted using realistic ambient temperatures and solar radiation conditions in SE England, for the 21st of January and 21st of June. The main results showed that a PCM-augmented cavity wall with 20 mm of GR27 and a 20 mm air space cavity can help maintaining the temperature of the interior wall surface, satisfying thermal comfort requirements and preventing the formation of condensation in the cavity of the wall during winter. Jin *et al.* [299] carried out an experimental study on the placement of a PCM layer within the cavity of buildings walls for heat transfer rate reduction in order to find the best position for the PCM layer.

De Grassi *et al.* [300] used statistical techniques to work out quantitative indexes from the data collected from experimental results carried out during the summer of 2003 within the C-Tide

European Project, whose aim was testing the possible profit of inserting PCM inside dry assembled walls, generally characterized by low thermal inertia. Darkwa and O'Callaghan [301] evaluated the thermal effectiveness of PCM-drywall samples (i.e. randomly-mixed and laminated PCM-drywalls) in a passive solar building model. The results showed that the laminated PCM sample with a narrow phase-change zone was capable of increasing the minimum room temperature at night by about 17% more than the randomly-mixed type.

In the last years, several authors have proposed the use of PCMs in ventilated active facades to combine the beneficial effects of a ventilated facade with the suitable advantages of PCMs. Diarce *et al.* [302] experimentally evaluated the thermal performance of a ventilated active facade with PCMs in its external layer by considering a real-scale PASLINK test call facility located in Vitoria-Gasteiz, Spain. The measurements were carried out during March, 2010. The experimental results showed that phase-change processes of PCM led to an increment of the heat absorption from solar gains, which reduces the overheating of the facade. The authors also compared the thermal performance of the PCM ventilated active facade with other traditional envelopes. For this purpose, simulations were performed using the *Design Builder* software. Diarce *et al.* [230] carried out a comparative study of the CFD modeling of a ventilated active facade which includes a PCM in its outer layer. The numerical results were validated against experimental data obtained by means of the real-scale PASLINK test facility. Recently, de Gracia *et al.* [303] evaluated the energy performance of a ventilated double skin facade with PCMs under different climatic conditions. The potential benefits of this new system were experimentally evaluated for Mediterranean-continental climate, and extended by means of a numerical model to several climates. The results showed mainly three potential benefits of the ventilated facade with PCMs: free cooling, cold storage and prevention of solar radiation incidence. Ventilated facades with PCMs were also used in the research carried out by Álvarez *et al.* [304], which aims at taking advantage of PCMs for natural cooling of buildings.

Li and Liu [305] carried out a numerical and experimental study to evaluate the thermal performance of a solar chimney system incorporating organic PCMs (RT-42) under different heat fluxes conditions. The results showed that the performance of the system is strongly dependent on the solar radiation and the authors suggested that the application of high effective thermal conductivity enhancers can further improve the performance of the solar chimney system under lower solar radiation conditions. Liu and Li [306] further numerically evaluated the effects of seven design and operational parameters on the heating performance of a solar chimney with PCMs: latent heat of fusion, heat flux, inlet air temperature, absorber thermal conductivity, thermal conductivity of insulation material, transmissivity of glass cover and absorptivity of the absorber surface.

Lai and Hokoi [307] proposed a new aluminum honeycomb wallboard incorporating a microencapsulated PCM. The aluminum surface structure is used to enhance the thermal

conductivity in the prototype wall in order to rapidly transfer the heat flux to the PCM. Biswas and Abhari [308] proposed a new PCM-based system made of naturally occurring fatty acids/glycerides trapped into high density polyethylene (HDPE) pellets. These authors experimentally and numerically evaluated the performance of the PCM–HDPE pellets in a building envelope application in order to show the energy-saving potential of the new TES system. Sun *et al.* [309] evaluated the energy and economic impacts related to the application of a PCM-board in building enclosures during the cooling season in different climate regions of China. Kong *et al.* [310] carried out a numerical study to evaluate the thermal performance of building walls and roofs incorporating PCM-panels for passive cooling. These authors have proposed two new PCM-based systems: capric acid contained in the panels installed on the outside surface of building and capric acid and 1-dodecanol contained in the panels installed on the inside surface of building.

V.2.3 SSPCM enhances elements

As it was discussed in section II.2.1, the integration of SSPCMs into construction elements to enhance the energy performance of buildings have been studied by many authors in the recent years [101–108,111–119,311,312]. Aiming to help the selection of SSPCMs and their applications in passive solar buildings, Zhou *et al.* [111] carried out one-dimensional numerical simulations to investigate the performance of SSPCM wallboards with sinusoidal heat flux waves on the outer surface. The results were compared with those related with traditional building materials such as brick, foam concrete and expanded polystyrene. The thermal characteristics of a SSPCM wallboard with sinusoidal temperature wave on the outer surface were also numerically investigated by Zhou *et al.* [112] and compared with the same traditional construction materials.

The simulation results of air-conditioned office buildings with SSPCMs in typical subtropical and dry continental climates achieved by Zhu *et al.* [106] showed that the use of SSPCMs in building envelopes can significantly improve the energy performance of buildings under both time-based pricing policy and energy-plus-demand-based pricing policy, and they can improve the indoor thermal comfort by reducing the indoor temperature swing. Zhou *et al.* [105] numerically investigated the performance of a hybrid space-cooling system with night ventilation and thermal storage using SSPCM plates as the inner linings of walls and ceiling. The authors indicated that the thermal storage effect of SSPCM plates, combined with night ventilation, could improve the indoor thermal comfort level and save 76% of daytime cooling energy consumption during summer in Beijing (compared to the case without SSPCM and night ventilation). Zhou *et al.* [115] also evaluated the effect of SSPCM walls/ceiling plates combined with night ventilation during summer, in Beijing. The numerical results showed that the SSPCM plates could decrease the daily maximum temperature by up to 2 °C due to

the cool storage at night. For the winter climatic conditions of Beijing, Zhou *et al.* [114] numerically optimized the thermal performance of a south-facing direct-gain room with SSPCM plates using an enthalpy model, and they pointed out that SSPCM plates create a heavyweight response to lightweight constructions with an increase of the minimum room temperature at night by up to 3 °C for the case studied. The comparison between the thermal performance of two PCM-composites was numerically evaluated in a passive solar building in Beijing by Zhou *et al.* [113]. The results showed that both mixed type PCM-gypsum and SSPCM plates effectively shave the indoor temperature swing by 46% and 56%, respectively, and that the SSPCM plates respond more rapidly than the mixed type PCM-gypsum.

A simplified dynamic model of building structures integrating SSPCM walls was developed and validated by Zhu *et al.* [101]. The physical model represented the wall by three resistances and two capacitances and the PCM layer by four resistances and two capacitances. The parameters of the simplified model were identified using genetic algorithm based preprocessors developed to identify the optimal parameters, resistances and capacitances, of the model by frequency-domain regression and time-domain regression, respectively. The validation results showed that the simplified model can represent lightweight and medianweight walls integrating SSPCM with good accuracy.

V.2.4 PCM-bricks

Alawadhi [313] presented a thermal analysis of a two-dimensional model for a common building brick with cylindrical holes containing PCMs for hot climates. In the author's view, the objective of the PCM brick system is to reduce the heat flow from outdoors during the daytime by absorbing the heat gain in the brick before it reaches the indoor space. The effects of different design parameters such as the PCM's quantity, type, and location in the brick was investigated and the results showed that, for the best configuration, the heat flux at the indoor space can be reduced by 17.55% when three PCM cylinders are introduced and placed at the centerline of the bricks. Zhang *et al.* [314] evaluated the thermal response of a brick wall filled with PCMs under fluctuating outdoor temperatures using a thermal conduction model with phase-change based on the enthalpy-porosity technique. The results showed that, in comparison with a common solid brick wall, the thermal storage capacity of the PCM brick wall is higher, and the incorporation of PCMs in the bricks is beneficial for the thermal insulation, temperature regulation and thermal comfort for occupancy.

Castell *et al.* [166] experimentally evaluated the benefits of using PCM in conventional and alveolar brick construction for passive cooling in Spanish continental climate. Several cubicles were built (with and without PCMs) and their thermal performance throughout the time was measured. For each type of construction material used, a macro-encapsulated PCM was added in one cubicle

(RT-27 and SP-25 A8). The cubicles have a domestic heat pump as a cooling system and the energy consumption is registered to determine the energy savings achieved. The main results of this study pointed out that a cooling strategy (either natural or mechanical) must be defined during the night to improve the performance of the PCM under free-floating conditions. Furthermore, when considering a heat pump to set and control the indoor temperature of the experimental cubicles, the results showed that the energy consumption of the cubicles containing PCM was reduced about 15% compared to the cubicles without PCM. Silva *et al.* [222] evaluated the potential of incorporating macroencapsulated paraffin into a typical Portuguese clay brick masonry wall. The experimental results revealed that the incorporation of the PCM contributes for the attenuation of indoors temperature swing, reducing from 5–10°C the thermal amplitude, as well as increasing the time delay of about three hours. Lai and Chiang [315] studied the incorporation of PCM in hollow thermal-insulation bricks. The authors found that PCM bricks have better daytime insulation effect when exposed to solar radiation than untreated bricks. The maximum underside temperature of PCM bricks was 31.7 °C which was 4.9 lower than that of the untreated bricks. Cheng *et al.* [316] pointed out the importance of the accurate measurement of the thermophysical properties of a PCM-concrete brick for the simulation and evaluation of its energy saving performance. Indeed, these authors proposed a new method based on the inverse problem, which deals with the measurements of thermal conductivity and specific heat of the PCM-concrete brick during the phase-change process.

V.2.5 PCM enhanced concrete systems and mortars

Cabeza *et al.* [317] studied a new innovative concrete with PCMs in order to develop a product which would not affect the mechanical strength of the concrete wall. They set up two real size concrete cubicles in Lleida, Spain, to demonstrate the possibility of using a microencapsulated PCM (with a melting point of 26 °C) in concrete to enhance its thermal performance. They concluded that the concrete reached a compressive strength over 25 MPa and a tensile splitting strength over 6 MPa, and no difference occurred in the effects of the PCM after six months of operation. The experimental results also showed that the energy storage in the concrete enhanced walls leads to an improved thermal inertia as well as lower inner temperatures, in comparison with conventional concrete. A similar study was also carried out by Cabeza *et al.* [318]. Chandra *et al.* [319] concluded that a PCM wall of smaller thickness is more desirable in comparison to an ordinary masonry concrete wall for providing efficient TES as well as better thermal comfort in buildings.

Entrop *et al.* [320] studied a PCM enhanced concrete to store solar thermal energy in floors for moderate sea climates. The experimental results showed that, for the experimental setup

considered, the application of microencapsulated PCMs in concrete floors resulted in a reduction of maximum floor temperatures up to 16 ± 2%, and an increase of minimum temperatures up to 7 ± 3%. Arnault *et al.* [321] implemented a numerical model to determine the thermal performance of internal surfaces including PCMs, which was exploited to compare a typical concrete floor with a floor with a PCM for Québec city weather conditions. The authors parametrically studied both systems, and optimized their configuration based on distinct objective functions. The results showed that the thickness of the concrete floor could be optimized and the floor performance may be enhanced by the inclusion of a PCM layer.

A concrete roof with cone frustum holes filled with PCM was investigated by Alawadhi and Alqallaf [322] as a method to reduce the heat gains during the working hours. The results for the best configuration indicated that the heat flux can be reduced by up to 39% when the PCM is introduced in the roof. Pasupathy and Velraj [323] studied the effect of a double PCM layer in a concrete slab roof for year-round thermal management in a residential building located in Chennai, India. Zhang *et al.* [324] pointed out that an adequate amount of PCM can be incorporated into concrete by porous aggregates absorbing PCMs or produced with a normal mixing method to produce TES concrete. The experimental results showed that the thermal performance was affected by the porous structure of the aggregates and the volume fraction of PCM in concrete. Srinivasan and Ravikumar [325] numerically evaluated the heat transfer in a PCM-filled reinforced cement concrete roof for thermal management of buildings.

Several studies were devoted to the thermophysical characterization of PCM-enhanced concretes. Pomianowski *et al.* [98] proposed a new experimental method to determine the specific heat capacity as a function of temperature of concrete mixed with various amounts of microencapsulated PCMs. Eddhahak-Ouni *et al.* [184] also evaluated the thermophysical properties of Portland cement concrete modified with organic microencapsulated PCMs – Micronal® DS 5001 X. The results showed an improvement of the heat storage capacity of the PCM-concrete. The thermal, mechanical and microstructural analysis of concrete containing microencapsulated PCMs was also investigated by Dehdezi *et al.* [326]. Thiele *et al.* [327] investigated the benefits of adding microencapsulated PCMs to concrete used in building envelopes to reduce energy consumption and costs. These authors have proposed a time-dependent homogeneous thermal model to establish design guidelines that can help the selection of microencapsulated PCMs for concrete walls in different climates. An updated review on the use of PCMs for thermal energy storage in concrete was recently carried out by Ling and Poon [328]. These authors have reviewed the feasibility of using PCMs in concrete, the predominant methods for incorporating PCMs in concrete (immersion, impregnation and direct mixing) and the influence of PCMs in the mechanical and thermophysical properties of the PCM-enhanced concretes.

Sá *et al.* [329] studied a new thermally enhanced mortar with 25% of microencapsulated PCM on the mass fraction. The results showed that the incorporation of the PCM in the mortar did not compromise the properties that are desirable for their application as plastering materials. The incorporation of microencapsulated PCMs in cement mortars was also evaluated by other authors. In their work, Joulin *et al.* [96] developed a method for the thermal characterization of cement-mortars incorporating microencapsulated PCMs from simultaneous heat flux and temperature measurements. The results showed that the composite PCM has potential thermal energy storage purpose for buildings. However, the results also showed a negative effect on the thermal conductivity by incorporating PCMs in the cement mortar, which may be disadvantageous for heat transfer. Franquet *et al.* [94] also carried out an experimental and theoretical modeling analysis of a cement mortar containing microencapsulated PCMs in order to characterize the thermal behavior of the composite during heating and cooling processes. Tittelein *et al.* [93] evaluated three different phase-change models for predicting the energy behavior of a PCM cement mortar sample: the apparent specific capacity method, the enthalpy method assuming a pure body and the enthalpy method assuming a binary mixture. The results showed that the last model gives better results. Nepomuceno and Silva [330] experimentally evaluated the mechanical and thermophysical properties of cement mortars with PCMs incorporated via lightweight aggregate (LWA). Three groups of LWA mortars were investigated: one with pre-soaked LWA and the others with PCM-filled LWA combining two different impregnation methods and PCM dosages. The authors reported that high thermal inertia and low mass are compatible in PCM-filled LWA mortars and that the thermal response increases with the PCM to a certain limit and then decrease [330]. Kheradmand *et al.* [331] evaluated the thermal behavior of cement based plastering mortars containing hybrid microencapsulated PCMs. By "hybrid", the authors mean the simultaneous incorporation of more than one type of PCM into the mortar. Zhang *et al.* [205] investigated the behavior of a cement mortar with a composite PCM based on n-octadecane and expanded graphite to help to decrease the energy consumption of buildings. Lecompte *et al.* [95] evaluated the mechanical and thermophysical behavior of concrete and mortars containing up to 29% in volume of microencapsulated PCMs. The results showed that PCMs can have a beneficial effect on the thermal behavior of walls, keeping a consistent mechanical strength.

Li *et al.* [332] investigated new thermal energy storage composites developed by incorporating granular PCMs (Rubitherm® PX25) into cement past. To avoid paraffin leakage during fabrication, the influence of several modifiers were investigated. Desai *et al.* [333] evaluated the viability of incorporating a paraffin PCM into an engineered cementitious composite. The results showed that the inclusion of 3% of PCM by mass increases the specific heat capacity of the composite by 40% at phase-change temperature, by maintaining a 28 MPa compressive strength and a 4% tensile strain capacity on average. Ventolà *et al.* [97] proposed a newly-designed traditional lime mortar with a PCM used as an addictive. The results showed that the PCM-enhanced lime mortar

has improved thermal insulation properties, compressive strength and carbonation rate in comparison to the classic lime mortar. These authors pointed out that this new material can be used in the retrofitting of architectural heritage and in the construction of new buildings where natural stone is used.

V.2.6 PCM Trombe wall

As suggested by Fang and Yang [334], passive solar heating of buildings is an area of great interest for renewable energy applications. Several authors have proposed the inclusion of PCMs in solar wall systems to replace masonry big volumes, and many experimental and theoretical tests have been conducted to investigate the reliability of PCMs in this kind of system [318,335–337]. Although the Trombe wall indirect solar gains concept was established decades ago and studied by many authors [338–340], cultural assimilation into architecture and design has been very sluggish. The new paradigm towards more green and zero-energy buildings and the introduction of PCMs in the construction industry give a new opportunity for the dissemination of this indirect solar gain technique. The introduction of PCMs in Trombe wall systems could contribute to the development of light, portable, movable and rotating systems fully adapted to the lightweight buildings category. In this new approach, the huge sensible thermal mass of a traditional Trombe wall and the big amount of material could be replaced by the latent heat from the PCMs phase-change processes, and less quantity of material will be necessary. Moghiman *et al.* [341] replaced the classic Trombe wall design by a set of rotating wall segments which can rotate around their vertical shafts. With this configuration, the rotating wall segments are a good absorber during the day and a good radiator during the winter nights. The results showed that, in comparison with classical solar walls, the rotating storage walls can be more efficient, even in cold climates.

V.2.7 PCM shutters, window-blinds and translucent PCM walls

Exterior PCM shutters containing PCMs are movable structural shading elements associated to window facades. The PCM shutters system must operate cyclically, reflecting the ongoing daily cycles of 24 hours. Similarly, the cyclically operation of the system should enable the melting of the PCM mass during the day and its solidification during the night, enabling the daily cyclic storage and release of thermal energy. Soares *et al.* [153] numerically optimized a southward PCM-shutter system to take advantage of solar thermal energy for winter night time indoor heating in Coimbra, Portugal. Exterior window shading elements with PCMs were also studied by other authors [266,267]. A new kind of interior PCM-shutters was recently proposed and evaluated by Silva *et al.* [229] and Silva *et al.* [228].

An interior sun protection system consisting of vertical slats filled with a PCM was installed in westward office rooms located in Karlsruhe and in southeast office rooms located in Kassel, and monitored from winter 2008 until summer 2010 by Weinlaeder *et al.* [342]. The system showed a significant cooling potential in summer and even some advantages in winter compared to a conventional blinds system without PCMs. During summer, while conventional systems often heat up to temperatures of 40 °C or more, the monitored results showed that the surface temperature on the interior side of the PCM-filled slats hardly ever exceeded the PCM melting-peak temperature of 28 °C. The PCMs also reduced the solar heat gain coefficient of the sun protection. The authors recommended the use of a ventilation system in combination with tilted windows to enhance the discharge of the system during the night. Wang and Zhao [343] proposed an interior flexible and low cost PCM-curtain system to reduce solar heat gains in hot summers. The numerical results showed that the average heat transfer rate into the indoor space during working hours can be reduced by as much as 30.9% when using a 15 mm thick PCM-layer with a melting temperature of 29 ºC in the hottest summer days in Shanghai [343].

A TIM-PCM external wall system for solar space heating and daylighting composed of transparent insulation material (TIM) and translucent PCM was theoretically and experimentally investigated by Manz *et al.* [344]. This system enables selective optical transmittance of solar radiation: the visible light is transmitted and invisible radiation is mainly absorbed and converted to heat. The main results showed the promising thermal-optical behavior of the TIM-PCM system for a Swiss lowland climate, even during the month with the lowest irradiation. Bontemps *et al.* [345] carried out an experimental and numerical simulation study to assess the impact of a wall made of hollow glass bricks filled with PCMs for the thermal management of an outdoors passive solar test-room. Reasonable agreement between the simulation and the experimental results was observed, and the authors pointed out the importance of conceiving systems with PCMs coupled with efficient night ventilation. Weinlader *et al.* [346] studied a PCM-facade-panel for daylighting and room heating. The double glazing system combined with PCMs transmits enough light and, because of the latent heat storage effect of the PCM, it also has a more equalized energy balance during the day in comparison with double glazing facades without PCMs. The results showed that this system could be a good choice for lightweight construction. In winter, especially during evenings, the PCM-facade-panel provided homogeneous illumination and less heat losses improving the thermal comfort. In summer, the results showed low heat gains, which reduces peak cooling loads during the day. Goia *et al.* [347] evaluated the spectral and angular behavior of different PCM-glazing samples, characterized by different thicknesses of PCMs. Goia *et al.* [348] carried out an experimental analysis of the energy performance of a full-scale PCM-glazing prototype. These authors claim that the innovative PCM-glazing system can take advantage of phase-change processes to achieve a dynamic and responsive

behavior. Moreover, coupling PCM and glass can improve the low thermal inertia of fenestrations and contribute for the effective thermal management of solar energy.

An updated review on PCMs integrated into transparent building elements was recently carried out by Fokaides *et al.* [349]. Cuce and Riffat [350] provided a state-of-the-art review on innovative glazing technologies including those incorporating PCMs. Several PCM-glazing systems were also reviewed and described by Hee *et al.* [351]. Finally, several solar facades were reviewed by Lai and Hokoi [352], including those with PCMs.

V.2.8 Future outlook

In the works available in the literature, most of the systems are numerically or experimentally studied/optimized for extreme winter or summer conditions and few studies are carried out for autumn and spring conditions. Typically, passive systems are also optimized to solve only either the winter or the summer problem and few studies are carried out about their behavior in both seasons, and more so, also during the remaining seasons. There is no reason to assume that the PCM will behave as a sensible material outside the season studied in a particular work, and indeed, the real effect of PCMs in those seasons could be disadvantageous. A large part of the passive TES systems with PCMs are validated against laboratory conditions. Further work should be done to accurately assess the effect of these systems in real dynamic conditions and for different occupancy scenarios.

Further work should be also done in order to integrate the construction solutions with PCMs in the buildings' thermal regulation codes worldwide, e.g. some methodologies must be developed to take into account the latent heat from the phase-change processes of PCMs in the design of buildings, mainly for the cases where the dynamic simulation of the energy throughout the year is not mandatory.

Some building envelope solutions are studied like one-layer PCM material. This does not agree with the real life building construction where more layers of other materials may be necessary because of architectural, aesthetic, regulatory or structural purposes. Hence, many layers of other materials (e.g. a mortar, a brick, a concrete or any other layer enhanced with PCMs) should be considered as a part of a passive system, and the system must be optimized as a whole.

Emerging economies in high need of housing, and the thermal refurbishment of existing buildings in the developed countries are great opportunities for the development of new construction solutions with PCMs. Further work should be done to convert new types of PCMs, new methods to incorporate them into building materials and new heat transfer enhancement techniques in the design of new passive TES systems. The most promising passive TES systems with PCMs to be developed for building applications are those related with harnessing solar thermal energy for heating

during winter and those optimized to reduce the overheating problem during summer. The development of hybrid and adaptable systems to solve the winter and the summer challenge at the same time is a fertile area of research. For example the development of rotary, portable, movable and reconfigurable systems, mainly those associated with glazed facades, is a great challenge to solve in the near future. This could be materialized in the design of portable, rotary and movable Trombe wall systems, or even shutters or window blinds systems, giving rise to a new generation of "PCM Trombe wall systems".

V.3 Dynamic simulation of energy in buildings with PCM-based passive TES systems

A good knowledge on the dynamic energy performance of buildings incorporating passive TES systems with PCMs is essential for building researchers and practitioners to better understand the buildings temperature response characteristics and the economic feasibility of using PCMs. This knowledge is also important to take further proper actions to fully utilize PCMs to enhance indoor thermal comfort and the overall energy performance of buildings. Nowadays, there are many building energy simulation tools for the DSEB assessment: *BLAST*, *BSim*, *DeST*, *DOE*, *ECOTECT*, *Ener-Win*, *Energy Express*, *Energy-10*, *EnergyPlus*, *eQUEST*, *ESP-r*, *IDA-ICE*, *IES*, *HAP*, *HEED*, *PowerDomus*, *SUNREL*, *Tas*, *TRACE*, *TRNSYS*, etc. [353]. The *EnergyPlus*, *ESP-r* and *TRNSYS* are highlighted for their versatility and reliability [354]. A recent updated review on the main numerical methods for latent heat evolution in building simulation programs was carried out by Al-Saadi and Zhai [47]. These authors presented the numerical formulation, the numerical method used for latent heat evolution and the time stepping scheme behind the most known PCM modules used in different building simulation programs (mainly *EnergyPlus*, *TRNSYS* and *ESP-r*). The authors also pointed out the limitations and constrains of the most known modules. A particular attention was given to the validation of the PCM modules.

V.3.1 Energy Plus

EnergyPlus is an energy analysis and thermal load simulation program that models heating, cooling, lighting, ventilation and other energy flows in buildings and includes some important simulation capabilities such as variable time steps, user-configurable modular systems that are integrated with a heat and mass balance-based zone simulation [355], multizone air flow, thermal comfort and natural ventilation. In *EnergyPlus*, a PCM-module is introduced using an implicit conduction finite-difference solution algorithm which includes both phase-change enthalpy and a temperature dependant thermal conductivity. Pedersen [356] evaluated the effect of using PCMs in several positions within a wall

configuration, and presented some examples of the annual energy performance changes caused by the integration of PCMs. No significant energy benefits are found. The author found the implicit numerical solution to be the most flexible method. The scheme of carrying the node enthalpy along with the simulation has proven to be very robust, and provides a completely accurate accounting for the phase-change enthalpy.

Tardieu *et al.* [357] used *EnergyPlus* to predict the thermal performance of office size test rooms located in Auckland, New Zealand. The long term measurements conducted for these test rooms showed a good agreement with the simulation results. They showed that PCM-gypsum wallboard provided significant TES benefits. The simulated results also showed that the additional thermal mass of the PCM can reduce the daily indoor temperature fluctuation by up to 4 °C on a typical summer day. Tetlow *et al.* [358] also used *EnergyPlus* for parametrically evaluating the potential benefits and limitations of incorporating PCMs into an internal wall insulation system for retrofitting "hard to treat" houses in the UK. Shrestha *et al.* [359] presented a model of a PCM-enhanced dynamic-insulation system in *EnergyPlus* and compared the simulation results against field measured data. The results indicated that the predicted daily average heat flux through walls from the simulation was within 9% of field measured data. Kosny *et al.* [360] presented experimental and numerical results from thermal performance studies of wall and attic applications of the blown fiberglass insulation modified with a novel spray-applied microencapsulated PCM. They used *EnergyPlus* to simulate the whole building energy performance for different US climates.

Kosny *et al.* [361] evaluated bio-based PCM encapsulated between two layers of plastic film and discussed an experimental-analytical methodology that can be used in the analysis of insulation assemblies containing array of PCM pouches. The authors also estimated the reduction in the annual wall-generated heating and cooling load due to the use of PCMs to be 10%. Evola *et al.* [362] used *EnergyPlus* to simulate the behavior of PCMs for the improvement of thermal comfort in lightweight buildings. The parametric DSEB results supported the definition of new indicators, which allow to better manage the use of PCMs in buildings for thermal comfort purposes. Tabares-Velasco *et al.* [363] verified, validated, and improved an *EnergyPlus* PCM model using analytical verification, comparative verification, comparative testing and empirical validation of three PCM applications: PCM distributed in drywall, PCM distributed in fibrous insulation, and thin concentrated PCM layers. The authors identified a few key limitations of using the *EnergyPlus* PCM model.

In their work, Al-Saadi and Zhai [364] carried out a systematic evaluation of several mathematical methods and numerical schemes for modeling PCM-enhanced building enclosure. The models were validated and further verified against *EnergyPlus* PCM model. Ascione *et al.* [365] used *EnergyPlus* to evaluate the energy savings and indoors comfort improvement during the cooling season in Mediterranean climates by using PCMs in the energy refurbishment of existing buildings.

Alam *et al.* [366] used *EnergyPlus* PCM model to assess the energy saving potential of PCMs in major Australian cities. The results showed that the effectiveness of the PCM strongly depends on local weather, thermostat range, thickness of the PCM layer and surface area. Evola and Marletta [367] carried out dynamic simulations using *EnergyPlus* to evaluate the effectiveness of PCM-wallboards for the energy refurbishment of lightweight buildings. A sample office building was considered for the simulations, and several locations with different climatic conditions were investigated. Sajjadian *et al.* [368] evaluated the potential of PCMs to reduce domestic cooling energy loads for current and future UK climates scenarios using the dynamic thermal simulation software *DesignBuilder*, which employs *EnergyPlus* as its calculation engine. Evola *et al.* [369] developed a methodology using *EnergyPlus* PCM model for investigating the effectiveness of PCM-wallboards for improving summer thermal comfort in lightweight buildings. Evola *et al.* [370] also used *EnergyPlus* for the dynamic simulation of a ventilated cavity used to improve the effectiveness of PCM-wallboards for summer thermal comfort in buildings. Recently, Sage-Lauck and Sailor [371] evaluated the use of PCMs for improving thermal comfort in a super-insulated residential case study passive house duplex located in Portland, Oregon, USA. One unit of the duplex was outfitted with PCMs while the other unit was used as a control unit. Both units were instrumented and several indicators were monitored. The performance of the PCM was then evaluated through analysis of the experimental data and through additional computer simulations using the *EnergyPlus* PCM model, which was validated against the experimental results.

Santos *et al.* [372] evaluated the influence of climate change scenarios on the energy efficiency of lightweight steel framed (LSF) residential buildings based on DSEB using *EnergyPlus* software and CFD models. Santos *et al.* [373] also carried out a parametric analysis of the annual thermal performance of LSF residential buildings in Mediterranean climate zones based on a numerical model which was experimentally validated. Both these works emphasized the importance of minimizing the energy demands for heating and cooling during the operational phase of the low thermal inertia building in order to enhance its energy efficiency. More analysis must be done considering the integration of PCMs in LSF residential buildings.

Some PCM models have also been developed for active systems. The comprehension of this models could contribute for the assessment of PCM-based passive TES systems. For example, Mazo *et al.* [374] described a model developed to simulate a radiant floor active system with PCM in simple building types. The building simulation model was validated by comparing its behavior with *EnergyPlus* simulation.

V.3.2 ESP-r

As stated by Almeida *et al.* [375], *ESP-r* is an advanced building energy simulation tool which allows for detailed thermal and optical description of buildings. The software discretizes the problem domain in a control volume scheme and solves the corresponding conservation equations for mass, momentum, energy, etc. *ESP-r* can integrate the effect of a variety of factors including, weather, external shading, occupancy gains, HVAC systems, and many others. Almeida *et al.* [375] have used *ESP-r* to evaluate the potential of using multiple layers of PCM versus using a single PCM layer. It was found that the application of PCMs can significantly affect the thermal performance of the building, and it was shown that multilayered PCM demonstrated more thermal benefit than single PCM layer.

In their work, Fernandes and Costa [376] also used *ESP-r* to analyze the comfort conditions and the energy savings obtained by incorporating PCMs in typical masonry Portuguese family houses, in summer, for three different Portuguese climatic locations. Kosny *et al.* [377] used *ESP-r* tool to evaluate the dynamic thermal characteristics of thick attic floor insulations and blends of PCMs with insulations. The results showed that both elements can provide reductions of thermal loads at the attic level. A significant time shift of peak-hour loads was verified due to PCMs. These authors pointed out that PCMs can be used for free cooling and to take advantage of double electrical tariffs with high daytime peak-hour electric energy cost and less-expensive off-peak energy cost. Heim and Clarke [273] considered the possibility to calculate non-linear thermal properties of PCMs in the simulation environment *ESP-r* to evaluate the potential of microencapsulated PCM mixed with gypsum for building wall applications. The behavior of PCMs was modeled using *ESP-r* special materials facility and the effect of phase-change was added to the energy balance equation as a latent heat generation term according to the effective heat capacity method. These authors carried out a set of numerical simulations for a multi-zone, highly glazed and naturally ventilated passive solar building, considering the weather data of Warsaw, Poland. They carried out comparative analysis between PCM-impregnated gypsum plasterboard and pure gypsum plasterboard and assessed the effect of latent heat storage on the thermal behavior of the building. The authors stated that this effect did not cause a substantial reduction in the diurnal temperature fluctuation. However, it decreased the internal air temperature in the transitions periods when the solar energy was effectively stored. The solar energy stored in the PCM-gypsum plasterboard can reduce the heating energy demand by up to 90% during the heating season studied.

Heim [274] also selected the effective heat capacity method for implementation into *ESP-r* tool and studied the yearly effect of isothermal storage of solar energy in building material components. Numerical simulations were conducted for two cases of multi-zone, highly glazed and naturally ventilated passive solar buildings, for moderate climatic conditions. In the first case study, a PCM-gypsum plasterboard was used as an internal room lining (direct gains room), and in the second

case study, a transparent insulation material combined with PCM was applied for the external south-faced wall (indirect solar gains wall). For both case studies, the author compared the air, surface and resultant temperatures with a reference no-PCM case study. The daylight period and the seasonal latent heat storage effect were also analyzed. The author concluded that the effect of latent heat storage depends on PCM layer thickness, phase-change temperature range and total latent heat of the phase-change. For direct gains zone, the thin layer with a high latent capacity was preferred against a thick layer with a relatively lower latent capacity. For indirect gains zone, thick elements provided a process continuing over time and allowed the energy stored to be used at night.

Few references of generalized DSEB of modular lightweight buildings with passive LHTES systems with PCMs are found in the literature. The work developed in this field by Hoes *et al.* [269] is particularly interesting due to its generalized approach. They used *ESP-r* for simulating the building dynamic behavior, and they evaluated a new concept that combines the benefits of buildings with low and high thermal mass, by applying hybrid adaptable TES systems to a lightweight building. The hybrid concept increases building performance and adaptability to seasonal variations and climate changes. Schossig *et al.* [91] simulated the thermal performance of a lightweight office using *ESP-r*. They concluded that the application of microencapsulated PCMs in interior wall materials prevents overheating and reduces the cooling load in summer. They also extend the study from building simulations to first measurements of full-size rooms with PCMs.

V.3.3 TRNSYS

The *TRNSYS* software is used for building dynamic simulation based on transfer functions technique, it is modular in nature and contains many subroutines for various systems including buildings [378]. In their work, Ibáñez *et al.* [354] describe a simple methodology for the energy simulation of buildings with PCMs using *TRNSYS*. The storage and release effects of PCMs were simulated using the active layer tool Type 56. The methodology was presented and experimentally validated in a building such as a prototype room built with concrete panels with PCM. They evaluated the influence of walls, ceiling and floor with PCMs in the whole energy balance of a building considering free cooling. Taking into account several recommendations to minimize the amount of PCM used, the results showed an average maximum ambient temperature decrease of up to 3 °C. In the work of Bontemps *et al.* [345], the energy performance of a dividing wall model was also evaluated with the *TRNSYS* Type 56.

In the work of Ahmad *et al.* [284], a numerical simulation with *TRNSYS* was carried out by adding a new module representing the new PCM-wallboard. The model consisted in 729 finite volume nodes, 9 nodes in each direction of the wall. The high node number slows down the simulations. Furthermore, the specific heat capacity is fixed to a top hat temperature function. The

model showed a good agreement with experimental results. Kuznik *et al.* [353] developed and validated through experimental results, a new *TRNSYS* Type, called Type 260, to model the thermal behavior of a PCM external wall. Stovall and Tomlinson [276] also used a verified *TRNSYS* code to show the potential of PCMs to improve buildings thermal comfort and to decrease peak-loads. The potential benefits of using a PCM-wallboard for passive solar applications with thermostat control were analyzed by the authors. The results showed that the PCM-wallboard did not improve the occupants comfort level with the traditional thermostat control, but can provide considerable load management relief. Lu *et al.* [379] developed an apparent specific heat capacity phase-change heat transfer model and a new *TRNSYS* component called Type 272. The proposed PCM room's TRNSYS heat transfer model is based on the latent heat utilization ratio to treat the melting and solidification processes. The model was validated against experimental results. The new model can be used to accurately simulate indoor temperature and surface temperatures of the walls. As suggested by the authors, it can also be used to optimize the design of the PCM room by simulating different kinds of PCMs, locations, and different combinations with cold and heat source [379]. Meng *et al.* [380] experimentally and numerically investigated the thermal performance of a new PCM room, which aims to control the indoor air temperature and improve indoor thermal comfort. For this purpose, a new model called Type 188 was developed in *TRNSYS*17.

Koschenz and Lehmann [157] developed a new model to be integrated in *TRNSYS* allowing the investigation of the behavior of real buildings with PCM active ceiling panels. As stated before, the comprehension of PCM models for the DSEB of active TES systems can contribute for the assessment of passive TES systems. Belmonte *et al.* [381] have used *TRNSYS* for the thermal simulation and system optimization of a chilled ceiling coupled with a floor containing a PCM. Lin *et al.* [382] investigated a ceiling ventilation system enhanced by solar photovoltaic thermal collectors and PCMs. The performance of the system was numerically evaluated based on a Solar Decathlon house using *TRNSYS*.

An updated review on the main Types in *TRNSYS* used to simulate PCMs was provided by Al-Saadi and Zhai [47].

V.3.4 Future outlook

Further work still needs to be done in the research field of DSEB considering the latent heat from phase-change processes of PCMs. There is still a simulation and analysis gap in the DSEB with respect to PCM benefits and modeling, in the development of comprehensive PCM models validation, in the cover of a wide range of PCM types, their location within passive TES systems and the best positions of this systems in the building. There is also an analysis gap with respect to the comparison between

the existing PCM modules for several DSEB tools in order to evaluate the accordance between them. A comparison assessment should also be done to validate the different PCM modules considering the same reference and to evaluate the accuracy of each module. The validation of DSEB results against experimental results in real scale building conditions is an active area of research in the future as well as the comparison between DSEB results and other numerical and CFD results. To predict the appropriate material properties for passive heating during winter, and cooling during summer, a wider analysis using multi-criteria and optimization is required.

Another future active area of research is the multi-objective optimization of buildings configurations with PCM passive TES systems. Several multi-objective optimization methods are reviewed in ref. [383]. The decision-maker has to compensate environmental, energy, financial and social factors in order to reach the best possible solution that will ensure the maximization of the energy efficiency of the building, satisfying at the same time the building's final user/occupants needs [4]. Multi-objective optimization techniques coupled to DSEB must be considered in the problem of improving the energy efficiency of buildings with passive latent heat TES systems with PCMs, so that the maximum possible number of alternative solutions may be considered, as well as the competitiveness between the decision criteria. Thereby, this will allow searching for feasible solutions according to the cost and energy savings objectives, helping decision-making.

V.4 Lifecycle assessment of passive TES systems with PCMs

Considering the integration of passive TES system with PCMs within the building, a lifecycle assessment (LCA) study is important to determine if the reduction of the energy consumption for heating and cooling during the operational stage of the building can balance out the embodied energy (EE) of PCMs. Few references of such analysis are found in the literature. De Gracia *et al.* [87] evaluated the environmental impact of incorporating PCMs in typical masonry Mediterranean building. They developed an LCA study based on the Ecoindicator 99 (EI99) method for three monitored cubicles built in Lleida, Spain, with different envelope solutions. The energy savings for cooling the cubicles during the summer was measured in order to evaluate the influence of PCMs during the operational stage of the cubicles. Results showed that the addition of PCMs in the building envelope, although decreasing the energy consumption during the operation stage, does not significantly reduce the global impact throughout the lifetime of the building. However, for the hypothetical scenario of considering summer conditions all year round and a lifetime of the building of 100 years, the use of PCMs reduces the overall impact by more than 10%. In the authors view, the global benefit of using PCMs in buildings can be maximized by designing both the building and the PCM for a long term operation. From the lifetime analysis of the real scenario, the global impact payback time was estimated at 25 years for the hydrated salts and at 61 years for the paraffins.

Menoufi *et al.* [384] have also developed an LCA study based on EI99 for 7 experimental masonry cubicles built in Lleida, Spain, to test different construction techniques, building materials, insulating materials and PCMs, in order to point out the most sustainable solution with lower energy demand during the operational phase. Results showed that although some of these materials are able to reduce the energy demand, and consequently the environmental impact during the operational phase, they still have high EE that can cause high environmental impact during the manufacturing phase.

Many studies have shown the contribution of the building's thermal mass for the lifecycle energy consumption and environmental impact of the building [385,386]. These studies should be extended to include the incorporation of PCMs within buildings. Regarding LCA studies, to determine if the energy savings for heating and cooling (due to PCMs) during the operational phase of the building can balance out the high EE of PCMs, further work must be done in order to make a sensitive analysis on the influence of the lifecycle impact assessment (LCIA) method chosen. Further work should also be done to assess the best types of PCMs in a life cycle thinking way. Further scenarios, other than those already found in the literature, must be evaluated and more methodological strategies coupling the DSEB techniques and the LCA techniques should be developed in order to assess the real potential of passive LHTES systems with PCMs in a lifecycle thinking way. Further work should also be done in order to evaluate the real environmental benefits of including passive TES systems with PCMs in building solutions. For example, studies as the one developed by Dylewski and Adamczyk [387] to assess the economic and environmental benefits of thermal insulation of building external walls could be extended to the consideration of PCM passive TES systems in the building's walls.

V.5 Economic impact analysis

In its "Advanced Phase Change Material Market: Global Forecast (2010-2015)" [388] *MarketsandMarkets* reports that the increasing demand for energy-saving and environment-friendly technology is driving the growth of the global PCM market. Furthermore, they stated that the global PCM market is expected to grow from $300.8 million in 2009 to $1,488.1 million in 2015, at an estimated Compound Annual Growth Rate of 31.7% from 2010 to 2015. Another study presented the economic feasibility of using PCM storage for peak shaving [171]. As the authors stated, one of the merits of peak shaving is the cost effectiveness: PCMs could store energy of discounted tariff or free one from natural environment. However, savings by PCMs should compensate the cost of installation, by using payback years. The authors concluded that the economic feasibility of a PCM storage system could be evaluated from a number of times of usage until the investment paid back: payback cycle. It was showed that the payback cycle of a system with PCMs is strongly affected by the price of the PCM used and by the price of the energy saved. The technical-economic analysis of

the impact of including PCM-based passive TES systems in buildings (hardly ever treated in many previous studies and economical life cycle analysis) should be performed to determine into which conditions TES systems with PCMs should be used. Furthermore, the use of PCM-based systems compared to standard sensible heat systems should be further discussed to assess their cost-effectiveness and to help decision-making.

In their work, Shilei *et al.* [175] showed that the studied PCM-wallboard enhanced room could greatly reduce the operating cost of HVAC systems in summer by transferring electric power peak load to valley. Peippo *et al.* [389] also evaluated the effect of PCM-wallboards in energy savings. The PCM-wallboard reduces the supplementary heating energy by approximately 2 GJ/year (or about 6%) for the climatic conditions in Helsinki, which means an annual benefit of $34 for a cost of heat of approximately 17 $/GJ, resulting in a payback time of 18 years, assuming a cost of 1.5 $/kg for the PCM. Considering another PCM and the climatic conditions of Madison (Wisconsin), the simulations showed that the PCM-wallboard reduces the supplementary heating energy by approximately 3 GJ/year (or about 15%), resulting in a payback time of 9 years assuming a cost of 1.5 $/kg for the PCM and a cost of heat of approximately 17 $/GJ. Stovall and Tomlinson [276] also concluded that the integration of PCM-wallboards in the simulated house in Boston could save $190 annual cost saving with a 3–5 years payback period. Zhu *et al.* [106] investigated the impacts of integrating SSPCMs into the office building envelope considering different control strategies on the energy consumption and peak-load demand, as well as electricity cost of building air-conditioning systems at typical summer conditions in subtropical and dry continental climates policies (*i.e.*, time-based pricing and energy-plus-demand-based pricing). The results showed that the use of SSPCMs in the building could reduce the building electricity cost significantly (over 11% in electricity cost reduction and over 20% in peak-load reduction).

Habeebullah [390] investigated the economic feasibility of both building an ice thermal storage and structure a time of rate tariff for the unique air conditioning plant of the Grand Holy Mosque of Makkah in Saudi Arabia. Rismanchia *et al.* [391] also evaluated the energetic, economic and environmental benefits of utilizing ice thermal storage systems for office building applications. These studies are based on active latent heat TES systems and they are out of the scope of this thesis. However, they allow to conclude that technical-economic studies should be developed to relate the potential of integrating PCM-based passive TES systems in buildings with the energy peak load reduction/shifting potential, the energy savings and the tariff structure. Studies as the one developed by Ozel [392] to assess the optimum insulation thicknesses, energy savings and payback periods calculated by using lifecycle cost analysis over a lifetime of 20 years of the building, should be extended to PCM applications.

V.6 Contribution of passive TES systems towards NZEBs

Nowadays there is a significant potential for cost-effective energy savings in the buildings sector that would lead to significant economic, social and environmental benefits. To address the buildings sector, EU regulators have published the Energy Performance of Buildings Directive (EPBD) [393], and its recast [394]. The EPBD mainly focuses on reducing the operational energy consumption of buildings, but it also establish that by 2020, every new building in the EU must be a "nearly-zero" energy building (NZEB), which means to reduce the building energy demand and to produce energy on building site (or nearby) to attain energy balance in a cost-effective way. The concepts and details of NZEBs have been widely discussed in the literature [395–398]. However, no reference about the benefits of including passive LHTES systems with PCMs in NZEBs are found in the literature.

As stated by Marszal and Heiselberg [397], in order to build a cost-effective NZEB, the energy use should be reduced to a minimum leaving just a small amount of left energy use to be covered by renewable active energy generation. Hence, the construction should be optimized to ensure reduced consumption before renewable active systems are integrated to obtain an energy balance. It is known by now that the integration of passive latent heat TES systems with PCMs in buildings can contribute to reduce the energy consumption for heating and cooling but further research should be done to find the most cost-effective solutions with PCMs for each building and climatic conditions, and to help decision-making.

Further work should also be done to sketch a methodology for evaluating the potential of PCMs towards NZEBs. This is challenging because several techniques should be coupled, mainly the DSEB, the economic analysis, the multi-criteria or even the multi-objective analysis in order to find out the best configuration for the passive TES systems with PCMs and their position within the NZEB.

CHAPTER VI

Optimizing the incorporation of PCM-drywalls in LSF residential buildings in different European climates

In this chapter, a holistic model is developed to optimize the incorporation of PCM-drywalls in an air-conditioned LSF residential room, considering real-life conditions and several European climates. The main goal is to maximize the heating and cooling energy savings in a passive way. A multi-dimensional optimization study is carried out by combining *EnergyPlus* and *GenOpt* tools. The CondFD-algorithm is used in *EnergyPlus* to simulate phase-changes. For the optimization, the PSOCC-algorithm is used considering a set of predefined discrete construction solutions. These variables are related with the thermophysical properties of the PCM (enthalpy-temperature and thermal conductivity-temperature functions), the solar absortance of the inner surfaces, and the thickness and location of the PCM-drywalls in the room. Indices of energy-savings for heating, cooling and for both heating and cooling are defined to evaluate the energy performance of the PCM-drywalls enhanced rooms. Some guidelines for the incorporation of PCM-drywalls in LSF residential buildings in Europe are provided. This chapter summarizes the results which have been published in the paper "*Multi-dimensional optimization of the incorporation of PCM-drywalls in lightweight steel-framed residential buildings in different climates*" by Soares *et al.* [399]. Chapter VI is divided into four sections. Section IV.1 provides the framework of the optimization problem to be investigated. Section IV.2 introduces the problem, the methodology carried out and the main design variables considered in the optimization model. The reference room and the performance indicators are also presented in this section. The *EnergyPlus* PCM model used in the DSEB approach is also presented in Section IV.2. Section IV.3 presents and discusses both annual and monthly assessment basis results. Section IV.4 provides the final remarks and the main conclusions of the study.

VI.1 Introduction

LSF construction has been attracting interest worldwide and its popularity is increasing for use in both residential houses and apartment blocks. It presents certain advantages over heavyweight construction such as: low weight; reduced disruption on site and speed of construction; almost 100% recyclability, and architectural flexibility for retrofitting purposes and modular construction. LSF construction is also particularly suited to the economy of mass production, due to a superior quality and high standards achieved by off-site manufacture control.

The main disadvantage of LSF construction can be its low thermal mass and the consequential risk of comfort problems (*e.g.* overheating). It is also more vulnerable to large temperature fluctuations, which may lead to higher heating and cooling energy demands. To overcome these problems, drywalls with PCMs can be incorporated allowing the building's thermal storage capacity to adapt to the needs. In LSF construction, drywalls (which are very suitable for the incorporation of microencapsulated PCMs) are widely used. As reviewed in the last chapter, many studies (numerical [113,164,174,275,277,278,288], experimental [175,281–283] or both numerical and experimental [91,162,172,178,180,186,220,284,285]) have been carried out to assess the performance of PCM-

drywalls. In recent years further studies concerning the application of these elements in real buildings have been carried out in order to evaluate the influence of PCM-drywalls in more real-life conditions [177,400].

The efficiency of these elements depends on numerous factors, such as: (*i*) their location in the building; (*ii*) their volume and thermophysical properties; (*iii*) the phase-change temperature range; (*iv*) the latent heat capacity; (*v*) the climatic conditions; (*vi*) the internal and solar gains; (*vii*) the reflectivity and orientation of the surfaces; (*viii*) the ventilation rates; (*ix*) the air-conditioning controls, and (*x*) the architectural characteristics. Therefore, the optimization of the incorporation of PCM-drywalls in LSF residential buildings is a complex task as several modeling parameters must be taken into account to realistically describe the real-life performance of the PCM-enhanced building. Besides, the relationship between the set of parameters may not be simply understood due to the nonlinearity of the problem. As a result, the evaluation of the impact of alternative scenarios on the performance of the building requires exploring a large decision space (due to its combinatorial nature) which can be very time consuming and inefficient in a traditional parametric and iterative process.

As found by many authors, combining DSEB and optimization tools can help to optimize the design of buildings and HVAC systems in a more efficient way [401–404]. Particularly, *GenOpt* [405] is an optimization tool that can be used for the minimization/maximization of a predefined cost function (or objective function) that is evaluated by an external building energy simulation program. As stated in Chapter V, nowadays there are many DSEB tools. *EnergyPlus* [406], *ESP-r* [407] and *TRNSYS* [408] are highlighted for their versatility and reliability [354]. They are able to model PCMs for different applications in buildings as shown in works carried out using *EnergyPlus* [356,363,369,409], *ESP-r* [91,269,273,274,376] and *TRNSYS* [157,284,345,353,354]. The implemented models varied from early PCM models, to empirical models using an equivalent heat transfer coefficient, to fully implemented finite difference models and control volume models [363]. The *EnergyPlus* PCM model uses a one-dimensional conduction finite-difference (CondFD) solution algorithm which was recently validated against multiple test suites (analytical verification, comparative testing, and empirical validation) by Tabares-Velasco *et al.* [363].

The work presented in this chapter aims at evaluating the impact of PCM-drywalls in the annual and monthly heating and cooling energy savings of an air-conditioned LSF residential single-zone building (living-room), considering real-life conditions and several European climates. To accomplish this, a multi-dimensional optimization approach is proposed by combining *EnergyPlus* 8.0.0 and *GenOpt* 3.1.0 tools. To find the optimum solution for each climate, a set of discrete variables are considered in the model, namely those related with the thermophysical properties of the PCM (enthalpy-temperature and thermal conductivity-temperature functions), solar absorptance coefficient

of the inner surfaces (α) and thickness and location of the PCM-drywalls. Several parameters are included in the model to better simulate real-life conditions mainly those related with the air-conditioning set-points, air infiltration rates, solar gains, internal gains from occupancy, equipment and lighting. The final goal of this chapter is to provide some guidelines for the optimum incorporation of PCM-drywalls in LSF residential buildings in Europe.

VI.2 Methodology

VI.2.1 Problem description and design variables

In this study, a simulation-based optimization scheme is developed to account for the annual cooling and heating energy savings due to the incorporation of PCM-drywalls in a reference model. This scheme is based on the combination of *EnergyPlus* with the optimization engine *GenOpt*, as sketched in Fig. VI.1. *GenOpt* can automatically rewrite the input files for *EnergyPlus*, changing the independent variables considered, run the DSEB program, read (from the simulation result file) the output value of the objective function (OF) to be minimized/maximized and then determine the new set of input parameters for the next run. This iterative process is repeated until a predefined criterion of convergence is fulfilled or the maximum number of iterations is reached. The methodology carried out is divided in three main environments: the simulation environment iteratively linked to the optimization environment for determining the optimized solution; plus, the post processing environment, which is based on the optimized solution previously found (Fig. VI.I).

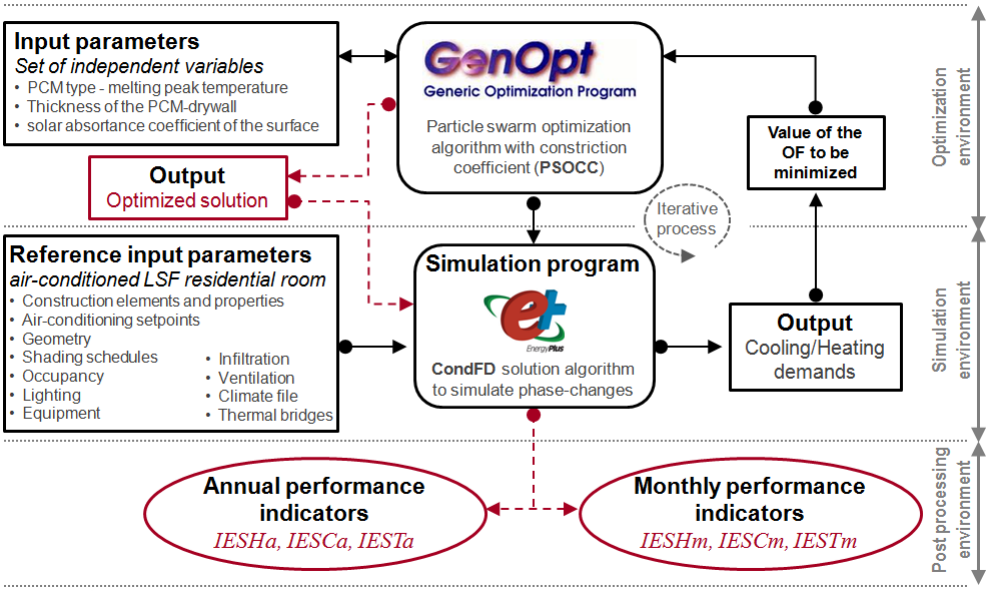

Fig. VI.1 Sketch of the methodology carried out.

A reference air-conditioned LSF single-zone room is defined in Section VI.2.6 for each climate presented in Section VI.2.4. The annual heating and cooling energy demands are determined for each reference room and then compared through simulation with the total heating and cooling energy demands of the correspondent PCM-enhanced room. This is attained by varying the location of the PCM-drywall elements (walls and ceiling), their thickness, the melting temperature of the PCM and the α–value (solar absortance coefficient) of the inner surfaces. A set of constant parameters is used to simulate the real-life behavior of the room (which remains constant for all the case studies). These parameters are also described below in Section VI.2.6 and summarized in Fig. VI.1.

The incorporation of PCM-drywalls in the LSF single-zone building is taken as a single objective multi-dimensional optimization problem. The objective function (OF) f: $\mathbf{X} \rightarrow \mathbb{R}$ (f: $\mathbb{Z}^{nd} \rightarrow \mathbb{R}$) is to be minimized, *i.e.* finding $\min_{x \in \mathbf{X}} f(x)$ subject to $\mathbf{X} \triangleq \{x \in \mathbb{Z}^{nd} \mid x^i, i \in \{1, \ldots, nd\}\}$. The $x \in \mathbf{X}$ is defined as the vector of independent variables and $\mathbf{X} \subset \mathbb{Z}^{nd}$ is the constraint set. All design solutions incorporating PCM-drywalls are specified as discrete independent variables that can only take predefined discrete values defined in $\mathbb{Z}^{nd}$. These predefined construction solutions are function of the melting-peak temperature of the PCM (T_{mp}), the thickness of the PCM-drywall (e_{PCM}) and the α-value of the inner surfaces. Six PCM-drywalls with melting-peak temperatures of 18, 20, 22, 24, 26 and 28 °C are considered for the optimization problem. The e_{PCM}–value can assume one of the seven possible values: 1.0, 1.5, 2.0, 2.5, 3.0, 3.5 and 4.0 cm. Drywalls are typically 1 to 2 cm thick. Therefore, the maximum thickness considered for the PCM-drywall is 4 cm to keep physical practicality. The α–value is related to the color of the surface (selective inks can be used) and it can be equal to 0.3, 0.5, 0.7 or 0.9. Regarding the combination of all referred values, a set of 169 predefined discrete solutions can be considered for each surface of the room (reference solution + 6 PCMs × 7 e_{PCM}–values × 4 α–values).

Five categories of enhanced surfaces with PCM-drywalls are involved in the optimization problem: external southern (S), western (W) and eastern (E) walls; northern partition wall (N) and ceiling (C). S, W, E, N and C represent the set of predefined admissible discrete solutions for each corresponding surface. Hence, this optimization setup is five-dimensional (nd = 5). Constraint sets for the independent variables are defined as $x^1 = \{ S_j, j \in \{0, \ldots, 169\}\}$, $x^2 = \{ W_k, k \in \{0, \ldots, 169\}\}$, $x^3 = \{ E_l, l \in \{0, \ldots, 169\}\}$, $x^4 = \{ N_m, m \in \{0, \ldots, 169\}\}$, and $x^5 = \{ C_p, p \in \{0, \ldots, 43\}\}$. In the optimization model, vector C has only 43 admissible values as the solar absortance of the ceiling is kept constant and equal to 0.3.

VI.2.2 Optimization approach

The OF to be minimized (Eq. VI.1) for each climate is based on the annual heating and cooling energy savings from the replacement of the inner gypsum plasterboard layer of the reference surfaces by a PCM-drywall. In other words, the main goal is to maximize the energy savings due to the incorporation of PCM-drywalls in the model. $E_{\text{heat,ref,a}}$ and $E_{\text{cool,ref,a}}$ are the annual energy demand for heating and cooling, respectively, derived from the simulation of the reference room. $E_{\text{heat,PCM,a}}$ and $E_{\text{cool,PCM,a}}$ are also predicted by simulation and they correspond to the annual energy demand for heating and cooling, respectively, after including PCM-drywalls in the model. For each optimization problem, with the corresponding weather data, $x^* \in \mathbf{X}$ denotes the iterated solution with the lowest cost function value. It can also be defined as $x^* = \{S_j, W_k, E_l, N_m, C_p\}_{\text{opt}}$.

$$\text{OF}(x) = E_{\text{heat,PCM,a}}(x) + E_{\text{cool,PCM,a}}(x) - E_{\text{heat,ref, a}} - E_{\text{cool,ref, a}} \quad \text{(VI.1)}$$

The efficiency and success of an optimization process is strongly affected by the properties and the formulation of the OF, and by the selection of an appropriate optimization algorithm [410]. The full enumeration (exhaustive search) of the design parameters space requires more than 35×10^9 *EnergyPlus* simulation runs, corresponding to 43 ceilings × 169 southern × 169 western × 169 eastern × 169 northern walls. To avoid looking for the independent variables that yield better performance in the entire design parameter space, which is very time consuming, the particle swarm optimization algorithm with constriction coefficient (PSOCC) described in ref. [410] is used.

Particle swarm optimization (PSO) algorithms are from a family of meta-heuristic population-based and stochastic optimization techniques first proposed by Kennedy and Eberhart [411,412]. At each iteration step, PSO compares the cost function value of a finite set of points, called particles. The set of potential solutions (particles) is called a population. The next populations are computed using a particle update equation. As summarized by Wetter and Wright [401], the change of each particle from iteration to iteration is modeled based on the social behavior of flocks of birds or schools of fish. Each particle attempts to change its location in $\mathbf{X}$ source to a point where it had a lower cost function value at previous iterations (cognitive behavior modeling), and in a direction where other particles had a lower cost function value (social behavior modeling) [401]. In this study, the simulation model is computationally expensive due to the big dimension of the vectors that describe the possibilities for each discrete variable. PSOCC algorithm is used with the *von Neumann* neighborhood topology, a population size of 25 particles with a maximum of 1500 generations, a seed of 1, a cognitive acceleration constant of 2.8, a social acceleration constant of 1.3, a velocity clamping with a maximum velocity gain of 4 and a constriction gain of 0.5.

VI.2.3 Performance indicators: indices of energy savings

Three indices of energy savings are defined to evaluate the energy performance of the PCM-drywall enhanced room for each climate under investigation, namely the indices of energy savings for heating ($IESH_i$), for cooling ($IESC_i$) and for both heating and cooling ($IEST_i$), respectively defined as:

$$IESH_i = 1 - E_{\text{heat,PCM},i} / E_{\text{heat,ref},i}, i = \{a, m\} \quad \text{(VI.2)}$$

$$IESC_i = 1 - E_{\text{cool,PCM},i} / E_{\text{cool,ref},i}, i = \{a, m\} \quad \text{(VI.3)}$$

$$IEST_i = 1 - E_{\text{tot,PCM},i} / E_{\text{tot,ref},i}, i = \{a, m\} \quad \text{(VI.4)}$$

where, $E_{\text{tot,ref},i}$ and $E_{\text{tot,PCM},i}$ are the total energy demand for heating and cooling considering the reference room and the PCM-drywalls enhanced room, respectively. Subscript i refers to time period assessment. The subscripts a and m correspond to the annual and the monthly assessment basis, respectively.

VI.2.4 Characterization of the European climates

Seven climate files provided by the International Weather for Energy Calculation (IWEC) [406] for different cities were considered to cover the main European climatic regions according to the Köppen-Geiger classification [413]. Table VI.1 presents the Köppen-Geiger classification and the description of the seven reference climates selected for this study.

Table VI.1 Characterization of the European climates: Köppen-Geiger climate classification and description. Climates provided by the International Weather for Energy Calculation (IWEC) files [406].

Location	Köppen-Geiger classification	Climate description [406]
Seville, Spain	Csa	Mediterranean climate (dry hot summer, mild winter, lat. 30–45°N)
Coimbra, Portugal	Csb	Mediterranean climate (dry warm summer, mild winter, lat. 30–45°N)
Milan, Italy	Cfa	Humid subtropical (mild with no dry season, hot summer, lat. 20–35°N)
Paris, France	Cfb	Marine west coastal (warm summer, mild winter, rain all year, lat. 35–60°N)
Bucharest, Romania	Dfa	Humid continental (hot summer, cold winter, no dry season, lat. 30–60°N)
Warsaw, Poland	Dfb	Moist continental (warm summer, cold winter, no dry season, lat. 30–60°N)
Kiruna, Sweden	Dfc	Subarctic (cool summer, severe winter, no dry season, lat. 50–70°N)

The European climates were divided into two main groups, warm temperate (C) and snow (D), and several subtypes regarding average values of precipitation – fully humid (f) and summer dry

(s) – and temperatures – hot summer (a), warm summer (b) and cool summer (c). Basically, the European climates change with latitude, altitude and coast vicinity. In southern Europe, the climate of regions with lower latitudes (below 45°N) is generally classified as Csa and Csb. Above these latitudes (between 45–55°N) the climate is mainly labelled as Cfb and Dfb, for western and eastern central European countries, respectively. In Northern Europe, in regions with latitudes above 55°N, the climate is typically classified as Dfc.

VI.2.5 EnergyPlus PCM model

EnergyPlus 8.0.0 includes the CondFD model proposed by Pederson [356] and improved by Tabares-Velasco *et al.* [363]. It is an implicit finite difference scheme coupled with an enthalpy-temperature function to account for phase-change energy accurately. Eq. (VI.5) represents the implicit formulation for an internal node:

$$\rho c_{\mathrm{p}} \Delta x \frac{T_{i,\mathrm{new}} - T_{i,\mathrm{old}}}{\Delta t} = k_{\mathrm{int}} \frac{T_{i+1,\mathrm{new}} - T_{i,\mathrm{new}}}{\Delta x} + k_{ext} \frac{T_{i-1,\mathrm{new}} - T_{i,\mathrm{new}}}{\Delta x} \tag{VI.5}$$

where,

$$k_{\mathrm{int}} = \left(k_{i+1,\mathrm{new}} + k_{i,\mathrm{new}}\right)/2 \tag{VI.6}$$

$$k_{\mathrm{ext}} = \left(k_{i-1,\mathrm{new}} + k_{i,\mathrm{new}}\right)/2. \tag{VI.7}$$

Subscripts refer to nodes and applicable time step. The new and old time steps are the present and the previous time steps, respectively. The node i is the node being modeled and the nodes i+1 and i–1 are the adjacent nodes to the inner and outer sides of the construction, respectively. The space between nodes used as the finite difference layer thickness is denoted Δx. In the CondFD algorithm, all elements are discretized using Eq. (VI.8) which depends on a space discretization constant (c), the thermal diffusivity of the material (α^*), and the time step (Δt). Eq. (VI.8) can also be written as function of the Fourier number (Fo):

$$\Delta x = \sqrt{c\alpha^* \Delta t} = \sqrt{\frac{\alpha^* \Delta t}{Fo}}. \tag{VI.8}$$

Eq. (VI.5) is coupled by Eq. (VI.9) and Eq. (VI.10) that relate the enthalpy (h) and the thermal conductivity (k) of the PCM with the temperature (T), respectively.

$$h_i = h\left(T_{i,\text{new}}\right) \tag{VI.9}$$

$$k_i = k\left(T_{i,\text{new}}\right) \tag{VI.10}$$

An equivalent variable specific heat ($c_{\text{p,eq}}$) at each time step can be defined as:

$$c_{\text{p,eq}}(T) = \frac{h_{i,\text{new}} - h_{i,\text{old}}}{T_{i,\text{new}} - T_{i,\text{old}}}. \tag{VI.11}$$

In a recent work, Tabares-Velasco *et al.* [363] identified some guidelines for using the *EnergyPlus* PCM model. They found that time steps equal to or shorter than three minutes should be used. They also stated that the default CondFD model can be used with acceptable monthly and annual results (Fo = 1/3 and c = 3). However, if accurate hourly performance and analysis is required, a smaller node space (1/3 of the default value) should be used at the expense of longer run times. In this study, the CondFD default model with 20 time steps per hour (Δt equal to three minutes) is used for the monthly and annual analysis of the heating and cooling energy demands (for both the reference and the PCM-enhanced rooms).

As stated above, the *EnergyPlus* PCM model requires an enthalpy-temperature function and a thermal conductivity-temperature function, both using data supplied as input. These functions are not linear for most PCMs and frequently not known in detail. Furthermore, obtaining these data could be challenging because careful selection of heating/cooling rates and calibration of instrumentation are needed [409]. In his recent work, Tabares-Velasco [409] investigated the energy impacts of the nonlinear behavior of enthalpy-temperature functions considering the CondFD model. These authors stated that a linear function could facilitate parametric and optimization analysis as well as broad analysis that would design generic PCMs that manufactures could later produce following specific guidelines [409]. He concluded that annual energy savings are not very sensitive to the linearization of the enthalpy-temperature curve. For hourly analysis, the simpler linear profiles should be specified in a way that the melting range covers roughly 80% of the latent heat, otherwise, hourly results can differ by up to 20% [409].

In the present study, the energy impacts of linear enthalpy-temperature functions are considered for microencapsulated PCMs distributed in drywalls. The DuPont™ Energain® PCM product was considered as a reference PCM-drywall. This material has a nonlinear enthalpy-temperature function, a melting temperature range centered around 21.7 °C, a latent heat of 70 kJ kg^{-1}, a density of 855 kg m^{-3}, a specific heat of 2500 J kg^{-1} K^{-1} and a variable thermal conductivity [363]. Based on the nonlinear enthalpy-temperature function of the reference material (PCMref), a new linear function was plotted for a hypothetical material (PCM22) with the melting range covering

roughly 80% of the latent heat (Fig. VI.2a). This new material has a melting temperature range between 18 °C and 26 °C centered around 22 °C. Five other hypothetical materials with the same latent heat characteristics were further defined to investigate the impact of different melting-peak temperatures. Therefore, six PCM-drywalls with different melting-peak temperatures are considered in the optimization problem. Fig. V1.2a and Fig. V1.2b show, respectively, the enthalpy-temperature and the thermal conductivity-temperature functions for the reference PCM-drywall and for the other six hypothetical materials defined.

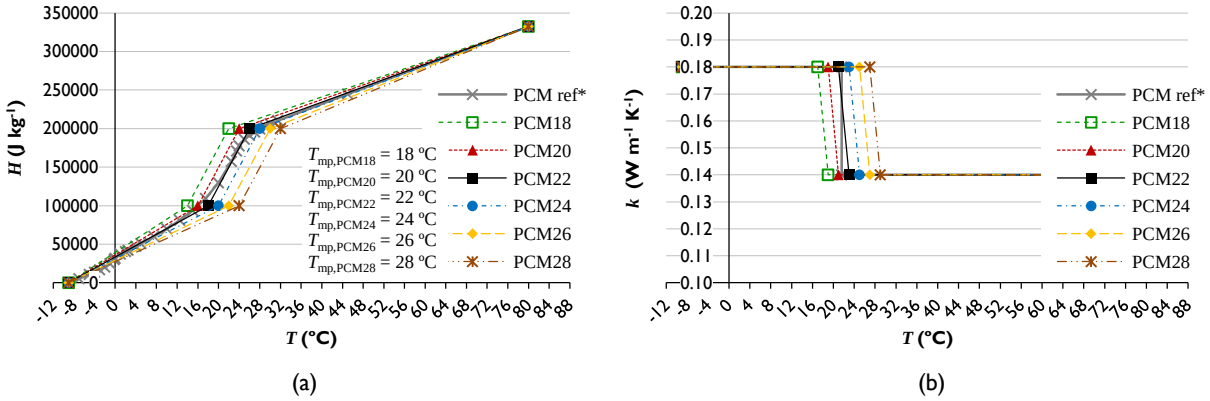

(a) (b)

Fig. VI.2 (a) Enthalpy-temperature and (b) thermal conductivity-temperature functions for the reference PCM-drywall and for other six hypothetical materials defined. *Data for DuPont™ Energain® PCM product obtained from differential scanning calorimeter (DSC) measurements with a heating rate of 0.05 °C min^{-1} [414].

The *EnergyPlus* PCM model described above simulates neither hysteresis of the PCM nor subcooling, and only the enthalpy-temperature information for the heating mode is inputted. Therefore, as found by Tabares-Velasco *et al.* [363], accuracy issues can arise when modeling PCMs with strong hysteresis. Hence, for the purpose of this study, subcooling and hysteresis are not considered in the simplified model. Another limitation of the *EnergyPlus* PCM model is that variations of the PCM density cannot be modeled to account for changes in volume during phase-change transitions. Additionally, the heat transfer by natural convection cannot be simulated using the pure diffusion *EnergyPlus* PCM model. This is not critical for problems considering microencapsulated PCMs dispersed in gypsum boards, but it may be particularly critical when evaluating free-form PCMs incorporated in envelope solutions. In these cases, a macrocapsule is normally considered to avoid leakage, and the heat transfer by natural convection and the volume variations must be considered in the model as discussed in Chapter III. For the purpose of this study, the density value is assumed constant and no changes in volume are considered.

VI.2.6 Reference rooms

For each climate considered, a reference room is defined based on an air-conditioned LSF residential single-zone (living room) with dimensions 8 m wide × 6 m long × 2.7 m high (Fig. VI.3). The reference room looks very similar to the one specified in ASHRAE 140 standard [415]. The total floor area of the room is 48 m² with a slab-on-grade foundation. The model is perfectly east-west oriented with a total window area of 12 m² on the south facade (solar factor G = 0.7). For an efficient use of solar heat gains, windows are provided with an external movable shading device (horizontal blinds with high reflectivity slats). From October to May, blinds are pulled back during the day to maximize solar gains (from 8am to 6pm). During the night (from 6pm to 8am) blinds are lowered and closed to reduce heat losses through the windows (slat angle set to 3°). From June to September, blinds are lowered with slats set to 90° during the day (from 8am to 8pm) to reduce solar gains. During summer nights blinds are retracted (from 8pm to 8am). Concerning boundary conditions, all vertical surfaces are considered external walls except the northern surface, which is a partition wall. For this surface, an adiabatic boundary condition is considered in the model, assuming that no heat exchanges occur between the living room and the other building zones (Fig. VI.3). The existence of interior doors is neglected in the simplified model.

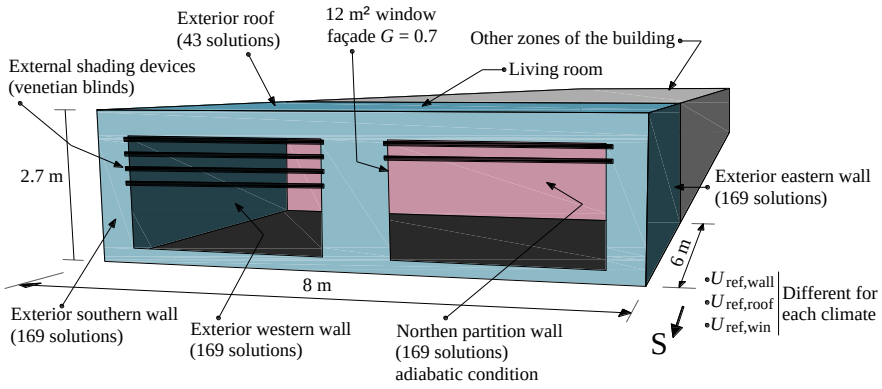

Fig. VI.3 Sketch of the case study living room facing the south facade.

Regarding internal heat gains, the living room is occupied by a maximum of 4 people in sedentary activity with a constant metabolic rate of 1.2 met (126 W person^{-1}). To simulate a real-lifestyle, the room is considered occupied during the weekend days and weekday evenings. The maximum heat loads due to equipments and lighting are 400 W and 120 W, respectively. Fig. VI.4. shows the occupancy, lighting and equipment schedules considered in the model. The reference rooms are air-conditioned considering an *ideal loads air system model* (in the *EnergyPlus* simulations) to obtain the rooms' thermal loads. When the living room is occupied, the thermostat is set with a dead

band so heating takes place for temperatures below 20 °C and cooling for temperatures above 25 °C. When the room is not occupied, the air temperature heating and cooling set-points are set to 15 °C and 30 °C, respectively. An infiltration rate of 0.5 air changes per hour is considered in the simulations. During summer nights (from June to September), when the room is empty (from 1 am to 8 am), a ventilation rate of 1.5 air changes per hour is also considered.

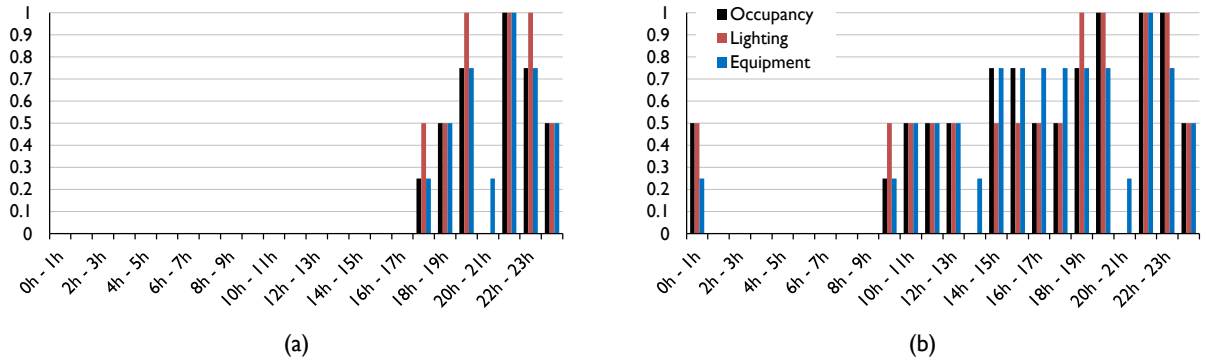

Fig. VI.4 Occupancy, lighting and equipment schedules during (a) weekdays and (b) weekends.

Generally speaking, there are three design types of LSF constructions: (*i*) cold framed construction; (*ii*) warm framed construction, and (*iii*) hybrid construction. In this study a hybrid framed construction is adopted with insulation tightly fitted between the steel studs in addition to insulation at the external side of the studs. Fig. VI.5 illustrates the cross-sections of the LSF walls (Fig. VI.5a), roof (Fig. VI.5b), slab-on-grade (Fig. VI.5c) and partition walls (Fig. VI.5d). Hybrid construction differs from cold framed construction because in the latter one, all the insulation is included within the thickness of the steel components and the steel members entirely bridge the insulation layer. Therefore, this construction has a higher degree of thermal bridging. In warm framed construction, all the insulation is placed outside the steel framing [416]. Table VI.2 lists the thermophysical properties of the materials considered in this study.

The set of parameters described above prevails for all the reference rooms. Variations in thermal insulation standards are to be expected from the north to the south European countries. In fact, the maximum U–value of the envelope elements are fixed by the building regulations of each country [417] as the result of the implementation of the Energy Performance of Buildings Directive (EPBD) by each state. In this work, different reference U–values are considered for the exterior walls, roof and windows of each climate as shown in Table VI.3. The reference U–values are considered equal to the correspondent maximum U–values specified in the regulation of each country according to ref. [417]. In Section VI.2.7 a simplified method for calculating U–values of LSF construction elements is described to account for thermal bridging effect. U–values are obtained by

varying the thickness of the outer insulation layers, $e_{ins,wall}$ and $e_{ins,roof}$ (Fig. VI.5). In the PCM-drywalls enhanced rooms, the inner plasterboard layers of the exterior walls, roof and partition wall are replaced by a PCM-drywall layer as explained before.

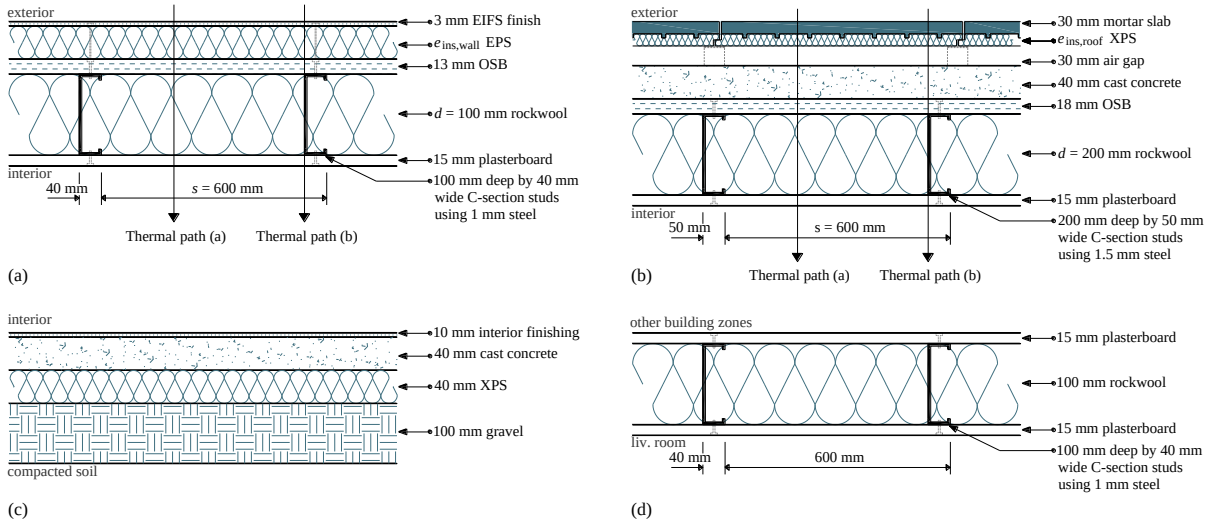

Fig. VI.5 Cross-section of the construction elements considered in the model: (a) exterior wall, (b) roof, (c) slab-on-grade and (d) partition wall.

Table VI.2 Thermophysical properties of the building components.

Material	k (W m^{-1} K^{-1})	c_p (J kg^{-1} K^{-1})	ρ (kg m^{-3})
EIFS finish	1.150	1500	1050
EPS	0.040	1400	15
XPS	0.034	1400	35
Rockwool	0.040	840	30
OSB	0.130	1700	650
Plasterboard	0.250	1000	900
Mortar slab	0.880	896	2800
Cast concrete	0.380	1000	1200
Gravel	2.800	800	2500
Interior finishing	0.170	1400	1200
Steel	50.000	450	7800

Table VI.3 Reference U–values (and correspondent insulation thicknesses) of the exterior opaque elements and windows for the different climates according to the building regulations of each country.

	Csa Seville	Csb Coimbra	Cfa Milan	Cfb Paris	Dfa Bucharest	Dfb Warsaw	Dfc Kiruna
$U_{ref,wall}$ (W m^{-2} K^{-1})	0.82	0.70	0.34	0.45	0.57	0.30	0.18
$U_{ref,roof}$ (W m^{-2} K^{-1})	0.45	0.50	0.30	0.28	0.20	0.25	0.13
$U_{ref,win}$ (W m^{-2} K^{-1})	5.20	4.30	2.20	2.00	1.30	1.70	1.30
$e_{ins,wall}$ (mm)	0.60	6.00	53.00	30.00	15.50	65.00	140.00
$e_{ins,roof}$ (mm)	5.00	0.50	30.00	38.00	73.00	47.00	150.00

VI.2.7 U–values in lightweight steel framing and thermal bridging in EnergyPlus

The effects of non-homogenous layers and thermal bridges (when the difference between the thermal conductivity of materials is large) should be considered in the calculation of the U–value of LSF elements [418]. Indeed, as suggested by Gorgolewski [419], depending on the details of the construction, ignoring the effect of the steel can lead to an overestimation of the thermal resistance by up to 50%. In this section, a simplified method to account for thermal bridging effects in *EnergyPlus* simulations is presented. A fictitious equivalent material is defined to replace the heterogeneous layer composed by insulation and steel frames. The thermal conductivity of the equivalent layer material is adjusted for each climate so that the effective thermal resistance is equal to that of the insulation panel with metallic frames. U–values listed in Table VI.3 are used to determine the equivalent thermal conductivities. The density and the specific heat of these equivalent materials are also adjusted to match the thermal capacity of the insulation with metal frames according to Eqs. (VI.12) and (VI.13), respectively,

$$\rho_{\mathrm{eq}} = \sum_{i=1}^{n} \rho_i \phi_i \tag{VI.12}$$

$$c_{\mathrm{p,eq}} = \frac{1}{\rho_{\mathrm{eq}}} \sum_{i=1}^{n} \phi_i \rho_i c_{\mathrm{p},i} \tag{VI.13}$$

where: ρ_{eq} is the density of the equivalent layer (kg m^{-3}); ρ_i is the density of the material i (kg m^{-3}); ϕ_i is the volumetric fraction of the material i; $c_{\mathrm{p,eq}}$ is the specific heat of the equivalent layer (J kg^{-1} K^{-1}) and, $c_{\mathrm{p,i}}$ is the specific heat of the material i (J kg^{-1} K^{-1}).

Table VI.4 lists the values of the thermal conductivity of the equivalent homogeneous layer materials for each climate. Considering the exterior and partition walls elements, the density and the specific heat of the equivalent homogeneous material are equal to 116 kg m^{-3} and 549.7 J kg^{-1} K^{-1}, respectively, for all the climates. As for the exterior roof elements, these values are 123 kg m^{-3} and 544 J kg^{-1} K^{-1}, respectively.

Table VI.4 Thermal conductivity of the equivalent homogeneous layer materials for each climate.

		Csa Seville	Csb Coimbra	Cfa Milan	Cfb Paris	Dfa Bucharest	Dfb Warsaw	Dfc Kiruna
Exterior walls	$k_{\mathrm{eq,wall}}$ (W m^{-1} K^{-1})	0.114	0.107	0.077	0.086	0.096	0.073	0.061
Exterior roof	$k_{\mathrm{eq,roof}}$ (W m^{-1} K^{-1})	0.140	0.147	0.114	0.109	0.092	0.104	0.077
Partition wall	$k_{\mathrm{eq,part}}$ (W m^{-1} K^{-1})	0.112	0.112	0.112	0.112	0.112	0.112	0.112

The simplified method of calculating U–values in LSF hybrid construction proposed in refs. [416,419] is used in this study. This method is similar in principle to that used in BS EN ISO 6946 [420] but adapted to increase accuracy for hybrid LSF construction. It was found by Gorgolewski [419] that with the proposed method the mean error of prediction compared with finite element modeling is less than 3% with a maximum error of 8% for a range of 52 assessed constructions. The method involves the calculation of the upper and lower limits of thermal resistance. The upper limit of thermal resistance (R_{max}) is calculated by combining in parallel the total resistances of the heat-flow paths through the building element (thermal paths (a) and (b) illustrated in Fig. VI.5). The conductance associated with R_{max} is calculated by combining the conductance through paths (a) and (b) (Fig. VI.5) on an area-weighted basis. The lower limit of thermal resistance (R_{min}) is calculated by combining in parallel the resistances of the heat flow paths of each layer separately and then summing the resistances of all layers of the building element. The conductance of the bridged layer is also calculated on an area-weighted basis. The fraction of the area taken up by the webs of the steel studs, noggins and braces adds up to 0.56% and 0.76% for the exterior walls and roof, respectively. The internal surface resistance (R_{si}) is equal to 0.13 m^2 K W^{-1} (horizontal heat flow) or 0.10 m^2 K W^{-1} (heat flow upwards). The external surface resistance (R_{se}) is equal to 0.04 m^2 K W^{-1} (horizontal or upwards heat flow). The U–value is calculated by:

$$U = \left(1 / R_T\right) \tag{VI.14}$$

where the total thermal resistance (R_T) is obtained by

$$R_T = pR_{max} + (1 - p)R_{min}\,. \tag{VI.15}$$

The p–value is calculated according to Eq. (VI.16) and it is influenced by several factors, including the flange width, the spacing between studs (s) and the depth of the stud (d). The s–value and the d–value in Eq. (VI.16) must be expressed in mm. Eq. (VI.16) is valid when the flange widths are known not to exceed 50 mm. It should be remarked that only the webs of the steel studs, noggins and braces are included in the calculation of R_{max} and R_{min} as the effects of the flanges are taken into account in the formula for p.

$$p = 0.8\left(R_{min} / R_{max}\right) + 0.32 - 0.2\left(600 / s\right) - 0.04\left(d / 100\right) \tag{VI.16}$$

The U–value corrections for air gaps and fixings proposed in ref. [419] are not considered in this study as the design consists of two layers of insulation (one between studs, the other as a continuous layer covering the first one) and plastic fixings are expected to be used in the steel flanges to attach the external sheathing board to the studs.

VI.3 Results and discussion

VI.3.1 Annual assessment basis

In this section, the annual energy savings for heating and cooling by incorporating the optimum PCM-drywalls in the model are presented. Table VI.5 shows the values of the independent variables that yield better performance for each climate (lowest cost function value). It can be seen that a 4.0 cm PCM-drywall is the optimum thickness for all the surfaces (considering the set of e_{PCM}–values evaluated). The optimum T_{mp}–value is different regarding the orientation of the surface and the climate considered. Generally speaking, the T_{mp}–value is lower for the partition wall than for the other surfaces. The T_{mp}–value is higher for the warmer climates and lower for the colder climates. Concerning the optimum α–value, it also varies according to the orientation of the surface and the climate. Inner surfaces with higher α–value are better for colder climates. Table VI.6 lists the annual heating and cooling energy demands of the reference and the PCM-drywalls enhanced rooms, for each climate. It also lists the annual heating and cooling energy savings considering the optimized solution x^*.

Table VI.5 Values of the independent variables that yield better performance for each climate, *i.e.* $x^* = \{S_{\mathrm{j}}, W_{\mathrm{k}}, E_{\mathrm{l}}, N_{\mathrm{m}}, C_{\mathrm{p}}\}_{\mathrm{opt}}$.

		Csa Seville	Csb Coimbra	Cfa Milan	Cfb Paris	Dfa Bucharest	Dfb Warsaw	Dfc Kiruna
Partition northern wall N_m	e_{PCM} (cm)	4.0	4.0	4.0	4.0	4.0	4.0	4.0
	T_{mp} (°C)	24.0	22.0	22.0	22.0	22.0	22.0	20.0
	α	0.3	0.3	0.3	0.9	0.3	0.9	0.9
Exterior western wall W_k	e_{PCM} (cm)	4.0	4.0	4.0	4.0	4.0	4.0	4.0
	T_{mp} (°C)	26.0	24.0	24.0	22.0	24.0	22.0	20.0
	α	0.3	0.3	0.9	0.9	0.9	0.9	0.9
Exterior eastern wall E_l	e_{PCM} (cm)	4.0	4.0	4.0	4.0	4.0	4.0	4.0
	T_{mp} (°C)	26.0	24.0	24.0	24.0	24.0	22.0	18.0
	α	0.3	0.3	0.9	0.9	0.9	0.9	0.9
Exterior southern wall S_j	e_{PCM} (cm)	4.0	4.0	4.0	4.0	4.0	4.0	4.0
	T_{mp} (°C)	26.0	24.0	24.0	22.0	24.0	22.0	20.0
	α	0.3	0.3	0.3	0.9	0.3	0.9	0.9
Exterior ceiling C_p	e_{PCM} (cm)	4.0	4.0	4.0	4.0	4.0	4.0	4.0
	T_{mp} (°C)	26.0	24.0	24.0	22.0	22.0	22.0	24.0
	α	0.3	0.3	0.3	0.3	0.3	0.3	0.3

Fig. VI.6 shows the annual heating and cooling energy demands for both the reference and the PCM-drywalls enhanced rooms for each climate and the associated indices of annual energy savings. The bars in grayscale correspond to the heating and cooling energy demands (read on the left axis) of the reference room for each climate and the colored bars correspond to the energy demands of the PCM-enhanced rooms. Additionally, the bullets on the graph indicate the indices of

annual energy savings (read on the right axis) for each climate. The $IESH_a$ varies between 0.07 (Dfc-Kiruna) and 0.92 (Csa-Seville); $IESC_a$ between 0.43 (Csa-Seville) and 0.87 (Dfc-Kiruna); and $IEST_a$ varies between 0.10 (Dfc-Kiruna) and 0.62 (Csb-Coimbra). Therefore, results show that the energy performance of LSF air-conditioned residential buildings can be significantly improved with the incorporation of PCM-drywalls in all the climates evaluated.

Table VI.6 Annual heating and cooling energy demands for the reference and the PCM-drywalls enhanced rooms for each climate, and annual energy savings considering the optimized solution $x^* = \{S_j, W_k, E_l, N_m, C_p\}_{opt}$.

Annual energy demand (kWh m^{-2} year^{-1})		Csa Seville	Csb Coimbra	Cfa Milan	Cfb Paris	Dfa Bucharest	Dfb Warsaw	Dfc Kiruna
Cooling	$E_{cool,ref}$	78.45	40.37	27.11	14.21	32.73	9.92	3.76
	$E_{cool,PCM}$	44.52	15.58	14.81	4.02	16.32	2.58	0.48
	Savings	33.94	24.78	12.30	10.18	16.40	7.34	3.28
Heating	$E_{heat,ref}$	4.65	5.64	27.56	30.67	33.64	47.31	98.96
	$E_{heat,PCM}$	0.36	1.69	21.70	24.77	25.15	40.96	92.38
	Savings	4.30	3.95	5.86	5.90	8.49	6.34	6.58
Total	$E_{tot,ref}$	83.10	46.01	54.67	44.88	66.37	57.23	102.72
	$E_{tot,PCM}$	44.87	17.27	36.51	28.80	41.47	43.55	92.86
	Savings	38.23	28.74	18.16	16.08	24.90	13.68	9.86

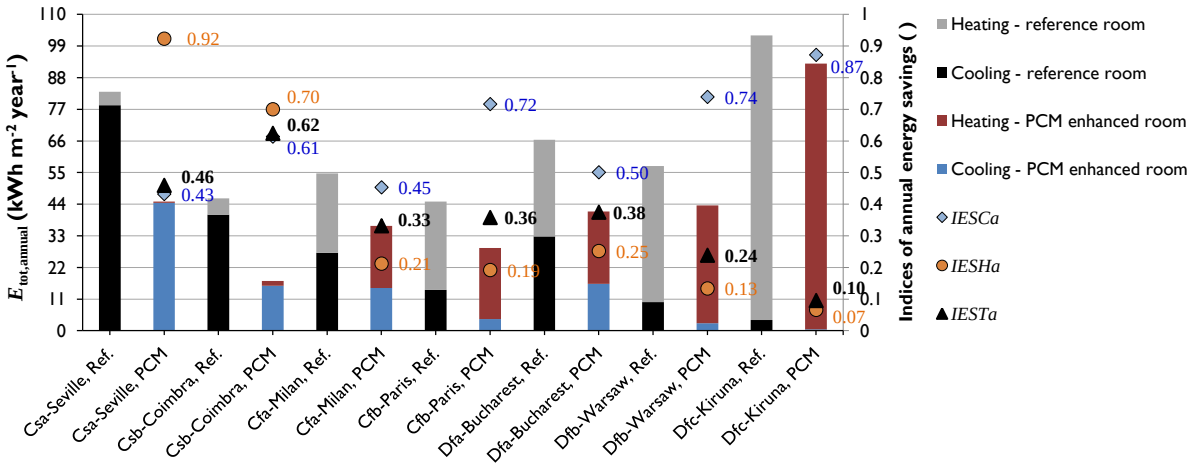

Fig. VI.6 Annual heating and cooling energy demands for both the reference and the PCM-enhanced rooms for each climate. Indices of annual energy savings for each climate considering the optimized solution $x^* = \{S_j, W_k, E_l, N_m, C_p\}_{opt}$.

The impact mentioned above is more significant for the warmer climates where the total energy savings for both heating and cooling reach 46% (38.23 kWh m^{-2} year^{-1}) and 62% (28.74 kWh m^{-2} year^{-1}) for the Csa-Seville and Csb-Coimbra climates, respectively. This is particularly due to the reduction in the energy demand for cooling, *i.e.* 43% (33.94 kWh m^{-2} year^{-1}) and 61% (24.78 kWh m^{-2} year^{-1}) for the Csa-Seville and Csb-Coimbra climates, respectively. For these climates the reference

energy demand is lower for heating than for cooling. However, the optimized incorporation of PCM-drywalls in the model also significantly reduces the heating energy demand, *i.e.* 92% (4.3 kWh m^{-2} $year^{-1}$) and 70% (3.95 kWh m^{-2} $year^{-1}$) for the Csa-Seville and Csb-Coimbra climates, respectively.

Regarding colder climates (Dfb-Warsaw and Dfc-Kiruna), the impact of PCM-drywalls in the total energy savings is not so significant, *i.e.* 24% (13.68 kWh m^{-2} $year^{-1}$) and 10% (9.86 kWh m^{-2} $year^{-1}$) for the Dfb-Warsaw and Dfc-Kiruna climates, respectively. This is particularly due to the decrease in the energy demand for heating, *i.e.* 13% (6.34 kWh m^{-2} $year^{-1}$) for the Dfb-Warsaw and 7% (6.58 kWh m^{-2} $year^{-1}$) for the Dfc-Kiruna climates. Another attractive feature is that the optimized incorporation of PCM-drywalls in the room significantly reduces cooling energy demand, *i.e.* 74% (7.34 kWh m^{-2} $year^{-1}$) and 87% (3.28 kWh m^{-2} $year^{-1}$) for the Dfb-Warsaw and Dfc-Kiruna climates, respectively.

Concerning the other climates (Cfa-Milan, Cfb-Paris and Dfa-Bucharest), results show that the optimum incorporation of PCM-drywalls in the room reduces both the annual cooling and heating energy demands. The index $IESH_a$ varies between 0.19 (Cfb-Paris) and 0.25 (Dfa-Bucharest); $IESC_a$ between 0.45 (Cfa-Milan) and 0.72 (Cfb-Paris), and $IEST_a$ between 0.33 (Cfa-Milan) and 0.38 (Dfa-Bucharest). Therefore, for these climates, the energy savings are particularly due to the reduction in the energy demand for cooling.

VI.3.2 Monthly assessment basis

In this section, the monthly assessment basis results of the energy savings for heating and cooling due to PCM-drywalls are presented to show the impact of the annual optimized solution x^* on the energy demands throughout the year. Fig. VI.7 shows the monthly heating and cooling energy demands for both the reference and the PCM-enhanced rooms for each climate investigated. It also shows the indices of energy savings for each month (for each climate) considering the optimized solution x^*. The bars in grayscale correspond to the heating and cooling energy demands (read on the left axis) for the reference room. Next to each of these, the colored bars correspond to the PCM-enhanced room energy demands for the same month. Additionally, the bullets on the graph indicate the indices of energy savings (read on the right axis) for each month. Table VI.7 lists the monthly heating and cooling energy savings for the investigated climates considering the optimized solution x^*. To prevent this section from becoming too long, only the graphs of Fig. VI.7a and Fig. VI.7g are discussed in detail. These graphs concern to the warmer (Csa-Seville) and colder (Dfc-Kiruna) climates, respectively.

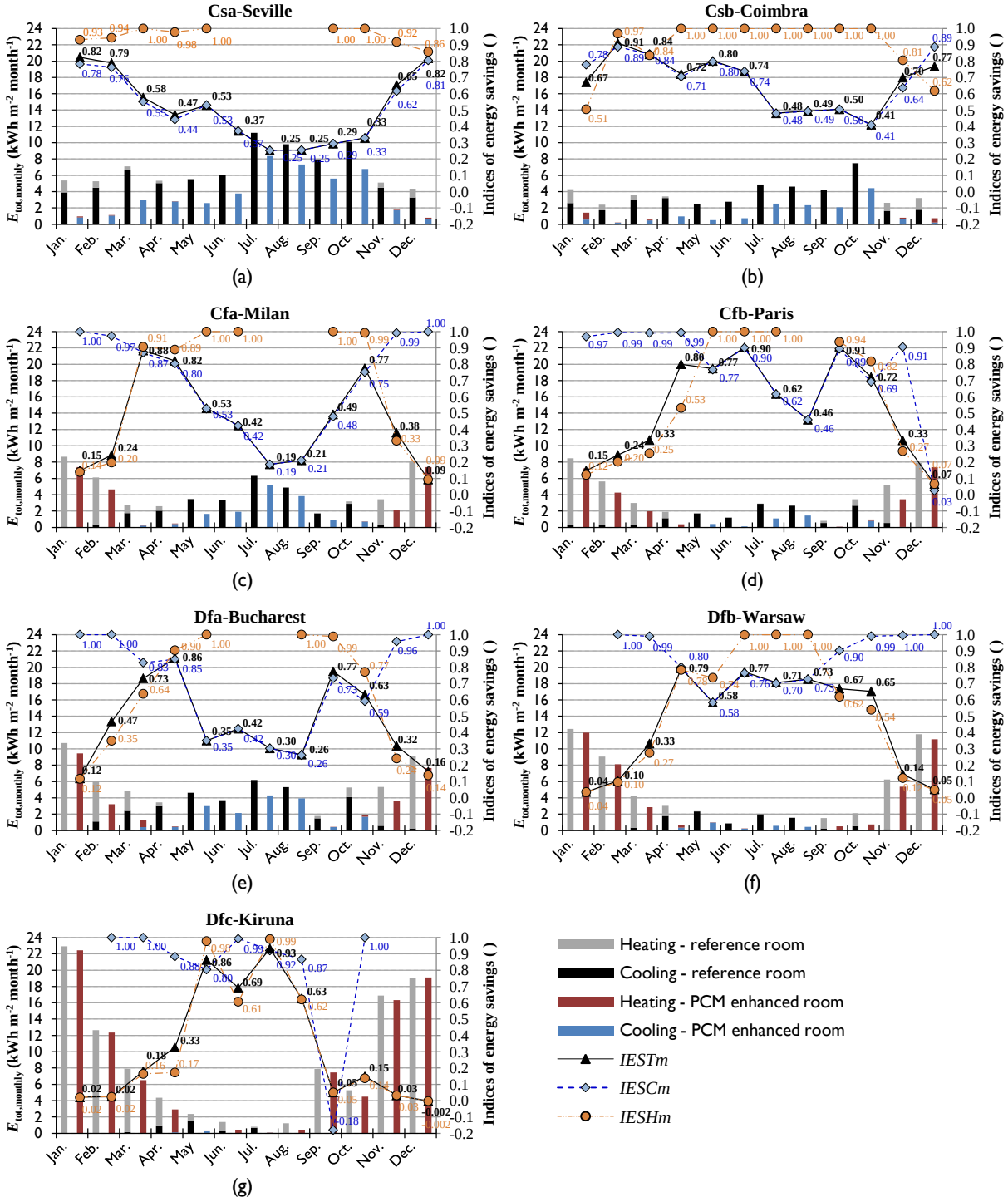

Fig. VI.7 Monthly heating and cooling energy demands for both the reference and the PCM-enhanced rooms for the (a) Csa-Seville, (b) Csb-Coimbra, (c) Cfa-Milan, (d) Cfb-Paris, (e) Dfa-Bucharest, (f) Dfb-Warsaw and (g) Dfc-Kiruna climates. Indices of energy savings for each month considering the optimized solution $x^* = \{S_j, W_k, E_l, N_m, C_p\}_{opt}$ for each climate.

For the Csa-Seville climate (see Fig. VI.7a), the energy demand in summer is mainly due to cooling. During this season, the cooling and the total energy savings due to PCMs vary both between 25% in July and 37% in June. The $IESH_m$ is not defined during summer because no heating is required.

Regarding the swing seasons (spring and autumn), the optimized incorporation of PCM-drywalls almost eliminates heating energy demands (savings from 92% in November to 100% in March, May, September and October), and leads to cooling savings between 29% in September and 62% in November. The total energy savings vary between 29% in September and 65% in November. During winter, the heating savings range from 86% in December to 94% in February; the cooling savings from 76% in February to 81% in December; and the total energy savings vary between 79% in February and 82% in January. January is the month with the highest level of total energy savings, *i.e.* 4.43 kWh m^{-2} month^{-1} (see Table VI.7).

Table VI.7 Monthly heating and cooling energy savings for the analyzed climates considering the optimized solution $x^* = \{S_j, W_k, E_l, N_m, C_p\}_{opt}$.

Climate	Energy savings (kWh m^{-2} month^{-1})	Jan.	Feb.	Mar.	Apr.	May	Jun.	Jul.	Aug.	Sep.	Oct.	Nov.	Dec.
Csa Seville	Cooling	3.04	3.43	3.70	2.22	2.93	2.24	2.82	2.50	2.33	3.31	2.77	2.63
	Heating	1.39	0.72	0.40	0.29	0.00	0.00	0.00	0.00	0.00	0.01	0.57	0.92
	Total	4.43	4.15	4.10	2.51	2.93	2.24	2.82	2.50	2.34	3.32	3.33	3.55
Csb Coimbra	Cooling	2.02	1.53	2.51	2.27	1.98	2.04	2.33	2.29	2.11	3.05	1.06	1.58
	Heating	0.86	0.67	0.49	0.18	0.05	0.00	0.00	0.01	0.00	0.03	0.79	0.88
	Total	2.88	2.20	3.00	2.46	2.04	2.05	2.33	2.29	2.11	3.08	1.84	2.46
Cfa Milan	Cooling	0.08	0.35	1.52	1.65	1.83	1.41	1.18	1.03	0.82	2.18	0.25	0.01
	Heating	1.20	1.14	0.87	0.49	0.02	0.01	0.00	0.00	0.04	0.29	1.06	0.75
	Total	1.27	1.49	2.39	2.14	1.85	1.42	1.18	1.03	0.87	2.47	1.31	0.76
Cfb Paris	Cooling	0.26	0.29	0.33	1.11	1.31	1.08	1.77	1.23	0.48	1.83	0.49	0.00
	Heating	1.00	1.08	0.67	0.43	0.05	0.03	0.01	0.00	0.24	0.65	1.24	0.51
	Total	1.25	1.37	1.00	1.54	1.36	1.10	1.78	1.23	0.72	2.48	1.72	0.51
Dfa Bucharest	Cooling	0.03	1.11	1.98	2.53	1.61	1.57	1.87	1.38	1.10	2.43	0.55	0.25
	Heating	1.24	1.73	1.54	0.41	0.00	0.00	0.00	0.03	0.29	0.89	1.15	1.22
	Total	1.27	2.84	3.52	2.94	1.62	1.57	1.87	1.41	1.39	3.32	1.70	1.47
Dfb Warsaw	Cooling	0.00	0.09	0.34	1.42	1.37	0.66	1.37	1.13	0.24	0.52	0.16	0.04
	Heating	0.44	0.86	1.07	0.98	0.00	0.03	0.04	0.01	0.77	0.84	0.74	0.56
	Total	0.44	0.95	1.41	2.40	1.37	0.69	1.41	1.13	1.01	1.36	0.90	0.60
Dfc Kiruna	Cooling	0.00	0.02	0.15	0.84	1.26	0.31	0.61	0.02	-0.00	0.07	0.00	0.00
	Heating	0.47	0.30	1.28	0.59	0.78	0.66	0.14	0.74	0.40	0.72	0.55	-0.04
	Total	0.47	0.31	1.43	1.43	2.04	0.97	0.75	0.77	0.40	0.78	0.55	-0.04

Regarding warmer climates, most studies found in literature deal with the optimization of the incorporation of PCM-drywalls for summer without assessing the impact of the latent heat in the remaining seasons [369,376]. For the Csa-Seville climate, results show that PCM-drywalls can also have a significant impact in the reduction of the heating and cooling energy demands during the swing seasons and winter. Therefore, high levels of energy reduction occur from January to March and from October to December, as it can be seen in Table VI.7. These results are explained by the extra thermal capacity of the envelope provided by the incorporation of PCMs.

The energy demands for the Dfc-Kiruna climate (see Fig. VI.7g) is mainly due to heating during winter and swing seasons. Nevertheless, a remaining energy demand is required for cooling

during summer, which is significantly reduced with the optimized solution: $IESC_m$ between 0.87 in August and 0.99 in June; $IESH_m$ between 0.61 in June and 0.99 in July; and $IESTm$ between 0.63 in August and 0.93 in July. During the swing seasons the total energy savings vary from 3% in November to 86% in May; the heating savings from 3% in November to 98% in May; and the cooling savings from 80% in May to 100% in March and October. An interesting result is the negative value of $IESC_m$ in September, which means that the incorporation of PCM-drywalls in the room increases the cooling energy demand during this month. This means that some stored energy (for instance during summer) is released indoors and more 18% of energy is required for cooling.

During winter, the $IESH_m$ and the $IEST_m$ are both equal to 0.02 in January and February. The $IEST_m$–value is negative in December, which means that the annual optimized solution has a negative impact in the monthly energy demand. Another interesting result is the negative value of $IESH_m$ in December, which means that the incorporation of PCM-drywalls increases the heating energy demand in 0.2%. In February, the $IESC_m$ is equal to 1.0 and no energy is required for cooling due to PCMs. The $IESC_m$ is not defined in January and December because no cooling is required. May is the month with the highest level of total energy savings, *i.e.* 2.04 kWh m^{-2} $month^{-1}$ (see Table VI.7). The negative value of the cooling energy savings in September indicates that an extra energy of 0.001 kWh m^{-2} $month^{-1}$ is required for cooling due to PCMs-drywalls incorporation. The same happens with the negative value of the heating savings in December. During this month more 0.04 kWh m^{-2} $month^{-1}$ are required for heating due to PCMs.

VI.4 Conclusion

In this chapter, the impact of PCM-drywalls in the annual and monthly heating and cooling energy savings of an air-conditioned LSF residential single-zone room was evaluated based on the combination of an optimization model in *GenOpt* with dynamic energy simulations using *EnergyPlus*. A holistic approach was carried out to simulate more real-life conditions and the influence of several European climates.

Using the methodology proposed in this chapter, it is concluded that an optimum solution incorporating PCM-drywalls can be found for each climate, leading to significant annual energy savings considering both cooling and heating energy demands. The results indicate an optimum thickness of the PCM-drywalls equal to 4.0 cm for all the case studies (considering the set of thicknesses evaluated). The optimum melting-peak temperature of the PCM is higher for the warmer climates: between 22 and 26 °C, against 18 to 24 °C for the colder climates. Inner surfaces with higher solar absortance (α = 0.9) are better for colder climates and surfaces with lower solar absortance (α = 0.3)

are better for warmer climates. These results can be taken as important guidelines for the incorporation of PCM-drywalls in LSF residential buildings in Europe. This is considering the value of the melting-peak temperature of the PCM, the thickness of the PCM-drywall and the use of selective inks (mainly in colder climates) to control the α–value of the inner surfaces. The results also show that the optimum solution for one surface of the room can differ from the others. This may be a problem for on-site manufacture control as it enhance the complexity of construction and ordering, but it can be very easy to accomplish during off-site manufacture control. Therefore, the results achieved are particularly interesting for the modular LSF construction industry, as the configuration of the building is controlled in the factory.

It is also concluded that the energy savings effect is more evident for the warmer climates, where the total energy savings due to PCM-drywalls reach 46% and 62% for the Csa-Seville and Csb-Coimbra climates, respectively. It is also concluded that PCM-drywalls can be used to significantly reduce not only the cooling energy demand in the warmer climates, but also the heating energy demand. PCM-drywalls are also very attractive for colder climates (Dfb-Warsaw and Dfc-Kiruna), with a predominance of the heating energy demand reduction. However, the impact of PCMs in the total energy savings is not so significant for these climates (24% and 10% for the Dfb-Warsaw and Dfc-Kiruna climates, respectively). Regarding the other climates, Cfa-Milan, Cfb-Paris and Dfa-Bucharest, PCM-drywalls could be used to reduce the total energy demand for heating and cooling between 33% and 38%.

Regarding the monthly assessment basis, it is concluded that the optimum annual solution can increase the monthly energy performance of the LSF single-zone room for all the climates, except for the case of the Dfc-Kiruna climate. For this colder climate, the optimum solution faces a decrease in the energy efficiency during December. It is also concluded that the enhancement of the thermal capacity of the LSF envelope via PCM-drywalls changes the behavior of the room every months.

The present study shows the importance of optimizing the incorporation of PCM-drywalls in an annual assessment basis rather than in a seasonal basis. Considering the Csa-Seville and the Csb-Coimbra climates, the total energy savings for heating and cooling are greater for the winter and swing seasons' months. For the Cfa-Milan and Dfa-Bucharest climates, the total energy savings are greater during the swing seasons. For the remaining climates considered (Cfb-Paris, Dfb-Warsaw and Dfc-Kiruna), the total energy savings are greater for the summer and swing seasons' months.

The overall methodology proposed herein was focused on a single-zone room model. Therefore, the results can only be carefully extrapolated and generalized to more complex models and real multi-zone LSF buildings. Further work should be done to apply the presented methodology to more complex buildings by including more real-life indoor heat loads schedules, air infiltration

models and heating/cooling systems operation. The study can also be extended to the optimization of the incorporation of real-commercialized PCM-drywalls (with different melting ranges) in real LSF buildings, for instance for retrofitting purposes.

CHAPTER VII

PCM-drywalls to reduce cooling energy demand and peak-loads in residential heavyweight buildings in Kuwait

This chapter evaluates the impact of incorporating PCM-drywalls in air-conditioned residential buildings in Kuwait. Using an *EnergyPlus* single-zone building model, a parametric study is carried out by considering several window-to-wall ratios, different solar orientations and some PCM-drywalls configurations. The main goals are to: (*i*) discuss the existence of an universal and fully-customized PCM-drywall solution for Kuwait regarding its thickness and the melting-peak temperature of the PCM; (*ii*) evaluate the impact of PCM-drywalls in the reduction of both cooling energy demand and peak-loads, and (*iii*) provide some guidelines for incorporating PCM-drywalls in Kuwait. Chapter VII is divided into four sections. Section VII.1 introduces the background information about the energy consumption in Kuwait and the problem to be studied. Section VII.2 presents the methodology carried out for the parametric study. Section VII.3 presents and discusses the results in an annual, monthly and daily assessment basis. Section VII.4 provides the main conclusions of the study.

VII.1 Introduction

Between 2008 and 2009, the energy and power demand in Kuwait increased at a rate of 6% per year, suggesting that the peak power demand could reach 27 GW in 2025 if the same trend persists [421]. In fact, the annual energy consumption per capita in Kuwait is among the highest in the world (13000 kWh person^{-1}) [5]. On the other hand, Kuwait is an oil-exporting country, which is the country's only natural resource and the main source of revenue [421]. As stated by Alotaibi [5], only 10% of the produced energy was consumed locally in 1980, but this percentage is expected to reach 40% by 2015. Therefore, to balance the domestic and international demand, the government might be forced to increase production or to reduce exportation of oil. Both options may cause several problems in meeting future goals due to the dependence of the country on oil as source of income [5].

Kuwait is seen as one of the leading countries in the Middle East in terms of construction activity [422] and several cities are being planned and designed. This boost in construction is the result of the rapid economic development, and the need to accommodate the growing population which has been increasing with an average growth rate of about 3.3% [5]. Regarding the distribution of electricity consumption by end-user sector, Krarti and Hajiah [423] reported that the building

sector represents 90% of the electricity consumption of the country. The authors also reported that the residential sector (including privately owned residences and rental apartment units) were responsible for over 70% of Kuwait's electrical peak power demand in 2004 [423]. This great energy demand is caused by a high standard of living and harsh summer climatic conditions which push the use of air-conditioning in all types of buildings to reach indoor thermal comfort. In Kuwait, air-conditioning accounts for 70% of the annual electricity peak-loads, 45% of the overall annual electricity consumption, and more than 20% of the fossil fuel consumption [421]. Therefore, the peak-hours are already problematic regarding the imbalance between energy supply and demand and, in the last years, recurrent electricity blackouts during summer have affected some residential areas.

Besides the increase in energy demand for cooling, there is a significant amount of inefficient use of energy which increase the insufficiency of the energy supply. This is caused by inefficient construction practices and installed equipment as well as energy-intensive lifestyle choices. It should be remarked that the country's energy supply is highly subsidized by the government. It should therefore become a government priority to manage and reduce building energy use in Kuwait to ensure the country's long-term prosperity. To further this goal, the energy conservation code of the Ministry of Electricity and Water [421] establishes several recommendations to enhance the energy efficiency of buildings (including insulation, glazing, lighting and ventilation requirements) and to reduce power ratings of air-conditioning systems. Al-ajmi and Hanby [424] carried out a parametric study on the simulation of the energy consumption of residential buildings in Kuwait using a *TRNSYS*-IISIBAT environment [424]. The authors proposed several features that should be adopted to achieve more energy efficient buildings in Kuwait including: (*i*) the use of the classical wall type; (*ii*) the reduction of the amount of uncontrolled air infiltration rates, and (*iii*) the control of the window area and the orientation and placement of the main window facades (windows in the Kuwaiti environment should face toward the north-south direction), and the use of certain treatments to the glazing to reduce heat gains. However, only traditional sensible materials are considered in both documents. To complement these works, this study explores the incorporation of PCM-drywalls in building envelope solutions in Kuwait.

As reviewed in Chapter V, the advantages of incorporating PCMs in buildings have been pointed out by many authors and several studies have been carried out to evaluate the energy performance of PCM-drywalls as they can be widely used as an inner finishing layer of the opaque envelope. However, no guidelines about the incorporation of PCM-drywalls in heavyweight construction in the dry desert climate conditions of Kuwait are found in the literature.

The main goals of this study are to: (*i*) discuss the existence of a fully-customized PCM-drywall solution that could be used in generalized applications; (*ii*) evaluate the impact of PCM-drywalls in the reduction of both the cooling energy demand and peak-loads, and (*iii*) provide some

guidelines for the incorporation of PCM-drywalls in residential buildings in Kuwait. This study forms part of an MIT-Kuwait Signature Project called *Sustainability of Kuwait's Built Environment* which aims at promoting an energy and carbon-efficient built environment in Kuwait. This project is a collaboration between the Kuwait-MIT Center for Natural Resources and the Environment (CNRE), the Kuwait Foundation for the Advancement of Sciences (KFAS), the MIT Sustainable Design Lab, the Kuwait Institute for Scientific Research and the Kuwait University.

VII.2 Methodology

A parametric study is carried out by using the *EnergyPlus* 8.3 [425] dynamic simulation tool and considering an air-conditioned residential single-zone building model built according to the 2010 building energy code of Kuwait [421]. The KISR Kuwait Intl Airport - KWT weather data file is used to simulate Kuwaiti climate (Fig. VII.1) [425]. Some internal loads and six window-to-wall ratios (WWR) of the main solar oriented window facade are considered in the study. The energy impact of incorporating seven different PCM-drywalls in the model is then evaluated in order to find the fully-customized PCM-drywall solution that could be used in generalized applications, which is suitable to the economy of mass production. A set of discrete variables is considered in the parametric study, namely those related with the thermophysical properties of the PCM (enthalpy-temperature and thermal conductivity-temperature functions) and thickness of the PCM-drywalls. In order to evaluate the influence of the cooling setpoint temperature (T_{th}) of the air-conditioning system in the selection of the fully-customized PCM-drywall solution, five values of T_{th} are considered in the study.

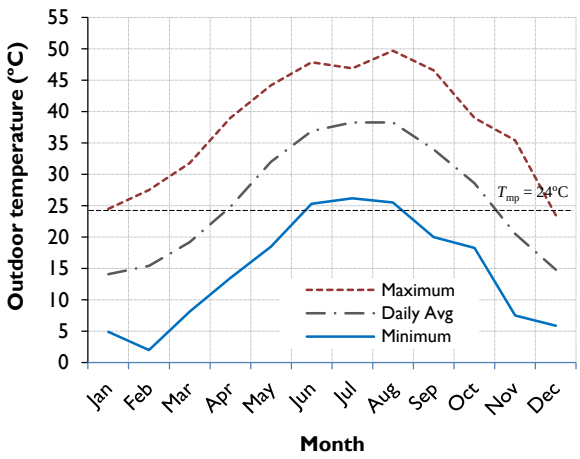

Fig. VII.1 Monthly statistics for the evolution of the dry bulb temperatures in Kuwait (KISR Kuwait Intl Airport – KWT weather data [425]).

VII.2.1 Reference models

To mimic a typical residence in Kuwait, 28 single-zone, fully air-conditioned models with seven WWRs and facing the four cardinal directions were built with interior dimensions of 8 m × 6 m × 2.7 m = 129.6 m³ as shown in Fig. VII.2 (the interior air volume remains as specified in ASHRAE 140 standard [415]). The buildings were assumed to have their windows concentrated on one side to reflect current, relatively dense construction practices in Kuwait with windows mainly facing the street. The total floor area of the room is 48 m² with a slab-on-grade foundation. All vertical surfaces are considered as external walls. The model is not obstructed by neighboring buildings and the ground reflectance is equal to 0.2. Table VII.1 shows the specific glazing types for different WWR values in accordance with the requisites of the building energy code of Kuwait [421]. The different WWRs are obtained by changing the fenestration area as shown in Fig. VII.2. Table VII.1 shows that the higher the value of the WWR, the more selective the requirements of the glazing type, with lower U and $SHGC$ values. This is a way to prevent the boost of cooling energy demand when increasing the fenestration area.

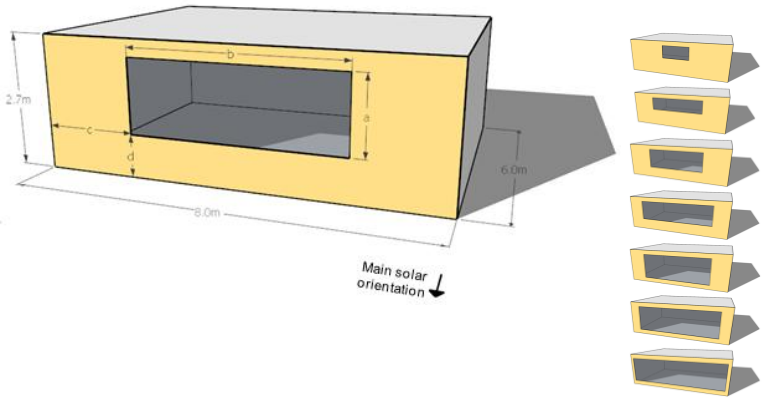

Room - WWR	Window			
	a (m)	b (m)	c (m)	d (m)
R1 - 10%	1.00	2.16	2.92	1.35
R2 - 20%	1.00	4.32	1.84	1.35
R3 - 30%	1.50	4.32	1.84	0.85
R4 - 40%	1.50	5.76	1.12	0.85
R5 - 50%	2.00	5.4	1.3	0.35
R6 - 60%	2.00	6.48	0.76	0.35
R7 - 70%	2.00	7.56	0.22	0.35

Fig. VII.2 Perspective view of the reference room and window-to-wall ratio layouts of the main solar oriented facade.

Table VII.1 Different types of glazing for different WWR in accordance with the building energy code of Kuwait [421].

WWR (%)	Glazing type required	U (W m^{-2} °C^{-1})	$SHGC$
10	6-mm double-tinted	3.42	0.360
20	6-mm double-reflective	3.38	0.245
30	6-mm double-reflective	3.38	0.245
40	6-mm double-reflective	3.38	0.245
50	6-mm double-spectrally selective	1.71	0.230
60	6-mm double-spectrally selective	1.71	0.230
70	6-mm double-spectrally selective	1.71	0.230

In their work, Al-ajmi and Hanby [424] describe the typical Kuwaiti residential building. According to them, the traditional flat roof is almost universal in Kuwait and the prevailing exterior walls are of two types: the autoclaved aerated concrete (AAC) walls and the concrete block walls (the so called "classical wall"). The latter type shows some advantages comparing to the first one: (*i*) it is cheaper – however if insulation is added the price will increase; (*ii*) the blocks are largely available and produced locally in Kuwait by many factories; (*iii*) it is structurally stronger; (*iv*) it is widely accepted by the buildings industry, and (*v*) the appropriate-skilled manpower for its construction is available in Kuwait [424]. The AAC blocks also work as thermal insulation layer, which can be an advantage. However, there are few factories producing these blocks locally and its price is higher [424]. Moreover, Al-ajmi and Hanby [424] suggested that the classical wall type is more energy-efficient regarding annual energy demand. Therefore, for the purpose of this study, the classical wall typology will be considered in the simulations.

Fig. VII.3 shows the cross-section of the construction elements used and Table VII.2 lists the thermophysical properties of the required materials. The reference U–value for each element is considered equal to the corresponding maximum U–value specified in the regulation (for heavy construction and medium-light external color) [1], *i.e.*, 0.568 W m^{-2} °C^{-1} for the walls and 0.397 W m^{-2} °C^{-1} for the roof. Changes in the U–value of the construction elements can be achieved by varying the thickness of the insulation layers $tck_{\text{ins,wall}}$ and $tck_{\text{ins,roof}}$. For the reference rooms, the thickness of the insulation layer is equal to 4.5 cm and 6.0 cm for the wall and roof, respectively.

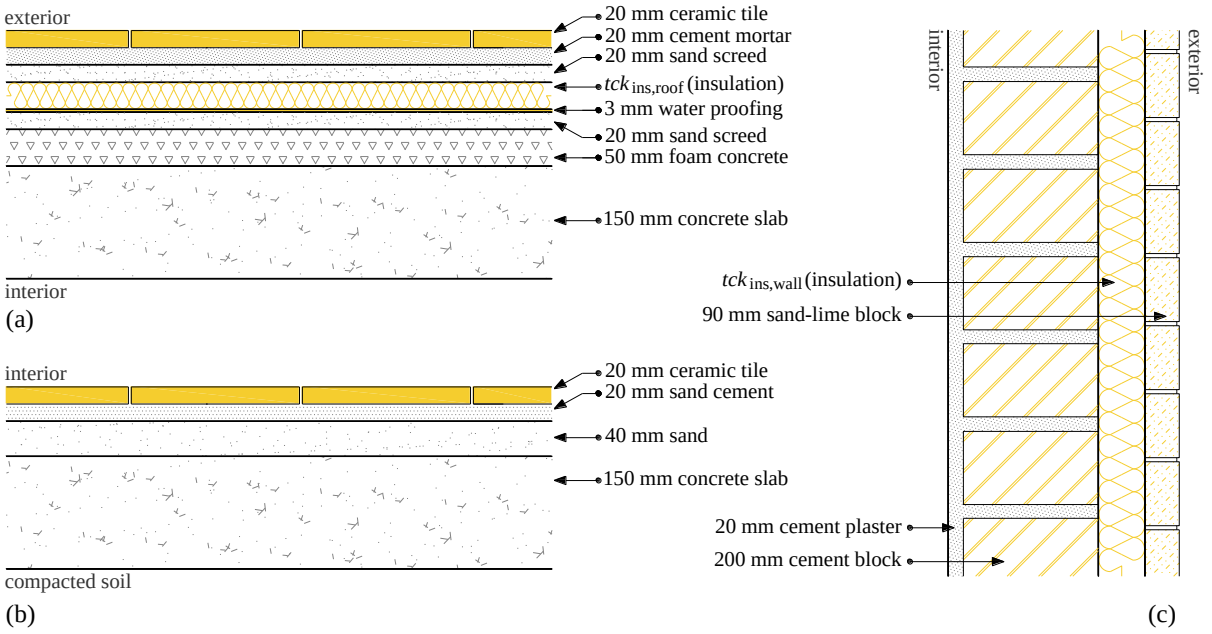

Fig. VII.3 Cross-section of the construction elements used in the model: (a) roof; (b) floor, and (c) exterior wall (adapted from ref. [424]).

Table VII.2 Thermophysical properties of the sensible construction materials [424].

Material	k (W m^{-1} °C^{-1})	c_p (J kg^{-1} K^{-1})	ρ (kg m^{-3})
Sand-lime block	1.310	795	1918
Cement block	1.640	910	2011
Cement plaster	0.944	840	2085
Cement mortar	0.944	840	2085
Concrete slab	1.214	921	2297
Foam concrete	0.210	879	351
Sand cement	0.944	840	2080
Sand screed	0.944	840	2080
Sand	0.337	920	1800
Ceramic tile	1.104	800	2284
Insulation	0.032	1120	30
Water proofing	0.140	1507	934

Regarding internal heat gains, the building model is occupied by a maximum of 4 people in sedentary activity with a constant metabolic rate of about 1.2 met (126 W person^{-1}). During the Sunday-Thursday 8am – 4pm weekdays hours, only 1 of the assumed 4 residents works or stays at home. During the weekdays and weekends, from 1am to 6am, only 1 person may stay in the room. The remaining periods are considered at 100% occupancy. A maximum design lighting level of 10 W m^{-2} is considered in the model [421]. The maximum load of 8 W m^{-2} is considered for equipments. Fig. VII.4 shows the occupancy, lighting and equipment schedules during the week. The room is air-conditioned considering an *ideal loads air system model* in the *EnergyPlus* simulations. Regarding air temperature control, the thermostat is set with a cooling setpoint temperature of 24 °C. A ventilation rate of 0.5 air changes per hour is considered in the model [421].

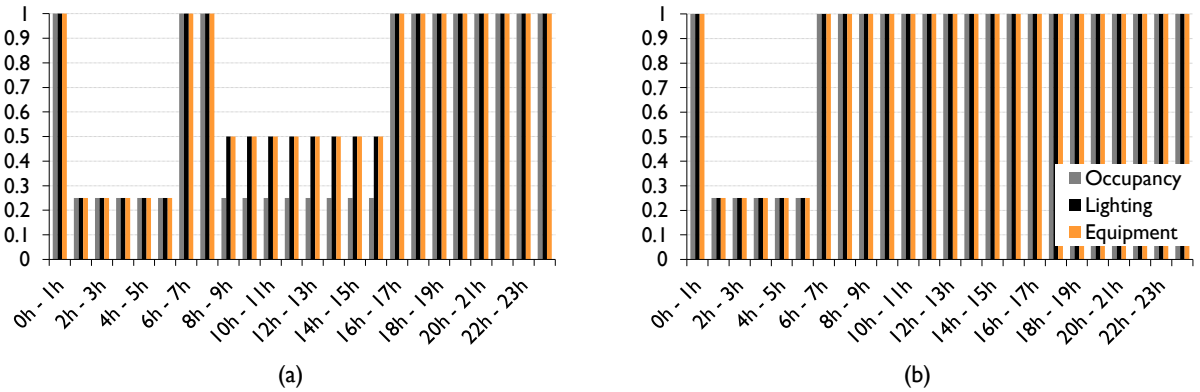

Fig. VII.4 Occupancy, lighting and equipment schedules during (a) Sunday-Thursday weekdays and (b) Friday-Saturday weekends.

VII.2.2 Problem description and design variables

The monthly and annual cooling energy demands are determined for each reference model without PCM-drywalls and then compared through simulation with the monthly and annual cooling energy demands of the correspondent PCM-enhanced model. The CondFD algorithm is used in *EnergyPlus* 8.3 [425] to simulate phase-change processes. As stated in Chapter VI, it is an implicit finite difference scheme coupled with an enthalpy-temperature function to account for phase-change energy accurately. The default CondFD model (Fo = 1/3 and c = 3) can be used with acceptable monthly and annual results, but a smaller node space should be used if accurate hourly analysis is required [363]. In this chapter, the default CondFD model with 20 time steps per hour is used for assessing the monthly and annual cooling energy demand, for both the reference and the PCM-enhanced models. For the hourly analysis, the CondFD model is used with the node space equal to 1/3 of the default value as suggested by Tabares-Velasco *et al.* [363]. As pointed out in Chapter VI, the CondFD model neither simulates hysteresis of the PCM nor does it simulate subcooling during discharging, and only the enthalpy-temperature information for the heating mode is given by the user. For the purpose of this study, the hysteresis and the subcooling phenomena are not considered in the simplified model.

The PCM-enhanced model is attained by including a PCM-drywall on the inner surface of the walls and ceiling of the reference model. Afterwards, a parametric analysis is carried out by varying the thickness of the PCM-drywall and the melting-peak temperature of the PCM incorporated in the drywall. In the parametric analysis, all the design solutions incorporating PCM-drywalls are specified as discrete independent variables that can only take predefined discrete values. The DuPontTM Energain® PCM product described in Chapter VI was considered as the reference PCM-drywall. As proposed by Soares *et al.* [399] and Tabares-Velasco [409], based on the nonlinear enthalpy-temperature function of the reference material, a new linear function can be plotted for an hypothetical PCM-drywall with the melting range covering roughly 80% of the latent heat. This new material has a melting range between 18 and 26 °C centered around 22 °C. A linear function facilitates the parametric analysis that would design generic PCM-drywalls that manufacturers could later produce.

In this study, more six hypothetical PCM-drywalls with the same latent heat characteristics (latent heat of 70 kJ kg^{-1}) but with different melting ranges centered at different melting-peak temperatures are defined. Therefore, seven PCM-drywalls with melting-peak temperatures (T_{mp}) of about 18, 20, 22, 24, 26, 28 and 30 °C are considered in the parametric study. Figs. VII.5a and VII.5b show, respectively, the enthalpy-temperature and the thermal conductivity-temperature functions for the reference PCM-drywall and for the other seven hypothetical materials defined. The thickness of

the PCM-drywall (tck_{PCM}) can be equal to 1.0, 1.5, 2.0, 2.5, 3.0, 3.5 and 4.0 cm. Regarding the combination of all the referred values, a set of 49 predefined discrete solutions can be considered for comparison with the reference model for each orientation of the window and for each WWR considered.

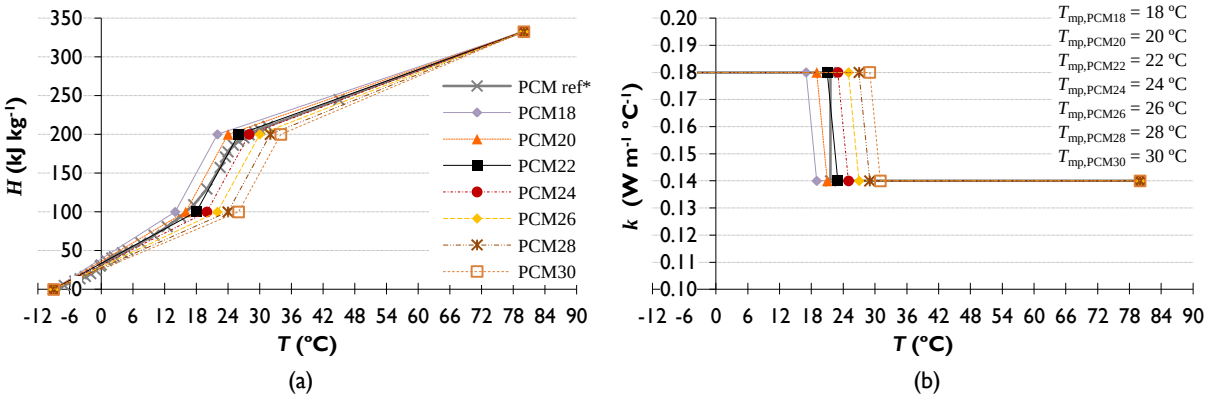

Fig. VII.5 (a) Enthalpy-temperature and (b) thermal conductivity-temperature functions for the reference PCM-drywall and other seven hypothetical materials.*Data for DuPont™ Energain® PCM product obtained from DSC measurements with a heating rate of 0.05 °C min^{-1} [414].

VII.3 Results and discussion

VII.3.1 Annual assessment basis – reference rooms

Fig. VII.6 shows the annual energy demand for cooling, $E_{cool,ref,a}$, for all the reference scenarios. As one would expect, the results show that the higher the WWR, the higher the annual cooling energy demand. When the WWR increases from 10% to 70%, considering the West-oriented room, the annual cooling energy demand increases by 20%. This value is about 16%, 17% and 9%, respectively, for the remaining East, South and North orientations. Windows facing West lead to highest solar heat gains, while windows facing North receive the least amount of solar radiation, becoming preferable for the climate of Kuwait. It should be noted that the increasingly stringent glazing type specifications required by the Kuwaiti building code (Table VII.1) [421] with growing WWR effectively mitigate the boost in cooling energy demand. If the same 6-mm double-tinted glazing type was used for West-oriented room with a 70% WWR, annual cooling demand would increase by 36% instead of 20% (considering the 6-mm double-spectrally selective glazing type).

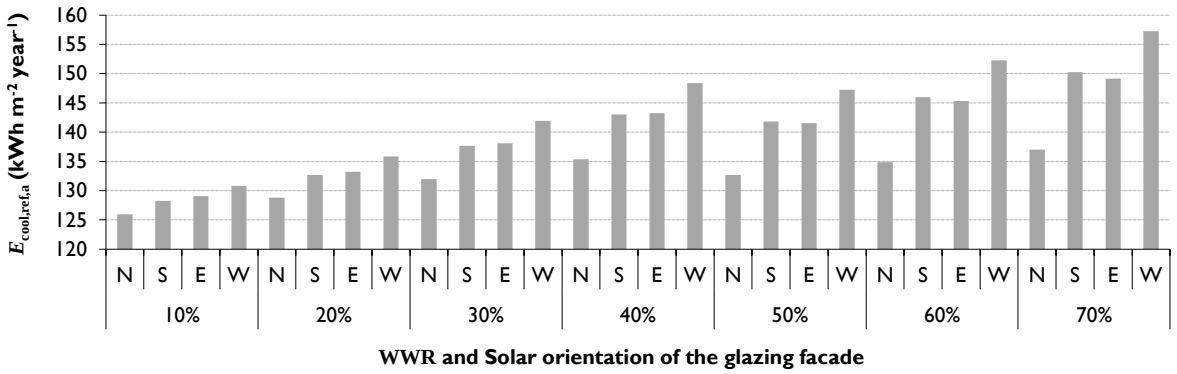

Fig. VII.6 Annual energy demand for cooling for the simulated reference rooms considering T_{th} = 24 °C.

VII.3.2 Annual assessment basis – fully-customized PCM-drywall solution

Fig. VII.7 shows the annual energy demand for cooling for the PCM-enhanced room facing West with WWR = 10% for different melting-peak temperatures and PCM thicknesses. The figure reveals that the best PCM-drywall for this configuration is the one with T_{mp} = 24 °C and the highest possible thickness considered, namely 4 cm. For the same PCM-drywall – PCM24, annual cooling energy savings of about 3.3% can be achieved by changing the thickness of the drywall from 1cm to 4 cm.

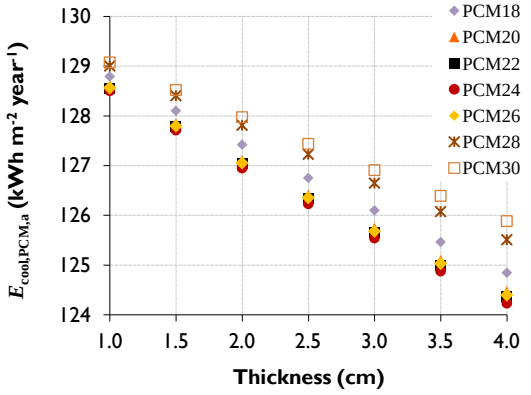

Fig. VII.7 Annual cooling energy demand for the PCM-enhanced room with WWR = 10% facing West and T_{th} = 24 °C considering different melting-peak temperatures and PCM thicknesses.

Fig. VII.8 shows the results of the parametric study carried out to evaluate the existence of a fully-customized PCM-drywall solution that could be used in generalized applications regarding the thickness of the wallboard and the melting-peak temperature of the PCM. The results show that the best solution for all the case-studies is the same 4 cm thick PCM-drywall with T_{mp} = 24 °C. The same trends described above about Fig. VII.7, can be applied to all of the case-studies shown in Fig. VII.8. An interesting feature is that the best value of the melting-peak temperature of the PCM is equal to the air-conditioning thermostat setpoint temperature for cooling. For T_{mp} values close to 24 °C, *i.e.*,

22 °C and 26 °C, the results achieved are very similar. For melting-peak temperatures of 28 °C and 30 ° C, and for the same mass of material, the energy required for cooling is higher. The same trend is verified for T_{mp} = 18 °C.

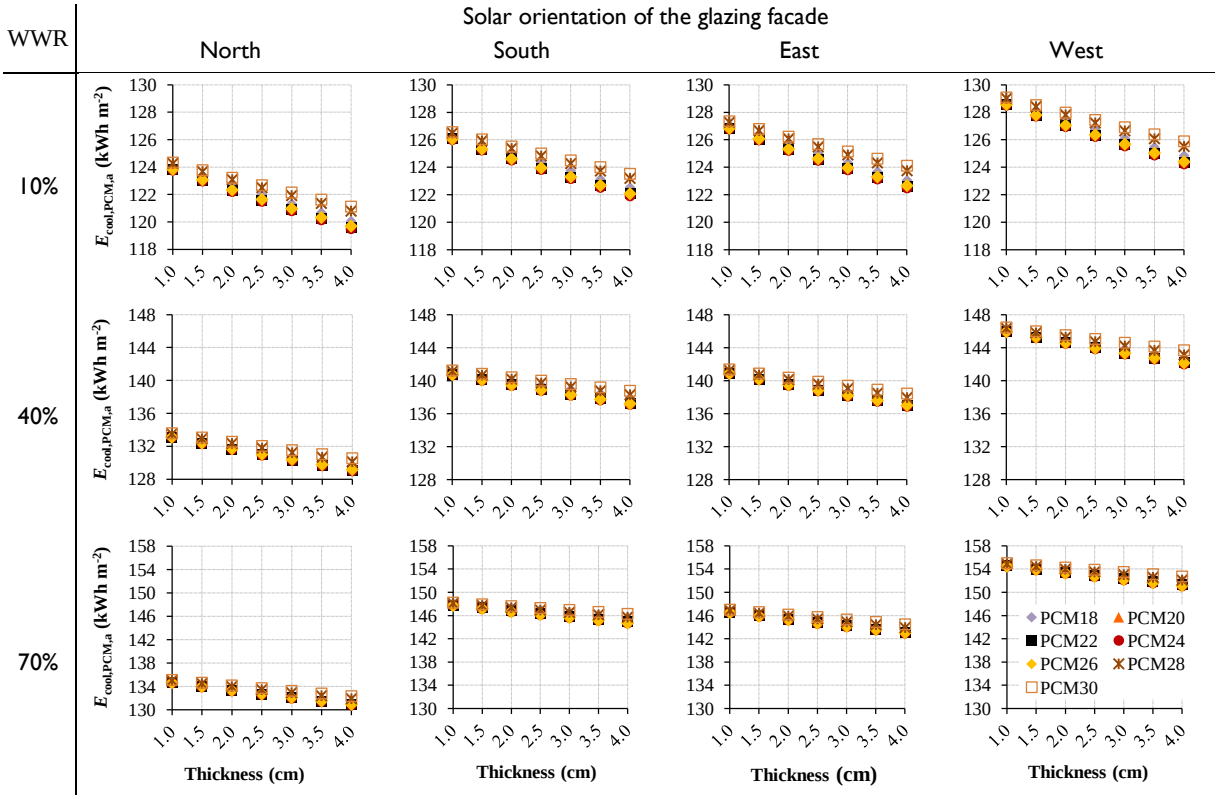

Fig. VII.8 Annual cooling energy demand for all the PCM-enhanced rooms scenarios – parametric study, T_{th} = 24 °C.

From the theoretical point of view, the goal is to increase the heat storage/release capacity using as little PCM as possible. As suggested by Soares *et al.* [1], the energy stored in a complete phase-change cycle is proportional to the PCM volume while the PCM is melting, after that, only sensible heat is absorbed. On the other hand, the energy released is proportional to the volume of PCM solidified during the discharging period. Therefore, insufficient thermal storage is achieved when the PCM solidifies or melts only partially. The optimum thermal storage/release capacity is reached through the optimum combination of the thickness of the PCM-drywall with the melting-peak temperature of the PCM. If the PCM mass is overestimated, or if the melting-peak temperature is too high, the time needed for the heat to penetrate the PCM could become larger than the charging period, and the melting process cannot be completed. Therefore some PCM mass could remain solid during several cycles. On the other hand, if the melting-peak temperature of the PCM is smaller than the air-conditioning setpoint temperature for cooling, and if the building is very thermal insulated on the outside, the PCM could remain liquid during several cycles. Likewise, if the PCM mass is

overestimated, the time needed for the heat to be released could become larger than the discharging period, and the solidification process cannot be completed. Considering all these features, *i.e.*, the existence of an insulation layer, the continuous air-conditioning model with a cooling setpoint temperature fixed at 24°C, the avoidance of an extra ventilation model during the discharging period, and the control of the solar heat gains through the $SHGC$ requirements of the glazing type, the impact of including PCM-drywalls in Kuwait for reducing cooling energy demand can be mitigated.

The index of annual energy savings for cooling ($IESC_a$) is used for quantifying the reduction of the energy demand for cooling and to evaluate the energy performance of the PCM-enhanced room. It is defined by:

$$IESC_i = 1 - E_{\text{cool,PCM,i}} / E_{\text{cool,ref,i}} \times 100\% \quad \text{(VII.1)}$$

Subscript i refers to the assessment time period. The subscripts a and m correspond to the annual and monthly assessment basis, respectively. Fig. VII.9 shows that the annual energy savings for cooling, by incorporating the fully-customized 4 cm thick PCM24-drywall solution in the reference models, can reach 4% to 5% in all the scenarios (5.5 to 6.6 kWh m^{-2} year^{-1}).

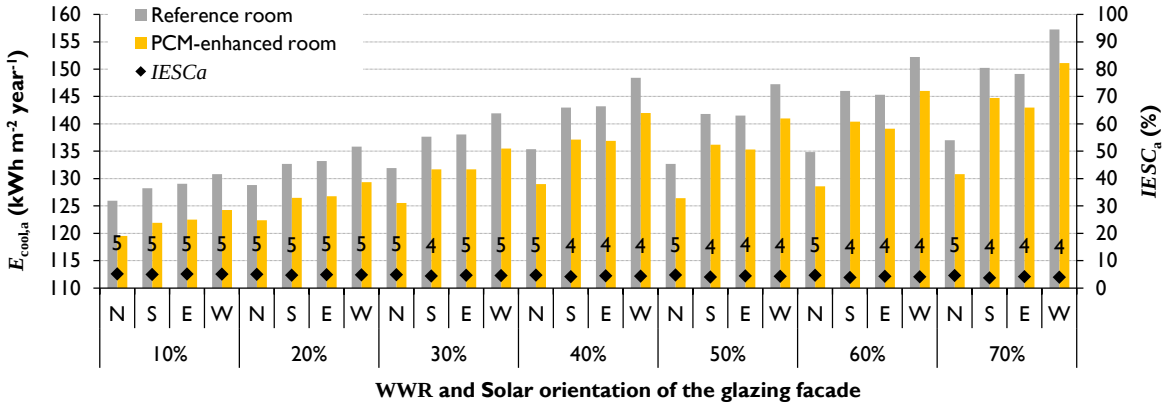

Fig. VII.9 Annual cooling energy demand for all the reference and PCM-enhanced models considering T_{th} = 24 °C. Index of annual energy savings for cooling by considering the incorporation of the fully-customized PCM-drywall solution in the reference rooms.

When the WWR increases from 10% to 70%, considering the West-oriented PCM-enhanced rooms, the annual energy demand for cooling increases by almost 22%. The results show again that the WWR plays an important role in the amount of energy required for cooling. As stated above, if the same 6-mm double-tinted glazing type was used in the two corresponding reference scenarios, the annual cooling demand would increase more than 36% instead of 20%. If the same 6-mm double-tinted glazing type was used combined with the incorporation of the fully-customized PCM-drywall

solution in the WWR = 70% case-study, the annual cooling demand would increase only 31% instead of 36%. This result shows that PCM-drywalls can be used for reducing the extra energy required for cooling due to the extra solar heat gains.

VII.3.3 Annual assessment basis – impact of the cooling setpoint temperature

The results shown in the previous section may suggest that the best melting-peak temperature of the PCM incorporated in the PCM-drywall is equal to the imposed cooling setpoint temperature of the air-conditioning system. Indeed, for T_{th} = 24 °C, the best melting-peak temperature of the PCM is equal to 24 °C. In order to evaluate the impact of the value of T_{th} on the results, the same analysis carried out in the previous section is repeated by considering T_{th} equal to 18, 20, 22 and 26 °C.

The bullets on the graph of Fig. VII.10 show the best value of T_{mp} for different values of T_{th} and for all the case-studies evaluated in the parametric study (read the value of $T_{mp,opt}$ on the right axis). Additionally, Fig. VII.10 shows the absolute annual energy savings for cooling (read on the left axis) by incorporating the best PCM-drywall solution for each scenario (with T_{mp} = $T_{mp,opt}$) in the simulations. Therefore, the absolute annual energy savings for cooling are presented as a function of the orientation of the window, the value of WWR, and the value of T_{th}. Results show that for T_{th} = 26 °C, the best melting-peak temperature of the PCM is also equal to T_{th}. However, for T_{th} = 18 and 20 °C, the best values of T_{mp} are 20 and 22 °C, respectively. Generally speaking, for T_{th} = 22 °C, the best T_{mp} is 22 °C for lower values of WWR and 24 °C for higher values of the same parameter. These results can be used as guidelines for the incorporation of PCM-drywalls in Kuwait.

Regarding the annual cooling savings by incorporating PCM-drywalls in the model, Fig. VII.10 shows that, in absolute terms, the lower the value of T_{th}, the higher the energy savings. However, in relative terms, *i.e.*, by evaluating the $IESC_a$ values, the lower the value of T_{th}, the lower the relative cooling energy savings as shown in Fig. VII.11. This is caused by the fact that the reference energy demand for cooling is higher for lower values of T_{th}. Therefore, a setpoint temperature of the air-conditioning system close to 22–24 °C can be a good compromise for reducing the energy consumption for cooling in Kuwait. In the next sections, the cooling setpoint temperature will be considered fixed at 24 °C as described in section VII.2.1.

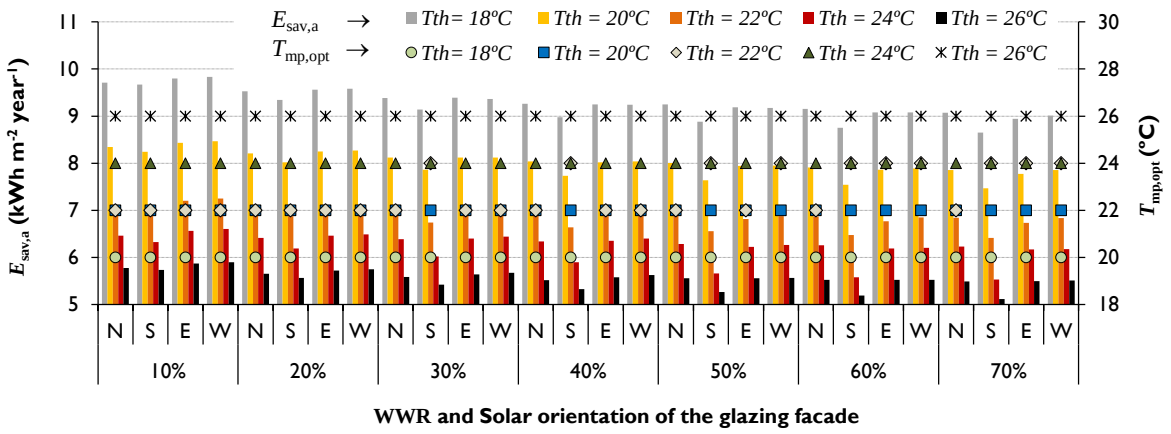

Fig. VII.10 Best value of T_{mp} for different values of T_{th} and for all the case-studies investigated in the parametric analysis (read the value of $T_{mp,opt}$ on the right axis). Annual absolute cooling energy savings (read on the left axis) by incorporating the best PCM-drywall solution for each scenario (with T_{mp} = $T_{mp,opt}$) in the simulations.

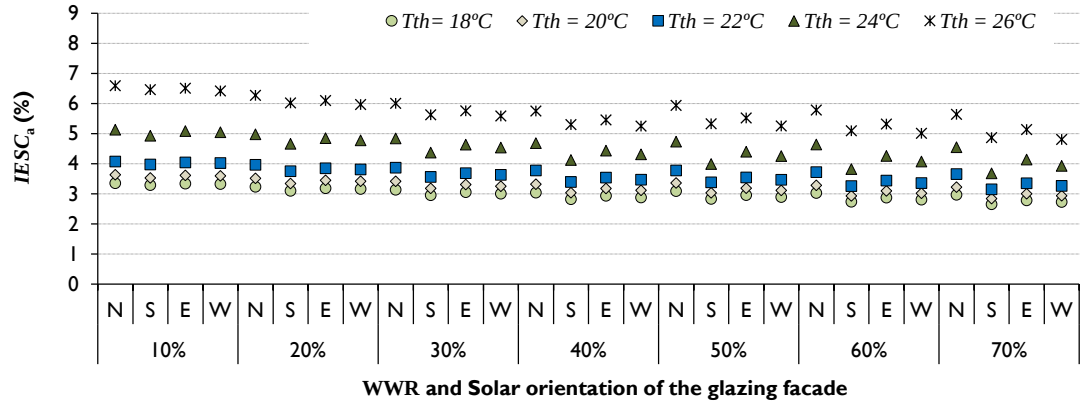

Fig. VII.11 Index of annual energy savings for cooling for all the case-studies investigated in the parametric study by considering the incorporation of the best PCM-drywall solution for each scenario (with T_{mp} = $T_{mp,opt}$) in the simulations.

VII.3.4 Monthly assessment basis

In this section, the impact of the fully-customized 4 cm thick PCM24-drywall solution on the energy demand throughout the year is investigated. Figs. VII.12a and VII.12b show the monthly cooling energy demand for both the reference and the PCM-enhanced models with WWR = 10% and 70%, respectively. They also show the index of energy savings for cooling, for each month, considering the incorporation of the PCM24-drywall solution in each reference room. To prevent this section from becoming too long, only the results for these two case-studies are presented. The same trends are verified for the other five scenarios investigated in the parametric study.

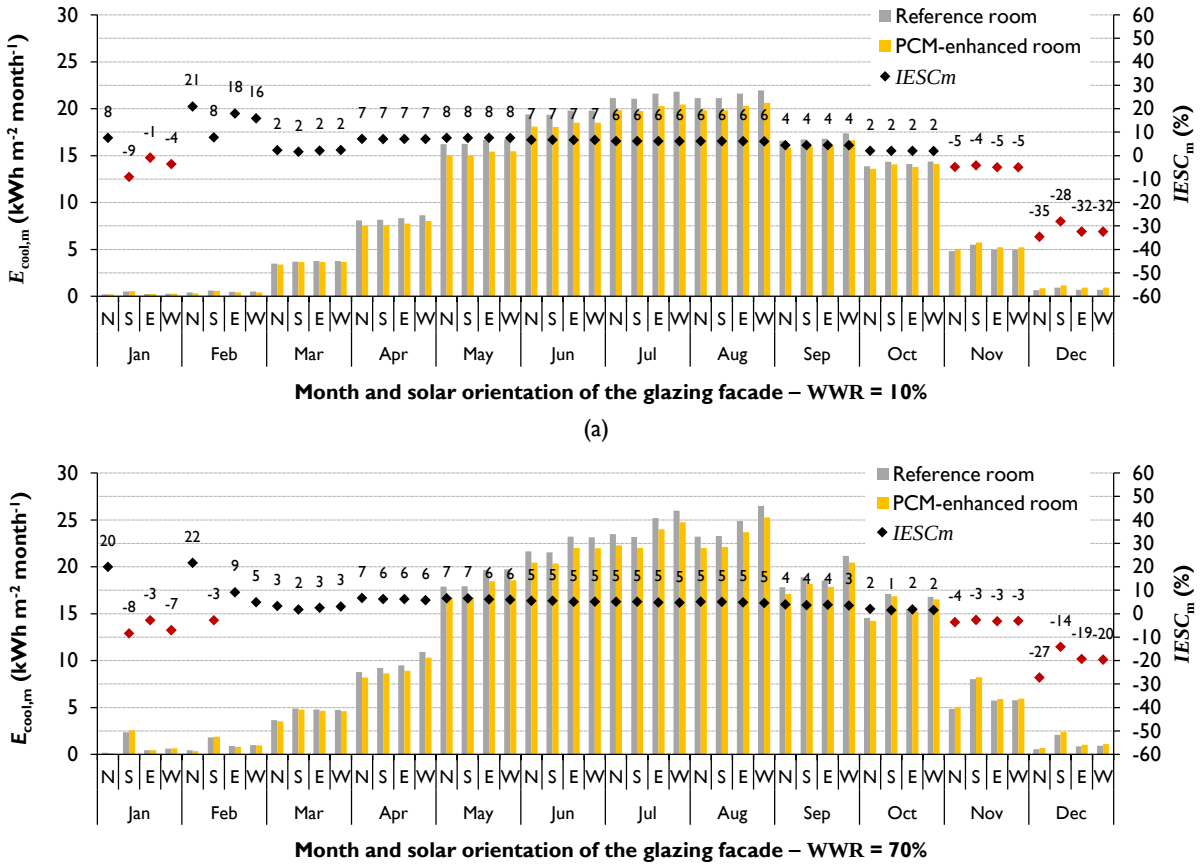

Fig. VII.12 Monthly cooling energy demand for both the reference and the PCM-enhanced rooms with (a) WWR = 10%, and (b) WWR = 70%. Index of monthly energy savings for cooling considering the incorporation of the 4 cm thick PCM24-drywall solution in the model and T_{th} = 24 °C.

The results show that the cooling demand is naturally higher during the summer months. During this period, the relative monthly energy savings for cooling can reach 5% to 7% (read the value of $IESC_m$ on the right axis). Therefore, it can be seen that PCMs are even more interesting for Kuwait, as they further reduce the cooling demand during the summer peak months. Another important feature is that the energy savings are even more significant during the spring months, April and May, reaching values of 6% to 8%. This trend is in accordance with the evolution of the dry bulb temperature throughout the year in Kuwait (Fig. VII.1). During April and May, the daily thermal amplitude is good enough to ensure the daily phase-change cycle of the PCM, considering T_{mp} = 24 °C. Moreover, extending the approach to the seasonal phase-change cycle, the PCM that was mostly solid during the winter time, can now be charged during the spring. On the other hand, the energy savings during the autumn are not so interesting (lower than 4%). During September and October, the difference between the maximum and the minimum dry bulb temperatures is not so high and the phase-change process could be hampered. Furthermore, considering the seasonal phase-change cycle approach, all the PCM volume, which was mostly charged during the summer, can start discharging

the stored heat indoors and more energy will be required for cooling. Other authors have also claimed that the daily phase-change cycle approach should be extended to the seasonal phase-change cycle approach as proposed in this study [273,274].

Another interesting feature is that the energy demand for cooling during the winter months increases by incorporating PCM-drywalls in the model ($IESC_m$ presents negative values). However, the absolute amount of energy required for cooling during the cold months is practically negligible when compared with the summer period. Fig. VII.13 summarizes the reduction of the monthly cooling load during the month with the highest average cooling load for each case-study evaluated. The results show that the monthly cooling loads can be reduced by 5% to 6% in all the scenarios.

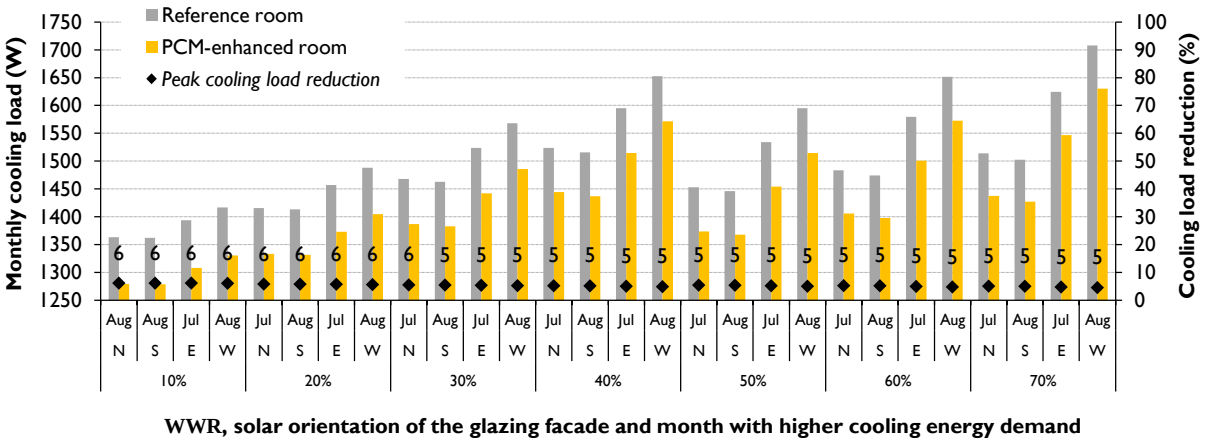

Fig. VII.13 Reduction of the monthly cooling load during the month with the highest average cooling load for all the case-studies considering T_{th} = 24 °C.

VII.3.5 Daily assessment basis

As it was remarked in the introduction section, the summer cooling peak hours are problematic in Kuwait, with the danger of recurring electricity blackouts during this period. In this section, the impact of the incorporation of the fully-customized 4 cm thick PCM24-drywall solution in the model is investigated in a daily assessment basis. For this purpose, the hourly evolution of the indoor air temperature (T_a), mean radiant temperature (T_{mr}), operative temperature (T_o) and outdoor temperature (T_{ext}) will be evaluated for the day with the highest average daily cooling load. The main idea is to evaluate how the incorporation of the PCM-drywall influences the thermal performance of the model if the air-conditioning system was turned off during the summer peak hours.

Fig. VII.14 shows the evolution of the average daily cooling load throughout the year for both the reference and the PCM-enhanced rooms with WWR = 10% and 70%, respectively. It can be seen

that the daily cooling load can be particularly reduced during the summer. The day with the highest average cooling load is the same for all the case-studies – the 5th of August. Fig. VI.15 summarizes the reduction of the average daily cooling load for all the case-studies (5% to 8%) for this day. The results show that the average daily cooling load can be reduced by 107 to 131 W.

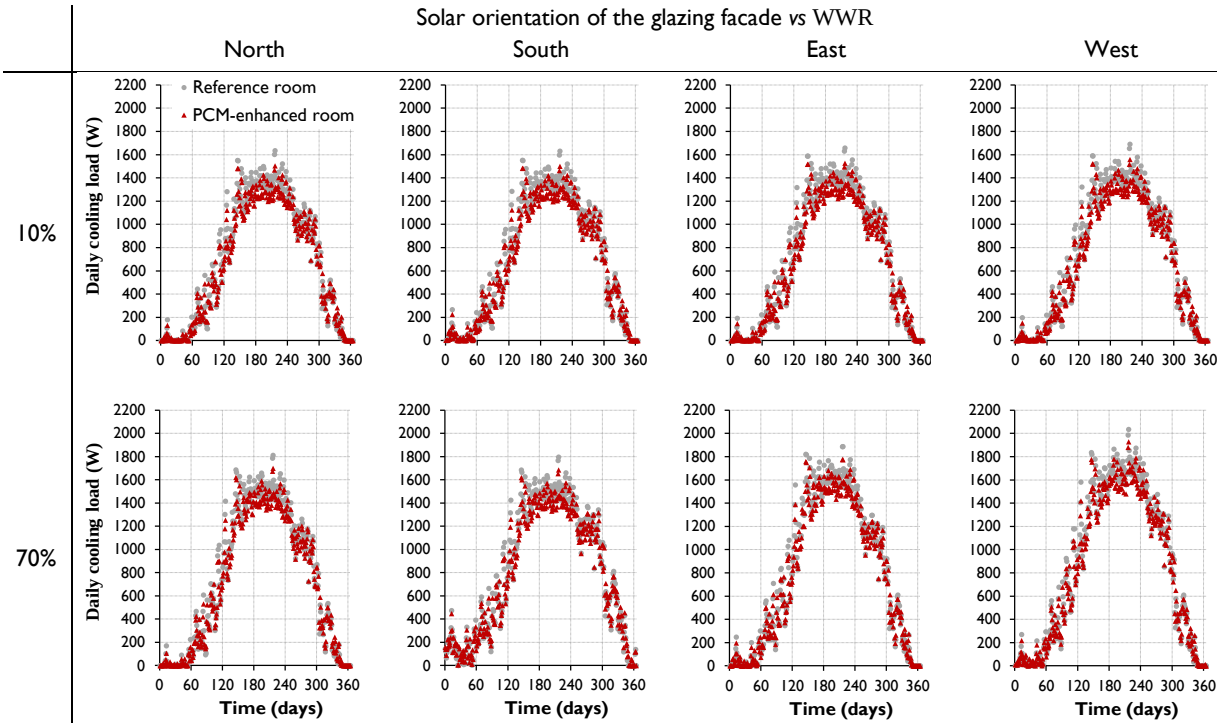

Fig. VII.14 Average daily cooling loads throughout the year for both the reference and the PCM-enhanced rooms with WWR = 10% and 70%. T_{th} = 24 °C.

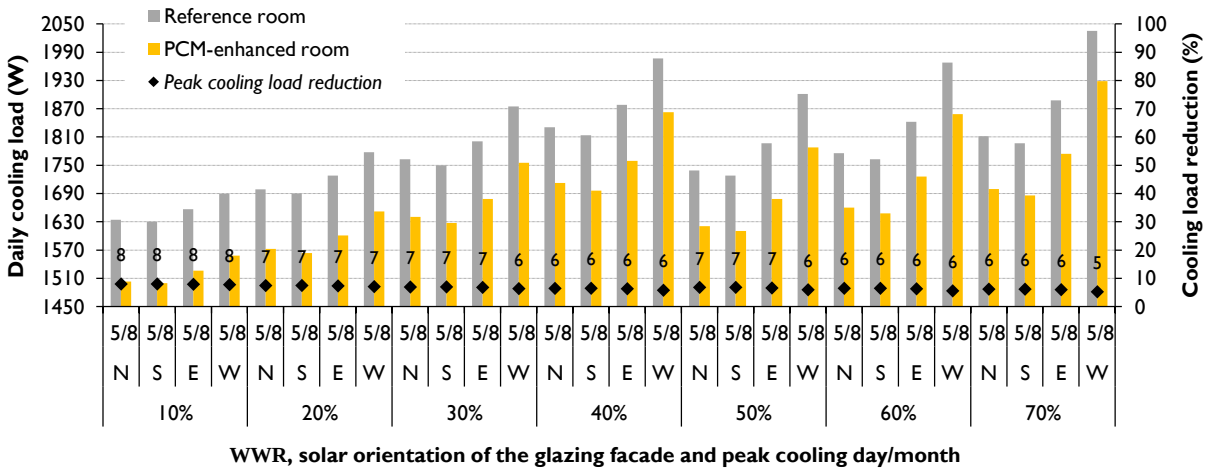

Fig. VII.15 Reduction of the average daily cooling load for the 5th of August, for all the case-studies evaluated and by considering T_{th} = 24 °C.

Fig. VII.16 shows the cooling profiles in an hourly assessment basis for the cooling peak day (5th of August) for both the reference and the PCM-enhanced models with WWR = 10% and 70%, respectively. The evolutions of T_a, T_{mr}, T_o and T_{ext} are also shown in the figure. The results show that the maximum cooling load of ≈3300 W is estimated for the West-oriented model with WWR = 70%, between 6pm and 7pm. The incorporation of the fully-customized 4 cm thick PCM24-drywall solution reduces the cooling load profiles of all the scenarios. An exception is the West-oriented room with WWR = 70%, where PCMs can increase the cooling loads during the peak hours.

Many times, the daily cooling profiles are simulated considering the PCMs completely discharged at the beginning of the day. In these cases, the reduction of the cooling loads is higher (with a significant delay of the peak hour) because more volume of PCM will be melted during the day and more latent heat will be stored. However, in real applications, mainly during the severe summer conditions of Kuwait, the PCM can be completely melted at the beginning of the summer peak day-cycle, which reduces the PCM capacity for latent heat storage. Moreover, large West-oriented windows are a major source of solar heat gains during the last sun-hours of the day, a period when the internal heat gains from occupancy, lighting and equipments also increase (see Fig. VII.4). Consequently, there is a boost in the energy demand for cooling, with no help from the latent heat loads from PCMs' phase-change processes, as they are completely melted at this time. In the East oriented rooms, a cooling peak is observed during the morning, which is caused by the morning solar heat gains and by the internal heat gains during these hours (see Fig. VII.4). Generally speaking, the cooling peak-loads are observed during the summer electricity demand peak hours, from 2pm to 4pm, which is problematic for the management of the energy supply in Kuwait.

Regarding the evolution of the temperature profiles during the cooling peak day, it is interesting to observe that the mean radiant temperature is reduced by almost 1 °C in most cases due to the incorporation of the fully-customized PCM-drywall solution. Consequently, the operative temperature is also reduced. As this temperature can be used for the thermal comfort analysis (ANSI/ASHRAE Standard 55 [426]), it is expected that the incorporation of PCM-drywalls contributes to increase indoor thermal comfort.

Fig. VII.17 shows the cooling loads and temperatures profiles for the same scenarios presented in Fig. VII.16 considering that the cooling system is turned off from 2pm to 4pm (to simulate the recurrent electricity blackout during the summer peak hours). For these *EnergyPlus* simulations, a maximum total cooling capacity of 3500 W was imposed in the *ideal loads air system model*. The results show that the air temperature in all the rooms immediately rises above 30 °C when the cooling system is turned off. For larger glazing areas, the indoor air temperature will be higher in the PCM-enhanced rooms. Moreover, when the system is turned on again at 4pm, the cooling loads are bigger for the rooms with PCM-drywalls. When the indoor temperature is lowered

by the air-conditioning, the PCMs will start discharging some sensible heat indoors and more energy will be required for cooling. Another important feature is that, during the cooling load cut period, both the mean radiant and the operative temperatures will be higher in the models with PCM-drywalls.

The results depicted in Figs. VII.16 and VII.17 also show that the incorporation of the fully-customized 4 cm thick PCM24-drywall solution in Kuwait can be used to reduce the hourly cooling loads when the cooling system is operating continuously. This feature may be very important for the design of the air-conditioning system. By downsizing the air-conditioning equipment capacities, a building owner not only will save on energy operating costs, but also on the initial equipment capitals costs. On the other hands, if the cooling system stops during the problematic summer peak hours in Kuwait, the inclusion of the fully-customized PCM-drywall solution can have a negative impact, as it may increase the indoor air temperature. As explained before, the PCM volume is already melted at this point, and no extra latent heat storage capacity exists to contribute for reducing the rise of the indoor temperature.

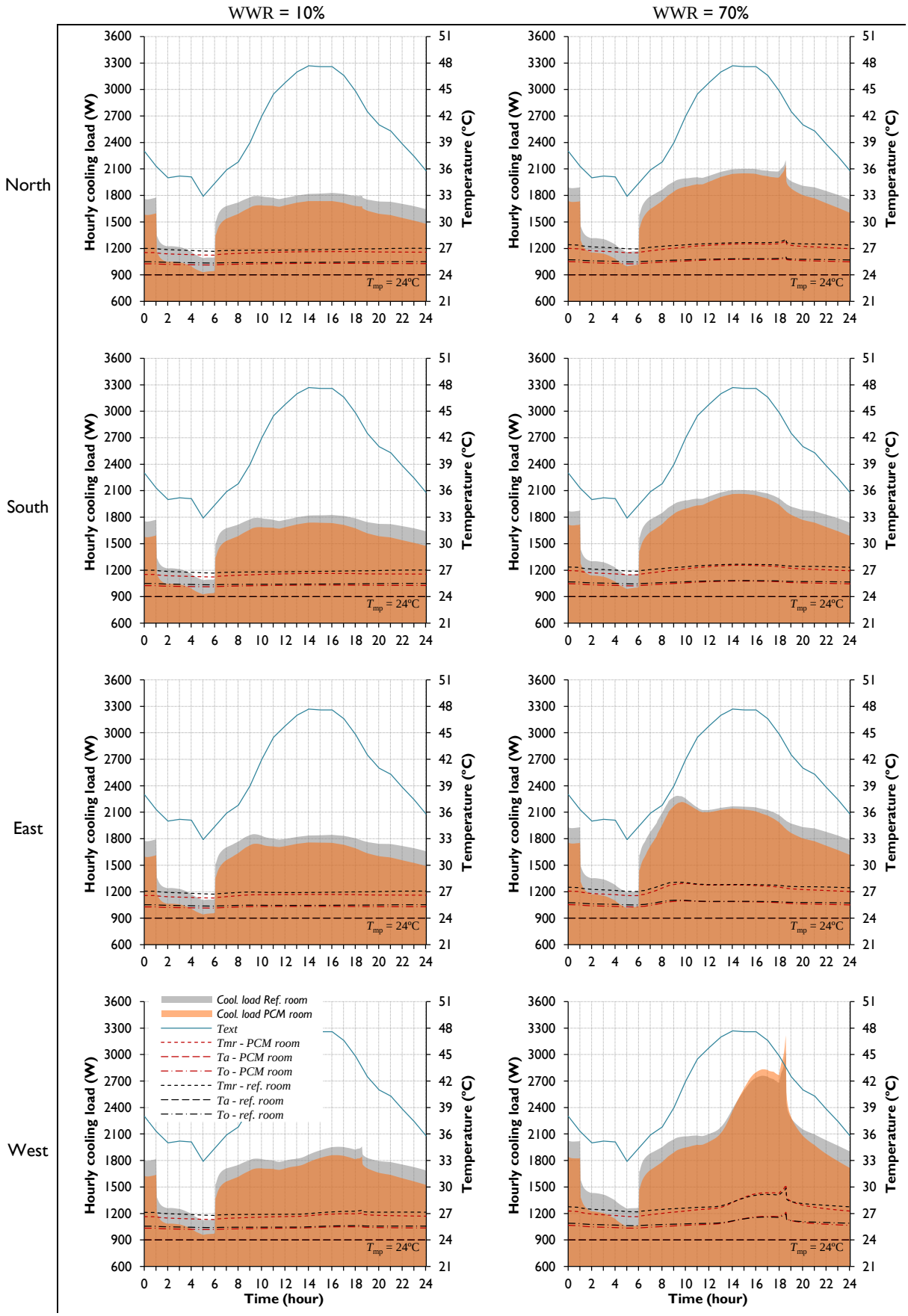

Fig. VII.16 Hourly cooling load profiles and evolution of the estimated temperatures for the cooling peak day (5th of August) for both the reference and the PCM-enhanced models with WWR = 10% and 70%. T_{th} = 24 °C.

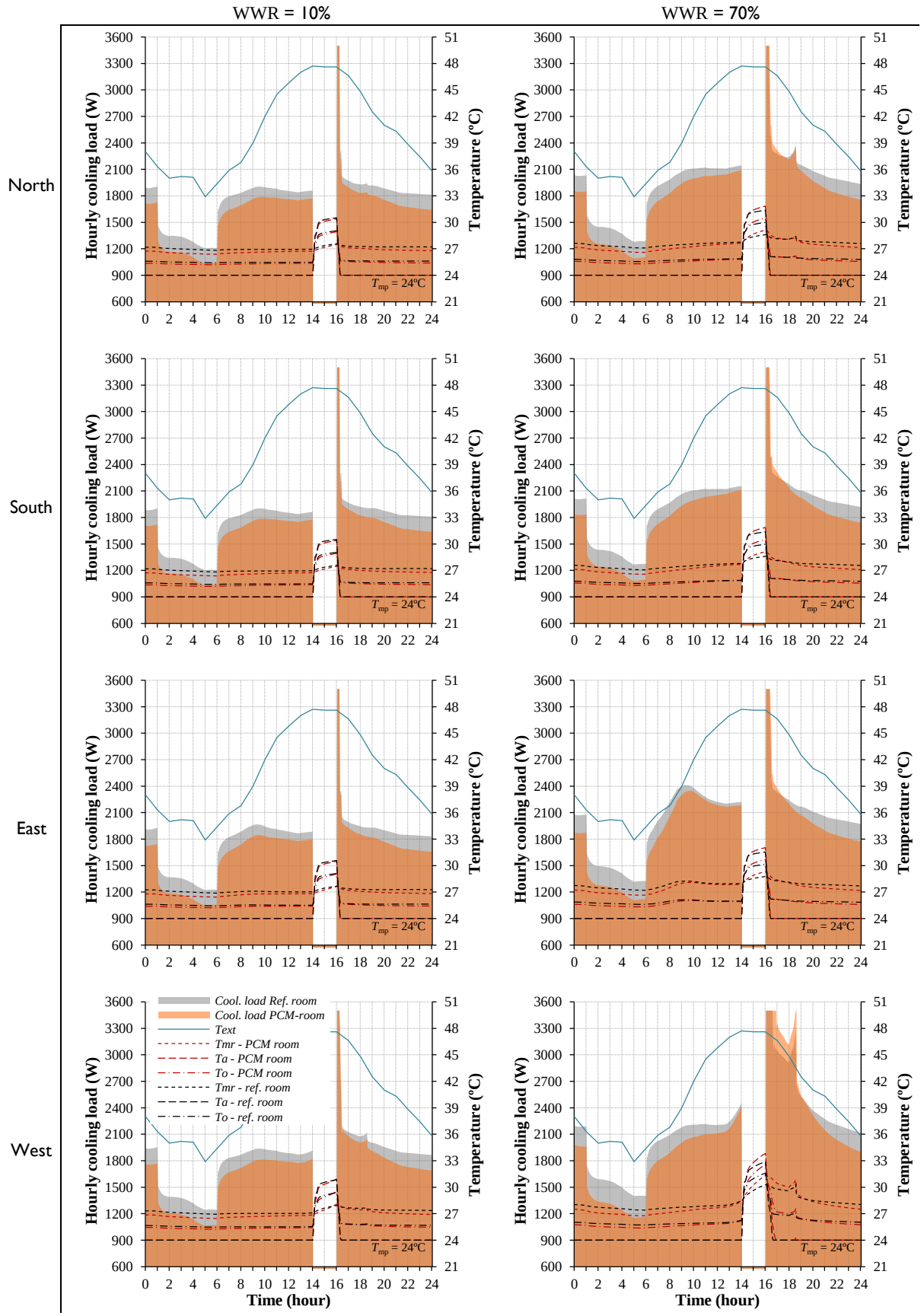

Fig. VII.17 Hourly cooling load profiles and evolution of the estimated temperatures for the cooling peak day (5th of August) for both the reference and the PCM-enhanced models with WWR = 10% and 70%. Cooling system turned off from 2 pm to 4 pm and T_{th} = 24 °C.

VII.4 Conclusion

Kuwait is one of the countries with the largest electricity usage per capita in the world. The country also faces a rapid urbanization due to the growing population number. Most of the energy demand is used for cooling. Indeed, the building sector is putting a big pressure on the electricity supply of the country. Consequently, the reduction of the energy consumption for cooling in the residential sector is a key target for reducing the overall electricity demand in Kuwait, reducing adverse environmental impacts and helping to foster economic growth.

In this chapter, the impact of incorporating PCM-drywalls in an air-conditioned residential single-zone model was investigated, aiming to find a fully-customized PCM-drywall solution to be used in generalized applications suitable to the economy of mass production. A parametric study was carried out by considering different WWR values, solar orientations and PCM-drywalls. The simulations were performed with the CondFD algorithm in the *EnergyPlus* software tool to simulate phase-change processes of PCMs. The requirements of the building energy code of Kuwait were also considered in the model.

A fully-customized PCM-drywall solution was found for the cooling setpoint temperature of the air-conditioning system fixed at 24 °C, leading to significant annual energy savings for cooling – a 4 cm thick PCM-drywall with a melting-peak temperature of the PCM of about 24 °C (considering the set of PCM-drywalls evaluated in the parametric study). By incorporating this PCM-drywall in all the reference case-studies, the annual cooling savings can reach 4% to 5% (energy savings of 5.5 to 6.6 kWh m^{-2} $year^{-1}$). Considering the impact of the fully-customized PCM-drywall solution throughout the year, both the cooling energy demand and the cooling peak-load can be reduced by 5% to 7% during the summer, and by 5% to 6% during the month with the highest average cooling load. The daily cooling load for the day with the highest average cooling load can be reduced by 5% to 8%. Therefore, it is concluded that the fully-customized PCM-drywall solution can be used for reducing both the cooling energy demand and the cooling peak-loads in residential buildings in Kuwait.

In order to provide some guidelines for the incorporation of PCM-drywalls in Kuwait, a sensitive analysis was carried out to evaluate the influence of the imposed cooling setpoint temperature of the air-conditioning system on the optimum value of the melting-peak temperature of the PCM. It was concluded that for setpoint temperatures equal to 24 °C and 26 °C, the melting-peak temperature of the PCM should be equal to 24 °C and 26 °C, respectively. For setpoint temperatures equal to 18 °C and 20 °C, the melting-peak temperature of the PCM should be slightly higher and equal to 20 °C and 22 °C, respectively. For the setpoint temperature fixed at 22 °C the melting-peak temperature should be equal to 22 °C and 24 °C, for lower and higher values of the

solar heat gains respectively. It was also concluded that choosing cooling setpoint temperatures close to 22–24 °C can be a good strategy for reducing the energy consumption for cooling in residential buildings in Kuwait.

Regarding the hourly assessment basis, it was concluded that PCM-drywalls can be used in Kuwait to reduce the hourly cooling loads when the cooling system is operating continuously. However, if the cooling system stops working during the problematic summer peak hours, the incorporation of PCM-drywalls has a negative impact for buildings with higher glazing areas, as the rise of the indoor air temperature is bigger.

Finally, it was concluded that the traditional daily phase-change cycle approach should be extended to the seasonal phase-change cycle approach in order to accurately evaluate the influence of the latent heat loads throughout the year. The overall methodology proposed herein was focused on a single-zone room model. Hence, the results cannot be directly extrapolated and generalized to more complex models. Further work should be done to apply the presented methodology to more complex buildings.

Chapter VIII

Conclusion

In this chapter, a general overview of the main results of the work carried out in this thesis is presented, along with the most important conclusions. Some limitations of the developed work and some recomendations for future research are also presented in this chapter.

VIII.1 General overview

This thesis was carried out in the framework of the Sustainable Energy Systems doctoral program of the MIT-Portugal program. In this work, *Buildings* were considered as the Energy System to be improved by reducing the energy demand for cooling and heating by taking advantage of renewable energy sources such as solar thermal energy. For that purpose, the use of latent heat from PCMs' solid–liquid phase-change processes was investigated. The core idea was to evaluate the potential of thermal energy storage with PCMs for the improvement of the energy performance of different typologies of buildings in different climates. This was done by evaluating the inclusion of PCMs in buildings from the scale of the envelope element to the scale of the entire building. The research was divided in two mains parts: Part A was devoted to the scale of a TES unit to be used in the design of new TES systems for buildings, and Part B was devoted to the scale of an entire room in order to evaluate the influence of PCMs in the thermal dynamic behavior of the building considering real-life conditions. The main goals of this thesis were: (*i*) to experimentally evaluate the heat transfer through a vertical stack of rectangular cavities filled with different types of PCMs (the so-called TES unit) and to make available a big amount of reliable experimental data for benchmarking and validation of numerical models and, (*ii*) to develop a holistic methodology to optimize the

incorporation of PCM-drywalls in different typologies of buildings and in different climates, providing some guidelines for the most effective use of this PCM-based TES system. The results of this thesis give new and relevant contributions to the present knowledge in the following research fields: (*i*) heat transfer with solid–liquid phase-change in vertical rectangular cavities considering the effects of subcooling and natural convection in the molten PCM; (*ii*) design and optimization of PCM-based TES systems for buildings; (*iii*) dynamic simulation of energy in buildings considering the latent heat from PCMs' phase change processes, and (*iv*) optimization of the incorporation of PCM-drywalls in different types of construction and climates.

VIII.2 Contribution of this thesis and main conclusions

In Part A of this thesis, the basic thermodynamics of TES in buildings and the most important fundamentals of the heat transfer with PCMs' solid–liquid phase-change processes were discussed. Particular attention was given to the thermophysical characterization of PCMs, as the thermophysical properties of PCMs and/or PCM composites must be known *a priori* when a new TES system is designed or optimized. Moreover, these properties directly influence the final thermal performance of the PCM-based TES system. It was concluded that the uncertainty of the measurements for characterizing PCMs is an active area of research, including the characterization of the PCM itself and/or the characterization of PCM composites and heterogeneous construction elements in a more macro-scale approach. It was also concluded that the numerical models to simulate solid–liquid phase-change processes in vertical rectangular cavities must be validated using appropriated experimental data. However, it was found that there was a lack of reliable experimental results in the literature that researchers could reproduce for validating their numerical models, this is including the influence of subcooling, hysteresis and natural convection phenomena.

Considering this, a new experimental setup was developed in the Mechanical Engineering Department of the University of Coimbra to evaluate the heat transfer through small TES units filled with different PCMs (the free-form PCM – Rubitherm® RT 28 HC and the microencapsulated PCM – Micronal® DS 5001 X). These TES units are intended to be integrated in the design of PCM-enhanced systems to improve the energy performance of buildings, such as PCM-bricks, PCM-shutters, PCM-window blinds, PV/PCM systems, SP/PCM systems, etc.. A parametric study was carried out to evaluate how the charging and discharging phases of PCMs are influenced by the configuration of the TES unit (aspect ratio of the rectangular cavities), by the boundary conditions imposed during the experiments and by the kind of PCM used to fill up the TES unit. The results achieved give new and relevant contributions to the present knowledge in the study of the heat transfer with solid–liquid

phase-change in vertical rectangular cavities. Moreover, a substantial amount of experimental data was made available to the scientific community for benchmarking and validation purposes. The main conclusions of the experimental study carried out in the first part of the thesis are:

- during charging of the free-form PCM, conduction is the initial dominant mode of heat transfer, although, after some time, the natural convection flow becomes the dominant heat transfer mechanism causing a thermal stratification in the TES unit;
- during charging of the free-form PCM, natural convection in the molten PCM and in the air-layer domain on the top of each cavity must be considered in every numerical simulation;
- during charging of the microencapsulated PCM, conduction is the dominant mode of heat transfer and natural convection can be neglected in the simulations;
- decreasing the aspect ratio of the cavities reduces the effect of natural convection during the charging of the free-form PCM, improves the heat transfer by conduction reducing the time required for melting all the PCM, reduces the value of the control-temperature on the hot surface of the TES unit and reduces the thermal-regulation period;
- decreasing the aspect ratio of the cavities filled with the microencapsulated PCM during charging increases the heat transfer rate by conduction but reduces the thermal-regulation period;

- during discharging of the free-form PCM, the effect of natural convection can be neglected but subcooling must be considered in the simulations;
- during discharging of the microencapsulated PCM, both natural convection and subcooling can be neglected in the simulations;
- decreasing the aspect ratio of the cavities filled with the free-form PCM enhances the subcooling effect by increasing the period during which subcooling occurs and by reducing both the temperature required to start crystallization and the phase-change temperature after subcooling;
- subcooling delays the discharging process of the free-form PCM and reduces the solidifying temperature of the PCM, which can increase the hysteresis problem;
- adding fins in both free-form and microencapsulated PCMs is a good technique for improving the discharging process by conduction;

- regarding building applications, TES units filled with the free-form PCM are more attractive to be used in TES systems in which the main purpose is to enhance the thermal-regulation period and to reduce the control-temperature value on the hot surface of the TES unit, and cavities filled with the microencapsulated PCM are better for elements where it is crucial to reduce the time required for melting all the PCM in the TES unit;

- regarding building applications, the higher the number of fins, the lower the volume of PCM and the lower the energy that can be stored and released during a potential charging/discharging cycle, and the heavier the system, which can be problematic for some vertical building applications.

In Part B, an overview on the main passive TES systems with PCMs for buildings and on the dynamic simulation of energy in buildings with PCMs is made available. Special attention was devoted to PCM-drywalls. The incorporation of this TES system in different types of buildings and in different climates was investigated during Part B. Firstly, a multi-dimensional optimization methodology combining *EnergyPlus* and *GenOpt* tools was defined to optimize the incorporation of PCM-drywalls in LSF residential buildings in different European climates. The attempt to develop specific solutions for different locations based on their climate is seen as a good approach to foster the implementation of a specific TES technology. Several variables were considered in the optimization problem, namely the thermophysical properties of the PCM-drywall (enthalpy-temperature and thermal conductivity-temperature functions), the solar absortance coefficient of the inner surfaces, and the thickness and location of the PCM-drywalls in the room. Secondly, an *EnergyPlus*-based parametric study was carried out to evaluate the influence of incorporating PCM-drywalls in heavyweight construction in Kuwait to reduce cooling energy demand and peak-loads. Several features were considered in the parametric study, such as different WWRs, solar orientations of the glazed facade and thermophysical properties and thicknesses of the PCM-drywall layer.

The main conclusions of Part B regarding the optimum incorporation of PCM-drywalls in LSF residential buildings in Europe are:

- considering the set of thicknesses evaluated for the PCM-drywall layer, an optimum thickness of 4.0 cm was found for all the surfaces and climates, based on the annual energy savings for air-conditioning;
- the optimum melting-peak temperature of the PCM varies according to the climate – it is higher for the warmer southern countries and between 22 °C and 26 °C against the 18 °C to 24 °C for the colder climates;
- inner PCM-drywalls surfaces with higher solar absorbance (α = 0.9) are better for colder climates while surfaces with lower solar absorbance (α = 0.3) are better for warmer climates;
- the annual energy savings for air-conditioning due to the incorporation of the optimum PCM-drywalls is higher for the warmer climates – 46% and 62% for the Csa-Seville and Csb-Coimbra climates, respectively – meaning that PCM-drywalls are particularly suitable for Mediterranean climates;
- PCM-drywalls reduce both the energy demand for cooling and heating in the warmer Southern climates;

- PCM-drywalls reduce mainly the annual energy demand for heating in the colder climates;
- the enhancement of the thermal capacity of the LSF envelope via PCM-drywalls changes the behavior of the building during every month of the year.

The main conclusions of Part B regarding the incorporation of PCM-drywalls in heavyweight residential buildings in Kuwait are:

- a fully-customized 4.0 cm thick PCM-drywall solution with a melting-peak temperature of 24 °C leads to the higher value of the annual energy savings for cooling, considering the set of thicknesses evaluated for the PCM-drywall, and the cooling setpoint temperature of the air-conditioning system fixed at 24 °C;
- the setpoint temperature of the air-conditioning system influences both the annual energy demand for cooling and the optimum melting peak-temperature of the PCM – considering the 4.0 cm thick PCM-drywall, for setpoint temperatures of 24 °C and 26 °C, the melting-peak temperature should be equal to 24 °C and 26 °C, respectively, for setpoint temperatures of 18 °C and 20 °C, the melting-peak temperature of the PCM should be equal to 20 °C and 22 °C, respectively, and for the setpoint temperature of the air-conditioning system fixed at 22 °C the melting-peak temperature should be equal to 22 °C and 24 °C, for lower and higher values of the solar heat gains, respectively;
- the fully-customized PCM-drywall solution reduces both the cooling energy demand and the cooling peak-loads;
- the annual cooling savings can reach 4% to 5% (energy savings of 5.5 to 6.6 kWh m^{-2} $year^{-1}$);
- both the cooling energy demand and the peak-loads can be reduced by 5% to 7% during the summer, and by 5% to 6% during the month with the highest average cooling load;
- the daily cooling load for the day with the highest average cooling load can be reduced by 5% to 8%;
- PCM-drywalls can be used in Kuwait to reduce the hourly cooling loads only if the cooling system operates continuously;
- if the cooling system stops working during the summer peak hours, the incorporation of PCM-drywalls has a negative impact.

VIII.3 Forthcoming work and future research

During the first part of this thesis, only small TES units were evaluated using the developed small-scale experimental setup. The next steps are: (*i*) to developed a validated CFD strategy for the parametric analysis and optimization of different small TES units; (*ii*) to define more complex CFD

simulations using, for example, the commercial code CFX from ANSYS®, to evaluate the heat transfer through large-scale TES prototypes incorporating the proposed TES units; (*iii*) to develop an experimental setup to evaluate the thermal performance of large-scale prototypes with TES units in a transient mode and to provide experimental data for validating more complex CFD models, and (*iv*) to propose new TES systems for buildings.

Regarding the development of a numerical model for the evaluation of the heat transfer through the small TES units, the two-dimensional phase-change heat diffusion model based on the enthalpy formulation described by Soares *et al.* in ref. [153] would be improved. The numerical model follows the finite-volume method with a fully-implicit formulation and allows the alternating melting and solidification of a pure PCM. This model neglects the advective term in the general equation for conservation of energy. To well describe the heat flow with phase-change, the model will be improved to consider the advective term in the conservation equations of energy and momentum. Moreover, the open-source code will be enhanced to simulate non-pure PCMs, taking into account the influence of natural convection, subcooling and hysteresis phenomena, as well as volume variation during phase-change. For that purpose, the model must consider the presence of a moving boundary between the PCM and the air-layer used to accommodate the PCM volume expansion. This problem can be overcome by using the Volume of Fluid (VoF) method. The code will be written in Fortran and the final goal is to propose a new type for the *TRNSYS* dynamic simulation tool that considers the influence of natural convection and subcooling in the heat transfer with solid–liquid phase-change. Indeed, the development of new validated PCM-models to be incorporated in DSEB tools to evaluate the thermal performance of more complex PCM-based systems for buildings is seen as an active area of research for the next years.

For measuring the thermal performance of large-scale prototypes incorporating rectangular cavities filled with PCMs, the Guarded Hot Box Apparatus developed in the Civil Engineering Department of the University of Coimbra will be used. The experimental characterization of the thermal transmittance value of non-homogeneous construction systems cannot be accurately carried out by using discrete measurements (of heat flux and surface temperatures) given the higher uncertainty caused by the lateral heat flows during the experiments. Nowadays, the most suitable experimental technique used for this purpose is the Hot Box method according to the procedures defined in ISO 8990 [427], as the measurements are performed in a wide representative continuous surface area. Furthermore, the Guarded Hot Box Apparatus was chosen for future work (instead of the Calibrated Hot Box) because it is easier and faster to calibrate and it is less sensible to external factors. Given the huge investment needed for the acquisition of this setup (about 400 k€), few Hot Boxes are available for the research community. Besides being more expensive, the commercial Hot Box standard apparatus typically allow testing samples with maximum size of 150 cm x 150 cm x 38

cm, which may not be enough for characterizing some construction elements. As far as the author knows, in Portugal there is only one Calibrated Hot Box available to perform the thermal characterization of construction elements following the prescriptions given in international standards (ISO 8990). Recently, a Guarded Hot Box test station was designed and assembled in the Civil Engineering Department of the University of Coimbra with a cost of about 20 k€. The cost of instrumentation complying with international standards (ISO 8990 [427], BS 874 [428] and ASTM C1363-11 [429]) was about 90 k€ considering heating/cooling systems, fans, sensors (thermocouples, airflow velocity meters, air pressure meters, heat flux meters and energy meters), data-acquisition and control systems. The developed experimental setup was less expensive than the reference commercial test stations. Moreover, the Guarded Hot Box Apparatus installed in the Civil Engineering Department allows testing samples with maximum size of 360 cm x 270 cm x 50 cm. The big challenge is to adapt the Guarded Hot Box Apparatus for measuring the transient heat transfer through elements considering solid–liquid phase-change processes. As the principle of the setup is based on steady-state experiments (ISO 8990), a methodology for carrying out transient experiments, allowing PCMs' phase-change and the imposition of variable boundary conditions must be proposed. This will require a big effort for performing calibration tests and to execute both steady-state and transient measurements in order to evaluate the thermal performance of PCM-enhanced prototypes and reference systems. Additionally, some infrared thermography may be used to evaluate the temperature distribution on the surfaces of the tested prototypes. The transient procedure will be configured to reproduce the daily outdoor temperature variation (or the sol-air temperature evolution) in one chamber. In the other chamber, the set temperature will simulate indoor thermal comfort conditions. At least two different daily cycles would be implemented: typical summer and winter days. Besides the trustworthy repeatability of the test conditions, the setup can also reproduce several ventilation conditions inside the test chambers by controlling the air velocity during the experiments. This feature is crucial to evaluate the influence of convection, mainly during the discharging of the TES systems (solidification of the PCM).

The experimental results of this thesis will be used to evaluate a PCM module in the commercial CFX tool from ANSYS®. Moreover, the experimental large-scale results are also expected to be used to validate the more complex numerical model. This model should reproduce the large-scale experimental domain and conditions, which are related with the temperature and ventilation imposed in the chambers (they can assume transient profiles). Radiation will not be considered in the experiments. However, some radiation models can be included in the numerical approach in order to evaluate the influence of solar radiation in the thermal performance of the TES systems. Firstly, solar radiation will be taken into account considering the sol-air temperature model. Afterwards, a multiband spectral model will be incorporated in the radiation model to take into

account the radiation properties of glass as a function of the wavelength. The validated CFD model will be used to evaluate the heat transfer through large-scale TES systems and to optimize the configuration and operation of several prototypes in a faster and robustly way. With this methodology, it would be possible to design and optimize several PCM-based TES systems to take advantage of solar thermal energy based on reliable and accurate numerical approaches.

The multi-dimensional optimization methodology proposed in the second part of this thesis, to find the best PCM-drywall solution for LSF residential buildings in different European climates, was focused on a single-zone room model. Therefore, the main findings can only be carefully generalized to more complex multi-zone models and further work should be done to apply the methodology to more complex models. The study should also be extended to the multi-objective optimization of the incorporation of PCM-drywalls in buildings in different climates by considering more than one Objective Function, such as cost (or retrofitting cost), energy savings and percentage of discomfort hours. These combinatorial multi-objective methodologies are particularly interesting to evaluate conflicting Objective Functions, and they can be used to help decision-making during the design and/or retrofitting of buildings with PCM-drywalls or other passive TES systems.

As pointed out in chapter V, further work needs to be done in the research field of DSEB considering the latent heat from solid-liquid phase change processes of PCMs and the influence of natural convection and subcooling in the dynamic simulations. The assessment of the accuracy of the DSEB results and the comparison between different PCM modules within different DSEB tools must also to be addressed. Moreover, more recommendations for future works can be noted, such as: the development of both environmental and economical lifecycle studies and the importance of coupling DSEB techniques with LCA techniques; the development of sensitive analysis to assess the influence of the LCIA method in LCA studies; and the evaluation of the potential of PCMs towards NZEBs.

To sum up, there is still a long way for the generalized use of PCM-based passive systems to improve the energy performance of buildings in a more sustainable way. Despite this criticism, the actual situation of our societies which puts energy consumption profiles, new and more demanding regulations, climate changes, security of the supplies, and fossil fuels depletion at the heart of economic and environmental discussions, will push forward towards guaranteeing a place for PCMs in global scientific, technological and economic research.

NOMENCLATURE

A	cavity aspect ratio (=H'/L)
C_{eff}	overall heat storage capacity (J kg^{-1})
c	space discretization constant ( )
c_p	specific heat (J kg^{-1} K^{-1})
DSC	differential scanning calorimetry
DTA	differential thermal analysis
e_{PCM}	thickness (cm)
E	energy (kWh m^{-2})
E_{cool}	energy demand for cooling (kWh m^{-2})
E_{heat}	energy demand for heating (kWh m^{-2})
E_{sav}	cooling energy savings (kWh m^{-2})
$E_{st,ex}$	stored energy (experimentally calculated) (J)
$E_{st,th}$	theoretical stored energy in the physical domain (J)
E_{tot}	total energy demand for heating and cooling (kWh m^{-2})
Fo	Fourier number ( )
FTIR	Fourier infrared spectroscopy
G	solar factor ( )
H	enthalpy (kJ kg^{-1})
H'	height of each cavity of the test-sample (m)
HF_1	average heat flux measured on the centre of the front surface of the TES unit (W m^{-2})
HF_2	average heat flux measured on the centre of the back surface of the TES unit (W m^{-2})
$IESC$	index of energy savings for cooling ( )
$IESH$	index of energy savings for heating ( )
$IEST$	index of energy savings for heating and cooling ( )
k	thermal conductivity (W m^{-1} °C^{-1})
L	width of each cavity of the test-sample (m)
L_f	latent heat of fusion (kJ kg^{-1})
LSF	lightweight steel-framed
m	mass (kg)
MDSC	modulated differential scanning calorimetry
OF	objective function
PCM	phase change material
PSO	particle swarm optimization
PSOCC	particle swarm optimization algorithm with constriction coefficient
PV	photovoltaic
Ra	Rayleigh number ( )
S	area of the front and back surfaces of the test-sample (m^2)

SEM	scanning electronic microscopy
$SHGC$	solar heat gain coefficient
SP	Solar panel
t	time (s)
T	temperature (°C)
T_a	indoor air temperature (°C)
T_C	average temperature on the surface of the TES unit facing the cold-plate (°C)
TCP	average temperature measured on the surface of the cold-plate facing the TES unit (°C)
t_{cr}	time required for starting the crystallization process of the free-form PCM (s)
T_{ext}	outdoor temperature (°C)
TES	thermal energy storage
T_H	average temperature on the surface of the TES unit facing the hot-plate (°C)
THP	average temperature measured on the surface of the hot-plate facing the TES unit (°C)
t_{liq}	time required for starting the solidification process of the microencapsulated PCM (s)
t_m	time required for complete melting of the PCM in the mid-plane of the TES unit (s)
T_{mp}	melting-peak temperature of the PCM (°C)
T_{mr}	mean radiant temperature (°C)
T_o	operative temperature (°C)
t_{reg}	thermal-regulation period (s)
T_{reg}	control-temperature reached on the hot surface of the TES unit (°C)
t_{sc}	period of subcooling in the free-form PCM (s)
t_{sol}	time required for solidifying all the PCM in the mid-plane of the TES unit (s)
ΔT_{sc}	difference between T_{sp} and T_{sp}*
T_{sp}	solidification temperature of the PCM (°C)
T_{sp}*	lowest temperature reached by the PCM at the end of the sensible cooling due to the subcooling (°C)
T_{th}	cooling thermostat setpoint temperature of the air-conditioning system (°C)
T_{water}	temperature of the cooling water (°C)
$tck_{ins,roof}$	thickness of the insulation layer of the roof (cm)
$tck_{ins,wall}$	thickness of the insulation layer of the wall (cm)
tck_{PCM}	thickness of the PCM-drywall (cm)
TPS	transient plane source method
U	coefficient of heat transfer (W m^{-2} $°C^{-1}$)
WWR	window-to-wall ratio

Greek letters

α	solar absortance coefficient ( )
ρ	density (kg m^{-3})

Subscripts

a, m	annual and monthly assessment basis
Al	aluminium
eq	Equivalent layer
ins	insulation layer
i,f	initial and final times considered for calculating the stored energy during charging
l	liquid
m	monthly assessment basis
opt	optimum value
part	partition wall
PCM	phase change material or PCM-enhanced room
s	solid
ref	reference room
roof	ceiling
wall	external wall
1,...,5	vertical position of the thermocouples in the mid-plane of the TES unit (from top to bottom)

REFERENCES

[1] N. Soares, J.J. Costa, A.R. Gaspar, P. Santos, Review of passive PCM latent heat thermal energy storage systems towards buildings' energy efficiency, Energy and Buildings 59 (2013) 82–103.

[2] L. Pérez-Lombard, J. Ortiz, C. Pout, A review on buildings energy consumption information, Energy and Buildings 40 (3) (2008) 394–398.

[3] E. Asadi, M. Gameiro, C. Henggeler, L. Dias, Multi-objective optimization for building retrofit strategies: a model and an application, Energy and Buildings 44 (2012) 81–87.

[4] C. Diakaki, E. Grigoroudis, D. Kolokotsa, Towards a multi-objective optimization approach for improving energy efficiency in buildings, Energy and Buildings 40 (2008) 1747–1754.

[5] S. Alotaibi, Energy consumption in Kuwait: prospects and future approaches, Energy Policy 39 (2011) 637-643.

[6] T. Kousksou, P. Bruel, A. Jamil, T. El Rhafiki, Y. Zeraouli, Energy storage: applications and challenges, Solar Energy Materials and Solar Cells 120 (2014) 59–80.

[7] Y. Yuan, N. Zhang, W. Tao, X. Cao, Y. He, Fatty acids as phase change materials: a review, Renewable and Sustainable Energy Reviews 29 (2014) 482–498.

[8] K. Pielichowski, Phase change materials for thermal energy storage, Progress in Materials Science 65 (2014) 67–123.

[9] H. Ge, H. Li, S. Mei, J. Liu, Low melting point liquid metal as a new class of phase change material: an emerging frontier in energy area, Renewable and Sustainable Energy Reviews 21 (2013) 331–346.

[10] B. Zalba, J.M. Marín, L.F. Cabeza, H. Mehling, Review on thermal energy storage with phase change: materials, heat transfer analysis and applications, Applied Thermal Engineering 23 (3) (2003) 251–283.

[11] A. Sharma, V.V. Tyagi, C.R. Chen, D. Buddhi, Review on thermal energy storage with phase change materials and applications, Renewable and Sustainable Energy Reviews 13 (2) (2009) 318–345.

[12] M.M. Farid, A.M. Khudhair, S. Ali, K. Razack, A review on phase change energy storage: materials and applications, Energy Conversion and Management 45 (2004) 1597–1615.

[13] Z. Rao, S. Wang, Z. Zhang, Energy saving latent heat storage and environmental friendly humidity-controlled materials for indoor climate, Renewable and Sustainable Energy Reviews 16 (5) (2012) 3136–3145.

[14] L.F. Cabeza, A. Castell, C. Barreneche, A. de Gracia, A.I. Fernández, Materials used as PCM in thermal energy storage in buildings: a review, Renewable and Sustainable Energy Reviews 15 (3) (2011) 1675–1695.

[15] S.D. Sharma, K. Sagara, Latent heat storage materials and systems: a review, International Journal of Green Energy 2 (1) (2005) 1–56.

[16] R.K. Sharma, P. Ganesan, V.V. Tyagi, H.S.C. Metselaar, S.C. Sandaran, Developments in organic solid–liquid phase change materials and their applications in thermal energy storage, Energy Conversion and Management 95 (2015) 193-228.

[17] S. Riffat, B. Mempouo, W. Fang, Phase change material developments: a review, International Journal of Ambient Energy 36 (3) (2015) 102–115.

[18] P. Tatsidjodoung, N. Le Pierrès, L. Luo, A review of potential materials for thermal energy storage in building applications, Renewable and Sustainable Energy Reviews 18 (2013) 327–349.

[19] S.A. Memon, Phase change materials integrated in building walls: a state of the art review, Renewable and Sustainable Energy Reviews 31 (2014) 870–906.

[20] W. Su, J. Darkwa, G. Kokogiannakis, Review of solid–liquid phase change materials and their encapsulation technologies, Renewable and Sustainable Energy Reviews 48 (2015) 373–391.

[21] V.V. Tyagi, D. Buddhi, PCM thermal storage in buildings: a state of art, Renewable and Sustainable Energy Reviews 11 (6) (2007) 1146–1166.

[22] M. Kenisarin, K. Mahkamov, Solar energy storage using phase change materials, Renewable and Sustainable Energy Reviews 11 (9) (2007) 1913–1965.

[23] L.F. Cabeza, C. Barreneche, I. Martorell, L. Miró, S. Sari-Bey, M. Fois, H.O. Paksoy, N. Sahan, R. Weber, M. Constantinescu, E.M. Anghel, M. Malikova, I. Krupa, M. Delgado, P. Dolado, P. Furmanski, M. Jaworski, T. Haussmann, S. Gschwander, A.I. Fernández, Unconventional experimental technologies available for phase change materials (PCM) characterization. Part 1. Thermophysical properties, Renewable and Sustainable Energy Reviews 43 (2015) 1399–1414.

[24] F. Kuznik, D. David, K. Johannes, J.-J. Roux, A review on phase change materials integrated in building walls, Renewable and Sustainable Energy Reviews 15 (1) (2011) 379–391.

[25] D. Zhou, C.Y. Zhao, Y. Tian, Review on thermal energy storage with phase change materials (PCMs) in building applications, Applied Energy 92 (2012) 593–605.

[26] R. Cheng, X. Wang, Y. Zhang, Energy-efficient building envelopes with phase-change materials: new understanding and related research, Heat Transfer Engineering 35 (11-12) (2014) 970–984.

[27] M.K. Rathod, J. Banerjee, Thermal stability of phase change materials used in latent heat energy storage systems: a review, Renewable and Sustainable Energy Reviews 18 (2013) 246–258.

[28] F. Agyenim, N. Hewitt, P. Eames, M. Smyth, A review of materials, heat transfer and phase change problem formulation for latent heat thermal energy storage systems (LHTESS), Renewable and Sustainable Energy Reviews 14 (2) (2010) 615–628.

[29] A. Waqas, Z.U. Din, Phase change material (PCM) storage for free cooling of buildings – a review, Renewable and Sustainable Energy Reviews 18 (2013) 607–625.

[30] A.F. Regin, S.C. Solanki, J.S. Saini, Heat transfer characteristics of thermal energy storage system using PCM capsules: a review, Renewable and Sustainable Energy Reviews 12 (2008) 2438–2458.

[31] Y. Zhang, G. Zhou, K. Lin, Q. Zhang, H. Di, Application of latent heat thermal energy storage in buildings: state-of-the-art and outlook, Building and Environment 42 (6) (2007) 2197–2209.

[32] P.B. Salunkhe, P.S. Shembekar, A review on effect of phase change material encapsulation on the thermal performance of a system, Renewable and Sustainable Energy Reviews 16 (8) (2012) 5603–5616.

[33] T.R. Whiffen, S.B. Riffat, A review of PCM technology for thermal energy storage in the built environment: part I, International Journal of Low-Carbon Technologies 0 (2012) 1–12.

[34] V.V. Tyagi, S.C. Kaushik, S.K. Tyagi, T. Akiyama, Development of phase change materials based microencapsulated technology for buildings: a review, Renewable and Sustainable Energy Reviews 15 (2) (2011) 1373–1391.

[35] C.Y. Zhao, G.H. Zhang, Review on microencapsulated phase change materials (MEPCMs): fabrication, characterization and applications, Renewable and Sustainable Energy Reviews 15 (8) (2011) 3813–3832.

[36] Z. Chen, G. Fang, Preparation and heat transfer characteristics of microencapsulated phase change material slurry: a review, Renewable and Sustainable Energy Reviews 15 (9) (2011) 4624–4632.

[37] A. Jamekhorshid, S.M. Sadrameli, M. Farid, A review of microencapsulation methods of phase change materials (PCMs) as a thermal energy storage (TES) medium, Renewable and Sustainable Energy Reviews 31 (2014) 531–542.

[38] L. Cao, D. Su, Y. Tang, G. Fang, F. Tang, Properties evaluation and applications of thermal energy storage materials in buildings, Renewable and Sustainable Energy Reviews 48 (2015) 500–522.

[39] M. Delgado, A. Lázaro, J. Mazo, B. Zalba, Review on phase change material emulsions and microencapsulated phase change material slurries: materials, heat transfer studies and applications, Renewable and Sustainable Energy Reviews 16 (1) (2012) 253–273.

[40] Z. Youssef, A. Delahaye, L. Huang, F. Trinquet, L. Fournaison, C. Pollerberg, C. Doetsch, State of the art on phase change material slurries, Energy Conversion and Management 65 (2013) 120–132.

[41] G. Fang, F. Tang, L. Cao, Preparation, thermal properties and applications of shape-stabilized thermal energy storage materials, Renewable and Sustainable Energy Reviews 40 (2014) 237–259.

[42] C. Yang, L. Fischer, S. Maranda, J. Worlitschek, Rigid polyurethane foams incorporated with phase change materials: a state-of-the-art review and future research pathways, Energy and Buildings 87 (2015) 25–36.

[43] M. Pomianowski, P. Heiselberg, Y. Zhang, Review of thermal energy storage technologies based on PCM application in buildings, Energy and Buildings 67 (2013) 56–69.

[44] S. Jegadheeswaran, S.D. Pohekar, Performance enhancement in latent heat thermal storage system: a review, Renewable and Sustainable Energy Reviews 13 (2009) 2225–2244.

[45] L. Fan, J.M. Khodadadi, Thermal conductivity enhancement of phase change materials for thermal energy storage: a review, Renewable and Sustainable Energy Reviews 15 (1) (2011) 24–46.

[46] S. Liu, Y. Li, Y. Zhang, Review on heat transfer mechanisms and characteristics in encapsulated PCMs, Heat Transfer Engineering 36 (10) (2015) 880–901.

[47] S.N. AL-Saadi, Z.(J.) Zhai, Modeling phase change materials embedded in building enclosure: a review, Renewable and Sustainable Energy Reviews 21 (2013) 659–673.

[48] A.A. Al-abidi, S.B. Mat, K Sopian, M.Y. Sulaiman, A.T. Mohammed, CFD applications for latent heat thermal energy storage: a review, Renewable and Sustainable Energy Reviews 20 (2013) 353–363.

[49] P. Verma, S.K. Varun, Singal, Review of mathematical modeling on latent heat thermal energy storage systems using phase-change material, Renewable and Sustainable Energy Reviews 12 (4) (2008) 999–1031.

[50] Y. Dutil, D.R. Rousse, N.B. Salah, S. Lassue, L. Zalewski, A review on phase-change materials: mathematical modeling and simulations, Renewable and Sustainable Energy Reviews 15 (1) (2011) 112–130.

[51] Y. Dutil, D. Rousse, S. Lassue, L. Zalewski, A. Joulin, J. Virgone, F. Kuznik, K. Johannes, J.-P. Dumas, J.-P. Bédécarrats, A. Castell, L.F. Cabeza, Modeling phase change materials behavior in building applications: Comments on material characterization and model validation, Renewable Energy 61 (2014) 132–135.

[52] R. Baetens, B.P. Jelle, A. Gustavsen, Phase change materials for building applications: a state-of-the-art review, Energy and Buildings 42 (9) (2010) 1361–1368.

[53] A. Pasupathy, R. Velraj, R.V. Seeniraj, Phase change material-based building architecture for thermal management in residential and commercial establishments, Renewable and Sustainable Energy Reviews 12 (1) (2008) 39–64.

[54] A.M. Khudhair, M.M. Farid, A review on energy conservation in building applications with thermal storage by latent heat using phase change materials, Energy Conversion and Management 45 (2) (2004) 263–275.

[55] N. Zhu, Z. Ma, S. Wang, Dynamic characteristics and energy performance of buildings using phase change materials: a review, Energy Conversion and Management 50 (12) (2009) 3169–3181.

[56] R. Parameshwaran, S. Kalaiselvam, S. Harikrishnan, A. Elayaperumal, Sustainable thermal energy storage technologies for buildings: a review, Renewable and Sustainable Energy Reviews 16 (5) (2012) 2394–2433.

[57] T.R. Whiffen, S.B. Riffat, A review of PCM technology for thermal energy storage in the built environment: part II, International Journal of Low-Carbon Technologies 8 (2013) 159–164.

[58] J. Jeon, J.-H. Lee, J. Seo, S.-G. Jeong, S. Kim, Application of PCM thermal energy storage system to reduce building energy consumption, Journal of Thermal Analysis and Calorimetry 111 (2013) 279–288.

[59] S.E. Kalnaes, B.P. Jelle, Phase change materials and products for building applications: a state-of-the-art review and future research opportunities, Energy and Buildings 94 (2015) 150–176.

[60] V. Basecq, G. Michaux, C. Inard, P. Blondeau, Short-term storage systems of thermal energy for buildings: a review, Advances in Building Energy Research 7 (1) (2013) 66–119.

[61] V.A.A. Raj, R. Velraj, Review on free cooling of buildings using phase change materials, Renewable and Sustainable Energy Reviews 14 (9) (2010) 2819–2829.

[62] E. Osterman, V.V. Tyagi, V. Butala, N.A. Rahim, U. Stritih, Review of PCM based cooling technologies for buildings, Energy and Buildings 49 (2012) 37–49.

[63] S. Kamali, Review of free cooling system using phase change material for building, Energy and Buildings 80 (2014) 131–136.

[64] A.A. Al-abidi, S.B. Mat, K. Sopian, M.Y. Sulaiman, C.H. Lim, A. Th, Review of thermal energy storage for air conditioning systems, Renewable and Sustainable Energy Reviews 16 (8) (2012) 5802–5819.

[65] X.Q. Zhai, X.L. Wang, T. Wang, R.Z. Wang, A review on phase change cold storage in air-conditioning system: materials and applications, Renewable and Sustainable Energy Reviews 22 (2013) 108–120.

[66] E. Rodriguez-Ubinas, L. Ruiz-Valero, S. Vega, J. Neila, Applications of phase change material in highly energy-efficient houses, Energy and Buildings 50 (2012) 49–62.

[67] D.N. Nkwetta, F. Haghighat, Thermal energy storage with phase change material – a state-of-the art review, Sustainable Cities and Society 10 (2014) 87–100.

[68] M.K.A. Sharif, A.A. Al-abidi, S. Mat, K. Sopian, M.H. Ruslan, M.Y. Sulaiman, M.A.M. Rosli, Review of the application of phase change material for heating and domestic hot water systems, Renewable and Sustainable Energy Reviews 42 (2015) 557–568.

[69] M.M. Alkilani, K. Sopian, M.A. Alghoul, M. Sohif, M.H. Ruslan, Review of solar air collectors with thermal storage units, Renewable and Sustainable Energy Reviews 15 (3) (2011) 1476–1490.

[70] Y. Tian, C.Y. Zhao, A review of solar collectors and thermal energy storage in solar thermal applications, Applied Energy 104 (2013) 538–553.

[71] L.A. Chidambaram, A.S. Ramana, G. Kamaraj, R. Velraj, Review of solar cooling methods and thermal storage options, Renewable and Sustainable Energy Reviews 15 (6) (2011) 3220–3228.

[72] S. Pintaldi, C. Perfumo, S. Sethuvenkatraman, S. White, G. Rosengarten, A review of thermal energy storage technologies and control approaches for solar cooling, Renewable and Sustainable Energy Reviews 41 (2015) 975–995.

[73] M. Chandrasekar, S. Rajkumar, D. Valavan, A review on the thermal regulation techniques for non integrated flat PV modules mounted on building top, Energy and Buildings 86 (2015) 692–697.

[74] T. Ma, H. Yang, Y. Zhang, L. Lu, X. Wang, Using phase change materials in photovoltaic systems for thermal regulation and electrical efficiency improvement: a review and outlook, Renewable and Sustainable Energy Reviews 43 (2015) 1273–1284.

[75] D. Du, J. Darkwa, G. Kokogiannakis, Thermal management systems for Photovoltaics (PV) installations: a critical review, Solar Energy 97 (2013) 238–254.

[76] Z. Ling, Z. Zhang, G. Shi, X. Fang, L. Wang, X. Gao, Y. Fang, T. Xu, S. Wang, X. Liu, Review on thermal management systems using phase change materials for electronic components, Li-ion batteries and photovoltaic modules, Renewable and Sustainable Energy Reviews 31 (2014) 427–438.

[77] A. Hasan, S.J. McCormack, M.J. Huang, B. Norton, Evaluation of phase change materials for thermal regulation enhancement of building integrated photovoltaics, Solar Energy 84 (9) (2010) 1601–1612.

[78] M.C. Browne, B. Norton, S.J. Mccormack, Phase change materials for photovoltaic thermal management, Renewable and Sustainable Energy Reviews 47 (2015) 762–782.

[79] A. Makki, S. Omer, H. Sabir, Advancements in hybrid photovoltaic systems for enhanced solar cells performance, Renewable and Sustainable Energy Reviews 41 (2015) 658–684.

[80] S. Jegadheeswaran, S.D. Pohekar, T. Kousksou, Exergy based performance evaluation of latent heat thermal storage system: a review, Renewable and Sustainable Energy Reviews 14 (9) (2010) 2580–2595.

[81] E. Oró, A. de Gracia, A. Castell, M.M. Farid, L.F. Cabeza, Review on phase change materials (PCMs) for cold thermal energy storage applications, Applied Energy 99 (2012) 513–533.

[82] D. Fernandes, F. Pitié, G. Cáceres, J. Baeyens, Thermal energy storage: "How previous findings determine current research priorities", Energy 39 (1) (2012) 246–257.

[83] S. Mondal, Phase change materials for smart textiles – an overview, Applied Thermal Engineering 28 (2008) 1536–1550.

[84] D.C. Hyun, N.S. Levinson, U. Jeong, Y. Xia, Emerging applications of phase-change materials (PCMs): teaching an old dog new tricks, Angewandte Chemie International Edition 53 (15) (2014) 3780–3795.

[85] X. Wang, Y. Zhang, W. Xiao, R. Zeng, Q. Zhang, H. Di, Review on thermal performance of phase change energy storage building envelope, Chinese Science Bulletin 54 (6) (2009) 920–928.

[86] P. Sittisart, M.M. Farid, Fire retardants for phase change materials, Applied Energy 88 (9) (2011) 3140–3145.

[87] A. de Gracia, L. Rincón, A. Castell, M. Jiménez, D. Boer, M. Medrano, L.F. Cabeza, Life cycle assessment of the inclusion of phase change materials (PCM) in experimental buildings, Energy and Buildings 42 (9) (2010) 1517–1523.

[88] H. Mehling, L.F. Cabeza, Heat and cold storage with PCM: an up to date introduction into basics and applications, Springer, 2008.

[89] X. Sun, Q. Zhang, M.A. Medina, K.O. Lee, Experimental observations on the heat transfer enhancement caused by natural convection during melting of solid–liquid phase change materials (PCMs), Applied energy 2015 (in press).

[90] D.W. Hawes, D. Feldman, D. Banu, Latent heat storage in building materials, Energy and Buildings 20 (1) (1993) 77–86.

[91] P. Schossig, H.-M. Henning, S. Gschwander, T. Haussmann, Micro-encapsulated phase-change materials integrated into construction materials, Solar Energy Materials and Solar Cells 89 (2–3) (2005) 297–306.

[92] T. Toppi, L. Mazzarella, Gypsum based composite materials with micro-encapsulated PCM: experimental correlations for thermal properties estimation on the basis of the composition, Energy and Buildings 57 (2013) 227–236.

[93] P. Tittelein, S. Gibout, E. Franquet, K. Johannes, L. Zalewski, F. Kuznik, J.-P. Dumas, S. Lassue, J.-P. Bédécarrats, D. David, Simulation of the thermal and energy behaviour of a composite material containing encapsulated-PCM: influence of the thermodynamical modelling, Applied Energy 140 (2015) 269–274.

[94] E. Franquet, S. Gibout, P. Tittelein, L. Zalewski, J.-P Dumas, Experimental and theoretical analysis of a cement mortar containing microencapsulated PCM, Applied Thermal Engineering 73 (2014) 32–40.

[95] T. Lecompte, P. Le Bideau, P. Glouannec, D. Nortershauser, S. Le Masson, Mechanical and thermo-physical behaviour of concretes and mortars containing phase change material, Energy and Buildings 94 (2015) 52–60.

[96] A. Joulin, L. Zalewski, S. Lassue, H. Naji, Experimental investigation of thermal characteristics of a mortar with or without a micro-encapsulated phase change material, Applied Thermal Engineering 66 (2014) 171–180.

[97] L. Ventolà, M. Vendrell, P. Giraldez, Newly-designed traditional lime mortar with a phase change material as an additive, Construction and Building Materials 47 (2013) 1210–1216.

[98] M. Pomianowski, P. Heiselberg, R.L. Jensen, R. Cheng, Y. Zhang, A new experimental method to determine specific heat capacity of inhomogeneous concrete material with incorporated microencapsulated-PCM, Cement and Concrete Research 55 (2014) 22–34.

[99] M.N.A. Hawlader, M.S. Uddin, M. Mya Khin, Microencapsulated PCM thermal-energy storage system, Applied Energy 74 (2003) 195–202.

[100] X.-xiang Zhang, Y.-feng Fan, X.-ming Tao, K.-lun Yick, Crystallization and prevention of supercooling of microencapsulated n-alkanes, Journal of Colloid and Interface Science 281 (2) (2005) 299–306.

[101] N. Zhu, S. Wang, X. Xu, Z. Ma, A simplified dynamic model of building structures integrated with shaped-stabilized phase change materials, International Journal of Thermal Sciences 49 (9) (2010) 1722–1731.

[102] M. Xiao, B. Feng, K. Gong, Preparation and performance of shape stabilized phase change thermal storage materials with high thermal conductivity, Energy Conversion and Management 43 (1) (2002) 103–108.

[103] A. Sarı, Form-stable paraffin/high density polyethylene composites as solid–liquid phase change material for thermal energy storage: preparation and thermal properties, Energy Conversion and Management 45 (13-14) (2004) 2033–2042.

[104] M. Xiao, B. Feng, K. Gong, Thermal performance of a high conductive shape-stabilized thermal storage material, Heat and Mass Transfer 69 (2001) 293–296.

[105] G. Zhou, Y. Yang, H. Xu, Energy performance of a hybrid space-cooling system in an office building using SSPCM thermal storage and night ventilation, Solar Energy 85 (2011) 477–485.

[106] N. Zhu, S. Wang, Z. Ma, Y. Sun, Energy performance and optimal control of air-conditioned buildings with envelopes enhanced by phase change materials, Energy Conversion and Management 52 (2011) 3197–3205.

[107] W.-l. Cheng, R.-m. Zhang, K. Xie, N. Liu, J. Wang, Heat conduction enhanced shape-stabilized paraffin/HDPE composite PCMs by graphite addition: preparation and thermal properties, Solar Energy Materials and Solar Cells 94 (2010) 1636–1642.

[108] Y. Zhang, J. Ding, X. Wang, R. Yang, K. Lin, Influence of additives on thermal conductivity of shape-stabilized phase change material, Solar Energy Materials and Solar Cells 90 (11) (2006) 1692–1702.

[109] A. Trigui, M. Karkri, I. Krupa, Thermal conductivity and latent heat thermal energy storage properties of LDPE/wax as a shape-stabilized composite phase change material Energy Conversion and Management 77 (2014) 586–596.

[110] M. Karkri, M. Lachheb, Z. Nógellová, B. Boh, B. Sumiga, M.A. AlMaadeed, A. Fethi, I. Krupa, Thermal properties of phase-change materials based on high-density polyethylene filled with micro-encapsulated paraffin wax for thermal energy storage, Energy and Buildings 88 (2015) 144–152.

[111] G. Zhou, Y. Yang, H. Xu, Performance of shape-stabilized phase change material wallboard with periodical outside heat flux waves, Applied Energy 88 (2011) 2113–2121.

[112] G. Zhou, Y. Yang, X. Wang, J. Cheng, Thermal characteristics of shape-stabilized phase change material wallboard with periodical outside temperature waves, Applied Energy 87 (2010) 2666–2672.

[113] G. Zhou, Y. Zhang, X. Wang, K. Lin, W. Xiao, An assessment of mixed type PCM-gypsum and shape-stabilized PCM plates in a building for passive solar heating, Solar Energy 81 (2007) 1351–1360.

[114] G. Zhou, Y. Zhang, K. Lin, W. Xiao, Thermal analysis of a direct-gain room with shape-stabilized PCM plates, Renewable Energy 33 (6) (2008) 1228–1236.

[115] G. Zhou, Y. Yang, X. Wang, S. Zhou, Numerical analysis of effect of shape-stabilized phase change material plates in a building combined with night ventilation, Applied Energy 86 (2009) 52–59.

[116] Y. Zhang, K. Lin, R. Yang, H. Di, Y. Jiang, Preparation, thermal performance and application of shape-stabilized PCM in energy efficient buildings, Energy and Buildings 38 (10) (2006) 1262–1269.

[117] X. Xu, Y. Zhang, K. Lin, H. Di, R. Yang, Modeling and simulation on the thermal performance of shape-stabilized phase change material floor used in passive solar buildings, Energy and Buildings 37 (2005) 1084–1091.

[118] W. Xiao, X. Wang, Y. Zhang, Analytical optimization of interior PCM for energy storage in a lightweight passive solar room, Applied Energy 86 (10) (2009) 2013–2018.

[119] N. Zhu, P. Hu, L. Xu, A simplified dynamic model of double layers shape-stabilized phase change materials wallboards, Energy and Buildings 67 (2013) 508–516.

[120] L. Cao, Y. Tang, G. Fang, Preparation and properties of shape-stabilized phase change materials based on fatty acid eutectics and cellulose composites for thermal energy storage, Energy 80 (2015) 98–103.

[121] S.A. Memon, T.Y. Lo, H. Cui, S. Barbhuiya, Preparation, characterization and thermal properties of dodecanol/cement as novel form-stable composite phase change material, Energy and Buildings 66 (2013) 697–705.

[122] O. Chung, S.-G. Jeong, S. Kim, Preparation of energy efficient paraffinic PCMs/expanded vermiculite and perlite composites for energy saving in buildings, Solar Energy Materials and Solar Cells 137 (2015) 107–112.

[123] Y. Wang, S. Wang, J. Wang, R. Yang, Preparation, stability and mechanical property of shape-stabilized phase change materials, Energy and Buildings (2014) 11–16.

[124] M. Sayyar, R.R. Weerasiri, P. Soroushian, J. Lu, Experimental and numerical study of shape-stable phase-change nanocomposite toward energy-efficient building constructions, Energy and Buildings 75 (2014) 249–255.

[125] C.A. Whitman, M.B. Johnson, M.A. White, Characterization of thermal performance of a solid-solid phase change material, di-n-hexylammonium bromide, for potential integration in building materials, Thermochimica Acta 531 (2012) 54–59.

[126] J. Darkwa, T. Zhou, Enhanced laminated composite phase change material for energy storage, Energy Conversion and Management 52 (2011) 810–815.

[127] E.-B.S. Mettawee, G.M.R. Assassa, Thermal conductivity enhancement in a latent heat storage system, Solar Energy 81 (7) (2007) 839–845.

[128] D. Zhou, C.Y. Zhao, Experimental investigations on heat transfer in phase change materials (PCMs) embedded in porous materials, Applied Thermal Engineering 31 (2011) 970–977.

[129] J.M. Marín, B. Zalba, L.F. Cabeza, H. Mehling, Improvement of a thermal energy storage using plates with paraffin–graphite composite, International Journal of Heat and Mass Transfer 48 (12) (2005) 2561–2570.

[130] A. Mills, M. Farid, J.R. Selman, S. Al-Hallaj, Thermal conductivity enhancement of phase change materials using a graphite matrix, Applied Thermal Engineering 26 (14-15) (2006) 1652–1661.

[131] X. Py, R. Olives, S. Mauran, Paraffin/porous-graphite-matrix composite as a high and constant power thermal storage material, International Journal of Heat and Mass Transfer 44 (2001) 2727–2737.

[132] K. Lafdi, O. Mesalhy, A. Elgafy, Graphite foams infiltrated with phase change materials as alternative materials for space and terrestrial thermal energy storage applications, Carbon 46 (1) (2008) 159–168.

[133] A. Sarı, A. Karaipekli, Thermal conductivity and latent heat thermal energy storage characteristics of paraffin/expanded graphite composite as phase change material, Applied Thermal Engineering 27 (8–9) (2007) 1271–1277.

[134] H. Yin, X. Gao, J. Ding, Z. Zhang, Experimental research on heat transfer mecha- nism of heat sink with composite phase change materials, Energy Conversion and Management 49 (6) (2008) 1740–1746.

[135] C.Y. Zhao, W. Lu, Y. Tian, Heat transfer enhancement for thermal energy stor- age using metal foams embedded within phase change materials (PCMs), Solar Energy 84 (2010) 1402–1412.

[136] Z. Chen, M. Gu, D. Peng, Heat transfer performance analysis of a solar flat-plate collector with an integrated metal foam porous structure filled with paraffin, Applied Thermal Engineering 30 (14-15) (2010) 1967–1973.

[137] J.P. Trelles, J.J. Dufly, Numerical simulation of porous latent heat thermal energy storage for thermoelectric cooling, Applied Thermal Engineering 23 (13) (2003) 1647–1664.

[138] K. Boomsma, D. Poulikakos, F. Zwick, Metal foams as compact high performance heat exchangers, Mechanics of Materials 35 (12) (2003) 1161–1176.

[139] K. Boomsma, D. Poulikakos, On the effective thermal conductivity of a three- dimensionally structured fluid-saturated metal foam, International Journal of Heat and Mass Transfer 44 (2001) 827–836.

[140] O. Mesalhy, K. Lafdi, A. Elgafy, K. Bowman, Numerical study for enhancing the thermal conductivity of phase change material (PCM) storage using high thermal conductivity porous matrix, Energy Conversion and Management 46 (6) (2005) 847–867.

[141] M.H.M. Isa, X. Zhao, H. Yoshino, Preliminary study of passive cooling strategy using a combination of PCM and copper foam to increase thermal heat storage in building facade, Sustainability 2 (8) (2010) 2365–2381.

[142] K. Nakaso, H. Teshima, A. Yoshimura, S. Nogami, Y. Hamada, J. Fukai, Extension of heat transfer area using carbon fiber cloths in latent heat thermal energy storage tanks, Chemical Engineering and Processing 47 (5) (2008) 879–885.

[143] Y. Hamada, W. Ohtsu, J. Fukai, Thermal response in thermal energy storage material around heat transfer tubes: effect of additives on heat transfer rates, Solar Energy 75 (4) (2003) 317–328.

[144] Y. Hamada, W. Otsu, J. Fukai, Y. Morozumi, O. Miyatake, Anisotropic heat transfer in composites based on high-thermal conductive carbon fibers, Energy 30 (2-4) (2005) 221–233.

[145] Y. Hamada, J. Fukai, Latent heat thermal energy storage tanks for space heating of buildings: comparison between calculations and experiments, Energy Conversion and Management 46 (20) (2005) 3221–3235.

[146] J. Fukai, Y. Hamada, Y. Morozumi, O. Miyatake, Effect of carbon-fiber brushes on conductive heat transfer in phase change materials, International Journal of Heat and Mass Transfer 45 (2002) 4781–4792.

[147] J. Fukai, Y. Hamada, Y. Morozumi, O. Miyatake, Improvement of thermal characteristics of latent heat thermal energy storage units using carbon-fiber brushes: experiments and modeling, International Journal of Heat and Mass Transfer 46 (23) (2003) 4513–4525.

[148] J. Fukai, M. Kanou, Y. Kodama, O. Miyatake, Thermal conductivity enhancement of energy storage media using carbon fibers, Energy Conversion and Management 41 (2000) 1543–1556.

[149] A. Elgafy, K. Lafdi, Effect of carbon nanofiber additives on thermal behavior of phase change materials, Carbon 43 (15) (2005) 3067–3074.

[150] C. Alkan, A. Sarı, A. Karaipekli, O. Uzun, Preparation, characterization, and thermal properties of microencapsulated phase change material for thermal energy storage, Solar Energy Materials and Solar Cells 93 (1) (2009) 143–147.

[151] A. Sarı, C. Alkan, A. Karaipekli, O. Uzun, Microencapsulated n-octacosane as phase change material for thermal energy storage, Solar Energy 83 (10) (2009) 1757–1763.

[152] C. Hasse, M. Grenet, A. Bontemps, R. Dendievel, H. Sallée, Realization, test and modelling of honeycomb wallboards containing a phase change material, Energy and Buildings 43 (2011) 232–238.

[153] N. Soares, J.J. Costa, A. Samagaio, R. Vicente, Numerical evaluation of a phase change material-shutter using solar energy for winter nighttime indoor heating, Journal of Building Physics 37 (4) (2014) 367–394.

[154] N. Soares, A. Samagaio, R. Vicente, J. Costa, Numerical simulation of a PCM shutter for buildings space heating during the winter, in: Proceedings of WREC – World Renewable Energy Congress 2011, Linköping, Sweden, 8–13 May, 2011.

[155] U. Stritih, Heat transfer enhancement in latent heat thermal storage system for buildings, Energy and Buildings 35 (11) (2003) 1097–1104.

[156] U. Stritih, An experimental study of enhanced heat transfer in rectangular PCM thermal storage, International Journal of Heat and Mass Transfer 47 (2004) 2841–2847.

[157] M. Koschenz, B. Lehmann, Development of a thermally activated ceiling panel with PCM for application in lightweight and retrofitted buildings, Energy and Buildings 36 (6) (2004) 567–578.

[158] P. Lamberg, R. Lehtiniemi, A.-M. Henell, Numerical and experimental investigation of melting and freezing processes in phase change material storage, International Journal of Thermal Sciences 43 (2004) 277–287.

[159] M. Huang, P. Eames, B. Norton, Comparison of a small-scale 3D PCM thermal control model with a validated 2D PCM thermal control model, Solar Energy Materials and Solar Cells 90 (13) (2006) 1961–1972.

[160] V. Shatikian, G. Ziskind, R. Letan, Numerical investigation of a PCM-based heat sink with internal fins, International Journal of Heat and Mass Transfer 48 (2005) 3689–3706.

[161] G. Susman, Z. Dehouche, T. Cheechern, S. Craig, Tests of prototype PCM 'sails' for office cooling, Applied Thermal Engineering 31 (5) (2011) 717–726.

[162] J. Koo, H. So, S.W. Hong, H. Hong, Effects of wallboard design parameters on the thermal storage in buildings, Energy and Buildings 43 (8) (2011) 1947–1951.

[163] A. Najjar, A. Hasan, Modeling of greenhouse with PCM energy storage, Energy Conversion and Management 49 (11) (2008) 3338–3342.

[164] D. David, F. Kuznik, J.-J. Roux, Numerical study of the influence of the convective heat transfer on the dynamical behaviour of a phase change material wall, Applied Thermal Engineering 31 (16) (2011) 3117–3124.

[165] A. Joulin, Z. Younsi, L. Zalewski, S. Lassue, D.R. Rousse, J.-P. Cavrot, Experimental and numerical investigation of a phase change material: thermal-energy storage and release, Applied Energy 88 (7) (2011) 2454–2462.

[166] A. Castell, I. Martorell, M. Medrano, G. Pérez, L.F. Cabeza, Experimental study of using PCM in brick constructive solutions for passive cooling, Energy and Buildings 42 (4) (2010) 534–540.

[167] C. Barreneche, A. Solé, L. Miró, I. Martorell, A.I. Fernández, L.F. Cabeza, Study on differential scanning calorimetry analysis with two operation modes and organic and inorganic phase change material (PCM), Thermochimica Acta 553 (2013) 23–26.

[168] C. Castellón, E. Gunther, H. Mehling, S. Hiebler, L.F. Cabeza, Determination of the enthalpy of PCM as a function of temperature using a heat-flux DSC - a study of different measurements procedures and their accuracy, International Journal of Energy Research 32 (2008) 1258–1265.

[169] E. Günther, S. Hiebler, H. Mehling, R. Redlich, Enthalpy of phase change materials as a function of temperature: required accuracy and suitable measurement methods, International Journal of Thermophysics 30 (2009) 1257–1269.

[170] J.-P. Dumas, S. Gibout, L. Zalewski, K. Johannes, E. Franquet, S. Lassue, J.-P. Bédécarrats, P. Tittelein, F. Kuznik, Interpretation of calorimetry experiments to characterise phase change materials, International Journal of Thermal Sciences 78 (2014) 48–55.

[171] A. Hauer, H. Mehling, P. Schossig, M. Yamaha, L. Cabeza, V. Martin, F. Setterwall, Annex 17: advanced thermal energy storage through phase change materials and chemical reactions-feasibility studies and demonstration projects. International energy agency implementing agreement on energy conservation through energy storage, 2005.

[172] F. Kuznik, J. Virgone, Experimental investigation of wallboard containing phase change material: data for validation of numerical modeling, Energy and Buildings 41 (5) (2009) 561–570.

[173] A. Lazaro, C. Peñalosa, A. Solé, G. Diarce, T. Haussmann, M. Fois, B. Zalba, S. Gshwander, L.F. Cabeza, Intercomparative tests on phase change materials characterisation with differential scanning calorimeter, Applied Energy 109 (2013) 415–420.

[174] F. Kuznik, J. Virgone, J. Noel, Optimization of a phase change material wallboard for building use, Applied Thermal Engineering 28 (11–12) (2008) 1291–1298.

[175] L. Shilei, F. Guohui, Z. Neng, D. Li, Experimental study and evaluation of latent heat storage in phase change materials wallboards, Energy and Buildings 39 (10) (2007) 1088–1091.

[176] M. Medina, J. King, M. Zhang, On the heat transfer rate reduction of structural insulated panels (SIPs) outfitted with phase change materials (PCMs), Energy 33 (4) (2008) 667–678.

[177] F. Kuznik, J. Virgone, K. Johannes, In-situ study of thermal comfort enhancement in a renovated building equipped with phase change material wallboard, Renewable Energy 36 (5) (2011) 1458–1462.

[178] F. Kuznik, J. Virgone, J.-J. Roux, Energetic efficiency of room wall containing PCM wallboard: a full-scale experimental investigation, Energy and Buildings 40 (2) (2008) 148–156.

[179] D. Banu, D. Feldman, D. Hawes, Evaluation of thermal storage as latent heat in phase change material wallboard by differential scanning calorimetry and large scale thermal testing, Thermochimica Acta 317 (1) (1998) 39–45.

[180] M. Ahmad, A. Bontemps, H. Sallée, D. Quenard, Experimental investigation and computer simulation of thermal behaviour of wallboards containing a phase change material, Energy and Buildings 38 (4) (2006) 357–366.

[181] Y. He, X. Zhang, Y. Zhang, Preparation technology of phase change perlite and performance research of phase change and temperature control mortar, Energy and Buildings 85 (2014) 506–514.

[182] S. Sari-Bey, M. Fois, I. Krupa, L. Ibos, B. Benyoucef, Y. Candau, Thermal characterization of polymer matrix composites containing microencapsulated paraffin in solid or liquid state, Energy Conversion and Management 78 (2014) 796–804.

[183] A. Sharma, A. Shukla, C.R. Chen, S. Dwivedi, Development of phase change materials for building applications, Energy and Buildings 64 (2013) 403–407.

[184] A. Eddhahak-Ouni, S. Drissi, J. Colin, J. Neji, S. Care, Experimental and multi-scale analysis of the thermal properties of Portland cement concretes embedded with microencapsulated phase change materials (PCMs), Applied Thermal Engineering 64 (2014) 32–39.

[185] A. Sarı, Fabrication and thermal characterization of kaolin-based composite phase change materials for latent heat storage in buildings, Energy and Buildings 96 (2015) 193–200.

[186] A.M. Borreguero, M.L. Sánchez, J.L. Valverde, M. Carmona, J.F. Rodríguez, Thermal testing and numerical simulation of gypsum wallboards incorporated with different PCMs content, Applied Energy 88 (3) (2011) 930–937.

[187] H.O. Paksoy, Determining thermal properties of heat storage materials using the twin bath method, Energy Conversion and Management 37 (3) (1996) 261–268.

[188] Y. Zhang, Y. Jiang, A simple method, the T-history method, of determining the heat of fusion, specific heat and thermal conductivity of phase-change materials, Measurement Science and Technology 10 (3) (1999) 201–205.

[189] A. Hasan, S.J. Mccormack, M.J. Huang, B. Norton, Characterization of phase change materials for thermal control of photovoltaics using differential scanning calorimetry and temperature history method, Energy Conversion and Management 81 (2014) 322–329.

[190] J.M. Marin, B. Zalba, L.F. Cabeza, H. Mehling, Determination of enthalpy temperature curves of phase change materials with the temperature-history method: improvement to temperature dependent properties, Measurement Science and Technology 14 (2) (2003) 184–189.

[191] H. Hong, S.K. Kim, Y.-S. Kim, Accuracy improvement of T-history method for measuring heat of fusion of various materials, International Journal of Refrigeration 27 (4) (2004) 360–366.

[192] J.H. Peck, J.-J. Kim, C. Kang, H. Hong, A study of accurate latent heat measurement for a PCM with a low melting temperature using T-history method, International Journal of Refrigeration 29 (7) (2006) 1225–1232.

[193] A. Lázaro, E. Gunther, H. Mehling, S. Hiebler, J.M. Marín, B. Zalba, Verification of a T-history installation to measure enthalpy versus temperature curves of phase change materials, Measurement Science and Technology 17 (2006) 2168–2174.

[194] A. Solé, L. Miró, C. Barreneche, I. Martorell, L.F. Cabeza, Review of the T-history method to determine thermophysical properties of phase change materials (PCM), Renewable and sustainable energy reviews 26 (2013) 425–436.

[195] C. Rathgeber, L. Miró, L.F. Cabeza, S. Hiebler, Measurement of enthalpy curves of phase change materials via DSC and T-History: when are both methods needed to estimate the behaviour of the bulk material in applications ?, Thermochimica Acta 596 (2014) 79–88.

[196] C. Barreneche, M.E. Navarro, A.I. Fernández, L.F. Cabeza, Improvement of the thermal inertia of building materials incorporating PCM. Evaluation in the macroscale, Applied Energy 109 (2013) 428–432.

[197] A. de Gracia, C. Barreneche, M.M. Farid, L.F. Cabeza, New equipment for testing steady and transient thermal performance of multilayered building envelopes with PCM, Energy and Buildings 43 (2011) 3704–3709.

[198] C. Barreneche, A. de Gracia, S. Serrano, M.E. Navarro, A.M. Borreguero, A.I. Fernández, M. Carmona, J.F. Rodriguez, L.F. Cabeza, Comparison of three different devices available in Spain to test thermal properties of building materials including phase change materials, Applied Energy 109 (2013) 421–427.

[199] I.D. Mandilaras, D.A. Kontogeorgos, M.A. Founti, A hybrid methodology for the determination of the effective heat capacity of PCM enhanced building components, Renewable Energy 76 (2015) 790–804.

[200] A. Eddhahak-Ouni, J. Colin, D. Bruneau, On an experimental innovative setup for the macro scale thermal analysis of materials: application to the phase change material (PCM) wallboards, Energy and Buildings 64 (2013) 231–238.

[201] S. Harikrishnan, M. Deenadhayalan, S. Kalaiselvam, Experimental investigation of solidification and melting characteristics of composite PCMs for building heating application, Energy Conversion and Management 86 (2014) 864–872.

[202] H. Fauzi, H.S.C. Metselaar, T.M.I. Mahlia, M. Silakhori, H.C. Ong, Thermal characteristic reliability of fatty acid binary mixtures as phase change materials (PCMs) for thermal energy storage applications, Applied Thermal Engineering 80 (2015) 127–131.

[203] S. Behzadi, M.M. Farid, Long term thermal stability of organic PCMs, Applied Energy 122 (2014) 11–16.

[204] S. Marchi, S. Pagliolico, G. Sassi, Characterization of panels containing micro-encapsulated Phase Change Materials, Energy Conversion and Management 74 (2013) 261–268.

[205] Z. Zhang, G. Shi, S. Wang, X. Fang, X. Liu, Thermal energy storage cement mortar containing n-octadecane expanded graphite composite phase change material, Renewable Energy 50 (2013) 670–675.

[206] C. Chen, W. Liu, Z. Wang, K. Peng, W. Pan, Q. Xie, Novel form stable phase change materials based on the composites of polyethylene glycol/polymeric solid-solid phase change material, Solar Energy Materials and Solar Cells 134 (2015) 80–88.

[207] A.I. Fernández, A. Solé, J. Giró-Paloma, M. Martínez, M. Hadjieva, A. Boudenned, M. Constantinescu, E.M. Anghel, M. Malikova, I. Krupa, C. Peñalosa, A. Lázaro, H.O. Paksoy, K. Cellat, J. Vecstaudža, D. Bajare, B. Sumiga, B. Boh, T. Haussmann, S. Gschwander, R. Weber, P. Furmanski, M. Jaworski, L.F. Cabeza, Unconventional experimental technologies used for phase change materials (PCM) characterization: part 2 – morphological and structural characterization, physico-chemical stability and mechanical properties, Renewable and Sustainable Energy Reviews 43 (2015) 1415–1426.

[208] A.S.T.M. Standard C177, Standard test method for steady-state heat flux measurements and thermal transmission properties by means of the guarded-hot-plate apparatus, ASTM International, West Conshohocken, PA, 2004.

[209] M. Jaworski, S. Abeid, Thermal conductivity of gypsum with incorporated phase change material (PCM) for building applications, Journal of Power Technologies 91 (2) (2011) 49–53.

[210] A. Boudenne, L. Ibos, E. Gehin, Y. Candau, A simultaneous characterisation of thermal conductivity and diffusivity of polymer materials by a periodic method, Journal of Physics D: Applied Physics 37 (1) (2004) 132–139.

[211] A. Boudenne, L. Ibos, Y. Candau, Analysis of uncertainties in thermophysical parameters of materials obtained from a periodic method, Measurement Science and Technology 17 (2006) 1870–1876.

[212] V.R. Voller, C.R. Swaminathan, B.G. Thomas, Fixed grid techniques for phase change problems: a review, International Journal for Numerical Methods in Engineering 30 (4) (1990) 875–898.

[213] M. Costa, D. Buddhi, A. Oliva, Numerical simulation of a latent heat thermal energy storage system with enhanced heat conduction, Energy Conversion and Management 39 (3) (1998) 319–330.

[214] R.C. Chen, A. Sharma, Numerical investigation of melt fraction of PCMs in a latent heat storage system, Journal of Engineering and Applied Sciences 1 (4) (2006) 437–444.

[215] A. Sharma, S.D. Sharma, D. Buddhi, L.D. Won, Effect of thermo physical properties of heat exchanger material on the performance of latent heat storage system using an enthalpy method, International Journal of Energy Research 30 (3) (2006) 191–201.

[216] C.R. Chen, A. Sharma, S.K. Tyagi, D. Buddhi, Numerical heat transfer studies of PCMs used in a box-type solar cooker, Renewable Energy 33 (5) (2008) 1121–1129.

[217] P. Brousseau, M. Lacroix, Numerical simulation of a multi-layer latent heat thermal energy storage system, International Journal of Energy Research 22 (1) (1998) 1–15.

[218] C.R. Swaminathan, V.R. Voller, On the enthalpy method, International Journal of Numerical Methods for Heat Fluid Flow 3 (3) (1993) 233–244.

[219] V.R. Voller, M. Cross, N.C. Markatos, An enthalpy method for convection/diffusion phase change, International Journal for Numerical Methods in Engineering 24 (1) (1987) 271–284.

[220] C. Chen, H. Guo, Y. Liu, H. Yue, C. Wang, A new kind of phase change material (PCM) for energy-storing wallboard, Energy and Buildings 40 (5) (2008) 882–890.

[221] N. Soares, A.R. Gaspar, P. Santos, J.J. Costa, Experimental study of the heat transfer through a vertical stack of rectangular cavities filled with phase change materials, Applied Energy 142 (2015) 192–205.

[222] T. Silva, R. Vicente, N. Soares, V. Ferreira, Experimental testing and numerical modelling of masonry wall solution with PCM incorporation: a passive construction solution, Energy and Buildings 49 (2012) 235–245.

[223] R. Vicente, T. Silva, Brick masonry walls with PCM macrocapsules: an experimental approach, Applied Thermal Engineering 67 (2014) 24-34.

[224] X. Shi, S.A. Memon, W. Tang, H. Cui, F. Xing, Experimental assessment of position of macro encapsulated phase change material in concrete walls on indoor temperatures and humidity levels, Energy and Buildings 71 (2014) 80–87.

[225] E.M. Alawadhi, Using phase change materials in window shutter to reduce the solar heat gain, Energy and Buildings 47 (2012) 421–429.

[226] N. Soares, J.J. Costa, R. Vicente, PCM_WindoWall – storage of solar thermal energy for buildings heating. in: 1st edition of the 'Prémio Ramos Catarino Inovação' Innovation Award, Coimbra, Portugal, February 4, 2012.

[227] N. Soares, Energy for sustainability initiative: an incubator for entrepreneurial and innovative technological ideas – proposal of a new latent heat solar thermal energy storage system. in: EFS 2011 Meeting – students and companies, MIT Portugal program, Civil Engineering Department of the University of Coimbra, Coimbra, Portugal, November 23, 2011.

[228] T. Silva, R. Vicente, F. Rodrigues, A. Samagaio, C. Cardoso, Development of a window shutter with phase change materials: full scale outdoor experimental approach, Energy and Buildings 88 (2015) 110–121.

[229] T. Silva, R. Vicente, F. Rodrigues, A. Samagaio, C. Cardoso, Performance of a window shutter with phase change material under summer Mediterranean climate conditions, Applied Thermal Engineering 84 (2015) 246–256.

[230] G. Diarce, Á. Campos-Celador, K. Martin, A. Urresti, A. García-Romero, J.M. Sala, A comparative study of the CFD modeling of a ventilated active façade including phase change materials, Applied Energy 126 (2014) 307–317.

[231] X. Kong, S. Lu, J. Huang, Z. Cai, S. Wei, Experimental research on the use of phase change materials in perforated brick rooms for cooling storage, Energy and Buildings 62 (2013) 597–604.

[232] R. Kandasamy, X.-Q. Wang, A.S. Mujumdar, Application of phase change materials in thermal management of electronics, Applied Thermal Engineering 27 (17-18) (2007) 2822–2832.

[233] M.J. Huang, P.C. Eames, B. Norton, Thermal regulation of building-integrated photovoltaics using phase change materials, International Journal of Heat and Mass Transfer 47 (12-13) (2004) 2715–2733.

[234] P.H. Biwole, P. Eclache, F. Kuznik, Phase-change materials to improve solar panel's performance, Energy and Buildings 62 (2013) 59–67.

[235] M.J. Huang, P.C. Eames, B. Norton, Phase change materials for limiting temperature rise in building integrated photovoltaics, Solar Energy 80 (2006) 1121–1130.

[236] M.J. Huang, P.C. Eames, B. Norton, N.J. Hewitt, Natural convection in an internally finned phase change material heat sink for the thermal management of photovoltaics, Solar Energy Materials and Solar Cells 95 (7) (2011) 1598–1603.

[237] M.J. Huang, The effect of using two PCMs on the thermal regulation performance of BIPV systems, Solar Energy Materials and Solar Cells 95 (3) (2011) 957–963.

[238] Y. Zhang, Z. Chen, Q. Wang, Q. Wu, Melting in an enclosure with discrete heating at a constant rate, Experimental Thermal and Fluid Science 6 (2) (1993) 196–201.

[239] P.D. Silva, L.C. Gonçalves, L. Pires, Transient behaviour of a latent-heat thermal-energy store: numerical and experimental studies, Applied Energy 73 (2002) 83–98.

[240] A. Joulin, Z. Younsi, L. Zalewski, D.R. Rousse, S. Lassue, A numerical study of the melting of phase change material heated from a vertical wall of a rectangular enclosure, International Journal of Computational Fluid Dynamics 23 (7) (2009) 553–566.

[241] M. Lacroix, M. Benmadda, Numerical simulation of natural convection-dominated melting and solidification from a finned vertical wall, Numerical Heat Transfer, Part A: Applications: An International Journal of Computation and Methodology 31 (1) (1997) 71–86.

[242] W.-B. Ye, D.-S. Zhu, N. Wang, Fluid flow and heat transfer in a latent thermal energy unit with different phase change material (PCM) cavity volume fractions, Applied Thermal Engineering 42 (2012) 49–57.

[243] H. Shokouhmand, B. Kamkari, Experimental investigation on melting heat transfer characteristics of lauric acid in a rectangular thermal storage unit, Experimental Thermal and Fluid Science 50 (2013) 201–212.

[244] H. El Qarnia, A. Draoui, E.K. Lakhal, Computation of melting with natural convection inside a rectangular enclosure heated by discrete protruding heat sources, Applied Mathematical Modelling 37 (6) (2013) 3968–3981.

[245] C.J. Ho, K.C. Liu, W.-M. Yan, Simulation on melting processes in a vertical rectangular enclosure with a free-moving ceiling, International Journal of Heat and Mass Transfer 83 (2015) 222–228.

[246] C.J. Ho, K.C. Liu, W.-M. Yan, Melting processes of phase change materials in an enclosure with a free-moving ceiling: an experimental and numerical study, International Journal of Heat and Mass Transfer 86 (2015) 780–786.

[247] S. Bouadila, M. Fteïti, M.M. Oueslati, A. Guizani, A. Farhat, Enhancement of latent heat storage in a rectangular cavity: solar water heater case study, Energy Conversion and Management 78 (2014) 904–912.

[248] K.C. Nayak, S.K. Saha, K. Srinivasan, P. Dutta, A numerical model for heat sinks with phase change materials and thermal conductivity enhancers, International Journal of Heat and Mass Transfer 49 (2006) 1833–1844.

[249] R. Akhilesh, A. Narasimhan, C. Balaji, Method to improve geometry for heat transfer enhancement in PCM composite heat sinks, International Journal of Heat and Mass Transfer 48 (2005) 2759–2770.

[250] S.K. Saha, P. Dutta, Heat transfer correlations for PCM-based heat sinks with plate fins, Applied Thermal Engineering 30 (2010) 2485–2491.

[251] L.-W. Fan, Y.-Q. Xiao, Y. Zeng, X. Fang, X. Wang,X. Xu, Z.-T. Yu, R.-H. Hong, Y.-C. Hu, K.-F. Cen, Effects of melting temperature and the presence of internal fins on the performance of a phase change material (PCM)-based heat sink, International Journal of Thermal Sciences 70 (2013) 114–126.

[252] S. Mahmoud, A. Tang, C. Toh, R. AL-Dadah, S.L. Soo, Experimental investigation of inserts configurations and PCM type on the thermal performance of PCM based heat sinks, Applied Energy 112 (2013) 1349–1356.

[253] S.K. Saha, P. Dutta, Performance analysis of heat sinks with phase-change materials subjected to transient and cyclic heating, Heat Transfer Engineering 36 (16) (2015) 1349–1359.

[254] B. Kamkari, H. Shokouhmand, F. Bruno, Experimental investigation of the effect of inclination angle on convection-driven melting of phase change material in a rectangular enclosure, International Journal of Heat and Mass Transfer 72 (2014) 186–200.

[255] B. Kamkari, H. Shokouhmand, Experimental investigation of phase change material melting in rectangular enclosures with horizontal partial fins, International Journal of Heat and Mass Transfer 78 (2014) 839–851.

[256] E. Assis, L. Katsman, G. Ziskind, R. Letan, Numerical and experimental study of melting in a spherical shell, International Journal of Heat and Mass Transfer 50 (2007) 1790–1804.

[257] RubiTherm GmbH. RT – data sheets, 2013, (http://www.rubitherm.com).

[258] F. Rouault, D. Bruneau, P. Sebastian, J. Lopez, Numerical modelling of tube bundle thermal energy storage for free-cooling of buildings, Applied Energy 111 (2013) 1099–1106.

[259] BASF SE Business Management Micronal® PCM – data sheets, 2009, (http://www.micronal.de).

[260] R. Cui, Effect of selected phase change materials concentration and manufacturing process on the properties of plaster mixture systems, Clemson University, 2011.

[261] J. Giro-Paloma, G. Oncins, C. Barreneche, M. Martínez, A.I. Fernández, L.F. Cabeza, Physico-chemical and mechanical properties of microencapsulated phase change material, Applied Energy 109 (2013) 441–448.

[262] J.J. Zhang, Z.G. Qu, Z.G. Jin, Experimental study on the thermal characteristics of a microencapsulated phase-change composite plate, Energy 71 (2014) 94–103.

[263] M. Longeon, A. Soupart, J.-F. Fourmigué, A. Bruch, P. Marty, Experimental and numerical study of annular PCM storage in the presence of natural convection, Applied Energy 112 (2013) 175–184.

[264] G.R. Solomon, S. Karthikeyan, R. Velraj, Sub cooling of PCM due to various effects during solidification in a vertical concentric tube thermal storage unit, Applied Thermal Engineering 52 (2013) 505-511.

[265] N. Soares, A.R. Gaspar, P. Santos, J.J. Costa (2015), Experimental evaluation of the heat transfer through small PCM-based thermal energy storage units for building applications (submitted for publication / under review).

[266] H. Mehling, Strategic project 'Innovative PCM-Technology' – results and future perspectives, in: 8th Expert Meeting and Workshop, Kizkalesi, Turkey, April 18–20 April, 2004.

[267] D. Buddhi, H.S. Mishra, A. Sharma, Thermal performance studies of a test cell having a PCM window in south direction. Annex 17, Indore, India, 2003.

[268] Y. Zhang, K. Lin, Q. Zhang, H. Di, Ideal thermophysical properties for free-cooling (or heating) buildings with constant thermal physical property material, Energy and Buildings 38 (10) (2006) 1164–1170.

[269] P. Hoes, M. Trcka, J.L.M. Hensen, B.H. Bonnema, Investigating the potential of a novel low-energy house concept with hybrid adaptable thermal storage, Energy Conversion and Management 52 (6) (2011) 2442–2447.

[270] U. Stritih, V. Butala, Experimental investigation of energy saving in buildings with PCM cold storage, International Journal of Refrigeration 33 (8) (2010) 1676–1683.

[271] A. Castell, M.M. Farid, Experimental validation of a methodology to assess PCM effectiveness in cooling building envelopes passively, Energy and Buildings 81 (2014) 59–71.

[272] M. Rostamizadeh, M. Khanlarkhani, S. Mojtaba Sadrameli, Simulation of energy storage system with phase change material (PCM), Energy and Buildings 49 (2012) 419–422.

[273] D. Heim, J.A. Clarke, Numerical modelling and thermal simulation of PCM-gypsum composites with ESP-r, Energy and Buildings 36 (8) (2004) 795–805.

[274] D. Heim, Isothermal storage of solar energy in building construction, Renewable Energy 35 (4) (2012) 788–796.

[275] Y. Zhang, K. Lin, Y. Jiang, G. Zhou, Thermal storage and nonlinear heat-transfer characteristics of PCM wallboard, Energy and Buildings 40 (9) (2008)1771–1779.

[276] T.K. Stovall, J.J. Tomlinson, What are the potential benefits of including latent storage in common wallboard? Journal of Solar Energy Engineering Transactions of the ASME 117 (4) (1995) 318–325.

[277] B.M. Diaconu, M. Cruceru, Novel concept of composite phase change material wall system for year-round thermal energy savings, Energy and Buildings 42 (10) (2010) 1759–1772.

[278] D.A. Neeper, Thermal dynamics of wallboard with latent heat storage, Solar Energy 68 (5) (2000) 393–403.

[279] D. Zhou, G.S.F. Shire, Y. Tian, Parametric analysis of influencing factors in phase change material wallboard (PCMW), Applied Energy 119 (2014) 33–42.

[280] A. Bastani, F. Haghighat, J. Kozinski, Designing building envelope with PCM wallboards: design tool development, Renewable and Sustainable Energy Reviews 31 (2014) 554–562.

[281] L. Shilei, Z. Neng, F. Guohui, Impact of phase change wall room on indoor thermal environment in winter, Energy and Buildings 38 (1) (2006) 18–24.

[282] S. Scalat, D. Banu, D. Hawes, J. Paris, F. Haghighata, D. Feldman, Full scale thermal testing of latent heat storage in wallboard, Solar Energy Materials and Solar Cells 44 (1996) 46–61.

[283] H. Liu, H.B. Awbi, Performance of phase change material boards under natural convection, Building and Environment 44 (9) (2009) 1788–1793.

[284] M. Ahmad, A. Bontemps, H. Sallée, D. Quenard, Thermal testing and numerical simulation of a prototype cell using light wallboards coupling vacuum isolation panels and phase change material, Energy and Buildings 38 (6) (2006) 673–681.

[285] A.K. Athienitis, C. Liu, D. Hawes, D. Banu, D. Feldman, Investigation of the thermal performance of a passive solar test-room with wall latent heat storage, Building and Environment 5 (1997) 405–410.

[286] T. Zhou, J. Darkwa, G. Kokogiannakis, Thermal evaluation of laminated composite phase change material gypsum board under dynamic conditions, Renewable Energy 78 (2015) 448–456.

[287] A. Oliver, Thermal characterization of gypsum boards with PCM included: thermal energy storage in buildings through latent heat, Energy and Buildings 48 (2012) 1–7.

[288] B.M. Diaconu, Thermal energy savings in buildings with PCM-enhanced envelope: influence of occupancy pattern and ventilation, Energy and Buildings 43 (1) (2011) 101–107.

[289] A. Bernardi, F. Becherini, M.D. Romero-Sanchez, A. Lopez-Buendia, A. Vivarelli, L. Pockelé, S. De Grandi, Evaluation of the effect of phase change materials technology on the thermal stability of cultural heritage objects, Journal of Cultural Heritage 15 (2014) 470–478.

[290] E. Rodriguez-Ubinas, B.A. Arranz, S.V. Sánchez, F.J.N. González, Influence of the use of PCM drywall and the fenestration in building retrofitting, Energy and Buildings 65 (2013) 464–476.

[291] D.A. Chwieduk, Dynamics of external wall structures with a PCM (phase change materials) in high latitude countries, Energy 59 (2013) 301–313.

[292] R. Barzin, J.J.J. Chen, B.R. Young, M.M. Farid, Application of PCM underfloor heating in combination with PCM wallboards for space heating using price based control system, Applied Energy 148 (2015) 39–48.

[293] K. Biswas, J. Lu, P. Soroushian, S. Shrestha, Combined experimental and numerical evaluation of a prototype nano-PCM enhanced wallboard, Applied Energy 131 (2014) 517–529.

[294] A.C. Evers, M.A. Medina, Y. Fang, Evaluation of the thermal performance of frame walls enhanced with paraffin and hydrated salt phase change materials using a dynamic wall simulator, Building and Environment 45 (8) (2010) 1762–1768.

[295] A. Carbonari, M. De Grassi, C. Di Perna, P. Principi, Numerical and experimental analyses of PCM containing sandwich panels for prefabricated walls, Energy and Buildings 38 (2006) 472–483.

[296] C.K. Halford, R.F. Boehm, Modeling of phase change material peak load shifting, Energy and Buildings 39 (3) (2007) 298–305.

[297] F. Mathieu-Potvin, L. Gosselin, Thermal shielding of multilayer walls with phase change materials under different transient boundary conditions, Inter- national Journal of Thermal Sciences 48 (9) (2009) 1707–1717.

[298] M. Huang, P. Eames, N. Hewitt, The application of a validated numerical model to predict the energy conservation potential of using phase change materials in the fabric of a building, Solar Energy Materials and Solar Cells 90 (13) (2006) 1951–1960.

[299] X. Jin, M.A. Medina, X. Zhang, On the placement of a phase change material thermal shield within the cavity of buildings walls for heat transfer rate reduction, Energy 73 (2014) 780–786.

[300] M. de Grassi, A. Carbonari, G. Palomba, A statistical approach for the evaluation of the thermal behavior of dry assembled PCM containing walls, Building and Environment 41 (4) (2006) 448–485.

[301] K. Darkwa, P.W. O'Callaghan, Simulation of phase change drywalls in a passive solar building, Applied Thermal Engineering 26 (8-9) (2006) 853–858.

[302] G. Diarce, A. Urresti, A. García-Romero, A. Delgado, A. Erkoreka, C. Escudero, Á. Campos-Celador, Ventilated active façades with PCM, Applied Energy 109 (2013) 530–537.

[303] A. de Gracia, L. Navarro, A. Castell, L.F. Cabeza, Energy performance of a ventilated double skin facade with PCM under different climates, Energy and Buildings 91 (2015) 37–42.

[304] S. Álvarez, L.F. Cabeza, A. Ruiz-Pardo, A. Castell, J.A. Tenorio, Building integration of PCM for natural cooling of buildings, Applied Energy 109 (2013) 514–522.

[305] Y. Li, S. Liu, Numerical study on thermal behaviors of a solar chimney incorporated with PCM, Energy and Buildings 80 (2014) 406–414.

[306] S. Liu, Y. Li, Heating performance of a solar chimney combined PCM: a numerical case study, Energy and Buildings 99 (2015) 117–130.

[307] C.-m. Lai, S. Hokoi, Thermal performance of an aluminum honeycomb wallboard incorporating microencapsulated PCM, Energy and Buildings 73 (2014) 37–47.

[308] K. Biswas, R. Abhari, Low-cost phase change material as an energy storage medium in building envelopes: experimental and numerical analyses, Energy Conversion and Management 88 (2014) 1020–1031.

[309] X. Sun, Q. Zhang, M.A. Medina, K.O. Lee, Energy and economic analysis of a building enclosure outfitted with a phase change material board (PCMB), Energy Conversion and Management 83 (2014) 73–78.

[310] X. Kong, S. Lu, Y. Li, J. Huang, S. Liu, Numerical study on the thermal performance of building wall and roof incorporating phase change material panel for passive cooling application, Energy and Buildings 81 (2014) 404–415.

[311] H. Ye, L. Long, H. Zhang, R. Zou, The performance evaluation of shape-stabilized phase change materials in building applications using energy saving index, Applied Energy 113 (2014) 1118–1126.

[312] W. Cheng, B. Xie, R. Zhang, Z. Xu, Y. Xia, Effect of thermal conductivities of shape stabilized PCM on under-floor heating system, Applied Energy 144 (2015) 10–18.

[313] E.M. Alawadhi, Thermal analysis of a building brick containing phase change material, Energy and Buildings 40 (3) (2008) 351–357.

[314] C. Zhang, Y. Chen, L. Wu, M. Shi, Thermal response of brick wall filled with phase change materials (PCM) under fluctuating outdoor temperatures, Energy and Buildings 43 (12) (2011) 3514–3520.

[315] C.-M Lai, C.-M Chiang, How phase change materials affect thermal performance: hollow bricks, Building Research and Information 34 (2) (2006) 118–130.

[316] R. Cheng, M. Pomianowski, X. Wang, P. Heiselberg, Y. Zhang, A new method to determine thermophysical properties of PCM-concrete brick, Applied Energy 112 (2013) 988–998.

[317] L.F. Cabeza, C. Castellón, M. Nogués, M. Medrano, R. Leppers, O. Zubillaga, Use of microencapsulated PCM in concrete walls for energy savings, Energy and Buildings 39 (2) (2007) 113–119.

[318] L.F. Cabeza, M. Medrano, C. Castellón, A. Castell, C. Solé, J. Roca, M. Nogués, Thermal energy storage with phase change materials in building envelopes, Contributions to Science 3 (4) (2007) 501–510.

[319] S. Chandra, R. Kumar, S. Kaushik, S. Kaul, Thermal performance of a non-air-conditioned building with PCCM thermal storage wall, Energy Conversion and Management 25 (1) (1985) 15–20.

[320] A.G. Entrop, H.J.H. Brouwers, A.H.M.E. Reinders, Experimental research on the use of micro-encapsulated phase change materials to store solar energy in concrete floors and to save energy in Dutch houses, Solar Energy 85 (5) (2011) 1007–1020.

[321] A. Arnault, F. Mathieu-Potvin, L. Gosselin, Internal surfaces including phase change materials for passive optimal shift of solar heat gain, International Journal of Thermal Sciences 49 (11) (2010) 2148–2156.

[322] E.M. Alawadhi, H.J. Alqallaf, Building roof with conical holes containing PCM to reduce the cooling load: numerical study, Energy Conversion and Management 52 (8-9) (2011) 2958–2964.

[323] A. Pasupathy, R. Velraj, Effect of double layer phase change material in building roof for year round thermal management, Energy and Buildings 40 (3) (2008) 193–203.

[324] D. Zhang, Z. Li, J. Zhou, K. Wu, Development of thermal energy storage concrete, Cement and Concrete Research 34 (6) (2004) 927–934.

[325] P.S.S. Srinivasan, M. Ravikumar, Heat transfer analysis in PCM-filled RCC roof for thermal management, Journal of Mechanical Science and Technology 28 (3) (2014) 1073–1078.

[326] P.K. Dehdezi, M.R. Hall, A.R. Dawson, S.P. Casey, Thermal, mechanical and microstructural analysis of concrete containing microencapsulated phase change materials, International Journal of Pavement Engineering 14 (5) (2013) 449–462.

[327] A.M. Thiele, G. Sant, L. Pilon, Diurnal thermal analysis of microencapsulated PCM-concrete composite walls, Energy Conversion and Management 93 (2015) 215–227.

[328] T.-C Ling, C.-S Poon, Use of phase change materials for thermal energy storage in concrete: an overview, Construction and Building Materials 46 (2013) 55–62.

[329] A.V. Sá, M. Azenha, H. de Sousa, A. Samagaio, Thermal enhancement of plastering mortars with phase change materials: experimental and numerical approach, Energy and Buildings 49 (2012) 16–27.

[330] M.C.S. Nepomuceno, P.D. Silva, Experimental evaluation of cement mortars with phase change material incorporated via lightweight expanded clay aggregate, Construction and Building Materials 63 (2014) 89–96.

[331] M. Kheradmand, M. Azenha, J.L.B. de Aguiar, K.J. Krakowiak, Thermal behavior of cement based plastering mortar containing hybrid microencapsulated phase change materials, Energy and Buildings 84 (2014) 526–536.

[332] H. Li, H. Chen, X. Li, J.G. Sanjayan, Development of thermal energy storage composites and prevention of PCM leakage, Applied Energy 135 (2014) 225–233.

[333] D. Desai, M. Miller, J.P. Lynch, V.C. Li, Development of thermally adaptive engineered cementitious composite for passive heat storage, Construction and Building Materials 67 (2014) 366–372.

[334] X. Fang, T. Yang, Regression methodology for sensitivity analysis of solar heating walls, Applied Thermal Engineering 28 (17-18) (2008) 2289–2294.

[335] C. Eiamworawutthikul, Investigation of phase-change thermal storage in passive solar design for light-construction building in the southeastern climate region. A research program to promote energy conservation and the use of renewable energy, Web accessed at http://energy.pratt.duke.edu/ document/Temporary/PDF%202.pdf

[336] A.J.N. Khalifa, E.F. Abbas, A comparative performance study of some thermal storage materials used for solar space heating, Energy and Buildings 41 (4) (2009) 407–415.

[337] A.A. Ghoneim, S.A. Klein, J.A. Duffie, Analysis of collector-storage building walls using phase-change materials, Solar Energy 47 (3) (1991) 237–242.

[338] S. Jaber, S. Ajib, Optimum design of Trombe wall system in Mediterranean region, Solar Energy 85 (9) (2011) 1891–1898.

[339] G. Quesada, D. Rousse, Y. Dutil, M. Badache, S. Hallé, A comprehensive review of solar facades. Opaque solar facades, Renewable and Sustainable Energy Reviews 16 (5) (2012) 2820–2832.

[340] F. Stazi, A. Mastrucci, C. di Perna, The behaviour of solar walls in residential buildings with different insulation levels: an experimental and numerical study, Energy and Buildings 47 (2012) 217–229.

[341] M. Moghiman, M. Hatami, M. Boghrati, Improvement the winter space heating by the effect of rotating thermal wall storage, in: Proceedings of ECOS 2011, Novi Sad, Serbia, July 4–7, 2011.

[342] H. Weinlaeder, W. Koerner, M. Heidenfelder, Monitoring results of an interior sun protection system with integrated latent heat storage, Energy and Buildings 43 (9) (2011) 2468–2475.

[343] Q. Wang, C.Y. Zhao, Parametric investigations of using a PCM curtain for energy efficient buildings, Energy and Buildings 94 (2015) 33–42.

[344] H. Manz, P.W. Egolf, P. Suter, A. Goetzberger, TIM-PCM, external wall system for solar space heating and daylight, Solar Energy 61 (6) (1997) 369–379.

[345] A. Bontemps, M. Ahmad, K. Johannès, H. Sallée, Experimental and modelling study of twin cells with latent heat storage walls, Energy and Buildings 43 (9) (2011) 2456–2461.

[346] H. Weinläder, A. Beck, J. Fricke, PCM-facade-panel for daylighting and room heating, Solar Energy 78 (2) (2005) 177–186.

[347] F. Goia, M. Zinzi, E. Carnielo, V. Serra, Spectral and angular solar properties of a PCM-filled double glazing unit, Energy and Buildings 87 (2015) 302–312.

[348] F. Goia, M. Perino, V. Serra, Experimental analysis of the energy performance of a full-scale PCM glazing prototype, Solar Energy 100 (2014) 217–233.

[349] P.A. Fokaides, A. Kylili, S.A. Kalogirou, Phase change materials (PCMs) integrated into transparent building elements: a review, Materials for Renewable and Sustainable Energy 4 (6) (2015) 1–13.

[350] E. Cuce, S.B. Riffat, A state-of-the-art review on innovative glazing technologies, Renewable and Sustainable Energy Reviews 41 (2015) 695–714.

[351] W.J. Hee, M.A. Alghoul, B. Bakhtyar, O. Elayeb, M.A. Shameri, M.S. Alrubaih, K. Sopian, The role of window glazing on daylighting and energy saving in buildings, Renewable and Sustainable Energy Reviews 42 (2015) 323–343.

[352] C.-M. Lai, S. Hokoi, Solar façades: a review, Building and Environment 91 (2015) 152–165.

[353] F. Kuznik, J. Virgone, K. Johannes, Development and validation of a new TRNSYS type for the simulation of external building walls containing PCM, Energy and Buildings 42 (7) (2010) 1004–1009.

[354] M. Ibáñez, A. Lázaro, B. Zalba, L.F. Cabeza, An approach to the simulation of PCMs in building applications using TRNSYS, Applied Thermal Engineering 25 (11–12) (2005) 1796–1807.

[355] D.B. Crawley, L.K. Lawrie, F.C. Winkelmann, W.F. Buhl, Y.J. Huang, C.O. Pedersen, R.K. Strand, R.J. Liesen, D.E. Fisher, M.J. Witte, J. Glazer, EnergyPlus: creating a new-generation building energy simulation program, Energy and Buildings 33 (4) (2001) 319–331.

[356] C.O. Pedersen, Advanced zone simulation in EnergyPlus: incorporation of variable properties and phase change material (PCM) capability, in: Proceedings of Building Simulation 2007, Beijing, China, 2007.

[357] A. Tardieu, S. Behzadi, J.J.J. Chen, M.M. Farid, Computer simulation and experimental measurements for an experimental PCM-impregnated office building, in: Proceedings of Building Simulation 2011, Sydney, Australia, 2011.

[358] D. Tetlow, Y. Su, S.B. Riffat, EnergyPlus simulation analysis of incorporating microencapsulated PCMs (Phase Change Materials) with internal wall insulation (IWI) for hard-to-treat (HTT) houses in the UK, in: 10th International Conference on Sustainable Energy Technologies, Istanbul, Turkey, 2011.

[359] S. Shrestha, W. Miller, T. Stovall, A. Desjarlais, K. Childs, W. Porter, M. Bhandari, S. Coley, Modeling PCM-enhanced insulation system and benchmarking EnergyPlus against controlled field data, in: Proceedings of Building Simulation 2011, Sydney, Australia, 2011.

[360] J. Kosny, D. Yarbrough, W. Miller, S. Shrestha, E. Kossecka, E. Lee, Numerical and experimental analysis of building envelopes containing blown fiber- glass insulation thermally enhanced with phase change material (PCM), in: Proceedings of the 1st Central European Symposium on Building Physics, Cracow, Poland, 2010.

[361] J. Kosny, S. Shrestha, T. Stovall, D. Yarbrough, Theoretical and experimental thermal performance analysis of complex thermal storage membrane containing bio-based phase-change material (PCM), in: Thermal Performance of the Exterior Envelopes of Whole Buildings XI, 2010.

[362] G. Evola, N. Papa, F. Sicurella, E. Wurtz, Simulation of the behaviour of phase change materials for the improvement of thermal comfort in lightweight buildings, in: Proceedings of Building Simulation 2011, Sydney, Australia, 2011.

[363] P.C. Tabares-Velasco, C. Christensen, M. Bianchi, Verification and validation of EnergyPlus phase change material model for opaque wall assemblies, Building and Environment 54 (2012) 186–196.

[364] S.N. Al-Saadi, Z.(J.) Zhai, Systematic evaluation of mathematical methods and numerical schemes for modeling PCM-enhanced building enclosure, Energy and Buildings 92 (2015) 374–388.

[365] F. Ascione, N. Bianco, R.F De Masi, F. de' Rossi, G.P. Vanoli, Energy refurbishment of existing buildings through the use of phase change materials: energy savings and indoor comfort in the cooling season, Applied Energy 113 (2014) 990–1007.

[366] M. Alam, H. Jamil, J. Sanjayan, J. Wilson, Energy saving potential of phase change materials in major Australian cities, Energy and Buildings 78 (2014) 192–201.

[367] G. Evola, L. Marletta, The effectiveness of PCM wallboards for the energy refurbishment of lightweight buildings, Energy Procedia 62 (2014) 13–21.

[368] S.M. Sajjadian, J. Lewis, S. Sharples, The potential of phase change materials to reduce domestic cooling energy loads for current and future UK climates, Energy and Buildings 93 (2015) 83–89.

[369] G. Evola, L. Marletta, F. Sicurella, A methodology for investigating the effectiveness of PCM wallboards for summer thermal comfort in buildings, Building and Environment 59 (2013) 517–527.

[370] G. Evola, L. Marletta, F. Sicurella, Simulation of a ventilated cavity to enhance the effectiveness of PCM wallboards for summer thermal comfort in buildings, Energy and Buildings 70 (2014) 480–489.

[371] J.S. Sage-Lauck, D.J. Sailor, Evaluation of phase change materials for improving thermal comfort in a super-insulated residential building, Energy and Buildings 79 (2014) 32–40.

[372] P. Santos, H. Gervásio, L.S. da Silva, A.G. Lopes, Influence of climate change on the energy efficiency of light-weight steel residential buildings, Civil Engineering and Environmental Systems 28 (4) (2011) 325–352.

[373] P. Santos, L.S. da Silva, H. Gervásio, A.G. Lopes, Parametric analysis of the thermal performance of light steel residential buildings in Csb climatic regions, Journal of Building Physics 35 (1) (2010) 7–53.

[374] J. Mazo, M. Delgado, J.M. Marin, B. Zalba, Modeling a radiant floor system with Phase Change Material (PCM) integrated into a building simulation tool: analysis of a case study of a floor heating system coupled to a heat pump, Energy and Buildings 47 (2012) 458–466.

[375] F. Almeida, D. Zhang, A.S. Fung, W.H. Leong, Investigation of multilayered phase-change-material modeling in ESP-r, in: International High Performance Buildings Conference, July 12–15, Purdue, USA, 2010.

[376] N.T.A. Fernandes, V.A.F. Costa, Use of phase-change materials as passive elements for climatization purposes in summer: the Portuguese case, International Journal of Green Energy 6 (3) (2009) 302–311.

[377] J. Kosny, A. Fallahi, N. Shukla, E. Kossecka, R. Ahbari, Thermal load mitigation and passive cooling in residential attics containing PCM-enhanced insulations, Solar Energy 108 (2014) 164–177.

[378] A. Chel, J.K. Nayak, G. Kaushik, Energy conservation in honey storage building using Trombe wall, Energy and Buildings 40 (9) (2008) 1643–1650.

[379] S. Lu, S. Liu, J. Huang, X. Kong, Establishment and experimental verification of PCM room's TRNSYS heat transfer model based on latent heat utilization ratio, Energy and Buildings 84 (2014) 287–298.

[380] E. Meng, H. Yu, G. Zhan, Y. He, Experimental and numerical study of the thermal performance of a new type of phase change material room, Energy Conversion and Management 74 (2013) 386–394.

[381] J.F. Belmonte, P. Eguía, A.E. Molina, J.A. Almendros-Ibáñez, Thermal simulation and system optimization of a chilled ceiling coupled with a floor containing a phase change material (PCM), Sustainable Cities and Society 14 (2015) 154–170.

[382] W. Lin, Z. Ma, M.I. Sohel, P. Cooper, Development and evaluation of a ceiling ventilation system enhanced by solar photovoltaic thermal collectors and phase change materials, Energy Conversion and Management 88 (2014) 218–230.

[383] M. Fadaee, M.A.M. Radzi, Multi-objective optimization of a stand-alone hybrid renewable energy system by using evolutionary algorithms: a review, Renewable and Sustainable Energy Reviews 16 (5) (2012) 3364–3369.

[384] K. Menoufi, A. Castell, L. Navarro, G. Pérez, D. Boer, L.F. Cabeza, Evaluation of the environmental impact of experimental cubicles using life cycle assessment: a highlight on the manufacturing phase, Applied Energy 92 (2012) 534–544.

[385] A. Utama, S.H. Gheewala, Life cycle energy of single landed houses in Indonesia, Energy and Buildings 40 (10) (2008) 1911–1916.

[386] J.N. Hacker, T.P. de Saulles, A.J. Minson, M.J. Holmes, Embodied and operational carbon dioxide emissions from housing: a case study on the effects of thermal mass and climate change, Energy and Buildings 40 (3) (2008) 375–384.

[387] R. Dylewski, J. Adamczyk, Economic and environmental benefits of thermal insulation of building external walls, Building and Environment 46 (12) (2011) 2615–2623.

[388] Markets and Markets, Advanced Phase Change Material Market Global Fore- cast (2010–2015), 2010.

[389] K. Peippo, P. Kauranen, P.D. Lund, A multicomponent PCM wall optimized for passive solar heating, Energy and Buildings 17 (4) (1991) 259–270.

[390] B.A. Habeebullah, Economic feasibility of thermal energy storage systems, Energy and Buildings 39 (3) (2007) 355–363.

[391] B. Rismanchi, R. Saidur, H.H. Masjuki, T.M.I. Mahlia, Energetic, economic and environmental benefits of utilizing the ice thermal storage systems for office building applications, Energy and Buildings 50 (2012) 347–354.

[392] M. Ozel, Cost analysis for optimum thicknesses and environmental impacts of different insulation materials, Energy and Buildings 49 (2012) 552–559.

[393] EPBD, Directive 2002/91/EC of the European Parliament and of the Council of 16 December 2002 on the energy performance of buildings, in Official Journal of the European Union (2003), L1/65–1/71.

[394] EPBD (recast), Directive2010/31/EU of the European Parliament and of the Council of 19 May 2010 on the energy performance of buildings (recast), in Official Journal of the European Union (2010), L153/13–153/35.

[395] D. Kolokotsa, D. Rovas, E. Kosmatopoulos, K. Kalaitzakis, A roadmap towards intelligent net zero- and positive-energy buildings, Solar Energy 85 (12) (2011) 3067–3084.

[396] I. Sartori, A. Napolitano, K. Voss, Net zero energy buildings: a consistent definition framework, Energy and Buildings 48 (2012) 220–232.

[397] A.J. Marszal, P. Heiselberg, Life cycle cost analysis of a multi-storey residential net zero energy building in Denmark, Energy 36 (9) (2011) 5600–5609.

[398] A.J. Marszal, P. Heiselberg, J.S. Bourrelle, E. Musall, K. Voss, I. Sartori, A. Napolitano, Zero energy building – a review of definitions and calculation methodologies, Energy and Buildings 43 (4) (2011) 971–979.

[399] N. Soares, A.R. Gaspar, P. Santos, J.J. Costa, Multi-dimensional optimization of the incorporation of PCM-drywalls in lightweight steel-framed residential buildings in different climates, Energy and Buildings 70 (2014) 411-421.

[400] I. Mandilaras, M. Stamatiadou, D. Katsourinis, G. Zannis, M. Founti, Experimental thermal characterization of a Mediterranean residential building with PCM gypsum board walls, Building and Environment 61 (2013) 93–103.

[401] M. Wetter, J. Wright, A comparison of deterministic and probabilistic optimization algorithms for nonsmooth simulation-based optimization, Building and Environment 39 (8) (2004) 989–999.

[402] E. Asadi, M.G. da Silva, C.H. Antunes, L. Dias, A multi-objective optimization model for building retrofit strategies using TRNSYS simulations, GenOpt and MATLAB, Building and Environment 56 (2012) 370–378.

[403] A. Hasan, M. Vuolle, K. Sirén, Minimisation of life cycle cost of a detached house using combined simulation and optimisation, Building and Environment 43 (12) (2008) 2022–2034.

[404] M. Fesanghary, S. Asadi, Z.W. Geem, Design of low-emission and energy-efficient residential buildings using a multi-objective optimization algorithm, Building and Environment 49 (2012) 245–250.

[405] GenOpt 3.1.0, Generic Optimization Program, 2013, (http://gundog.lbl.gov/GO/).

[406] EnergyPlus 8.0.0, Energy Simulation Software, 2013, (http://apps1.eere.energy.gov/buildings/energyplus/).

[407] ESP-r. http://www.esru.strath.ac.uk/Programs/ESP-r.htm, 2013.

[408] TRNSYS 17, A Transient Systems Simulation Program, 2013, (http://sel.me.wisc.edu/trnsys/).

[409] P. Tabares-Velasco, Energy impacts of nonlinear behavior of PCM when applied into building envelope, in: ASME 2012 sixth International Conference on Energy Sustainability and tenth Fuel Cell Science, Engineering and Technology Conference, San Diego, California, 2012.

[410] M. Wetter, GenOpt: Generic Optimization Program, User Manual Version 3.1.0, Lawrence Berkeley National Laboratory, 2011.

[411] R. Eberhart, J. Kennedy, A new optimizer using particle swarm theory, in: Sixth International Symposium on Micro Machine and Human Science, Nagoya, Japan, 1995, pp. 39–43.

[412] J. Kennedy, R. Eberhart, Particle swarm optimization, in: IEEE International Conference on Neural Networks, Volume IV, Perth, Australia, 1995, pp. 1942–1948.

[413] M. Kottek, J. Grieser, C. Beck, B. Rudolf, F. Rubel, World Map of the Köppen–Geiger climate classification updated, Meteorologische Zeitschrift 15(3) (2006) 259–263.

[414] S. Cao, A. Gustavsen, S. Uvsløkk, B.P. Jelle, J. Gilbert, J. Maunuksela, The effect of wall-integrated phase change material panels on the indoor air and wall temperature – hot box experiments, in: Proceedings of Renewable Energy Research Conference 2010, Trondheim, Norway, 2010.

[415] American Society of Heating, Refrigerating, and Air-Conditioning Engineers, ANSI/ASHRAE Standard 140-2004, Standard Method of Test for the Evaluation of Building Energy Analysis Computer Programs, American Society of Heating, Refrigerating, and Air-Conditioning Engineers, GA, Atlanta, 2004.

[416] S. Doran, M. Gorgolewski, U-values for light steel-frame construction, in: BRE Digest 465, Building Research Establishment, UK, 2002.

[417] Concerted action EPBD, Implementing the Energy Performance of Buildings Directive (EPBD) – Featuring Country Reports 2010, Brussels, April 2011.

[418] A.P. Gomes, H.A. de Souza, A. Tribess, Impact of thermal bridging on the performance of buildings using Light Steel Framing in Brazil, Applied Thermal Engineering 52 (1) (2013) 84–89.

[419] M. Gorgolewski, Developing a simplified method of calculating U-values in light steel framing, Building and Environment 42 (1) (2007) 230–236.

[420] European Committee for Standardization, Building components and building elements – thermal resistance and thermal transmittance – calculation method, in: EN ISO 6946, 1996.

[421] Ministry of Electricity and Water, Energy Conservation Program – Code of Practice, MEW, R-6, 2nd Ed, 2010.

[422] S. Alsanad, A. Gale, R. Edwards, Challenges of sustainable construction in Kuwait: investigating level of awareness of Kuwait stakeholders, Engineering and Technology 59 (2011) 2197–2204.

[423] M. Krarti, A. Hajiah, Analysis of impact of daylight time savings on energy use of buildings in Kuwait, Energy Policy 39 (2011) 2319–2329.

[424] F.F. Al-ajmi, V.I. Hanby, Simulation of energy consumption for Kuwaiti domestic buildings, Energy and Buildings 40 (2008) 1101–1109.

[425] EnergyPlus 8.3, Energy Simulation Software, 2013, (http://apps1.eere.energy.gov/buildings/energyplus/).

[426] ANSI/ASHRAE standard 55-2004, Thermal environment conditions for human occupancy, American Society of Heating, Refrigerating, and Air-Conditioning Engineers, Atlanta 2004.

[427] ISO 8990:1994, Thermal insulation - Determination of steady-state thermal transmission properties - Calibrated and guarded hot box.

[428] BS 874:1973, Methods for determining thermal insulating properties with definitions of thermal insulating terms.

[429] ASTM C1363 - 11, Standard test method for thermal performance of building materials and envelope assemblies by means of a hot box apparatus.